

AD-781 317

STRUCTURAL DYNAMIC PROPERTIES OF
TACTICAL MISSILE JOINTS--PHASE 3

George Lasker, et al

General Dynamics

Prepared for:

Naval Air Systems Command

May 1974

DISTRIBUTED BY:

NTIS

National Technical Information Service
U. S. DEPARTMENT OF COMMERCE
5285 Port Royal Road, Springfield Va. 22151

UNCLASSIFIED

AD 781 317

DOCUMENT CONTROL DATA - R & D		
Security Classification		
Pomona Division of General Dynamics Inc. 1615 W. Mission Boulevard Pomona, California 91766		UNCLASSIFIED
REPORT TITLE		
STRUCTURAL DYNAMIC PROPERTIES OF TACTICAL MISSILE JOINTS - PHASE 3		
1. DESCRIPTIVE NOTES (Type of report and inclusive dates) Final (May 1972 thru January 1974)		
2. AUTHOR(S) (First name, middle initial, last name) George Lasker, John G. Maloney, Michael T. Shelton and David A. Underhill		
3. REPORT DATE May 1974	4. TOTAL NO. OF PAGES 186	5. NO. OF REFS 7
6. CONTRACT OR GRANT NO. N00019-72-C-0507	7. ORIGINATOR'S REPORT NUMBER(S) C-6-348-945-003	
8. PROJECT NO.	9. OTHER REPORT NO(S) (Any other numbers that may be assigned this report)	
10. DISTRIBUTION STATEMENT Approved for public release, distribution unlimited.		
11. SUPPLEMENTARY NOTES		
12. SPONSORING/MONITORING AGENCY NAME(S) AND ADDRESS(ES) Naval Air Systems Command Department of the Navy Washington, D.C. 20361		
13. ABSTRACT The results of a third and final phase in a general study of the structural dynamic properties of tactical missile airframe joints are presented. The overall objectives of the study were to provide a better understanding of mechanical joint effects on missile dynamic response and to improve methods for predicting and representing their characteristics in system simulation and response studies. Finite element structural analysis techniques started in Phase 1 are shown to be capable of providing reliable estimates of joint compliance in complex actual missile structures. A technique for extracting joint compliance values from missile model test data started in Phase 1 is refined to improve convergence and user convenience. A user's manual for the joint compliance extraction digital computer code is included as an appendix to the report. An exploratory study of missile joint self-induced vibration is presented together with an initial evaluation of some promising methods for suppression and control. The report concludes with a proposed rating system for joints intended to integrate the many design considerations such as strength, weight, producibility, and maintainability, in addition to structural dynamic considerations, into overall system requirements.		
NATIONAL TECHNICAL INFORMATION SERVICE 705 Grafton Avenue Springfield, MA 01105		

DD FORM 1473

(PAGE 1)

GIC1-807-1801

UNCLASSIFIED

Security Classification

Security Classification

DD FORM 1473 (BACK)
(PAGE 2)

Security Classification

STRUCTURAL DYNAMIC PROPERTIES OF
TACTICAL MISSILE JOINTS - PHASE 3

Final Report

(May 1972 to January 1974)

May 1974

CR-6-348-945-003

By

G. Lasker
J. G. Maloney
M. T. Shelton
D. A. Underhill

Prepared Under Contract N00019-72-C-0507

for the

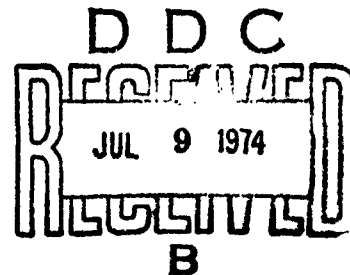
Naval Air Systems Command

by

Pomona Division

General Dynamics, Inc.

1675 W. Mission Blvd.
Pomona, California 91766



Approved for public release; distribution unlimited

ib

FOREWORD

This study has been conducted by the Pomona Division of General Dynamics Corporation for the Naval Air Systems Command under Contract N00019-72-C-0507.

The principal investigator for the study has been Mr. John G. Maloney. Dr. George Lasker has performed the finite element analysis presented in Section 3. The joint compliance extraction technique and computer code work was performed by Mr. M. T. Shelton. The direct technical supervisor has been Mr. David A. Underhill, Structural Dynamics Section Head.

Mr. George P. Maggos has been the Naval Air Systems Command technical monitor.

The authors wish to acknowledge the contributions of Messrs David O. Rife, James B. Samonte and Donald G. VandeGriff for providing assistance in various portions of the study.

TABLE OF CONTENTS

<u>Section</u>	<u>Title</u>	<u>Page</u>
1.0	SUMMARY	1
2.0	INTRODUCTION	2
3.0	JOINT COMPLIANCE ANALYSIS	8
	3.1 PROBLEM FORMULATION	8
	3.2 TEST CASE AND RESULTS	16
	3.3 CONCLUSIONS	19
4.0	JOINT COMPLIANCE EXTRACTION TECHNIQUE DEVELOPMENT	33
	4.1 METHOD OF ANALYSIS	34
	4.1.1 System Model	35
	4.1.2 Solution Method	36
	4.2 SPECIAL PARAMETERS	40
	4.2.1 Weighting Factors	40
	4.2.2 "Bite" Size Selection	43
	4.3 PROGRAM FEATURES ADDED	45
	4.3.1 Weighting Factor Generation	45
	4.3.2 Missing Mode Logic	45
	4.3.3 Number of Theoretical Modes	46
	4.3.4 Input Parameter 'CLOSE'	46
	4.3.5 Test Data Preparation	47
	4.4 TACTICAL MISSILE TEST CASE	48
	4.5 STATUS OF THE EXTRACTION TECHNIQUE	49
5.0	MISSILE JOINT SELF INDUCED VIBRATION	64
	5.1 FULL SCALE LAB TESTS	65
	5.2 MISSILE LEVEL QUALIFICATION AND FLIGHT TEST	66
	5.3 JOINT IMPACT MODEL DESIGN AND TEST	69

TABLE OF CONTENTS
(Cont'd.)

<u>Section</u>	<u>Title</u>	<u>Page</u>
	5.3.1 Model Joint Preload	70
	5.3.2 Model Vibration Test Setup and Results	71
	5.4 FULL SCALE IMPLICATIONS OF MODEL TEST RESULTS	72
6.0	INTEGRATION INTO OVERALL SYSTEM REQUIREMENTS	87
	6.1 SYSTEM CONSIDERATIONS	87
	6.1.1 Strength	87
	6.1.2 Weight	88
	6.1.3 Volumetric Efficiency	89
	6.1.4 Degree of Enclosure	89
	6.1.5 Producibility	90
	6.1.6 Maintainability	91
	6.2 INTEGRATION METHOD	91
REFERENCES		98
APPENDIX	JOINT COMPLIANCE EXTRACTION CODE USER'S MANUAL	99-175

LIST OF TABLES

<u>Table No.</u>	<u>Title</u>	<u>Page</u>
3-1	NASTRAN Computed Stiffness Coefficients for the Structure on Each Side of the Joint for 108 Harmonics	20
3-2	Data Used in Equation (3.44) to Compute Stiffness Coefficients for Harmonics Greater than 108	17
3-3	Harmonics Having Non Zero Stiffness Coefficients for the Various Fastener Arrangements	21
3-4	Phase 2 Measured Values of Stiffness for Various Numbers of Fasteners	17
3-5	Computed Joint Stiffness for Three Fasteners and Various Values of the Ratio of ϵ over the Bolt Diameter Enclosed Angle	22
3-6	Computed Equivalent Joint Stiffness for 3, 6, 9, 18 Fasteners Using a Value of 6.24 for the Ratio of ϵ Over the Bolt Diameter Enclosed Angle	23
3-7	Computed Joint Stiffness for Eighteen Fasteners and Various Values of the Ratio of ϵ over the Bolt Diameter Enclosed Angle	24
3-8	Computed and Measured Equivalent Joint Stiffness for 3, 6, 9, 12 and 18 Fasteners Using a Value of 1.544 for the Value of R	25
3-9	Computed Equivalent Joint Stiffness	26
5-1	Measured Noise Ratios for Discontinuous Land Joint with Different Surface Treatments	74
5-2	Basic Joint Model Dynamic Response	75
5-3	Teflon Coated Joint Model Dynamic Response	76
5-4	Basic/Teflon Joint Model Dynamic Response Comparison	77

LIST OF TABLES
(Cont'd.)

<u>Table No.</u>	<u>Title</u>	<u>Page</u>
6-1	Proposed Joint Attribute Rating Basis	93
6-2	Illustrative Rating Comparison for Three Joints	94

LIST OF FIGURES

<u>Figure No.</u>	<u>Title</u>	<u>Page</u>
2-1	Frequency Ratio Vs. Joint Stiffness Ratio, Uniform Beam - Midspan Joint	5
2-2	13.5 Inch Diameter Shear Bolt Joint Flexural Compliance Vs. Number of Fasteners	6
2-3	Generalized Shear Joint Compliance Versus Number of Fasteners	7
3-1	Sketch Showing Two Axisymmetric Shells Attached at a Discrete Set of Points	9
3-2	Area Over Which Bolt Acts as Defined in Math Model	9
3-3	Shear Bolt Joint Test Specimen and Section Modeled Using Finite Elements	27
3-4	Shell Element Model in the Region of the Shear Bolt Joint	28
3-5	Log-Log Plots of NASTRAN Computed Stiffness Coefficients Versus Harmonic Number for the Two Structures	29
3-6	Curve of Stiffness Versus Number of Fasteners for $R = 1.544$, $R = 6.24$ and Measured Results	30
3-7	Curve of Joint Stiffness Versus R for the Three Fastener Case	31
3-8	Curves of Computed Joint Stiffness Versus Highest Harmonic for the Three Fastener Joint and Various Values of R	32
4-1	Non-Uniform Bending Beam Properties	52
4-2	Non-Uniform Bending Beam Solution for Three Joint Compliances Using Two Modes, $r = 25\%$	53
4-3	Non-Uniform Bending Beam Solution for Three Joint Compliances Using Two Modes, $r = 1\%$	54

LIST OF FIGURES
(Cont'd.)

<u>Figure No.</u>	<u>Title</u>	<u>Page</u>
4-4	Non-Uniform Bending Beam Convergence Vs. Intermediate Step Size - r , Solving for Three Joint Compliances Using Two Modes	55
4-5 thru 4-7	Tactical Missile Measured Bending Modes	56-58
4-8	Tactical Missile Application Solution No. 1 Equal Weighting Factors	59
4-9 thru 4-11	Tactical Missile Application Comparison of Experimental and Theoretical Modes	60-62
4-12	Tactical Missile Application Solution No. 2 Unequal Weighting Factors	63
5-1	Discontinuous Land Ring Joint	78
5-2	Continuous Land Ring Joint	79
5-3	Test Setup - Joint Self Induced Vibration	80
5-4	Flight Test Missile Joint Locations	81
5-5	Teflon Coupling Ring Joint Impact Noise Suppression Versus Basic Joint Noise Factor	82
5-6	Idealized Ring Joint Model	83
5-7	Scale Model Ring Joint Preload Vs. Torque	84
5-8	Ring Joint Model Test Setup	85
5-9	Model 1st Mode Frequency Vs. Effective Joint Compliance	86
6-1	Continuous Land Ring Joint	95
6-2	Four Bolt Tension Joint	96
6-3	Eight Bolt Tension Joint	97

Section 1.0

SUMMARY

Results of a third and final phase in a general study of the structural dynamic properties of tactical missile joints are presented. This effort, undertaken by the Pomona Division of General Dynamics for the Naval Air Systems Command, has been intended to provide a better understanding of mechanical joint effects on missile dynamic response and improved methods for predicting and representing their characteristics in system simulation and response studies.

Highlights of the results obtained in the first two study phases (References 1 and 2) are reviewed, covering an industry survey, classification scheme, and parametric evaluation of joint compliance effects. Finite element structural analysis techniques started in Phase 1 and completed in this final study phase are shown to be capable of providing reliable estimates of joint compliance in complex actual missile structures.

Experimental methods are reviewed and a joint compliance extraction code designed to solve for joint properties from modal test data is described in some detail. This method, also started in the Phase 1 study, has been refined during the present phase to improve convergence and user convenience. A user's manual for this code is included as an Appendix.

An exploratory study of missile joint self-induced vibration is presented together with an initial evaluation of some promising methods for suppression and control. The report concludes with a discussion of a proposed rating system for tactical missile joints with the objective of offering the designer some perspective on integrating the many considerations such as strength, producibility, and maintainability, in addition to compliance, into overall system requirements.

Section 2.0

INTRODUCTION

The structural dynamic properties of tactical missile joints can play an extraordinarily important role in weapon system structural response characteristics. This report deals with the third and final phase of an exploratory study of the primary structural dynamic characteristics of missile mechanical joints and the analytical and experimental tools identified and developed for predicting their behavior.

The most conspicuous attribute of the average tactical missile joint is flexural compliance under applied bending moment. The first phase study was largely devoted to an examination of this characteristic starting with a literature search and an industry survey to sample others' experience followed by a parametric study of joint compliance effects, elastic coupling, the significance of stiffness discontinuities and the importance of considering actual load paths through joint elements. Based on the industry survey, it was concluded that investigators generally represent missile joints in analytical modeling by flexural springs selected by trial and error to match measured response characteristics. Joint compliance effects were typically found to account for more than 30 percent of the total elastic deformation of a missile in its primary bending modes.

A joint classification scheme proposed in a NASA study reported in Reference 3 suggested factors of ten increase in compliance progressing from each level - Excellent, Good, Moderate, and Loose. Thus, a "Moderate" joint would be 10 times as compliant as a "Good" joint and 100 times as compliant as an "Excellent" joint. Viewed in terms of stiffness loss in a typical missile airframe, a "Good" joint represents a local reduction in section properties of approximately 60 percent over a span of one half body diameter. A "Moderate" joint would correspondingly reduce local section properties 95 percent. Such gross structural inefficiencies are attributed to poor distribution of load paths through joint interfaces. Figure 2-1 shows the powerful influence of joint compliance on the first mode frequency of a missile idealized as a uniform beam.

From the standpoint of the structural dynamic analyst charged with the responsibility for developing adequate math models in developmental studies, methods for accurately estimating joint compliance are of paramount importance. The advent of finite element structural analysis techniques has offered some very promising tools for realistically representing detailed elastic behavior with joint elements. Finite element modeling of idealized joints was started in an exploratory effort

during Phase 1 and - based on encouraging results - considerably expanded during Phase 2 to encompass an actual missile joint design for which accurate compliance test data were available for correlation purposes. This effort has been continued during the present and final study phase with emphasis on computational economy and is presented in Section 3.0.

Experimental methods when test hardware is available offer another important approach to the determination of missile joint structural dynamic properties. An ideal test configuration for evaluating joint properties is considered to be a simple uniform structure on a free-free suspension to avoid external constraints and with the subject joint located at mid-span. The joint bending compliance then has a dominant effect on odd numbered modes (1, 3, . . .) and the joint shear compliance is exposed by even numbered modes (2, 4, . . .). Simple tests were performed during Phase 1 on tubular models to illustrate the basic test approach and to explore the effects of load path discontinuities. Actual missile joint hardware was employed in a series of four similar tests during the Phase 2 study, with data on two joint configurations being provided in a collaborative effort by Naval Weapon Center, China Lake personnel. One joint test of particular interest involved a shear joint with 18 radial screws. Joint compliance was evaluated parametrically as a function of number of fasteners, producing the surprisingly consistent and well ordered results shown in Figure 2-2. An exploratory generalization of this shear joint behavior is shown in Figure 2-3 with the cautionary comment that the derived compliance expression must be viewed with some skepticism since it considers only joint diameter and number of fasteners. Test data for two unrelated specimens are compared with the empirical compliance expression in the figure, however, and show better agreement than might be expected. The 8 fastener data point is taken from the 8-inch diameter shear joint tested at the Naval Weapons Center, China Lake and reported in the Phase 2 study. The 3 and 6 fastener data points are taken from the segmented tube test data in Phase 1 extrapolated to a "fastener" arc length of 2 degrees in order to correspond to the 1/4 inch bolts used with the 13.5 inch diameter data source.

The opportunity to test single joints in the "ideal" configuration is the exception rather than the rule, however, and more generally dynamic testing is performed on total airframes with many joints. The traditional approach consists of hand tuning compliance values to produce matching results between the mathematical model and measured mode shapes and frequencies. Since this is a laborious, time consuming, and often frustrating task, an automated and systematic approach is desirable. To these ends, an exploratory effort based on the optimization method of steepest descent was developed in Phase 1 of the study. This method of extracting joint compliance values from a set of measured missile elastic mode frequencies and shapes was shown to be feasible. However,

various limitations in the implemented method precluded full development. A more general approach developed by Hall, Calkin and Sholar, Reference 4, appeared in the literature and in Phase 2 their method was applied to the problem of extracting joint compliances. The result is a digital computer code. In Phase 3 refinements were added to the joint compliance extraction technique code to increase its utility and a user's manual was prepared for the code. Section 4 and the Appendix of the present report present the Phase 3 efforts on the joint compliance extraction technique.

Another important characteristic of missile airframe joints is that of self-induced vibration. This behavior is most usually associated with joint designs having inherently low interface preloads, and its presence can create unnecessarily severe environments in laboratory testing as well as in both captive and free-flight. Section 5 of this report describes an investigation of this phenomena covering both full scale and model exploratory testing.

The final section of this report, Section 6, illustrates a method of integrating the structural dynamic properties of joints with other important mechanical attributes that airframe joints must possess to meet overall system requirements.

FIGURE 2-1

FREQUENCY RATIO VS. JOINT STIFFNESS RATIO
UNIFORM BEAM - MIDSAN JOINT

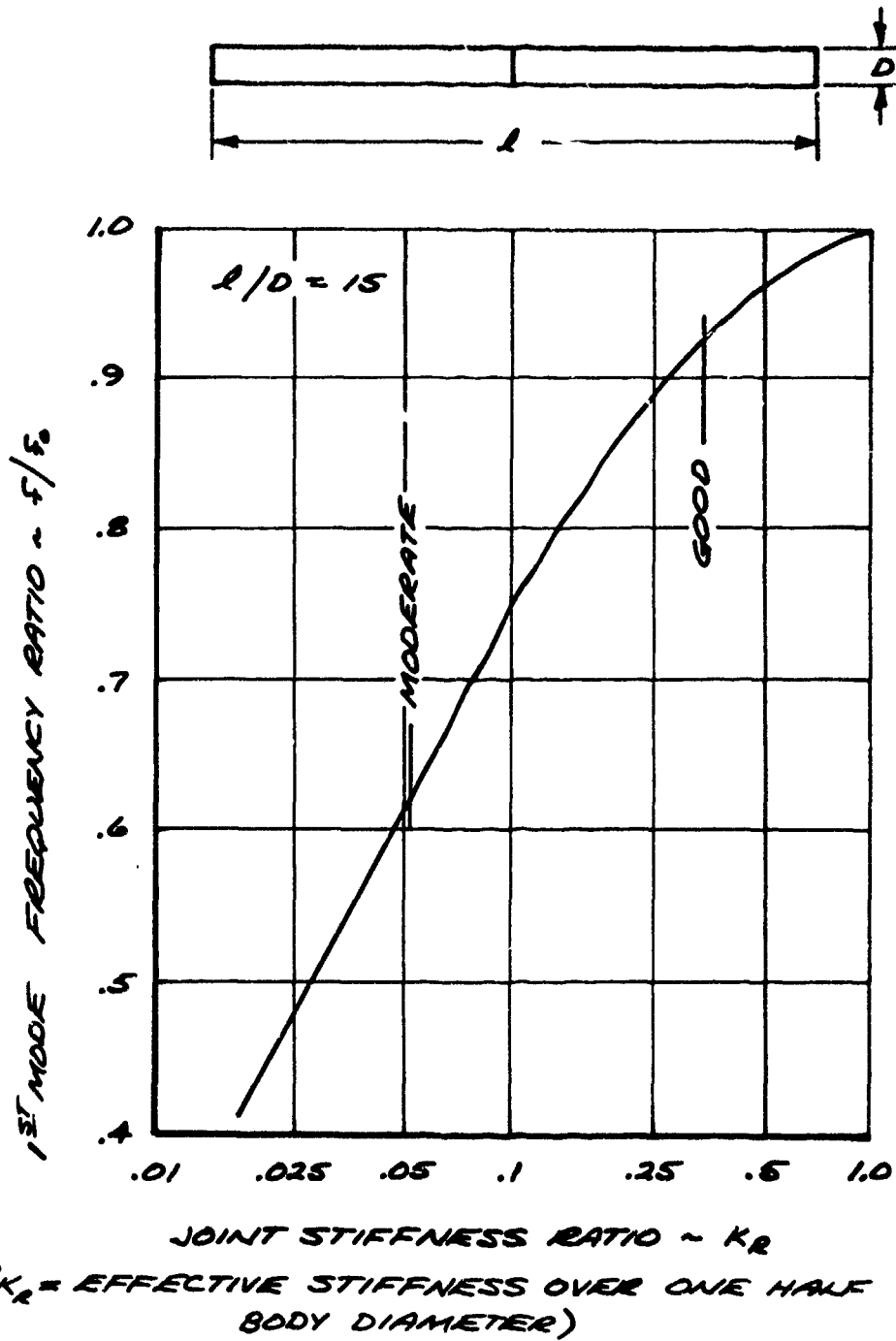


FIGURE 2-2

13.5 INCH DIAMETER SHEAR BOLT JOINT
FLEXURAL COMPLIANCE VS. NUMBER OF FASTENERS

$$C_0 = 12.71 (10)^{-8} / n^{1.404} \text{ RAD./IN.-LB.}$$

○ TEST DATA

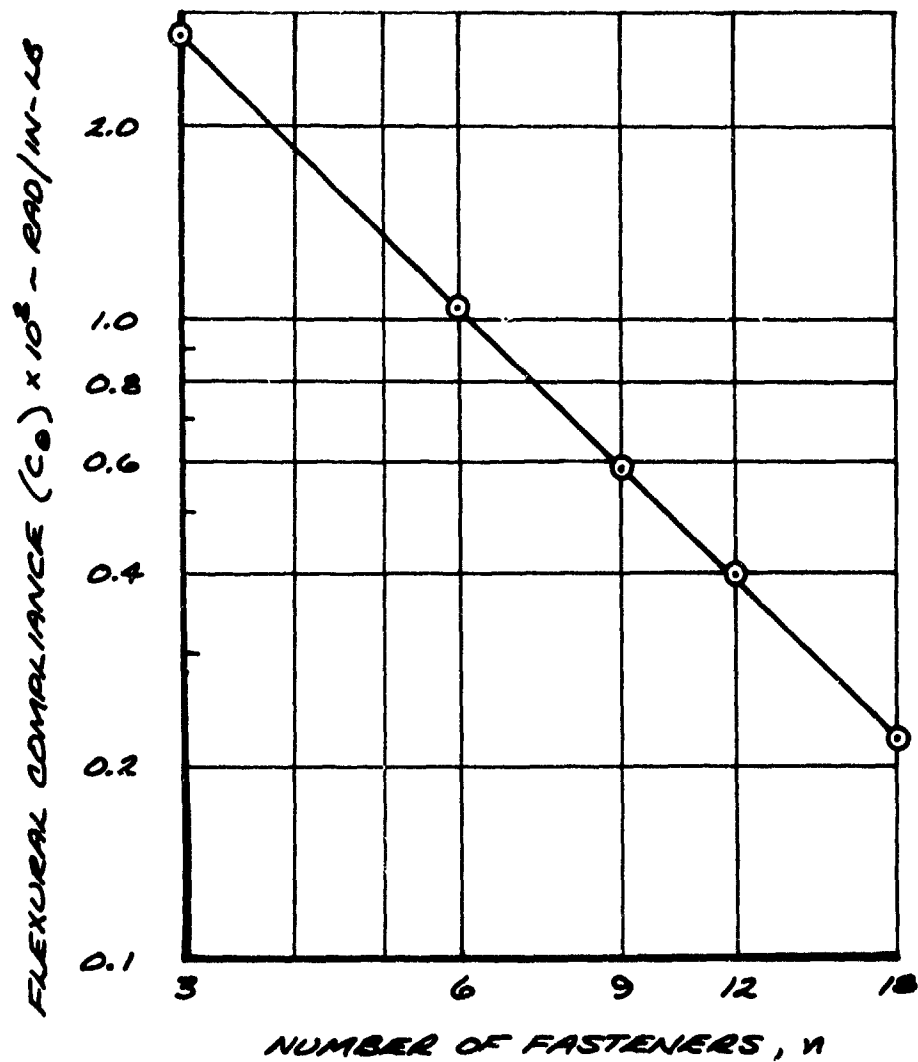
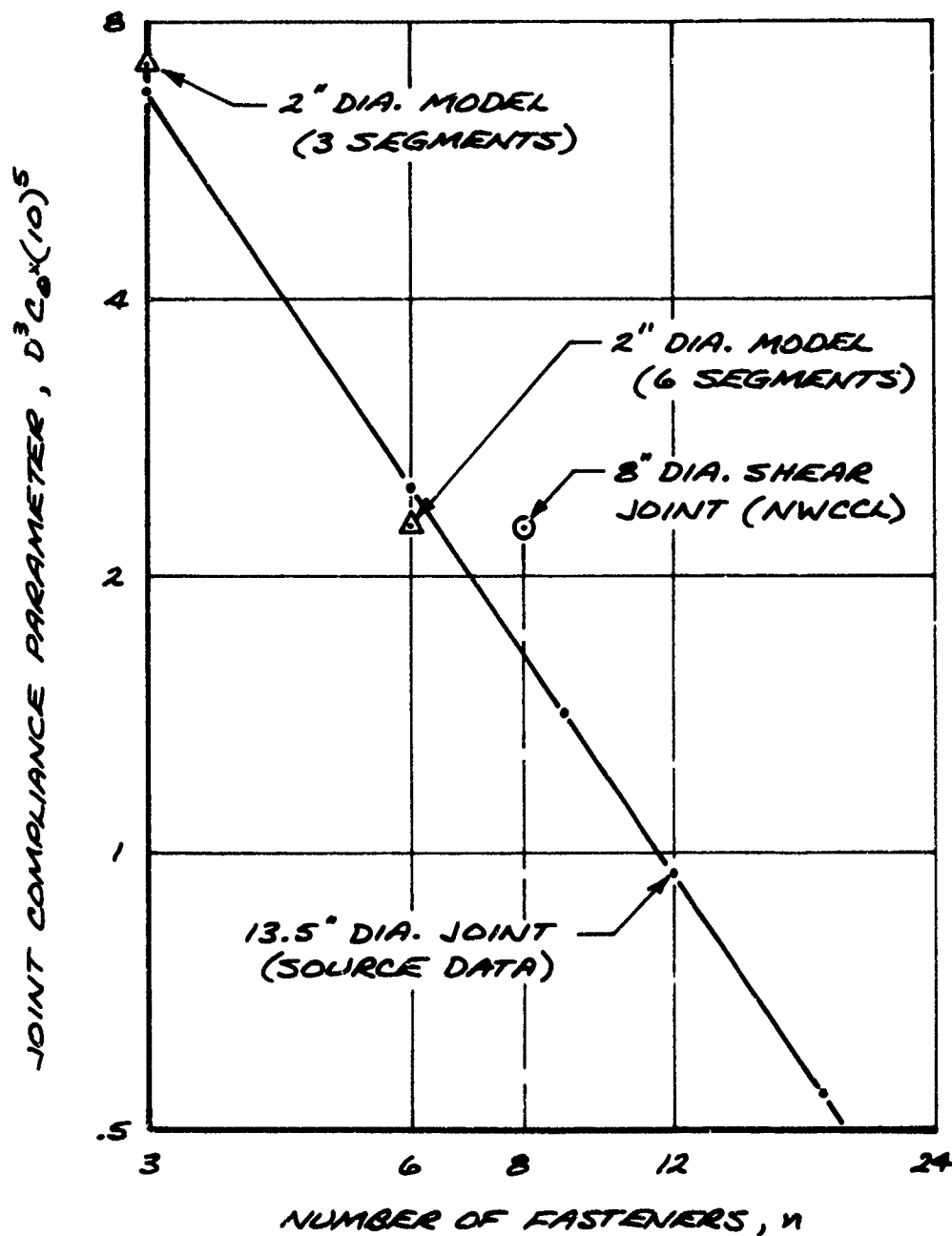


FIGURE 2-3
GENERALIZED SHEAR JOINT COMPLIANCE
VERSUS NUMBER OF FASTENERS

$$D^3 C_0 = 31.3 (10)^{-5} / n^{1.404}$$

WHERE D = JOINT DIA. IN INCHES

C_0 = COMPLIANCE, RAD./IN.-LB.



Reproduced from
best available copy.

Section 3.0

JOINT COMPLIANCE ANALYSIS

Finite element structural analysis methods have been shown in earlier study phases to offer considerable promise as means of predicting tactical missile mechanical joint properties. In the Phase 2 portion of the investigation a finite element type of analysis was performed on an eighteen fastener shear joint. The analysis made use of the NASTRAN computer program. The math model used described the structure on each side of the joint by means of a set of conical shell elements. Bolts were then described by discrete springs. Each spring constrains two corresponding points on each side of the joint. The solution process is based on a Fourier series expansion about the circumference. Thus forces and displacements are determined by summing a set of harmonic components. The compliance associated with various harmonics can be zero. The zero compliance harmonics are well defined for uniform bolt patterns. Thus for a joint with n bolts, the compliance associated with all harmonics are zero except for harmonics $0, 1, n-1, n+1, 2n-1, 2n+1, \dots$

In Phase 2 the problem was formulated and computations were performed entirely on NASTRAN. The cost per computer run was quite high even though only twelve harmonics were used. Two effects played a role in the high cost. If the structure was geometrically axisymmetric the stiffness matrix for each harmonic would be uncoupled from all others, however, due to the bolts the structure is asymmetric. Thus a coupling between harmonics results with a corresponding high computer solution time. The problem is aggravated to a considerable degree by the fact that the zero harmonics cannot be excluded from the solution process. Thus to solve this problem using say 50 harmonics is almost prohibitive.

On examining this problem it became apparent that it was not inherently expensive but rather due to limitations within the NASTRAN program. It also became apparent that a small efficient computer program could be written which used certain NASTRAN outputs. This was done as part of the Phase 3 finite element analysis effort.

The new computer program uses NASTRAN generated stiffness coefficients associated with each harmonic and the structure on each side of the joint.

3.1 PROBLEM FORMULATION

Consider two axisymmetric shells with a common axis of symmetry which are attached together with respect to a discrete set of points around the circumference as shown in Figure 3-1.

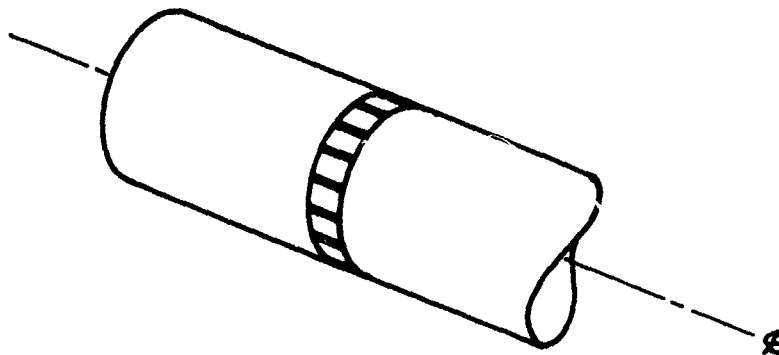


Figure 3-1. Sketch Showing Two Axisymmetric Shells Attached at a Discrete Set of Points

We require the attachments to be positioned so that they are symmetric with respect to a plane of symmetry which includes the missile longitudinal axis. The attachment forces do not act at points but rather over a small area defined by the thickness of the shell and an arc length defined by the enclosed angle ϵ as shown in Figure 3-2.

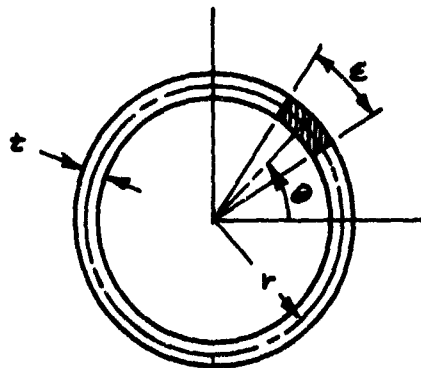


Figure 3-2. Area Over Which Bolt Acts as Defined in Math Model

Also the distribution of the load over the area is taken as uniform. Let P be the resultant bolt force acting on the area. The stress $\sigma(\theta)$ can then be expanded into a cosine series in the form

$$\sigma(\theta) = \frac{1}{t} \sum a_n \cos n\theta \quad (3.1)$$

On doing so we obtain

$$\sigma(\theta) = \frac{2p}{tE} \sum_{n=1}^{\infty} \frac{\sin(nE/2)}{n} \cos(n\theta) \quad (3.2)$$

or

$$a_n = \frac{2p}{nE} \sin(nE/2) \quad (3.3)$$

The use of the cosine series imposes the requirement that the horizontal plane be a plane of symmetry. The quantity $t\sigma(\theta)$ has units of load per unit arc length. The quantity $f(\theta) = t\sigma(\theta)$ can be expressed in the form

$$f(\theta) = f_1 \cos(\theta) + f_2 \cos(2\theta) + f_3 \cos(3\theta) + \dots \quad (3.4)$$

where

$$f_n = \frac{2p}{nE} \sin(nE/2) \quad (3.5)$$

It can be interpreted as a generalized force associated with the n th harmonic. Let f_{ni} be the generalized force associated with the n th harmonic and the i th bolt. Let the joint have b bolts and let p_i be the force resultant for the i th bolt acting at θ_i . Then the harmonic generalized forces f_n associated with the set of bolts used on the joint are

$$f_n = \sum_{i=1}^b f_{ni} = \sum_{i=1}^b \frac{2p_i}{nE} \sin(nE/2) \cos(n\theta_i) \quad (3.6)$$

Let us define a matrix with elements a_{ij}

$$a_{ij} = \frac{2}{iE} \sin(iE/2) \cos(n\theta_j) \quad (3.7)$$

Let f_i and p_i respectively be elements of column vectors $\{f_i\}$ and $\{p_i\}$. Then from (3.6) and (3.7) one can see that the following relationship holds

$$\{f_i\} = [a_{ij}] \{p_j\} \quad (3.8)$$

Let $[S_{ij}]$ be a diagonal matrix where element S_{ij} is a spring stiffness constant associated with the i th bolt and let $\{v_j\}$ be a column matrix associated with bolt elongations. Then the following relationship holds.

$$\{p_j\} = [S_{jk}] \{v_k\} \quad (3.9)$$

If we could assign a point on the circumference to each bolt then bolt elongation could be expressed by a set of generalized displacements u_n as follows:

$$v_i = \sum_{n=1}^{\infty} u_n \cos(n\theta_i) \quad (3.10)$$

Since the bolt load is associated with an area as shown in Figure 3-2 we cannot associate the bolt displacement with only one point. We will give an indirect definition which will implicitly contain an averaging over this area. Let the problem be limited to m harmonics and let $[c_{ij}]$ be an m by b matrix which relates bolt elongations $\{v_i\}$ to generalized harmonic displacements $\{u_j\}$ as follows

$$\{v_i\} = [c_{ij}] \{u_j\} \quad (3.11)$$

Then virtual bolt elongations $\{\delta v_i\}$ and virtual generalized displacements $\{\delta u_j\}$ are related by

$$\{\delta v_i\} = [c_{ij}] \{\delta u_j\} \quad (3.12)$$

We require the following to hold

$$\{p_i\}^T \{\delta v_i\} = \{f_j\}^T \{\delta u_j\} \quad (3.13)$$

That is, we require the virtual work associated with virtual elongation $\{\delta v_i\}$ to be equal to the virtual work associated with the corresponding generalized variables. On substituting from (3.8) and (3.12) into (3.13) we obtain

$$\{P_i\}^T [c_{ij}] \{\delta u_j\} = \{P_i\}^T [a_{ij}]^T \{\delta u_j\} \quad (3.14)$$

Equation (3.14) can hold for all virtual displacements $\{\delta u_j\}$ and all loads $\{P_i\}$ if and only if

$$[c_{ij}] = [a_{ij}]^T \quad (3.15)$$

Therefore from (3.7) and (3.15) it follows that

$$c_{ij} = \frac{2}{jE} \sin\left(\frac{jE}{2}\right) \cos(n\theta_i) \quad (3.16)$$

From (3.8), (3.9), (3.11), and (3.15) it follows that

$$\begin{aligned} \{f_i\} &= [a_{ij}] \{P_j\} \\ &= [a_{ij}] [S_{jk}] \{v_k\} \\ &= [a_{ij}] [S_{jk}] [a_{kl}]^T \{u_l\} \end{aligned} \quad (3.17)$$

Let

$$[\bar{S}_{il}] = [a_{ij}] [S_{jk}] [a_{kl}]^T \quad (3.18)$$

Thus $[\bar{S}_{il}]$ is a stiffness matrix which describes the stiffness of the set of joint bolts with respect to the generalized (harmonic) variables $\{f_i\}$ and $\{u_l\}$. Then (3.17) has the form

$$\{f_i\} = [\bar{S}_{ij}] \{u_j\} \quad (3.19)$$

We will now define the variables associated with the axisymmetric structures on each side of the joint. These structures will be interpreted as two free structures whose relative displacements are constrained by the bolt attachments. We will assume that there is no relative radial or circumferential motion across the joint. Since the two structures are unconstrained except by the joint it follows that the zero and first

harmonics of longitudinal relative displacements are respectively associated with relative longitudinal translation and pitch rigid body motions. The higher harmonics on the other hand are associated with shell deformation.

Using NASTRAN we can compute the displacement u_n associated with each higher harmonic load f_n acting on the joint. We can then compute two sets of stiffness coefficients associated with each of the structures as follows:

$$\begin{aligned} \kappa'_{ii} &= \frac{f_i'}{u_i'} \\ \kappa''_{ii} &= \frac{f_i''}{u_i''} \end{aligned} \quad (3.20)$$

where the single and double primes are used to distinguish the two structures. From the above discussion it follows that

$$\kappa'_{ii} = \kappa''_{ii} = 0 \quad (3.21)$$

The joint displacements can be described by relative generalized (harmonic) displacement parameters $\{u_i\}$ described earlier. They are related to the harmonic displacement parameters for the two structures as follows:

$$u_i = u_i' - u_i'' \quad (3.22)$$

Then from (3.17) and (3.19) it follows that

$$u_i = \frac{f_i'}{\kappa'_{ii}} - \frac{f_i''}{\kappa''_{ii}} \quad (3.23)$$

This is a consequence of the orthogonality of the set of cosine functions. Similarly joint equilibrium and harmonic function orthogonality requires

$$f_i' = -f_i'' = f_i \quad (3.24)$$

where f_i indicates that the prime will not be required below. Substituting (3.24) into (3.23) and simplifying we obtain

$$u_i = \left(\frac{K_{ii}' + K_{ii}''}{K_{ii}' K_{ii}''} \right) f_i \quad (3.25)$$

or

$$f_i = K_{ii} u_i \quad (3.26)$$

where

$$K_{ii} = \frac{K_{ii}' K_{ii}''}{K_{ii}' + K_{ii}''} \quad (3.27)$$

The parameters K_{ii} describe the effective stiffness associated with the set of harmonics for the axisymmetric structure on both sides of the joint. Let $[K_{ij}]$ be a diagonal matrix with diagonal elements K_{ii} . Then (3.26) can be expressed in the following matrix form

$$\{f_i\} = [K_{ij}] \{u_j\} \quad (3.28)$$

Note that

$$K_{ii} = 0 \quad (3.29)$$

Partition equation (3.19) and (3.28) as follows

$$\begin{Bmatrix} f_i \\ \{f_i\}_2 \end{Bmatrix} = \begin{bmatrix} \bar{S}_{ii} & [\bar{S}_{ij}]_{12} \\ [\bar{S}_{ij}]_{21} & [\bar{S}_{ij}]_{22} \end{bmatrix} \begin{Bmatrix} u_i \\ \{u_j\}_2 \end{Bmatrix} \quad (3.30)$$

$$\begin{Bmatrix} f_i \\ \{f_i\}_2 \end{Bmatrix} = \begin{bmatrix} 0 & 0 \\ 0 & [K_{ij}]_{22} \end{bmatrix} \begin{Bmatrix} u_i \\ \{u_j\}_2 \end{Bmatrix} \quad (3.31)$$

From (3.30) and (3.31) we obtain

$$f_i = \bar{S}_{ii} u_i + [\bar{S}_{ij}]_{12} \{u_j\}_2 \quad (3.32)$$

$$\{f_i\}_2 = [\bar{S}_{ij}]_{21} u_1 + [\bar{S}_{ij}]_{22} \{u_j\}_2 \quad (3.33)$$

$$\{f_i\}_2 = [\kappa_{ij}]_{22} \{u_j\}_2 \quad (3.34)$$

From (3.33) and (3.34) we obtain

$$\{u_j\}_2 = \left[[\kappa_{ij}]_{22} - [\bar{S}_{ij}]_{22} \right]^{-1} [\bar{S}_{jk}]_{21} u_1 \quad (3.35)$$

On substituting (3.35) into (3.32) we obtain

$$f_1 = \left(\bar{S}_{11} + [\bar{S}_{ij}]_{12} \left[[\kappa_{jk}]_{22} - [\bar{S}_{jk}]_{22} \right]^{-1} [\bar{S}_{kj}]_{21} \right) u_1 \quad (3.36)$$

Let A_{11} equal the quantity in brackets. Then (3.36) has the form

$$f_1 = A_{11} u_1 \quad (3.37)$$

The parameter u_1 is a measure of the maximum relative displacement around the circumference. We wish to relate the joint stiffness to more common parameters M and ϕ which correspond to joint bending moment and joint relative rotation. Now u_1 and ϕ are related by

$$u_1 = r \phi \quad (3.38)$$

where r is defined in Figure 3-2. We will define the relationship between M and f_1 by requiring that the following hold for all virtual displacements δu_1 and $\delta \phi$.

$$M \delta \phi = f_1 \delta u_1 \quad (3.39)$$

On substituting (3.38) into (3.39) we obtain

$$M \delta \phi = f r \delta \phi \quad (3.40)$$

For the above to hold for all virtual changes it follows that

$$M = r f \quad (3.41)$$

On substituting (3.38) into (3.37) and the resultant into (3.41) we obtain

$$M = r^2 A_{ii} \phi \quad (3.42)$$

The equivalent joint stiffness designated by H is related by

$$H = r^2 \left(\bar{S}_{ii} + [\bar{S}_{ij}]_{i2} \left[[K_{jk}]_{22} - [\bar{S}_{jk}]_{22} \right]^{-1} [\bar{S}_{kl}]_{2i} \right) \quad (3.43)$$

3.2 TEST CASE AND RESULTS

A computer program which can compute the effective joint stiffness as described above was written. The structural configuration used in the Phase 2 study was used in this study since comparative test data were available. Figure 3-3 describes the joint and Figure 3-4 describes the finite element model of shell elements used in all the NASTRAN analyses.

The NASTRAN computer program was used to compute the longitudinal harmonic stiffness coefficient designated by K'_{ii} and K''_{ii} for the first 108 harmonics. These stiffness coefficients are given in Table 3-1 and a log-log plot of the stiffness coefficient versus harmonic number is given in Figure 3-5.

As can be seen from Figure 3-5 the value of stiffness appears to approach a straight line for higher values of harmonic number. A straight line on a log-log plot implies the following continuous function relationship

$$\frac{K}{K_1} = \left(\frac{n}{n_1} \right)^\alpha \quad (3.44)$$

where K is the dependent stiffness variable, n is the independent harmonic number variable, (K_1, n_1) is a point on the line and α is a coefficient related by

$$\alpha = \frac{\log\left(\frac{K_2}{K_1}\right)}{\log\left(\frac{n_2}{n_1}\right)} \quad (3.45)$$

where (K_2, n_2) is a point on the line. For the two lines in Figure 3-5 associated with the two structures connected by the joint, the data used to compute higher harmonic stiffness coefficients are given in Table 3-2.

Table 3-2

Data Used in Equation (3.44) to Compute Stiffness Coefficients for Harmonics Greater than 108

	Structure 1	Structure 2
K_1	1.57×10^7	4.35×10^7
K_2	3.32×10^8	9.90×10^8
n_1	10	10
n_2	100	100

As pointed out earlier many harmonics do not influence the computation. Table 3-3 shows the harmonics which influence the computations as a function of number of fasteners.

Each bolt has an effective arc length over which it acts. As noted earlier this arc length is defined by the enclosed angle ϵ . Let us define the quantity R as the ratio of ϵ over the angle subtended by the bolt. The R can be interpreted as the effective number of bolt diameters over which the bolt load distributes at the joint.

The larger the value of R the higher the joint stiffness will be. To establish correct values of R computed values of stiffness were compared to measured results obtained in the Phase 2 study. Table 3-4 summarizes the Phase 2 measured values of stiffness.

Table 3-4

Phase 2 Measured Values of Stiffness for Various Numbers of Fasteners ($\times 10^8$ Inch Pounds per Radian)

Number of Fasteners	Stiffness
3	0.358
6	0.971
9	1.680
12	2.575 (interpolated)
18	4.440

Table 3-5 gives computed values of joint stiffness for the three fastener joint, for various values of R and for different values of the highest harmonic used in the calculations. The value of R equal to 6.24 gives results which are almost equal to the measured values. Table 3-6 shows results for 3, 6, 9 and 18 fastener cases using R equal to 6.24. Although the results match the experimental values for the three fastener case, they are quite in error for the 18 fastener case. The compliances of the 18 fastener case for various values of R are given in Table 3-7. As can be seen a value of R close to 1.5 is required if the 18 fastener case is to match measured results. Using a linear interpolation between the compliance values for R equal to 1.5 and 2.0 we conclude that a value of R equal to 1.544 will give a value very close to the measured compliance. Table 3-8 gives results for R equal to 1.544. Since R equal to 6.24 gives correct values for the 3 fastener case and R equal to 1.544 gives correct values for the 18 fastener case, we used a linear interpolation to establish values of R for the 6, 9 and 12 fastener case. Computed joint stiffness for these cases are given in Table 3-9. Figure 3-6 gives curves of stiffness versus number of fasteners of the measured results and of the computed results for R equal to 1.544 and 6.24.

As can be seen from the results described above there does not appear to be a simple way of describing bolt shell interaction. For the joint in question one shell surface overlaps the other and the bolt load acts on the two contacting surfaces. The above results imply that the fewer the bolts the more compliant the joint but the larger the effective contact area between the shells becomes. The results suggest that a more detailed analytical description of the bolt area is required.

Figure 3-7 shows the curve of joint stiffness versus R for the three fastener case. A dashed straight line referred to as the "reference line" is also shown in this figure. Before continuing our discussion of this curve note Figure 3-8 which shows curves of stiffness versus highest harmonic used in the computation for various values of R . In essence these curves show the way in which the cosine series converges. Note that the cosine series converges slower for smaller values of R and that all curves are monotonically decreasing. Now re-examine Figure 3-7. The separation of the curve for low values of R can partly be explained by the slow convergence, i.e., the values shown for the lower values of R are somewhat separated from the values at the point of convergence. The separation from the reference line associated with higher values of R can be explained in a different way. The assumption was made in the derivation that the load distribution along the arc length associated with the bolt load is uniform. This does not introduce very much error for small R however for large R the error is significant.

3.3 CONCLUSIONS

The analysis described here was motivated by the fact that comparable analyses performed using the NASTRAN computer program would have been prohibitive. A joint stiffness analysis performed entirely on NASTRAN during the Phase 2 study cost approximately \$300.00 per run for a case which used 12 harmonics. In the present analysis the determination of K' and K'' were made once for 109 harmonics using NASTRAN at a cost of \$2000.00 and all subsequent runs cost from \$0.10 to \$0.30. The relatively high cost in generating the K 's motivated use of formulas (3.44) for generating higher K values.

One of the problems with using NASTRAN to solve the complete problem is that one would have to use all the harmonics up to the highest one used. One could not exclude harmonics. Thus a run using the present method which used up to harmonic number 400 and costing \$0.30 would have cost in excess of \$5000.00 if done directly on NASTRAN. In the present study over 100 runs were made at a modest cost.

An unexpected problem was the one associated with selecting an appropriate bolt load distribution parameter (R). The effective load path area for each fastener in the shear bolt joint analyzed appears to decrease as the number of fasteners increases. It should be noted, however, that joint compliance estimates within 10 to 20 percent will in most cases be more than adequate for missile modal analysis purposes. Accuracy in compliance estimates is more important for compliant joints which have a greater influence on airframe modal characteristics than for stiff joints which have little effect on airframe response characteristics.

A useful effort which was not attempted in this study would be to develop a simple expression for estimating K_1 , n_1 , and α used in equation (3.44). Such an expression would allow the determination of joint compliance for shells of revolution.

TABLE 3-1 NASTRAN Computed Stiffness Coefficients for the Structure on
Each Side of the Joint for 108 Harmonics (amts x 10⁸ pounds per inch)

	Structure 1	Structure 2		Structure 1	Structure 2		Structure 1	Structure 2
1	0.04291	0.06538	37	0.95935	2.66935	73	2.12083	6.30799
2	0.04239	0.08109	38	0.98724	2.75904	74	2.15987	6.42760
3	0.04219	0.11913	39	1.01513	2.84877	75	2.19932	6.54837
4	0.04415	0.06769	40	1.04307	2.93862	76	2.23918	6.67031
5	0.05090	0.21266	41	1.07109	3.02867	77	2.27945	6.79342
6	0.06247	0.24588	42	1.09974	3.11901	78	2.32014	6.91770
7	0.07684	0.48946	43	1.12753	3.20969	79	2.36125	7.04316
8	0.08313	0.30330	44	1.15600	3.30079	80	2.40277	7.16979
9	0.11140	0.33731	45	1.18467	3.39238	81	2.44471	7.29760
10	0.13189	0.37756	46	1.21356	3.48451	82	2.48706	7.42659
11	0.15477	0.42459	47	1.24271	3.57724	83	2.52984	7.55677
12	0.18000	0.47815	48	1.27211	3.67062	84	2.57303	7.68813
13	0.20748	0.53858	49	1.30180	3.76470	85	2.61664	7.82067
14	0.23698	0.60538	50	1.33178	3.85953	86	2.66068	7.95439
15	0.26821	0.67771	51	1.36207	3.95515	87	2.70513	8.08928
16	0.33244	0.75520	52	1.39268	4.05158	88	2.75000	8.22535
17	0.33442	0.83705	53	1.42362	4.14888	89	2.79530	8.36258
18	0.36869	0.92249	54	1.45490	4.24706	90	2.84102	8.50097
19	0.40330	1.01082	55	1.48653	4.34616	91	2.88716	8.64049
20	0.43800	1.10136	56	1.51851	4.44621	92	2.93373	8.78115
21	0.47251	1.19358	57	1.55085	4.54722	93	2.98072	8.92287
22	0.50669	1.28663	58	1.58356	4.64922	94	3.02810	9.06563
23	0.54040	1.38028	59	1.61664	4.75223	95	3.07597	9.20931
24	0.57356	1.47360	60	1.65010	4.85627	96	3.12423	9.35370
25	0.60612	1.57804	61	1.68394	4.96135	97	3.17292	9.49853
26	0.63806	1.66562	62	1.71816	5.06749	98	3.22203	9.64273
27	0.66940	1.75835	63	1.75278	5.17471	99	3.27157	9.78316
28	0.70015	1.85126	64	1.78778	5.04321	100	3.32153	9.89900
29	0.73036	1.94382	65	1.82318	5.39240	101	3.37193	10.26364
30	0.76009	2.03090	66	1.85898	5.50289	102	3.42274	10.29839
31	0.78938	2.12750	67	1.89517	5.61450	103	3.47399	10.43826
32	0.81829	2.21863	68	1.93102	5.72724	104	3.52566	10.58834
33	0.84690	2.30934	69	1.96877	5.84112	105	3.57776	10.74234
34	0.70160	2.39970	70	2.00617	5.95611	106	3.63029	10.89874
35	0.90340	2.48976	71	2.04398	6.07225	107	3.68329	11.05698
36	0.93142	2.57962	72	2.08220	6.18955	108	3.73663	11.21680

**TABLE 3-3 Harmonics Having Non Zero Stiffness
Coefficients for the Various Fastener
Arrangements**

Number Of Fasteners									
3		6		9		12		18	
2	40	5	79	8	118	11	157	17	235
4	41	7	83	10	125	13	167	19	251
5	43	11	85	17	127	23	169	35	253
7	44	13	89	19	134	25	179	37	269
8	46	17	91	26	136	35	181	53	271
10	47	19	95	28	143	37	191	55	287
11	49	23	97	35	145	47	193	71	289
13	50	25	101	37	152	49	203	73	305
14	52	29	103	44	154	59	205	89	307
16	53	31	107	46	161	61	215	91	323
17	55	35	109	53	163	71	217	107	325
19	56	37	113	55	170	73	227	109	341
20	58	41	115	62	172	83	229	125	345
22	59	43	119	64	179	85	239	127	359
23	61	47	121	71	181	95	241	143	361
25	62	49	125	73	188	97	251	145	377
26	64	53	127	80	190	107	253	161	379
28	65	55	131	82	197	109	263	163	395
29	67	59	133	89	199	119	265	179	397
31	68	61	137	91	206	121	275	181	413
32	70	65	139	98	208	131	277	197	415
34	71	67	143	100	215	133	287	199	431
35	73	71	145	107	217	143	289	215	433
37	74	73	149	109	224	145	299	217	449
38	76	77	151	116	226	155	301	233	451

TABLE 3-5 Computed Joint Stiffness for Three Fasteners and Various
Values of the Ratio of ϵ over the Bolt Diameter Enclosed
Angle ($\times 10^7$ inch pound per radian)

Highest Harmonic	R (Values of ϵ Over Bolt Diameter Enclosed Angle)						
	$\frac{1}{2}$	1	3	5	6	6.2	10
1	10388.0	10387.0	10378.0	10359.0	10345.0	10342.7	10342.2
3	12.6700	12.6730	12.7050	12.7760	12.8372	12.8372	12.8851
6	5.1253	5.1308	5.1905	5.3076	5.3955	5.4142	5.4183
9	3.8632	3.8708	3.9532	4.1160	4.2386	4.2347	4.2703
12	3.3277	3.3374	3.4449	3.6567	3.8157	3.8496	3.8567
15	3.0494	3.0618	3.1941	3.4531	3.6449	3.6855	3.6941
18	2.8862	2.9009	3.0572	3.3584	3.5769	3.6225	3.6321
36	2.4698	2.5013	2.8092	3.2721	3.5359	3.5865	3.5971
64	2.2466	2.3132	2.7897	3.2592	3.5231	3.5741	3.5848
							4.6497
							4.6893
							4.6884
							4.6369
							4.6497

Table 3-6
 Computed Equivalent Joint Stiffness ($\times 10^8$ inch pound per radian)
 for 3, 6, 9, 18 Fasteners. All Computations Use 6.24 for the
 Value of ϵ Over the Bolt Diameter Enclosed Angle

Highest Harmonic	3	6	9	18
1	1034.22	2068.40	3102.62	6205.2
3	1.28851	- -	- -	- -
6	.54183	2.0828	- -	- -
9	.42703	- -	4.3292	- -
12	.38567	1.1690	- -	- -
15	.36941	- -	- -	- -
18	.36321	1.0632	2.5469	48.734
36	.35971	1.0470	2.4721	31.067
54	- -	- -	2.4547	29.7569
64	.35848	- -	- -	- -
72	- -	1.0412	2.4509	29.589
109	- -	1.0406	2.4486	29.356

Table 3-7
Computed Joint Stiffness for Eighteen Fasteners
and Various Values of the Ratio of ϵ over the
Bolt Diameter Enclosed Angle ($\times 10^8$ inch pounds
per radian)

Highest Harmonic	Values of ϵ Over Bolt Diameter Enclosed Angle			
	0.5	1.0	1.5	2.0
1	6232.9	6232.0	6230.2	6230.2
17	10.9580	11.2330	-	-
35	5.0374	5.2411	-	-
53	4.0392	4.3071	-	-
71	3.5954	3.9403	-	-
109	3.1513	3.6822	-	-
181	2.9575	-	4.4163	5.2684
253	2.9178	-	4.4128	5.2620
325	2.9140	-	4.4092	5.2597

Table 3-8
 Computed and Measured Equivalent Joint Stiffness
 (x 108 Inch Pounds per Radian) for 3, 6, 9, 12,
 and 18 Fasteners. All computations use 1.544 for
 the value of R.

Number of Fasteners	Highest Harmonic Number	Computed Joint Stiffness	Measured Joint Stiffness
3	55	.2445	.358
6	109	.6089	.971
9	163	1.163	1.680
12	217	1.962	2.573*
18	325	4.480	4.440

*Interpolated

Table 3-9
Computed Equivalent Joint Stiffness
($\times 10^8$ Inch Pounds per Radian)

Number of Fasteners	Highest Harmonic Number	R	Computed Stiffness	Test Data
3	55	6.240	0.3585	0.358
6	109	5.301	0.9430	0.971
9	163	4.361	1.8306	1.680
12	217	3.422	2.9524	2.573*
18	325	1.544	4.4798	4.440

*Interpolated

FIGURE 3-3
SHEAR BOLT JOINT
TEST SPECIMEN AND SECTION MODELED USING FINITE ELEMENTS

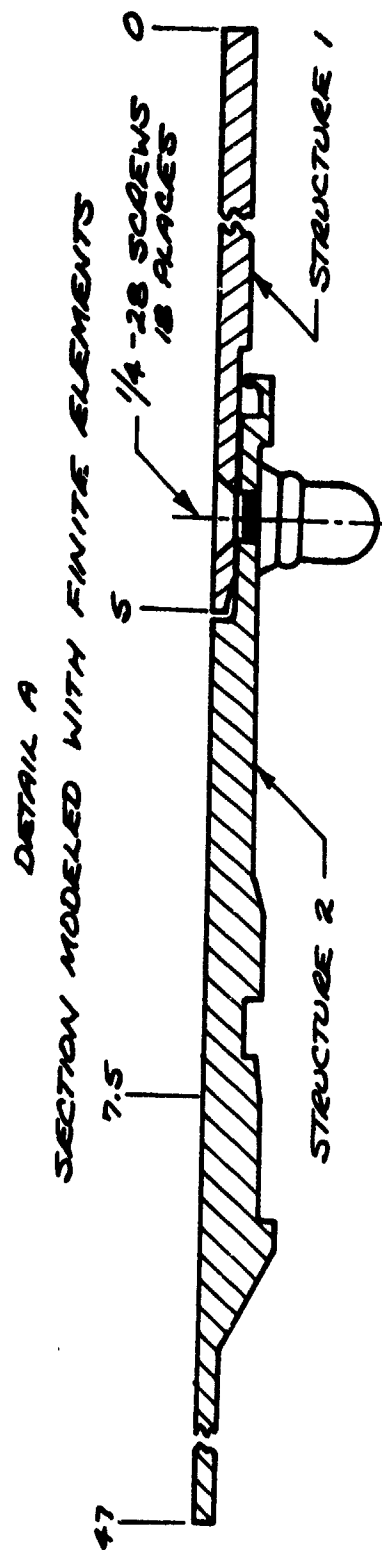
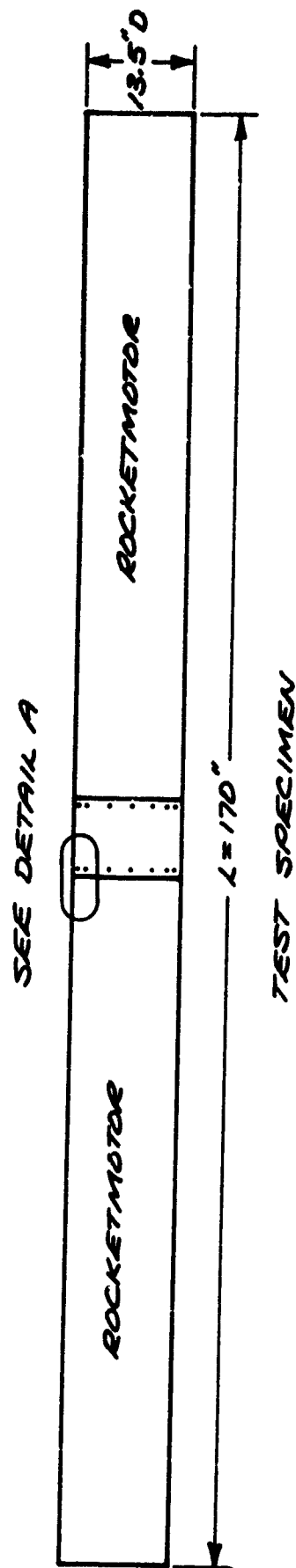
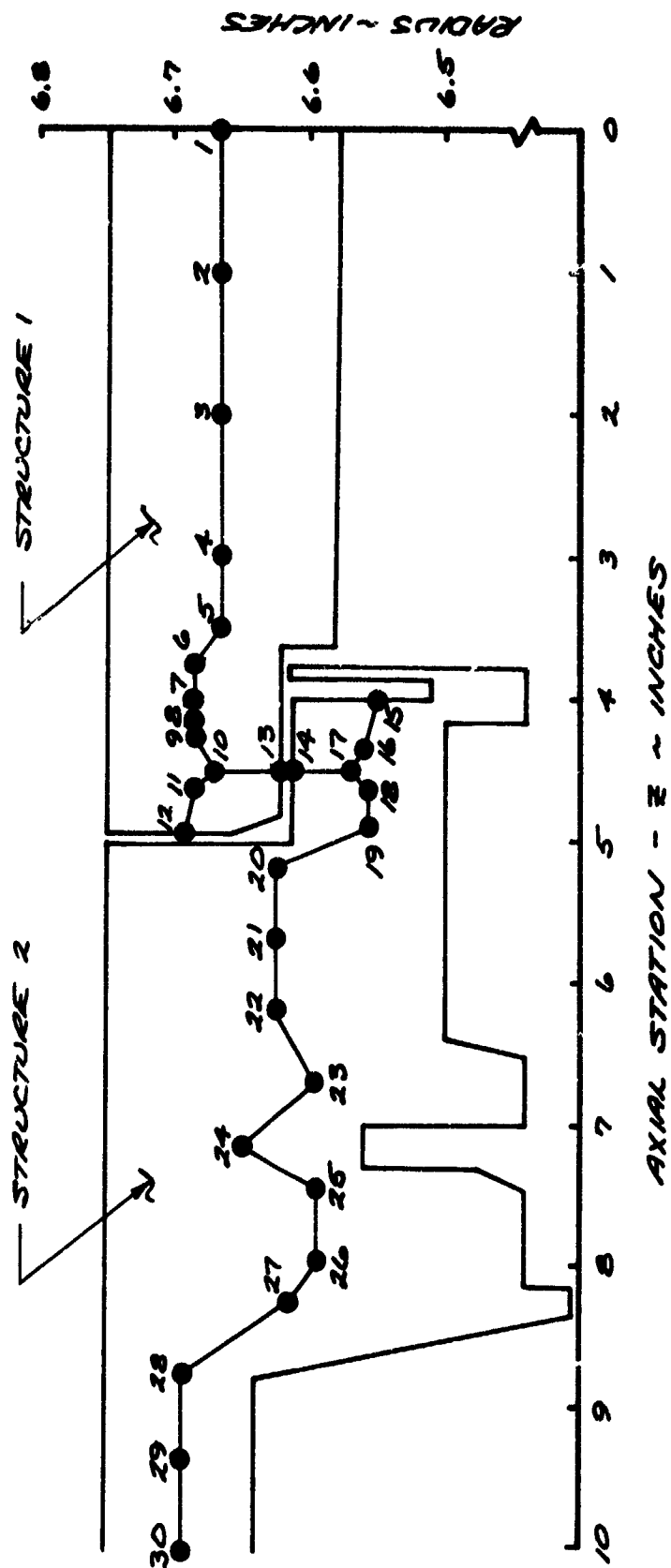


FIGURE 3-4
SHELL ELEMENT MODEL IN THE REGION OF THE
SHEAR BOLT JOINT



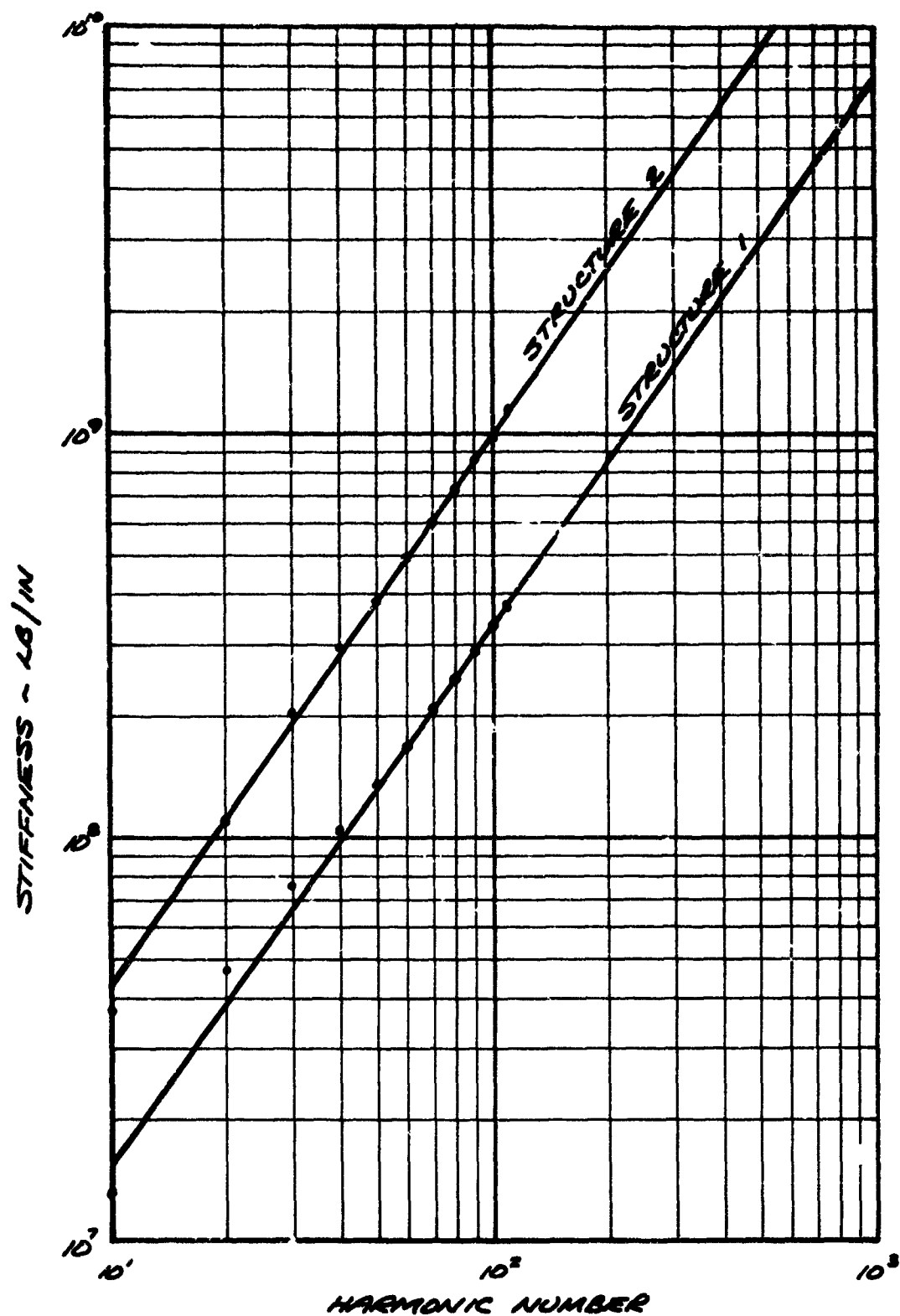


FIGURE 3-5 LOG-LOG PLOTS OF NASTRAN COMPUTED STIFFNESS COEFFICIENTS VERSUS HARMONIC NUMBER FOR THE TWO STRUCTURES

FIGURE 3-6

CURVE OF STIFFNESS VERSUS NUMBER OF FASTENERS
FOR $R = 1.544$, $R = 6.24$ AND MEASURED RESULTS

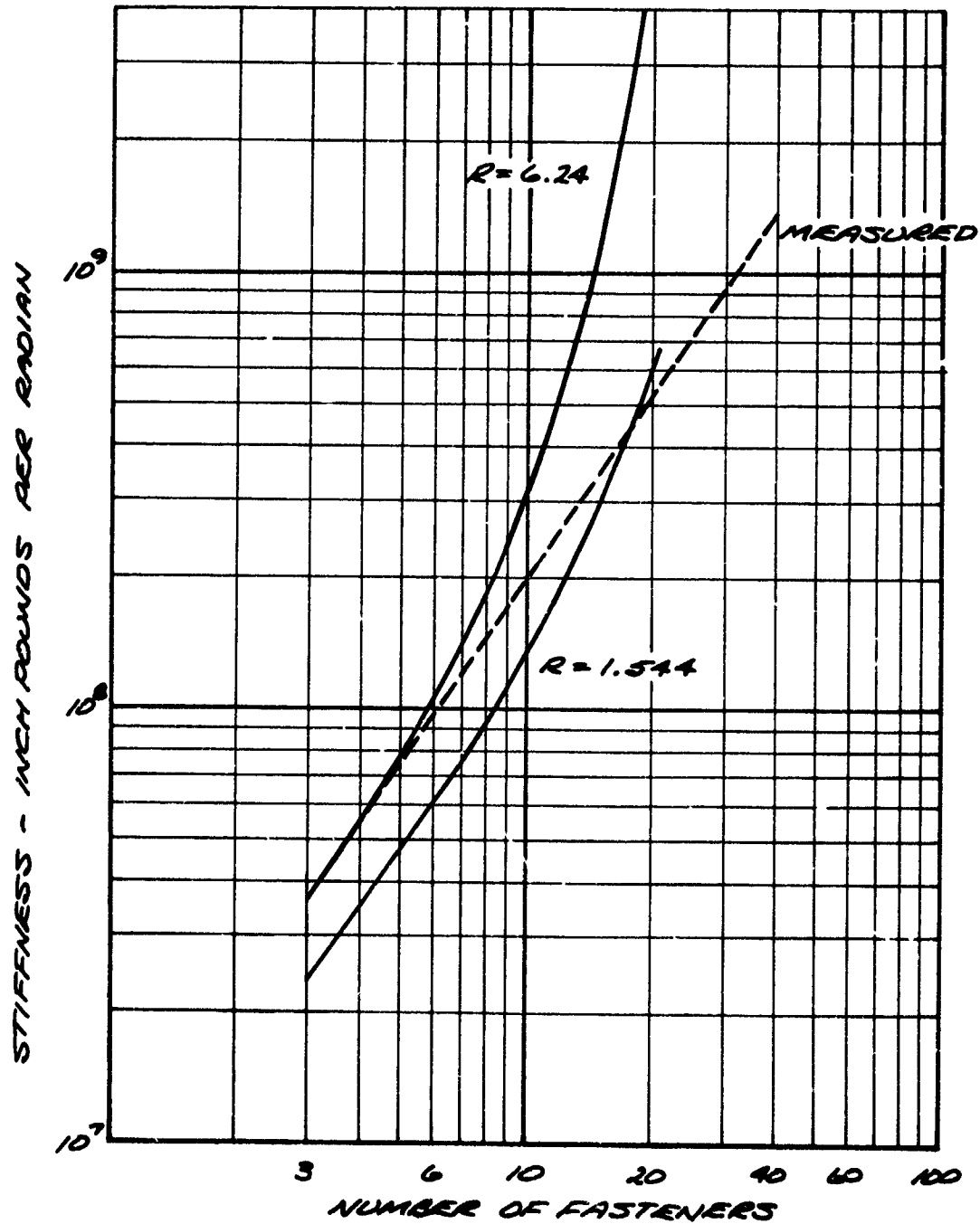


FIGURE 3-7

CURVE OF JOINT STIFFNESS VERSUS R (RATIO OF E OVER THE BOLT DIAMETER ENCLOSED ANGLE) FOR THE THREE FASTENER CASE.

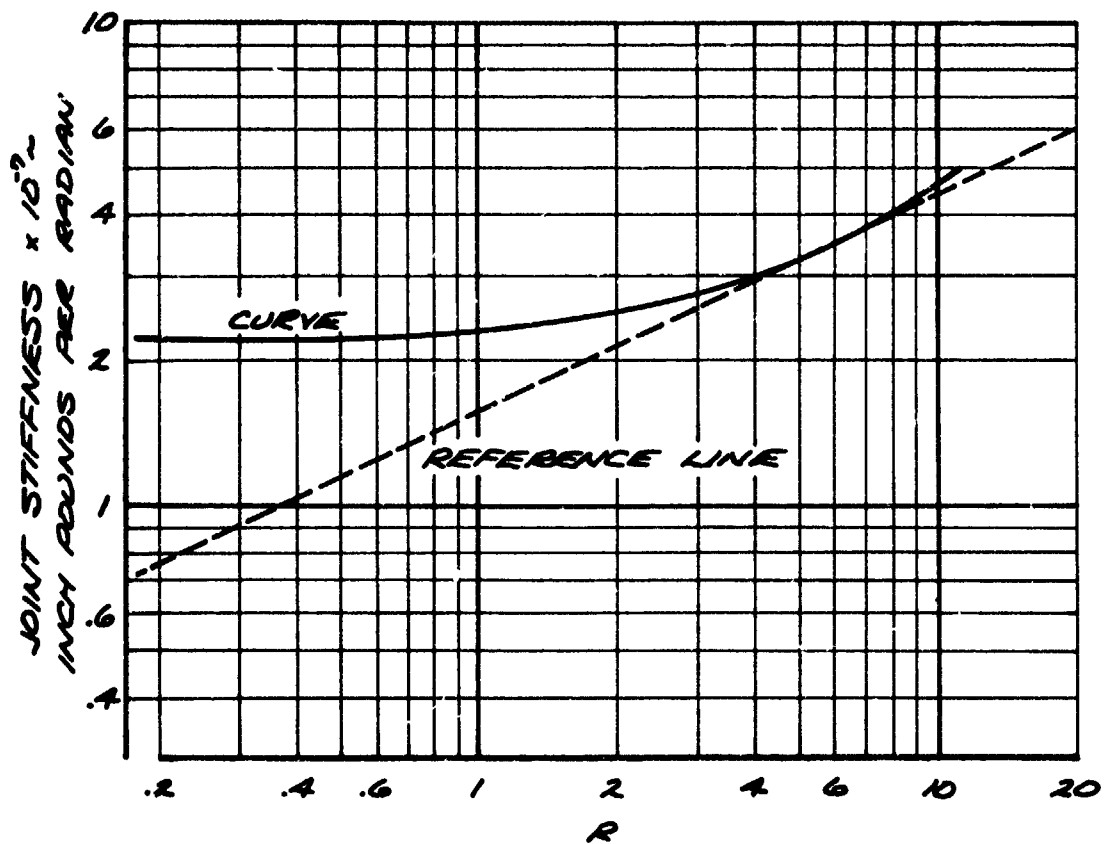
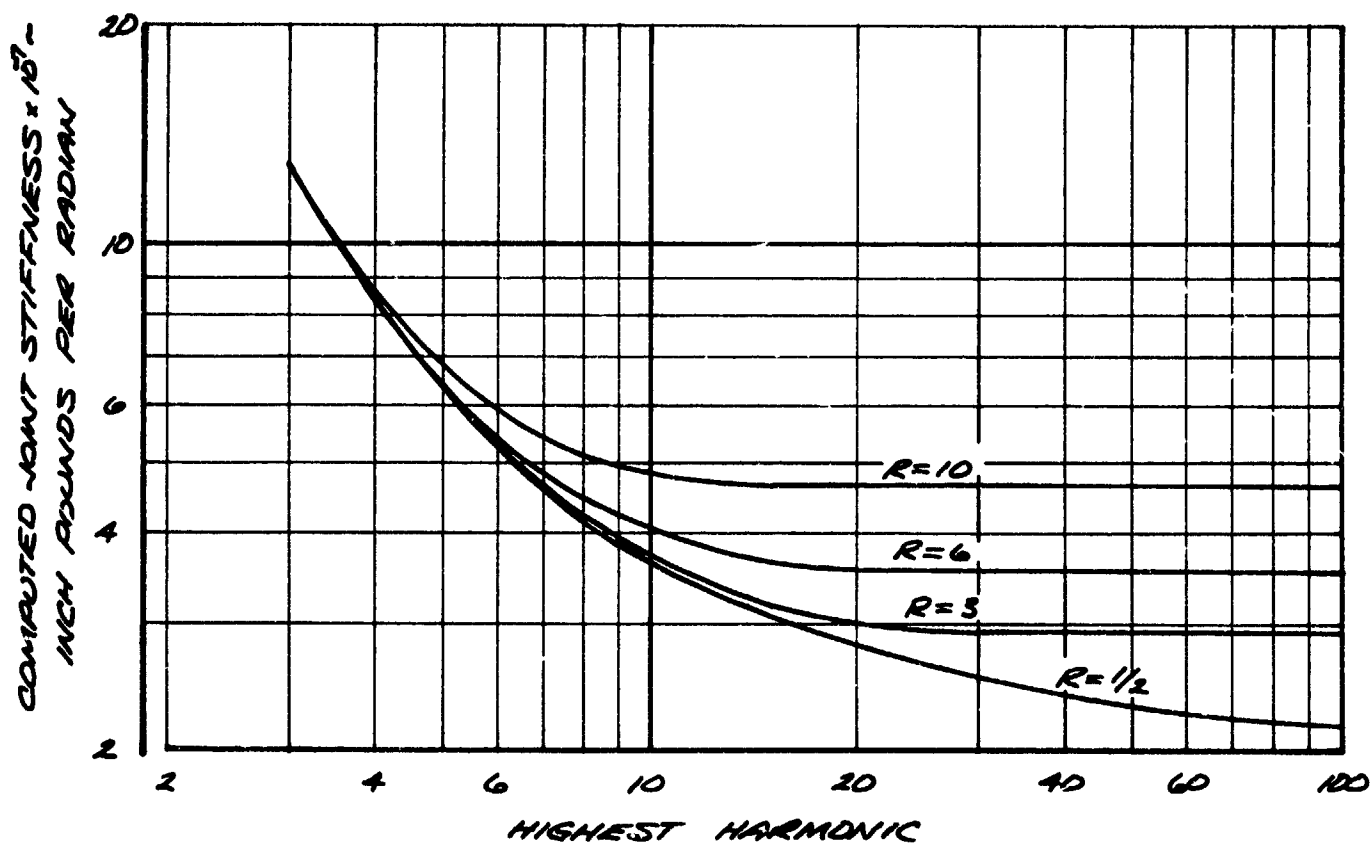


FIGURE 3-8

CURVES OF COMPUTED JOINT STIFFNESS VERSUS
HIGHEST HARMONIC FOR THREE FASTENER JOINT
AND VARIOUS VALUES OF R (RATIO OF E OVER
BOLT DIAMETER ENCLOSED ANGLE.)



Section 4.0

JOINT COMPLIANCE EXTRACTION TECHNIQUE DEVELOPMENT

Tactical missile joint compliances often represent one of the major uncertainties in developing an acceptable analytical model for dynamic response studies. This uncertainty tends to be reinforced if large differences are discovered between theoretical and experimental mode shapes and frequencies. If one assumes that errors in assumed joint compliances are totally responsible for the theory/test mismatch, then a method of solution for effective joint compliances is suggested through an iterative "best fit" between modal analysis and modal test data. Since distributed mass and missile airframe stiffness parameters are generally well defined, the assumption that all errors lie in the effective joint compliances is not usually unreasonable. For many years at the Pomona Division of General Dynamics a somewhat arbitrary trial and error "hand tuning" procedure was employed to arrive at a set of joint compliances which would yield an acceptable fit between analysis and test data. This procedure can become quite time consuming and cumbersome, however, when more than two or three unknown joint compliances are involved.

A joint compliance extraction technique was developed during Phase 1 of the study of structural dynamic properties of tactical missile joints (Reference 1). It utilized a steepest-descent method to solve for variable unknown spring rates based upon a weighted best fit match between experimental and theoretical mode shapes and natural frequencies. The method was tailored specifically to beam representations of missile structures. Unfortunately, the method as implemented had several limitations. One of the restrictions was that the number of modes used had to equal or exceed the number of unknown joints to obtain meaningful results. Also, only bending cases with free-free boundary conditions could be run, and no method of handling appendages had been devised.

Late in the Phase 1 study, a general method for estimating structural parameters from dynamic test data appeared in Reference 4 which looked promising for use in the extraction of missile airframe joint compliances. Subsequently this method was applied in Phase 2 to simple test cases with encouraging results. As confidence was gained in the optimization method, the method was programmed for use with a Control Data Corporation 6400 computer. Originally only first order gradient terms were used. The first order gradient method worked well with a small (two degree of freedom) system, but was inadequate for larger systems. Next a second order gradient method in which the second order terms were approximated by differences was tried and techniques developed to improve convergence of the method. The resulting computer program is called program JOINTS.

During the present and final phase of this study (Phase 3) a number of program refinements and improvements have been introduced and evaluated. These program additions include the following:

1. A time saving option is provided for generation of "Standard" weighting factors which weights all test mode shapes and frequencies equally. Provision still exists, of course, for input of alternate weighting factors if preferred.
2. Program logic has been added to preclude missing or skipping over needed theoretical modes by assuring theoretical/test mode correspondence both in number of nodes and polarity. This prevents sizable errors which can result from mode mismatching and avoids numerous program restarts, thus saving turn around time between computer runs.
3. An option is offered to use a greater number of theoretical modes than experimental modes in the calculation of the gradients of the cost function. This feature aids solution convergence when only a few experimental modes are available.
4. An interpolation/extrapolation program called FILLIN has been added which takes experimental modal data at any arbitrary set of test missile stations and generates modal displacement and slope data at missile stations consistent with the lumped parameter modal analysis model. This operation offers a substantial labor savings in the preparation of input data for the joint compliance extraction program.

Section 4.1 presents the theory that program JOINTS is based upon. Rationale in selecting iteration bite size and the considerations involved in choosing experimental mode shape and frequency weighting factors are discussed in Section 4.2 together with a review of some of the results obtained with a hypothetical test case during the Phase 2 study. Section 4.3 presents a discussion and summary of the new program features added during the present phase and Section 4.4 offers a program application test case based on a set of actual tactical missile modal test data. The joint compliance extraction technique user's manual, including a listing of the programs, and appropriate test cases are presented in the Appendix.

4.1 METHOD OF ANALYSIS

The joint compliance extraction technique is designed to determine mechanical joint compliances of an elastic missile structure by generating the "best" least square fit between a linear lumped parameter mathematical model and a given set of experimental modal data. A major assumption in the method is that the joint compliances constitute the principal unknowns in the lumped parameter system, with both distributed

mass and stiffness being precisely defined. Weighting factors which involve mode number, shape, and frequency acknowledge the existence of accuracy limitations in the test data. The joint compliances yielding a best fit are found by minimizing a quadratic function of the differences between corresponding theoretical and experimental eigenvalues and eigenvectors. This function, referred to as the cost function, is expressed as follows:

$$F = \frac{1}{2} \sum_{i=1}^N \{ W_{if} (\omega_{ie}^2 - \omega_{it}^2)^2 + (X_{ie} - X_{it})^T W_{ix} (X_{ie} - X_{it}) \} \quad (4.1)$$

The frequencies and mode shapes are denoted by ω and X , respectively. The weighting factor matrix is W and the index i is the mode number. If the mode shape slopes are used, they are treated as additional components of the X 's. The subscripts e and t denote experimental and theoretical values, respectively. The minimization of the cost function constitutes a nonlinear programming problem which is the subject of this section. Optimization problems not amenable to standard methods are more the rule than the exception. In this case the optimization is accomplished by a steepest descent method especially developed for this study. The basic concept originally appeared in Reference 4. Before proceeding with a detailed discussion of the method, the structural mathematical model utilized will be described.

4.1.1 System Model. The fundamental structural dynamic considerations of a tactical missile are often handled with a linear lumped parameter mathematical model. The one used in this study is typical. More expressly, the mathematical model simulates a beam-like body with a series of lumped masses connected by weightless beams. Discrete shear, compressive; torsional, and flexural springs may be included at any point in the model. The model can be used to analyze bending, torsion, and longitudinal motion. The model contains provisions for including appendages attached to the main body at arbitrary angles with arbitrary attachment springs. The appendages are modeled similarly to the main body. The boundary value problem that results from this representation can be expressed as an eigenvalue problem:

$$[K - \omega_{ie}^2 M] X_{ie} = 0 \quad i = 1, 2, \dots, N \quad (4.2)$$

where M and K are mass and stiffness matrices, respectively. The subroutine within the computer program which solves the eigenvalue problem uses the Holzer-Myklestad method. This numerical method utilizes transfer matrices from point to point on the model and finds the eigenvalues by satisfying the boundary conditions using an iterative procedure. A

complete description of the method is found in Reference 5. Limitations of the method and economy preclude extraction of all N modes where N is typically 50 to 200. It will be seen later that the lack of a complete set of modes introduces approximations into the optimization method and necessitates modifications.

4.1.2 Solution Method. The "best fit" values of the joint compliances, defined in a least square error sense, are determined by minimizing the cost function which is accomplished with a modified steepest descent method. Steepest descent or gradient methods as they are also known, iteratively converge on the location of the minimum, since an analytical solution of the condition for an extremum, $\nabla F = 0$, is not possible. The successive estimates of the minimizing values of the independent variables, in this case a vector the components of which are the unknown spring rates of the structural joints \underline{k} , are

$$\underline{k}^{(n+1)} = \underline{k}^{(n)} - \theta \nabla F \big|_{\underline{k}^{(n)}} \quad (4.3)$$

The superscript indicates the number of the estimate. If the quantity θ is a constant, the algorithm is a first order method commonly referred to as the steepest descent method. It is based on the intuitive notion that if one proceeds in the direction of the steepest descent, which Equation 4.3 does, in small steps one must arrive at a local minimum. It can also be proven rigorously (Reference 6). A very efficient second order method may be derived by applying the Newton-Raphson algorithm to the gradient of the cost function which yields the successive approximation,

$$\underline{k}^{(n+1)} = \underline{k}^{(n)} - S \left[\frac{\partial^2 F}{\partial k_i \partial k_j} \right] \nabla F \big|_{\underline{k}^{(n)}} \quad (4.4)$$

The matrix of second partial derivatives must be non-singular. Theoretically, the step size, S , is a scalar. However, in this study, it was necessary to generalize its definition. Equation 4.4 serves as the basis for the algorithm developed. The reasons for the modifications that were necessary will be explained as they are encountered.

The j^{th} component of the gradient of the cost function is

$$\frac{\partial F}{\partial k_j} = \sum_{i=1}^{N_i} \left\{ w_{if} (\omega_{ie}^2 - \omega_{ie}^2) \frac{\partial \omega_{ie}^2}{\partial k_j} + (x_{ie} - x_{ie})^T w_{ix} \frac{\partial x_{ie}}{\partial k_j} \right\} \quad (4.5)$$

where k_j is the j^{th} unknown spring rate. In order to calculate the partial derivatives of the eigenvalues and eigenvectors with respect to

the k_j 's, a departure was made from Reference 4. Here the modes were normalized to unity with respect to the generalized mass M ,

$$\underline{x}_{it}^T M \underline{x}_{jt} = \delta_{ij} \quad (4.6)$$

Also a joint compliance positioning matrix, K^j , is introduced which locates the unknown spring rates within the full spring matrix -

$$K = \bar{K} + \sum_{j=1}^N K^j K_j \quad (4.7)$$

\bar{K} is the matrix of known spring elements. Because of the peculiarities of the method used to solve the eigenvalue problem, the spring matrix, K , is not directly available and so neither are the variable spring positioning matrices, the K^j 's. However, they can be derived by considering the strain energy stored in the j th spring. For simplicity, assume that a separate spring rate is assigned to each joint. Then the strain energy associated with the j th spring is:

$$U_j = \frac{1}{2} K_j (\dot{x}_j - \dot{x}_j')^2 \quad (4.8)$$

where \dot{x}_j and \dot{x}_j' are the slopes to the left and to the right of the joint for the case of a rotational spring. The strain energy is also $U_j = 1/2 k_j \underline{x}^T T K_j \underline{x}$. Equating the two expressions and then the coefficients of like terms, it can be deduced that the matrix, K_j , must be the null matrix except for a submatrix,

$$\begin{pmatrix} 1 & -1 \\ -1 & 1 \end{pmatrix} \quad (4.9)$$

corresponding to the coordinates on either side of the joint. Then according to Reference 7 the partial derivatives are

$$\frac{\partial \omega_{it}^2}{\partial K_j} = \underline{x}_{it}^T K^j \underline{x}_{it} \quad (4.10a)$$

$$\frac{\partial \underline{x}_{it}}{\partial K_j} = \sum_{l \neq i}^N \frac{\underline{x}_{lt}^T K^j \underline{x}_{it}}{\omega_{it}^2 - \omega_{lt}^2} \underline{x}_{lt} \quad (4.10b)$$

Equations (4.10a) and (4.10b) can be expanded in terms of components of the normal coordinates by utilizing the strain energy relationship for each joint.

$$\begin{aligned}\frac{\partial \omega_{it}^2}{\partial K_j} &= x_{it, m_j} (x_{it, m_j} - x_{it, m_{j+1}}) + x_{it, m_{j+1}} (-x_{it, m_j} + x_{it, m_{j+1}}) \\ &= (x_{it, m_j} - x_{it, m_{j+1}})^2\end{aligned}\quad (4.11a)$$

$$\begin{aligned}\frac{\partial x_{it}}{\partial K_j} &= \sum_{l \neq i}^N (\omega_{it}^2 - \omega_{lt}^2)^{-1} \{ x_{lt, m_j} (x_{it, m_j} - x_{it, m_{j+1}}) \\ &\quad + x_{lt, m_{j+1}} (-x_{it, m_j} + x_{it, m_{j+1}}) \} x_{lt}\end{aligned}\quad (4.11b)$$

where the indices m_j and m_{j+1} refer to the components of the normal coordinates to the left and right of the j th joint respectively. The partial derivatives of the mode shapes were derived using the second formulation of Reference 7 which requires a complete set of theoretical modes. As pointed out previously the sum has to be truncated for reasons of accuracy and economy. This is usually the case in dynamic problems. Here the justification is a posteriori. The number of theoretical modes used in the computation of their derivatives is an option to be selected by the user.

$$\frac{\partial x_{it}}{\partial K_j} \cong \sum_{l \neq i}^N \frac{x_{lt}^T K_j^j x_{it}}{\omega_{it}^2 - \omega_{lt}^2} x_{lt} \quad (4.12)$$

The second partial derivative of the cost function with respect to the unknown spring rates, k_q and k_j , is

$$\begin{aligned}\frac{\partial^2 F}{\partial K_q \partial K_j} &= \sum_{i=1}^N \left\{ w_{if} \left[\frac{\partial \omega_{it}^2}{\partial K_q} \frac{\partial \omega_{it}^2}{\partial K_j} + (\omega_{it}^2 - \omega_{ie}^2) \frac{\partial^2 \omega_{it}^2}{\partial K_q \partial K_j} \right] \right. \\ &\quad \left. + \frac{\partial x_{it}^T}{\partial K_q} w_{ix} \frac{\partial x_{it}}{\partial K_j} + (x_{it} - x_{ie})^T w_{ix} \frac{\partial^2 x_{it}}{\partial K_q \partial K_j} \right\} \quad (4.13)\end{aligned}$$

The second partials of the eigenvalues and mode shapes are

$$\frac{\partial^2 \omega_{it}^2}{\partial K_q \partial K_j} = \frac{\partial X_{it}^T}{\partial K_q} K^j X_{it} + X_{it}^T K^j \frac{\partial X_{it}}{\partial K_q} \quad (4.14a)$$

$$\begin{aligned} \frac{\partial^2 X_{it}}{\partial K_q \partial K_j} \cong \sum_{l \neq i}^{N_i} (\omega_{it}^2 - \omega_{lt}^2)^{-1} \left\{ \left[-(\omega_{it}^2 - \omega_{lt}^2)^{-1} \left(\frac{\partial \omega_{it}^2}{\partial K_q} - \frac{\partial \omega_{lt}^2}{\partial K_q} \right) X_{lt}^T K^j X_{it} \right. \right. \\ \left. \left. + \frac{\partial X_{lt}^T}{\partial K_q} K^j X_{it} + X_{lt}^T K^j \frac{\partial X_{it}}{\partial K_q} \right] X_{lt} \right. \\ \left. + X_{lt}^T K^j X_{it} \frac{\partial X_{lt}}{\partial K_q} \right\} \quad (4.14b) \end{aligned}$$

During Phase 2 it was felt that direct calculation of the second partial derivatives of the eigenvalues and eigenvectors using the above equations were prohibitive because of computer memory size limits. It was subsequently realized that direct calculation of the second partial derivatives is very likely economically feasible since many of the terms are zero. However, since only a small number of unknown missile joints are assumed, the method employed in program JOINTS approximates the second partials by taking differences of the first partials. Such a numerical process tends to be accuracy sensitive and demands careful monitoring. Without resorting to double precision arithmetic, the step size must be large enough to yield a sufficient number of significant figures. On the other hand, too large a step size may enclose a region too large for the cost function to be represented by a quadratic. The procedure settled upon was the following. Using the current estimate $k^{(n)}$, the gradient of the cost function is computed with Equations (4.5), (4.11a) and (4.12). The current estimates of the unknown springs are successively incremented one at a time in the direction dictated by the corresponding component of the gradient:

$$K_j^{(n)} = K_j^{(n)} \left[1 + r \cdot \text{SGN} \left(\frac{\partial F}{\partial K_j} \Big|_{K^{(n)}} \right) \right] \quad (4.15)$$

The relative increment, r , is the same for all the unknown spring rates and fixed for a particular problem. The gradient is calculated at $k^{(n)}$ and the ratios of the differences of the respective components and the spring rate increments are computed. In order to improve the estimates of the second partial derivatives, corresponding off-diagonal estimates which theoretically should be equal are averaged as indicated below.

$$\frac{\partial^2 F^{(n)}}{\partial K_i \partial K_j} = \frac{\partial^2 F^{(n)}}{\partial K_j \partial K_i} \approx \frac{1}{2} \left\{ (K_i'^{(n)} - K_i^{(n)})^{-1} \left[\frac{\partial F^{(n)}}{\partial K_j} \right]_{K_i}^{K_i'} + (K_j'^{(n)} - K_j^{(n)})^{-1} \left[\frac{\partial F^{(n)}}{\partial K_i} \right]_{K_j}^{K_j'} \right\} \quad (4.16)$$

The Hessian, the matrix of second partial derivatives, is then inverted. The correction terms in Equation (4.4) are computed using a value of 1.0 for S. The sign and magnitude of each correction component are compared to those of the increment used to estimate the second partials. If the signs agree or if the magnitude is less than 2-1/2% of the current spring rate, the second order correction is utilized. If not, equation (4.15) is used. If the new spring rates, $k^{(n+1)}$, result in an increase in the cost function, the correction terms to $k^{(n)}$ are halved repeatedly until a decrease in the cost function is obtained. In any case, each variable spring rate is kept within prespecified limits. These procedures which taken together may be considered a complicated method of selecting a varying step size, S, evolved heuristically. Modifications which can be made to improve them and put them on a more rigorous basis are possible.

4.2 SPECIAL PARAMETERS

This section discusses two of the parameters important to the proper functioning of the method of solution. Both of these parameters are input quantities in the present version of Program JOINTS. These parameters are the set of weighting factors and the step size - r.

4.2.1 Weighting Factors. Ideally the weighting in the cost function should reflect both the relative accuracy of the experimental data and the relative importance of the information to be obtained from applications of the mathematical model. Often for missiles constructed with thin cylindrical shells, the experimental data will diverge from beam behavior in progressively higher modes. For many dynamic analyses (such as dynamic loads analyses and autopilot elastic mode coupling analyses), the contribution of the higher modes is less significant than the lower modes. If the above conditions hold for any given problem, then the weighting factors should decrease in some way with increasing mode number.

A derivation of the weighting factors is now developed. The cost function (Equation 4.1) may be broken down into two terms (mode shape and frequency) for each mode

$$F_i = F_{if} + F_{ix} \quad (4.17)$$

where

$$F_{if} = \frac{1}{2} W_{if} (\omega_{ie}^2 - \omega_{it}^2)^2 \quad (4.18)$$

$$F_{ix} = \frac{1}{2} (\underline{X}_{ie} - \underline{X}_{it})^T W_{ix} (\underline{X}_{ie} - \underline{X}_{it}) \quad (4.19)$$

Rewriting F_{ix} as a summation yields

$$F_{ix} = \frac{1}{2} W_{ix} \sum_k (\underline{X}_{ie_k} - \underline{X}_{it_k})^2 \quad (4.19a)$$

To see the size of terms produced in the cost function by an error in the eigenvalue or eigenvector, a relative error of size ϵ is assumed in each of the measured quantities. Then the cost function terms will be equated by proper selection of weighting factors. That is, an error of ϵ will be assumed in both ω^2 and X , and weighting factors will then be found which give equal size terms in the cost function. If the theoretical eigenvalues and eigenvectors are assumed correct, then an error of ϵ in the eigenvalue can be written as

$$\omega_{it}^2 = (1 + \epsilon) \omega_{ie}^2 \quad (4.20)$$

The frequency terms in the cost function become

$$\begin{aligned} F_{if} &= \frac{1}{2} W_{if} [\omega_{ie}^2 - (1 + \epsilon) \omega_{ie}^2]^2 \\ F_{if} &= \frac{1}{2} W_{if} [-\epsilon \omega_{ie}^2]^2 \\ F_{if} &= \frac{1}{2} W_{if} \epsilon^2 \omega_{ie}^4. \end{aligned} \quad (4.21)$$

This means that an error of ϵ in the eigenvalue will produce a residual term in the cost function proportional to the product of the fourth power of the frequency and the square of the error. Considering the same error applied to the mode shape contribution to the cost function yields

$$F_{ix} = \frac{1}{2} W_{ix} \sum_l [x_{ie_l} - (1+\epsilon) x_{ie_l}]^2$$

$$F_{ix} = \frac{1}{2} W_{ix} \sum_l \epsilon^2 x_{ie_l}^2 \quad (4.22)$$

The above equation shows that an error of ϵ in the eigenvector will produce a residual term in the cost function proportional to the product of the square of the eigenvector and the square of the error. Since the mode shapes are normalized to a unity generalized mass, then

$$1 = \sum_l m_l x_{ie_l}^2 \quad (4.23)$$

If assumptions are made that the test specimen is a slender beam with uniform mass and station distributions, then the above equation may be rewritten as

$$1 = \bar{m} \sum_l x_{ie_l}^2$$

$$\sum_l x_{ie_l}^2 = 1/\bar{m} \quad (4.23a)$$

and the mode shape portion of the cost function becomes inversely proportional to the mass

$$F_{ix} = \frac{1}{2} W_{ix} \epsilon^2 \frac{1}{\bar{m}} \quad (4.24)$$

where $\bar{m} = \frac{\text{mass of beam}}{\text{Number of stations}}$

F_{ix} is independent of frequency, and is dependent upon the mass, number of beam stations, and the square of the error.

To equate the size of the frequency terms in the cost function with each other, the following weighting factors were selected

$$w_{if} = \frac{\omega_{N/8}^4}{\omega_{1e}^4} \quad (4.25)$$

where

$\omega_{N/8}$ = highest experimental mode frequency

Equating the mode shape and frequency terms of the cost function yields

$$\begin{aligned}
W_{ix} \frac{1}{m} &= \frac{W_{N1e}^4}{W_{ie}^4} \quad W_{ie}^4 = W_{N1e}^4 \\
W_{ix} &= W_{N1e}^4 m \\
W_{ix} &= \frac{W_{N1e}^4 m}{N}
\end{aligned} \tag{4.26}$$

where m = mass of the missile (Lb-Sec²/In)
 N = number of internal stations

The above weighting factors then approximately weight the mode shape and frequency errors equally. These factors have been built into Program JOINTS along with a set of adjustable weighting factor coefficients. If unequal weights are desired, weighting factor coefficients are input to the program and these coefficients are multiplied by the above factors to obtain the new weighting factors used by the program. That is

$$W_{if} = WFC_{if} \left(\frac{W_{N1e}^4}{W_{ie}^4} \right) \tag{4.27}$$

$$W_{ix} = WFC_{ix} \left(\frac{W_{N1e}^4}{N} m \right) \tag{4.28}$$

where WFC_{if} and WFC_{ix} are input separately for each mode.

Some consideration was given to including provisions for weighting some mode components more than others, but this was concluded to be an impractical and unwarranted complexity in the operation of the program.

4.2.2 "Bite" Size Selection. The bite size being discussed in this section is r in equation (4.15), the increment each spring is altered during the intermediate calculation in the computation of the second order partials. The choice of the spring increment size, r , can cause a problem unless care is taken in its selection. The step size must be large enough to prevent incurring numerical accuracy problems, yet small enough to give an adequate estimate of the second order gradients of the cost function.

The present tolerance ratio on the frequency solution in the modal analysis routine in Program JOINTS is 1×10^{-5} . That is, the theoretical

frequency solutions will be no worse than .001 percent. In selecting a value of r to be used in Program JOINTS, a change in each individual spring equal to r times the spring rate should produce frequency changes greater than .01 percent in the theoretical modes. This change in frequency is dependent upon the joint locations and magnitude of compliances. Reference 1 (Phase 1 Report) provides an extensive discussion of these parameters. Another constraint on the step size to be considered is that if the originally assumed joint compliances are 'far from convergence' a first order gradient method is used rather than the second order gradient method. If the first order method is used, r is the amount the compliance is altered each iteration. If r is small, the solution time may be very large. The phrase 'far from convergence' is defined as a region which is determined by the directions indicated for changes in individual spring rates from the first order and the second order gradient methods. If the two methods indicate opposite directions should be taken for the change in spring rate, the first order method is used. As the cost function minimum is approached, the first and second order terms agree in sign for the change in spring rate so the magnitude determined from the second order method is used. This choice of either the first or second order method is made independently for each spring.

To illustrate the effect of the step size r , consider the non-uniform bending beam model shown in Figure 4-1. It consists of five beam sections connected by four flexural joints, each of "moderate" to "good" stiffness for the assumed test airframe. The Holzer Myklestad method (identical to what is used in Program JOINTS) was used to generate the required modal data for this test case. Since the modal data are "exact" for the lumped parameter model, a precise means for judging the accuracy of the JOINTS program solution is provided. Selected flexural joints were then assumed to be unknown, and arbitrary (incorrect) initial values selected.

Figure 4-2 shows the results obtained with Program JOINTS by using two modes to solve for three joint compliances. For this case, the compliance of the first of the four joints was assumed to be known correctly and the compliance of the last three were assumed high by a factor of two. The value of the intermediate step size, r , used in this case was 25%. Figure 4-2 shows the result of eighteen iterations. The convergence is seen to be quite slow. Other values of r have been considered with interesting results. Figure 4-3 shows the same example as Figure 4-2, except the value of r was changed from 25% to 1%. Here convergence to the three correct joint flexural compliances is achieved in four iteration cycles or about four times as fast. This points out the importance of the intermediate step size, r , used in approximating the second partial derivatives. In both of these examples, three unknown spring rates were solved using only two modes.

Figure 4-4 illustrates further the importance of the intermediate step size, r , in the convergence of the method. Values of r considered

in Figure 4-4 range from 25% to 1%. Very little difference is seen between 1% and 5%, suggesting that both approximate the second order gradients well. For this case, it can be seen that 25%, 20%, and 15% were all too large a value for r . All three values of r will produce the correct joint compliances but the run time is much longer for the larger values of r . The value of r for best convergence will not be the same for all cases. In fact, for some problems it might be more efficient to make two computer runs using two different values of r . In the beginning, use of a larger value of r may be required if the program employs the first order gradient method. However, the solution may be speeded up by using a smaller value of r as the cost function minimum is approached and the program uses the second order gradient method.

4.3 PROGRAM FEATURES ADDED

This section discusses some of the techniques developed during the Phase 3 study to increase the efficiency of Program JOINTS and to decrease the work required by the user. Covered in this discussion are the program generation of weighting factors, logic in JOINTS to correct for modes being missed by the eigenvalue extraction subroutine, and the benefits of using the input parameter 'CLOSE'. In addition, this section introduces the computer program (Program FILLIN) written as an aid for the user of Program JOINTS. Program FILLIN accepts measured modal data in a general format and interpolates between those data points to obtain a new set of data in the format appropriate for use in Program JOINTS. The changes to the input data are necessitated because Program JOINTS compares the experimental and theoretical modal data at identical missile stations.

4.3.1 Weighting Factor Generation. In the original program format, the weighting factors required to use Program JOINTS had to be calculated by the user. As an added convenience, it was decided to accomplish the major portion of the weighting factor computation within the program. Equations 4.25 and 4.26 of section 4.2.1 present the equations of the weighting factors now used in the program. The option is retained to input weighting factor coefficients desired by the user, but these weighting factor coefficients ($WFC_{i,f}$ and $WFC_{i,x}$ in equations 4.27 and 4.28) modify the factors computed by the program and do not replace them. If no values are input for $WFC_{i,f}$ and $WFC_{i,x}$, these coefficients are each assumed equal to 1.0. If the user, for example, wishes to weight the first mode shape and frequency a factor of two more than the other modes, he simply inputs the value 2.0 for $WFC_{1,f}$ and $WFC_{1,x}$ and 1.0 for all other modes.

4.3.2 'Missing' Mode Logic. Another option built into Program JOINTS during Phase 3 is a check to guard against missing modes in the eigenvalue extraction routine. This is accomplished by checking the computed modes against the experimental modes. For bending cases, the number

of slope sign changes in each theoretical mode shape is compared with each measured mode. Like modes are matched and if any modes are missing the program will go back and compute the missing modes. Because of the way the Myklestad subroutine treats redundant appendages, this check should not be used with a model that has redundant appendages.

4.3.3 Number of Theoretical Modes. Another improvement introduced to Program JOINTS is to allow the calculation and inclusion of more theoretical modes than experimental modes in the partial derivatives of the mode shape given in equation (4.11b). The partial derivative of the eigenvector for the i^{th} mode is expressed as the sum of contributions from all modes except the i^{th} mode. This sum is truncated at however many modes are available for the calculation. If only one mode is available, then the partial is approximated by zero. If two modes are available, then the partial is approximated by contributions from one mode. For a distributed system, the partial derivative would be computed from an infinite sum. The larger the number of modes, the closer the sum should approximate the partial derivatives. Using more modes in approximating the partial derivatives can be expected to produce more accurate values, aid in the problem solution, and accelerate the rate of convergence. The amount of computer time used per iteration cycle, however, is directly proportional to the number of theoretical modes used in the solution. Because of this cost consideration, the user would be advised to use an equal number of theoretical modes in the solution when three or more measured modes are available.

4.3.4 Input Parameter 'CLOSE'. The input parameter 'CLOSE', Table A-3, used in Program JOINTS is another parameter designed to save computer time. If a value is not input for 'CLOSE' into Program JOINTS, a continuous search is made for the required number of modes between specified frequency limits. Computer time may be saved by eliminating as much of the searching as possible. A way of eliminating the unnecessary searching is to start below but very near the answer. The reason for starting just below the answer is that the frequency search is done in an increasing order. For a model which matches the experimental data fairly closely, the search starting frequency for each mode may be selected close to the experimental frequencies. If a value of 'CLOSE' is input, the search for the i^{th} mode starts at the frequency equal to 'CLOSE' times the experimental frequency for the i^{th} mode.

Starting the search for the modes near the required solution has saved considerable computer time in several of the test cases. Using the tactical missile application of Section 4.4 as an example, a value of 'CLOSE' equal to 0.9 cost approximately 30% less than an identical run where a continuous search was used. However, care must be taken that 'CLOSE' times the experimental frequency for the i^{th} mode will not be less than the theoretical frequency for the $(i-1)^{\text{th}}$ mode, in which case the $(i-1)^{\text{th}}$ mode will be repeated for the i^{th} mode.

4.3.5 Test Data Preparation. One of the goals of the Phase 3 study was to simplify the tasks of the person using Program JOINTS. During the Phase 2 study, it became obvious that for Program JOINTS to be easily useable, a scheme was needed to reduce the amount of work required to get the experimental data in the format necessary for the program. As the cost function is formulated, the mode shape deflection and slope at every internal station are compared with a measured mode shape deflection and slope at that station. However, seldom are the measurements made at the station locations required by the mathematical model. In addition, the quantities most usually measured during test are the modal deflections and not the slopes. One way of handling this problem is to plot the measured deflection data. From these plots, a new set of modal deflections and slopes are read at the desired stations and key punched on cards. As an example of the size of this problem, the tactical missile test case discussed in Section 4.4 has a total of 78 stations. The number of data points read per mode is 156, and three modes were used for that case. It was for this reason that Program FILLIN was written.

Program FILLIN accepts modal data measured at a set of missile stations and the mathematical model data to be used in Program JOINTS. The program then interpolates using several simple curve fitting techniques. The program is primarily designed for bending mode cases. The method of interpolation to be used at a particular station is determined by the station type and the relative locations of stations at which experimental values are available. The types of stations considered include those not at a joint, those immediately to the right or left of joints, and those at the ends of the main beam or an appendage. The first class of stations includes the majority of stations. For these stations interpolation was accomplished with a sliding parabolic least square curve fit to four experimental values. That is the two nearest experimental values on either side of the station are used for the least square fit. If two experimental values are not available on both sides of the station, linear interpolation or if necessary extrapolation is resorted to. This also applies to stations at ends of appendages and to modal slopes at stations immediately to the right or left of rotational spring joints and to modal displacements at stations immediately to the right or left of shear spring joints. Modal slopes at a shear joint are the average of the two straight line slopes on each side of the joint.

One of the limitations of Program FILLIN is that appendages with 180° attachment angles will have slope values with the sign opposite to the Myklestad subroutine. This occurs because the Myklestad routine uses a different coordinate systems on appendages than it does on the main beam while FILLIN uses only one coordinate system. Another limitation of

FILLIN is that inaccuracies can occur at stations near joints and in slopes at roots of appendages. However, one of the advantages of the least square curve fit is that the method will smooth the experimental data.

4.4 TACTICAL MISSILE TEST CASE

To show the utility of Programs FILLIN and JOINTS, a set of measured bending modal data for an actual tactical missile were selected as a test case. The set of modal data had previously been matched with a mathematical model by a trial and error method. This method took approximately sixty computer runs. Previous test cases based on hypothetical models had shown that the method arrives at the correct joint compliances rapidly when an exact math model is used with no errors in the input data. The results obtained with this test case illustrate how well the program works when matching a lumped parameter model to actual measured data with its inherent experimental errors.

Figures 4-5, 4-6, and 4-7 present the three experimental modes and the curve fit values obtained from Program FILLIN for the tactical missile. There are slight discrepancies between the measured data points and the curve fit values, especially near the front end of the missile where few data points exist. The forward end of the missile is a radome shell and quite stiff for the weight it supports. It therefore bends very little in the lower bending modes. When the program fits the data points with a quadratic equation, the match is not perfect. Nevertheless the interpolated modal displacements and slopes are believed to be reasonable representations of the measured modes. Since the method tends to smooth the data, a test case with larger experimental errors in the measured modes would look more impressive.

The output displacements and slopes from Program FILLIN are punched on cards in the format for Program JOINTS. However, the punched output must be checked and corrected as 180 degree appendages will have the sign of the slopes out of phase with the Myklestad program. This is due to a different sign convention in the Myklestad subroutine for 180 degree appendages.

The data output from Program FILLIN was then used as the input modal data for Program JOINTS. The set of weighting factors selected for this application were chosen to equate all three modes (both frequencies and mode shapes) equally. The first three joint compliances (which represented airframe joints) were started approximately 300% higher than the hand tuned values. The fourth joint compliance represented the attachment compliance for an internal appendage. The originally assumed value of the fourth compliance was started high by 30% over the hand tuned value.

Figure 4-8 shows the rate of convergence obtained by Program JOINTS for the tactical missile application. The program was run for a total of eight iteration cycles. However, the cost function did not improve significantly after the third cycle. The final (iteration cycle eight) joint compliances obtained agree quite well with the hand tuned values. Figures 4-9, 4-10, and 4-11 present a comparison of the experimental and theoretical modes. It is apparent from the figures that a good match has been obtained between the two sets of data.

Next, a new set of weighting factors was chosen to see what effect different weighting factors had on the solution. It should also be noted that the test data was represented well by the beam model in the above solution. The set of frequency weighting factor coefficients selected were 100, 10, and 1 for the first, second, and third modes respectively. The corresponding mode shape weighting factor coefficients were 1, 0.1, and 0.01. Figure 4-12 shows the solution (No. 2) obtained for this condition. Comparison of Figures 4-8 and 4-12 shows that both sets of compliances obtained are close to the hand tuned values. The following is a comparison of the experimental frequencies and the frequencies obtained for the two sets of weighting factors.

Mode No.	Experimental Frequency (Hz)	Theoretical Frequency (Hz)	
		Solution No. 1	Solution No. 2
1	59.3	59.5	59.3
2	116.	114.4	116.0
3	153.	154.2	153.6

As shown above, the case where the frequencies are weighted more heavily than the mode shapes (solution number 2) does in fact exhibit a better match between the experimental and theoretical frequencies.

4.5 STATUS OF THE EXTRACTION TECHNIQUE

The joint compliance extraction technique in its present format is believed to offer a useful, convenient, and reliable method for estimating effective compliances of missile joints from modal test data. The method presumes that the missile airframe distributed stiffness and mass properties are known, the modal characteristics can be adequately modeled as a lumped parameter beam, and that all discrepancies between modal analysis and modal test data can be attributed to uncertainties in the joint compliance values. As in any analytical method, additional refinements and areas for improvement will become evident as applications are further explored with actual test data.

LIST OF SYMBOLS FOR SECTION 4.0

F	=	Cost Function of Error Terms
N_e	=	Number of Experimental Modes
\sum_i	=	Summation on Index i
ω	=	Mode Frequency
X	=	Mode Shape
W	=	Weighting Factor
$()^T$	=	Transpose of $()$
K	=	Stiffness Matrix
M	=	Mass Matrix
N	=	Number of Internal Stations in Model
K	=	Unknown Spring Components
n	=	Iteration Number
θ	=	Step Size
∇F	=	$\frac{\partial F}{\partial K}$ = Gradient of F
S	=	Step Size
$[]^{-1}$	=	Inverse of $[]$
δ_{ij}	=	Kronecker Delta $\begin{cases} = 1 & i = j \\ = 0 & i \neq j \end{cases}$
\bar{K}	=	Matrix of Known Spring Elements
N_j	=	Number of Joints
U	=	Strain Energy
x_j, x'_j	=	Slope to the Left and Right of Joint j
K'	=	Intermediate Spring Rate Used in Computing the Second Order Derivatives of F

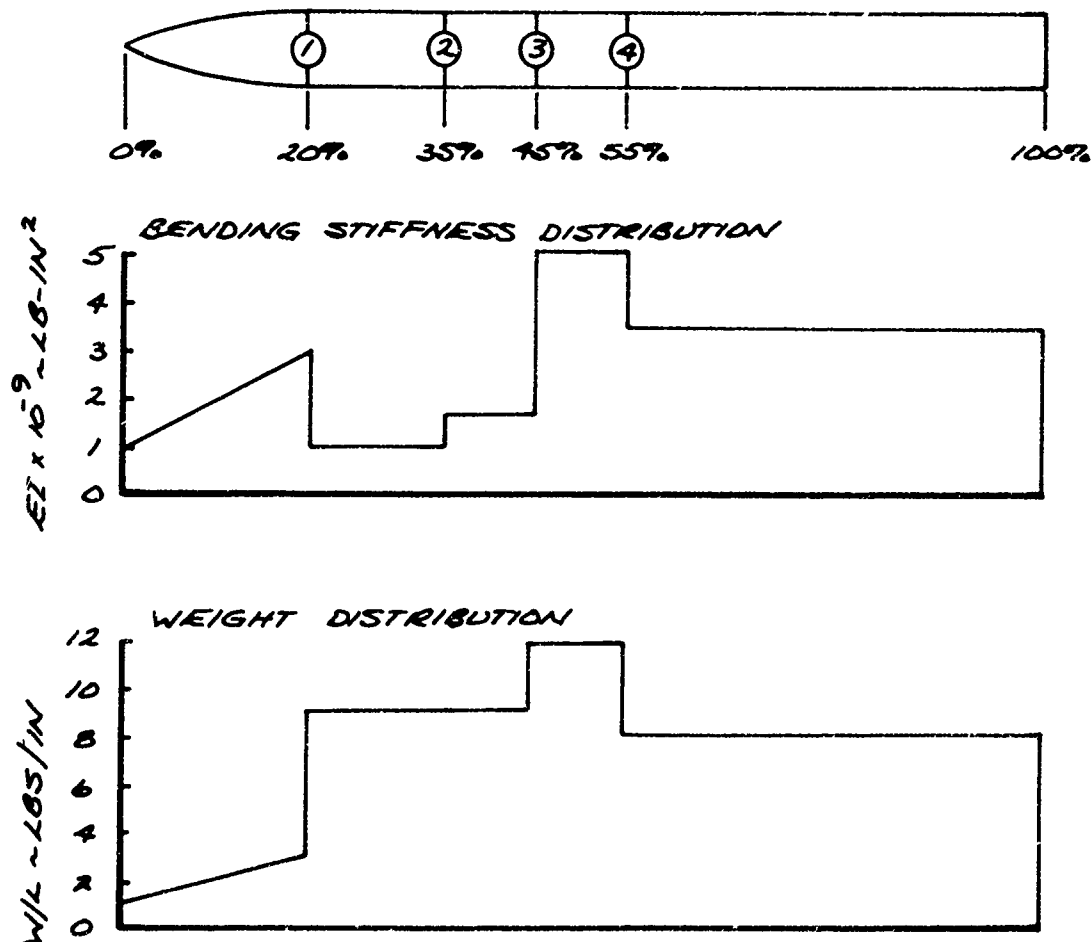
LIST OF SYMBOLS FOR SECTION 4.0 (Cont'd.)

- τ = Intermediate Step Size Used to Obtain K'
- $sgn()$ = The Sign of ()
- ϵ = Relative Error Size
- λ = ω^2 = Eigenvalue
- m = Mass of Missile
- w/c = Weighting Factor Coefficients

SUBSCRIPTS

- e = Experimental
- t = Theoretical
- x = Mode Shape
- f = Frequency
- i, j, l, m, q = Indices or Counters

FIGURE 4-1
NON-UNIFORM BENDING BEAM PROPERTIES



MODE NO.	FREQUENCY WITH JOINTS (Hz)	FREQUENCY W/O JOINTS (Hz)
1	35.9	50.4
2	100.7	118.3

JOINT NO.	COMPLIANCE RAD/IN-LB
1	.1 -7
2	.1 -7
3	.1 -7
4	.1 -7

FIGURE 4-2
 NON-UNIFORM BENDING BEAM
 SOLUTION FOR THREE JOINT COMPLIANCES
 USING TWO MODES, $r = 25\%$

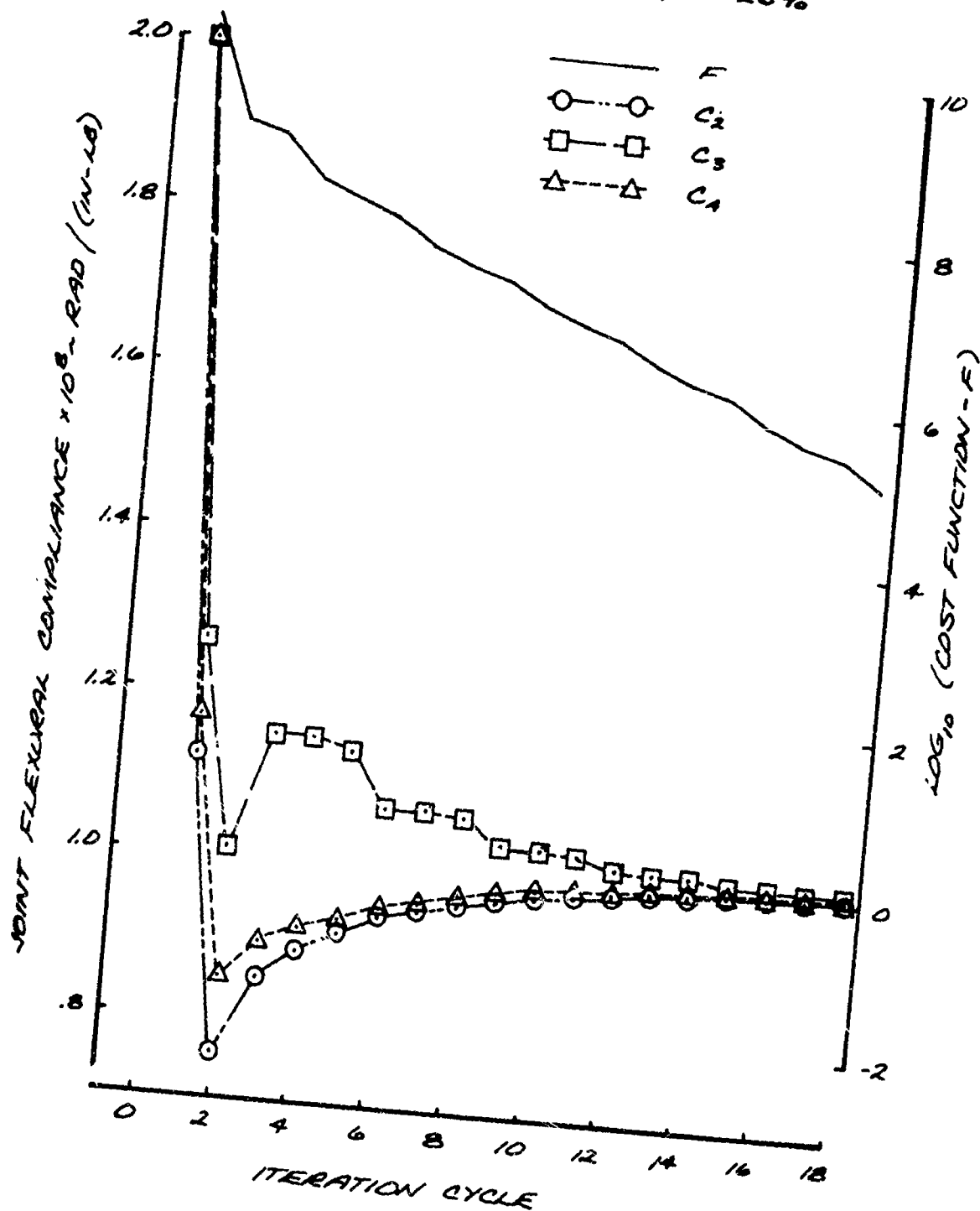


FIGURE 4-3

NON-UNIFORM BENDING BEAM
SOLUTION FOR THREE JOINT COMPLIANCES
USING TWO MODES, $\nu = 1\%$

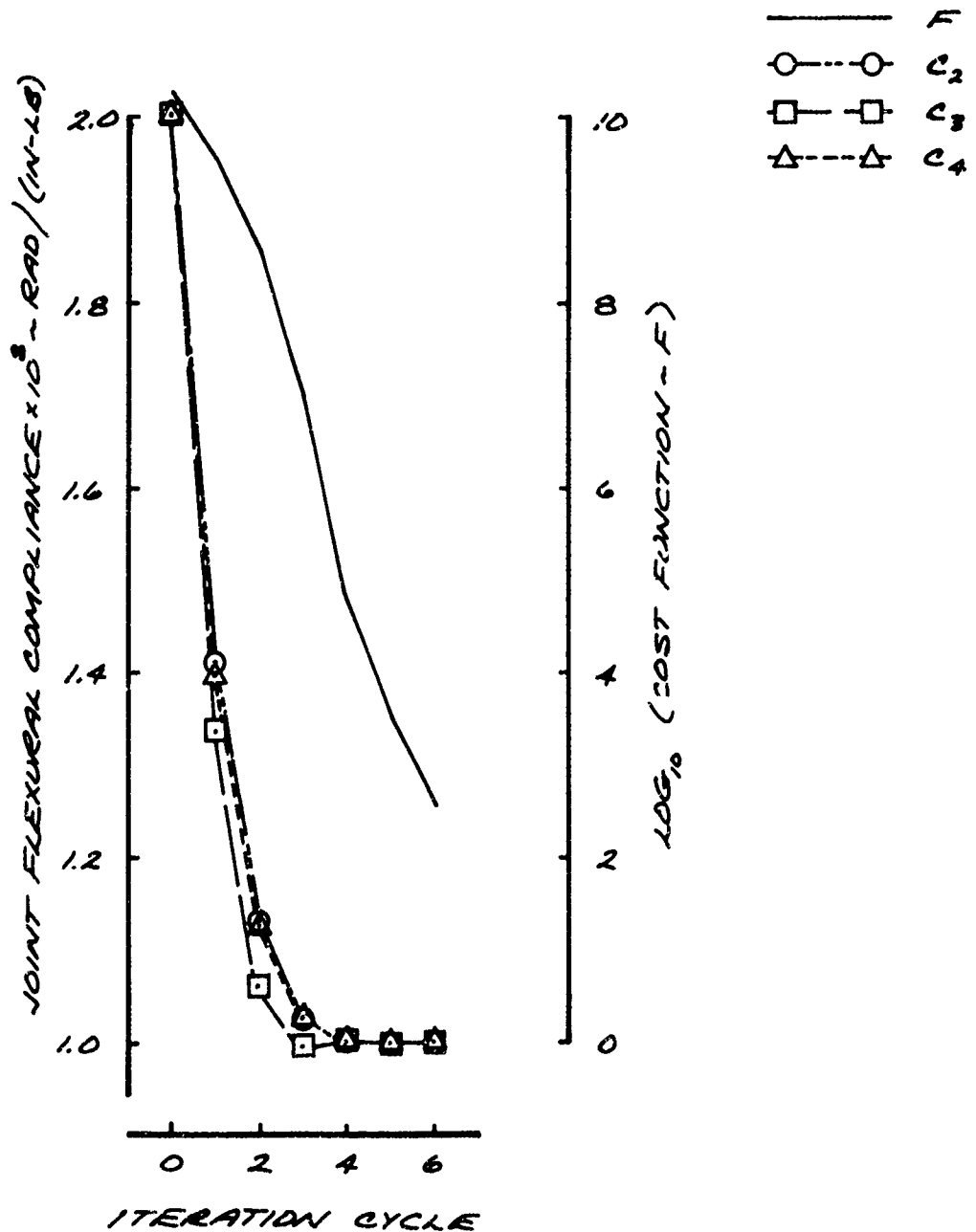


FIGURE 4-4

NON-UNIFORM BENDING BEAM
CONVERGENCE VS. INTERMEDIATE STEP SIZE - r
SOLVING FOR THREE JOINT COMPLIANCES
USING TWO MODES

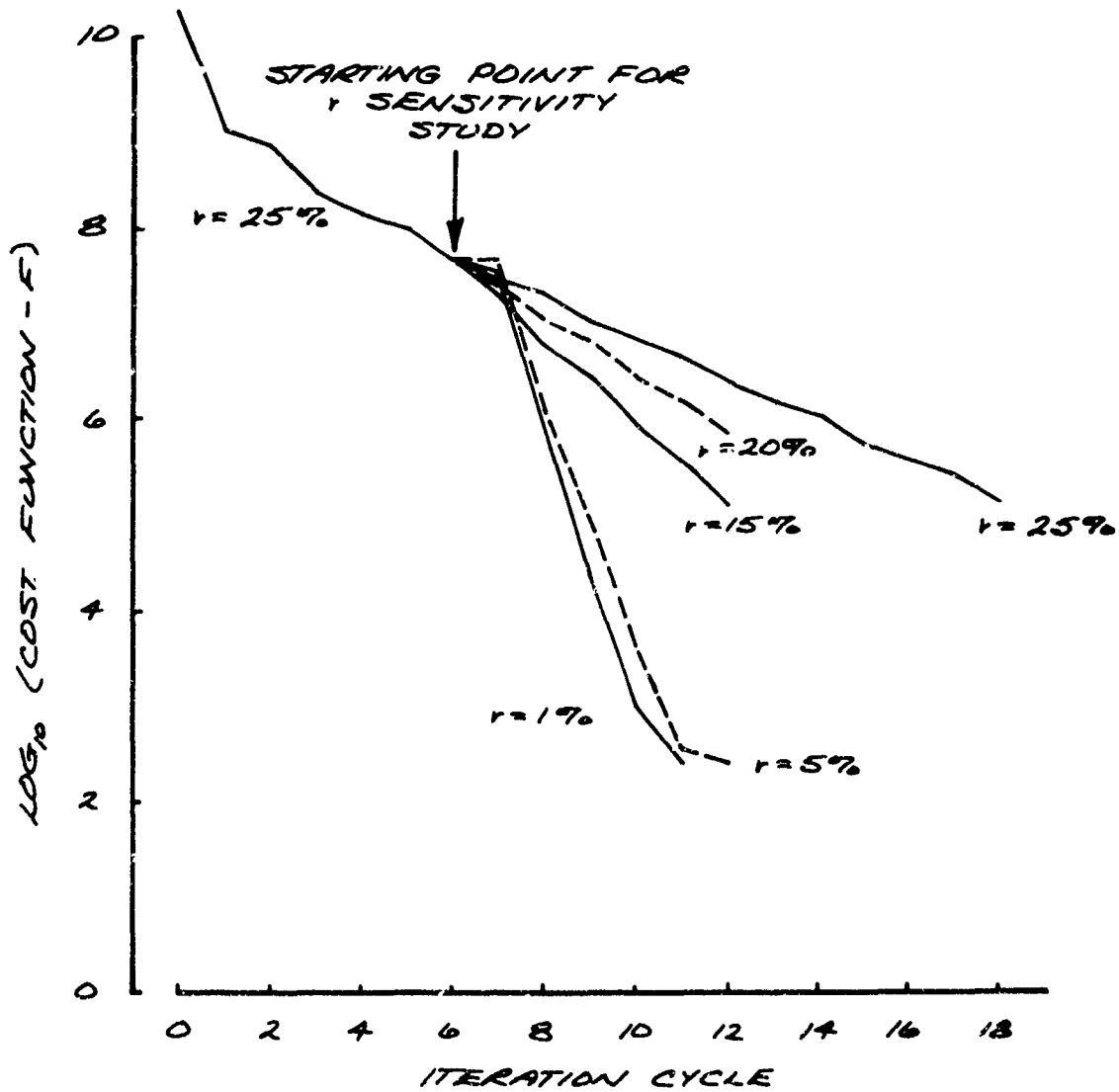


FIGURE A-5

TACTICAL MISSILE MEASURED BENDING MODES

FIRST MODE $f_E = 59.3 \text{ Hz}$

○ AIRFRAME DATA

△ APPENDAGE DATA

— PROGRAM FILIN CURVE FIT

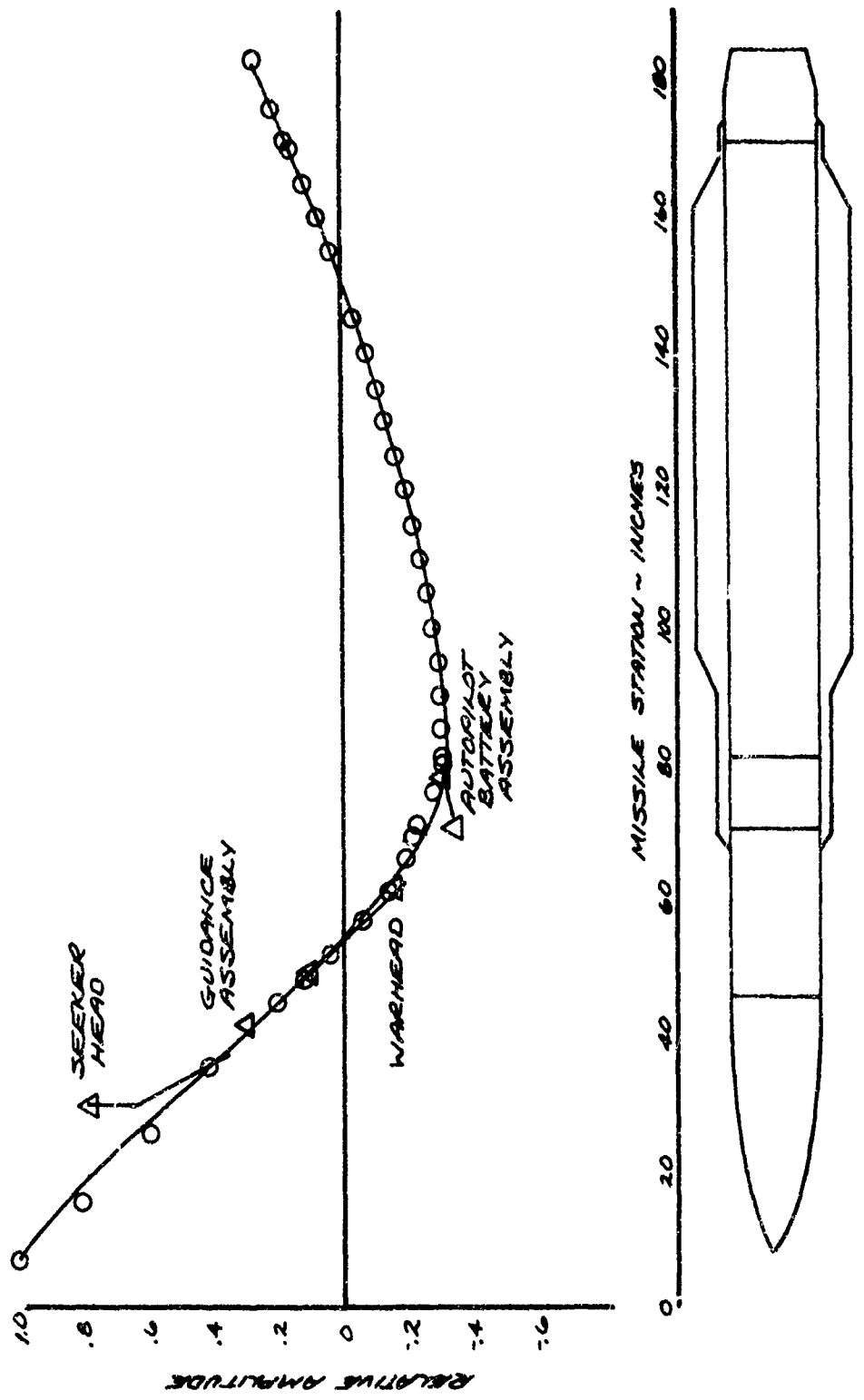


FIGURE A-6

TACTICAL MISSILE MEASURED BENDING MODES
SECOND MODE $f_R = 116 \text{ Hz}$

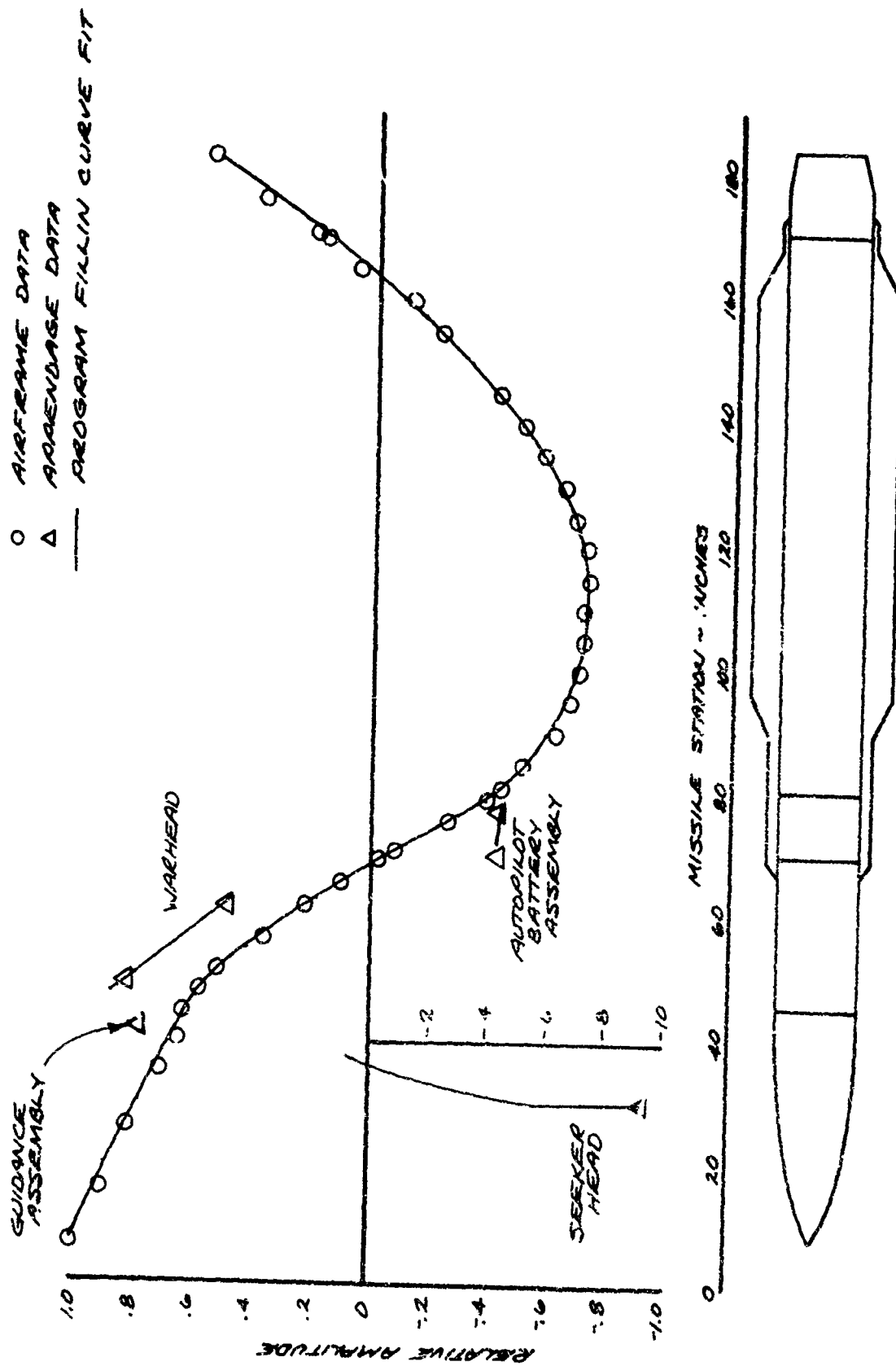


FIGURE 4-7

TACTICAL MISSILE MEASURED BENDING MODES
THIRD MODE $f_E = 153$ Hz

- AIRFRAME DATA
- △ APPENDAGE DATA
- PROGRAM FIT IN CURVE FIT

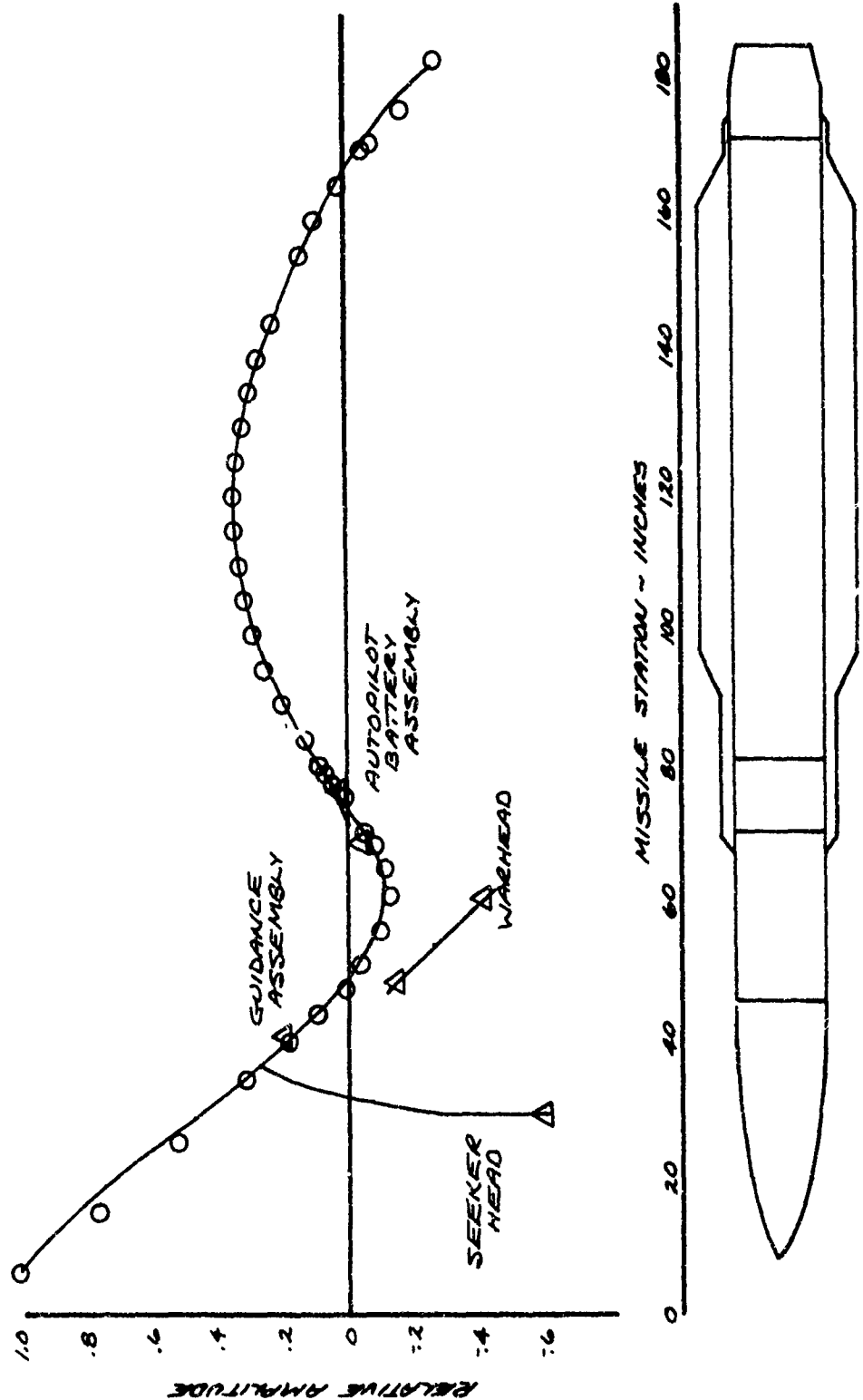


FIGURE 4-8
TACTICAL MISSILE APPLICATION
SOLUTION NO. 1
EQUAL WEIGHTING FACTORS

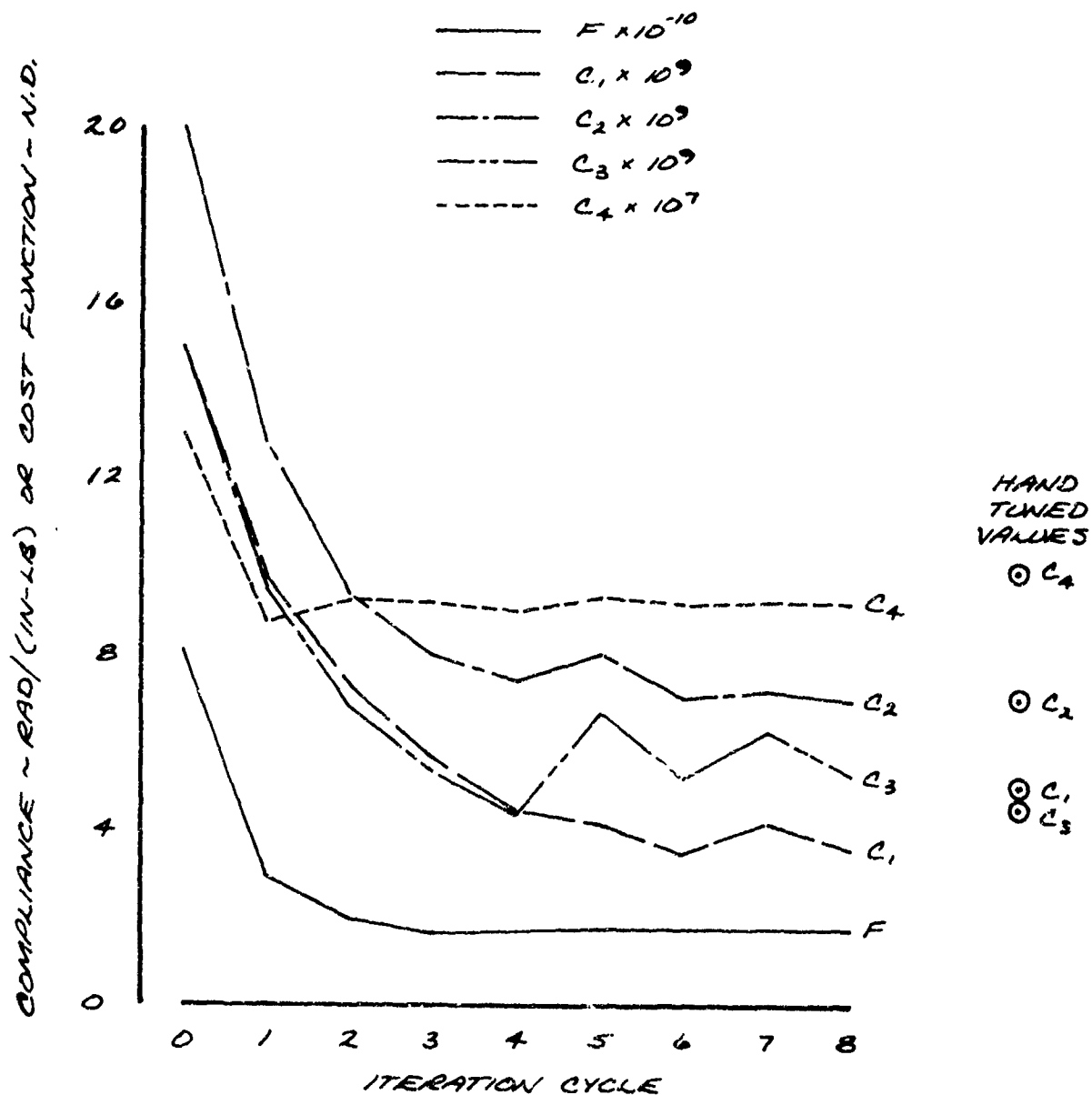


FIGURE 4-9

TACTICAL MISSILE APPLICATION
COMPARISON OF EXPERIMENTAL AND THEORETICAL FIRST MODES

— THEORETICAL, $f_T = 59.5$ ME
O, Δ EXPERIMENTAL, $f_E = 59.3$ ME

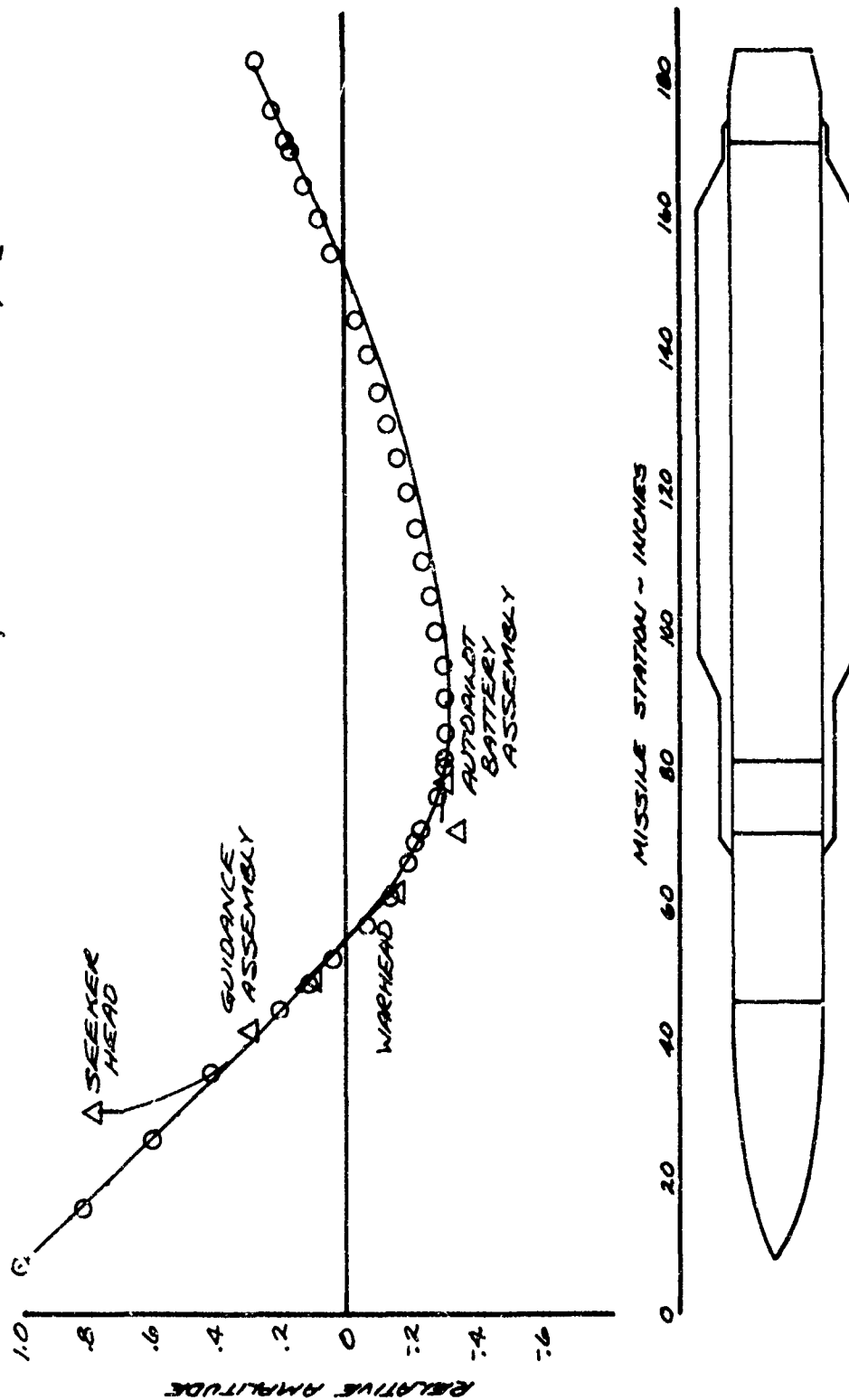


FIGURE A-10

TACTICAL MISSILE APPLICATION
COMPARISON OF EXPERIMENTAL AND THEORETICAL SECOND MISSILES

— THEORETICAL, $F_T = 114.4 \text{ ME}$
O, Δ EXPERIMENTAL, $F_E = 116 \text{ ME}$

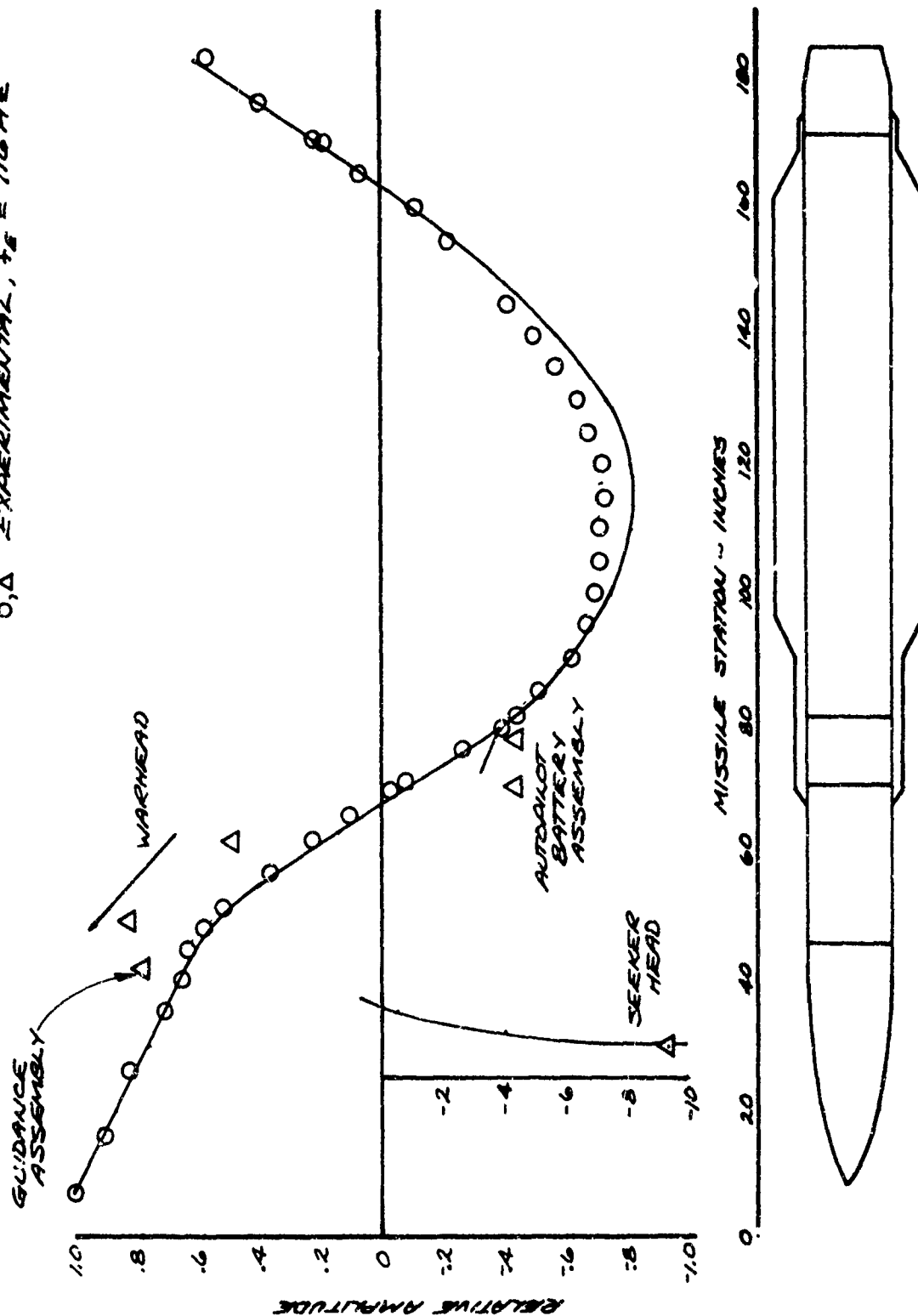


FIGURE 4-11
TACTICAL MISSILE APPLICATION
COMPARISON OF EXPERIMENTAL AND THEORETICAL THIRD MODES

— THEORETICAL, $f_T = 154.2 \text{ Hz}$
O, Δ EXPERIMENTAL, $f_E = 153 \text{ Hz}$

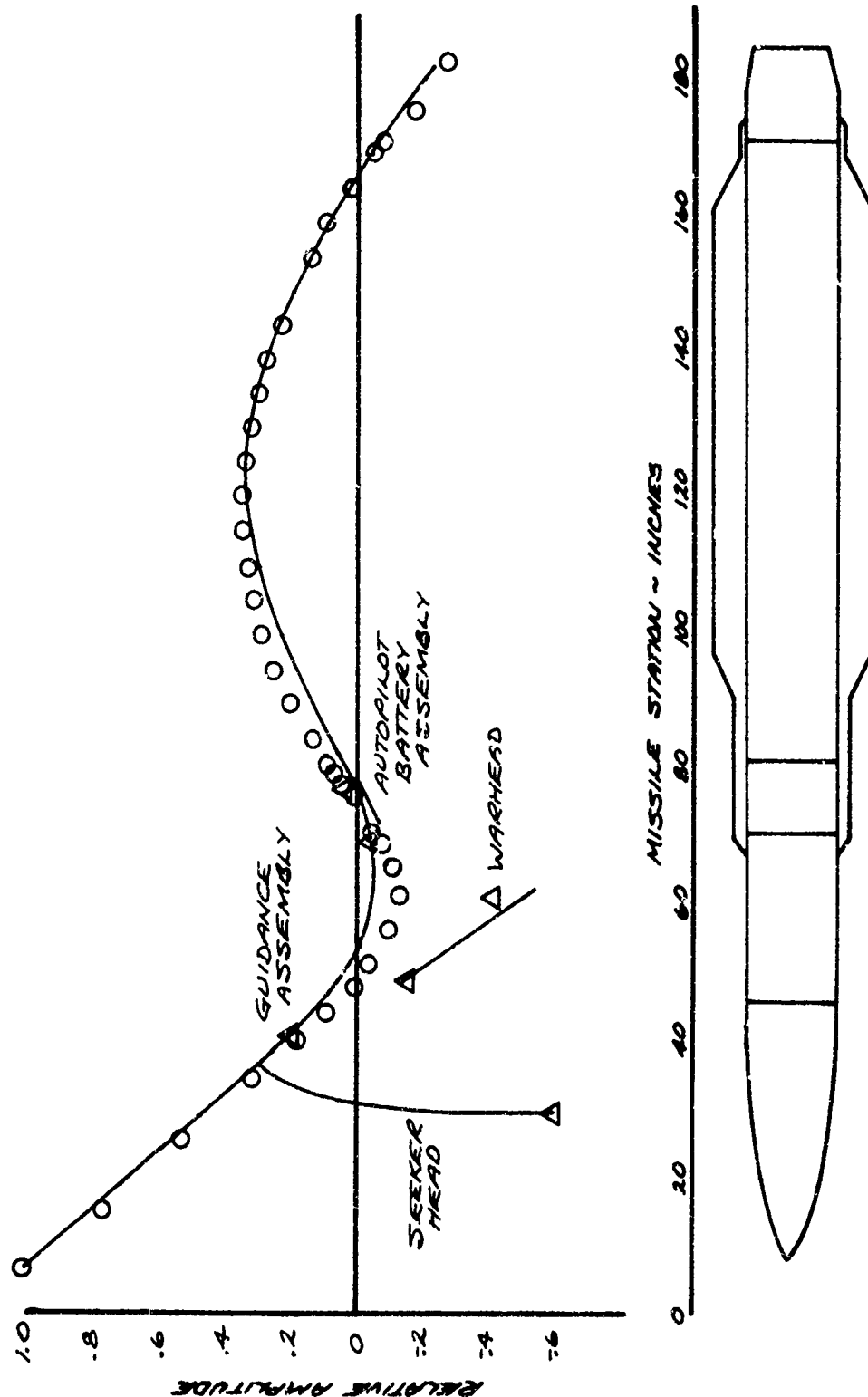
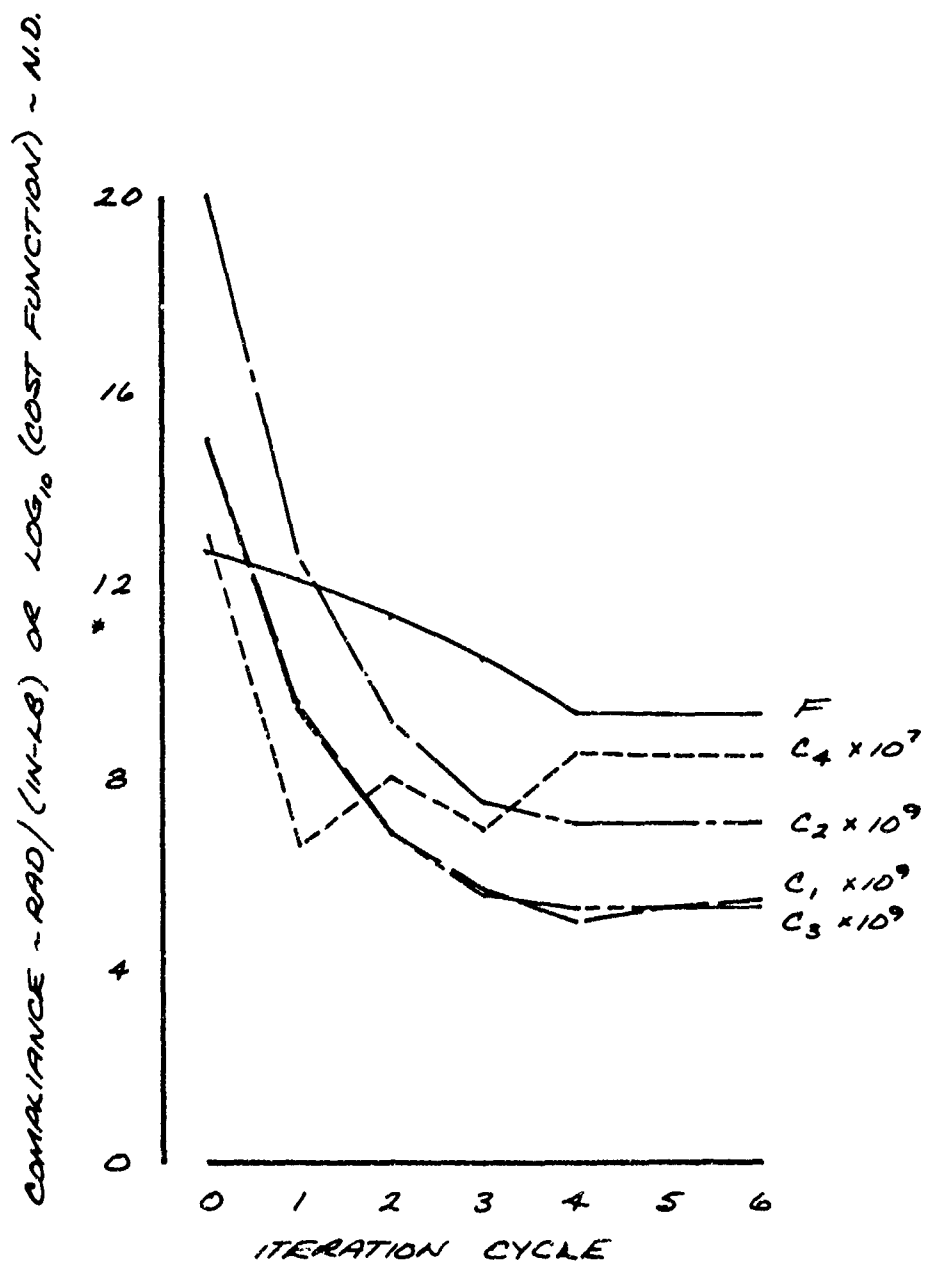


FIGURE 4-12
TACTICAL MISSILE APPLICATION
SOLUTION NO. 2
UNEQUAL WEIGHTING FACTORS



Section 5.0

MISSILE JOINT SELF INDUCED VIBRATION

Tactical missile airframe joints can become significant sources of mechanical shock and vibration under transient loading conditions which exceed mating surface interface preloads. If mating surface separation and impact occurs, shock transients generated at the interface will propagate from the airframe joints throughout the missile structure. Under oscillatory loading conditions, the repetitive shock transients - modified by strain wave reflections - often assume the appearance of broadband vibration when monitored at missile components.

One obvious potential problem area with noisy joints can occur in laboratory sinusoidal vibration testing where the test conditions are specified in terms of displacement or acceleration input at the test fixture/specimen interface. Since only the fundamental input levels at the excitation frequency are usually controlled, a significant overtone can result from uncontrolled broadband vibration induced by mechanical joint interface impact.

The vibration environment source characteristic can also be of concern in the case of air launched missiles which are often exposed to many captive flight hours. Excitation of comparatively low frequency aircraft and missile modes by aerodynamic turbulence and/or buffet may result in the secondary generation of high frequency vibration due to mechanical interface impact within missile airframe joints and in some instances at aircraft interface contact points such as sway brace pads and lugs.

Recent tactical missile flight vibration measurements, furthermore, provide suspicious evidence that for some current missile designs the joints may be a prime contributor to missile flight vibration and shock environments. If this premise is valid, then improvements in missile joint design may yield significant reductions in environmental exposure and support cost saving relaxations in environmental specifications.

This section presents the results of an exploratory investigation of the mechanism of joint self induced vibration and an initial evaluation of possible methods for control and suppression. The scope of the investigation has included tests of both full scale actual missile joints and an idealized subscale joint model. A design concept for a joint interface treatment to suppress self induced vibration involving flame deposited teflon was developed in missile section level testing with sufficient promise to warrant missile round level flight test evaluation. Test results from both laboratory section level (encouraging) and flight missile level (inconclusive) are reviewed and discussed. Due to the inconclusive results obtained in the missile level testing, a sub-scale

idealized joint model was designed with the objective of isolating and controlling some of the more elusive full scale test parameters. The model test results, while exhibiting some scatter, do show consistent trends and a significant improvement in joint preload, damping, and mechanical noise reduction when a teflon coating is present at the model joint interfaces.

More work clearly remains to be done in this area. The investigation thus far has shown that joint interface impact can be a powerful source of broadband vibration and that interface coatings can effect a substantial improvement in joints exhibiting these characteristics.

5.1 FULL SCALE LAB TESTS

The full scale joint designs selected for consideration in this study include a discontinuous land ring joint shown in Figure 5-1 and a continuous split ring joint shown in Figure 5-2. Both of these joints are highly compliant (rated about 'moderate' under the classification basis discussed in Section 2.0) with comparatively low interface contact preload (estimated to be approximately 12 pounds/inch) under design assembly torques. The low preload is best illustrated by the fact that in one tactical missile application, with the discontinuous land ring joint, the assembly preload is well exceeded in a one g environment; i.e. the static moment produced by the missile structure forward of the joint is nearly twice the preload induced moment.

Ring joints of this type have consistently demonstrated a capacity for generating joint interface impact vibration in section level vibration testing. In one instance of sinusoidal vibration testing of a missile guidance section, a 3g sweep was observed to produce 20g broadband when the fundamental passed through a joint impact resonance.

The initial hypothesis in searching for a fix for this behavior was that compliant material placed on the contacting surfaces of the joint would inhibit metal to metal impact and thus materially reduce the resulting vibration. It was further conjectured that any adverse effect of this compliant material on joint stiffness could be offset by a general improvement in load distribution resulting from filling voids and irregularities in the mating surfaces. Each of the ring joint designs has 3 contacting surfaces - two associated with the ring nut and subject to abrasion as the surfaces slide in contact during assembly, and one where the missile shroud sections butt together. With practical manufacturing tolerances, a perfect fit on the mating surfaces is virtually never achieved. The uncertain and variable load paths due to this feature are viewed as a major contributing factor to both high compliance and noise generation characteristics. Another obviously important parameter is the joint preload, with any increase achieved either through higher assembly torques or reduced friction in the sliding surfaces (threads) being beneficial.

A variety of candidate joint interface materials including epoxy, RTV, plastics, elastomers, and soft metals such as lead and aluminum were selected for evaluation. These materials, in general, were only introduced on the non-sliding surfaces of the joint. Epoxy and RTV were applied also to the sliding surfaces with the expectation that most of the coating would be wiped off points of contact but that some of the voids in the mating surfaces might be filled. The test set-up used to determine the effect on joint self induced vibration, shown in Figure 5-3, consisted of a missile nose section cantilevered from a discontinuous ring joint attached through a test fixture to an oil slide table. The basic test specimen when driven at resonance would exhibit an abrupt increase in broadband vibration when the joint preload was exceeded with the ratio of broadband to fundamental response at the joint exceeding a factor of 8 for one test point. The test was then repeated with each of the joint interface materials using a constant assembly torque and recording broadband (20 5000 Hz) response at the joint for several reference fundamental response levels. Table 5-1 presents the results obtained with the different interface coatings for two dynamic bending moment levels at the ring joint interface. These data should be considered qualitative at best with the test results generally showing poor repeatability with large variations for small changes in test conditions. The exception to this was the Teflon configuration which showed not only the best performance from the standpoint of minimum impact noise but also good repeatability and consistency in subsequent re-tests.

It should be noted that the teflon configuration represented the first effort to coat the sliding surfaces of the joint. Flame deposited teflon has sufficient bond strength on the coupling ring and low friction on the sliding surfaces to remain intact and not be wiped off the contacting surfaces during joint assembly. The low friction on the sliding surfaces in fact undoubtedly accounts for a major portion of the substantial improvement shown for this configuration by producing a large increase in joint interface preload for the same torque. The teflon coating was applied only to the coupling ring, rather than all joint contacting surfaces, not by choice but by expedience since the coating process was performed out of plant. One other potentially important characteristic of the teflon was observed to be an apparent significant increase in effective structural damping for the test specimen, with larger shaker output required for the same bending moment response. Based on these admittedly limited but encouraging results, the use of teflon on ring joint interfaces was concluded to have shown sufficient promise to warrant missile level evaluation.

5.2 MISSILE LEVEL QUALIFICATION AND FLIGHT TEST

A continuing series of test firings for an advanced version of a surface launched missile planned for the Spring of 1973 offered an opportunity for missile level flight evaluation of the effect of teflon coated joints on missile flight vibration. Environmental data obtained

on earlier flights of essentially the same missile airframe with unmodified joints provided a direct basis for comparison. The missile configuration in question employs six primary joints. Three of which are ring joints, two being of the discontinuous land type and one of the continuous split ring type. The remaining three joints are of the tension bolt type, considered to be very stiff and sufficiently preloaded under assembly torques to preclude any separation under flight loads. The missile profile and joint locations are shown in Figure 5-4.

A decision was made to treat only the ring joints and furthermore to confine the teflon coating to the coupling rings, recognizing that one of the interfaces for each joint, as was the case in the lab test configuration, would not be teflon coated. Prior to design release and acceptance for flight of this missile joint modification, several possible issues needed to be resolved in securing a design requalification. This effort included:

1. Proof load tests of the modified joints to demonstrate that the teflon coating had not compromised structural integrity.
2. Creep tests to provide assurance that missile assembly preloads (albeit low in the case of the ring joints) would not be seriously degraded.
3. Further lab evaluation to confirm the expected noise suppression characteristics of the teflon.

One facet of this phase of the investigation was a concerted attempt to devise a means for measuring the interface preload - both for the basic and teflon coated joints. This effort, unfortunately, was largely unsuccessful, precluding definition of this important parameter which would have been particularly useful in interpreting dynamic response and creep characteristics. Proof loads were successfully applied to the joints in question without incident, and the creep issue was qualitatively resolved by retorquing control joints after suitable aging and noting that no relative motion of the joint coupling ring occurred.

Joint impact noise suppression tests were carried out using essentially the same test set-up shown in Figure 5-3. In this case, however, three different test fixtures were required to represent the three different joint locations on the missile airframe. The test results for the three joints are plotted in Figure 5-5 in terms of noise suppression achieved by the teflon coating versus the basic joint noise factor, with these parameters defined as follows:

- g_F = in-plane fundamental response at the joint
 g_{BB} = in-plane broadband response at the joint (20-5000 Hz)
 $g_N = \bar{g}_{BB} - \bar{g}_F$ = in-plane noise at the joint
 (g_N/g_F) = joint noise factor
 $(g_N/g_F)_T / (g_N/g_F)_B$ = joint noise suppression factor - a ratio of
 teflon coated joint noise factor to basic joint
 noise factor.

The test results obtained in this series showed considerably less improvement in joint noise characteristics with teflon coated coupling rings than had been observed in the earlier testing. Previous lab data for Joint 1 are shown for comparison. Joint 3 at low response levels was "quieter" in the basic configuration than with teflon for the one specimen tested, although the performance of the teflon configuration improved rapidly as the excitation level was increased. Data points connected by straight lines in Figure 5-5 reflect the two different response levels for the same joint. These data would appear to indicate that "quiet" joints do not admit much improvement while considerable benefit from the teflon coating might be expected with "noisy" joints.

Since the teflon coated rings had satisfactorily passed all design qualification requirements, the configuration was released for flight test evaluation. A total of four instrumented test flights were made with complete data acquisition. From the standpoint of showing an improvement attributable to the teflon coated coupling rings, however, the flights were uniformly disappointing being virtually indistinguishable from the earlier flight series with the basic unmodified joints.

Possible interpretations of this test outcome include:

1. The importance of coating all three joint interface surfaces rather than just two may have been underestimated. Lab testing could have been misleading in this respect if excitation levels relative to joint preloads were not representative of the flight conditions.
2. Joint impact may not be a significant contributor to the flight vibration environment for this missile configuration. In this case, improvements in the joint response characteristics would not have been noticed.

In hopes of answering some of the questions associated with joint self induced vibration, an idealized ring joint model which would admit more precise measurements of the critical parameters was designed and tested.

5.3 JOINT IMPACT MODEL DESIGN AND TEST

The ideal test specimen for joint impact modeling was visualized (as in previous joint investigations) as a simple uniform structure with a single ring joint replica at the mid-span. Free-free boundary conditions would be used to avoid uncertainties in support constraints. As a result, the primary joint characteristics of interest (compliance, damping, impact noise generation) would dominate and be deducible from the test specimen dynamic response. The model joint replica design, while permitting considerable simplification, was required to simulate all of the important properties of a typical full scale missile ring joint including compliance, low interface preload, and similar assembly and interface contact characteristics. Additionally, the joint replica design approach must provide accurate and reliable means for measuring joint interface preload versus applied torque during assembly and as a function of time during creep investigations.

The joint replica designed to satisfy these requirements is illustrated in Figure 5-6. Joint preload is accomplished through a single strain gaged bolt on the center line of the aluminum test specimen, with this preload reacted circumferentially through a separate joint ring representing multiple joint interface contact surfaces. Interchangeable stainless steel "joint rings" provide a convenient means for investigating the effects of various joint interface materials. The model joint compliance is assumed to be provided primarily by the extensional elasticity of the center axis bolt estimated as follows:

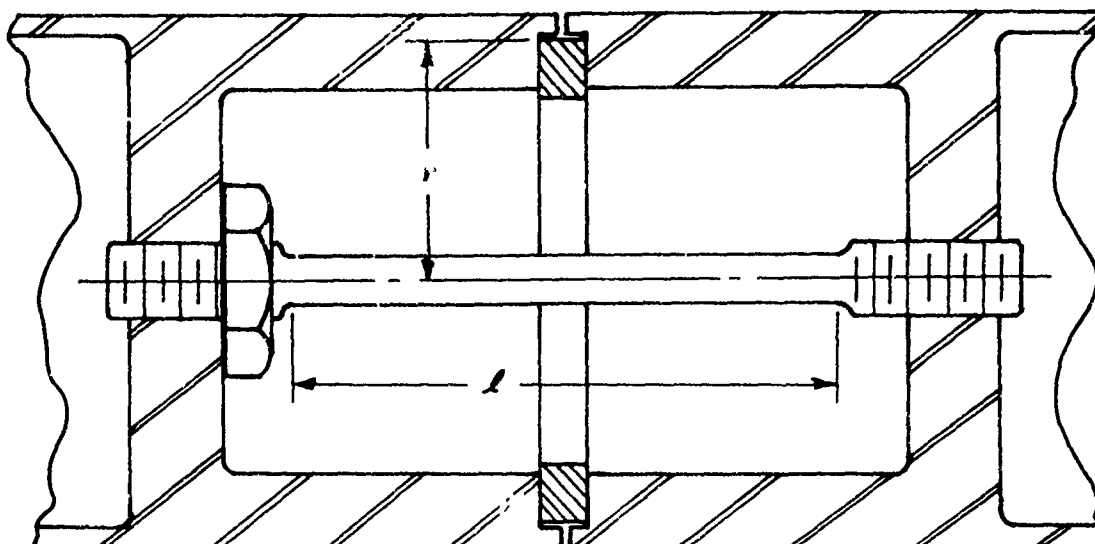
$$C_0 = \frac{l}{r^2 AE} \quad (5.1)$$

where: l = effective spring length, 3".

r = effective radius, 1.265 inches.

E = modulus of elasticity, $30 (10)^6$ #/in².

A = cross sectional area of spring elements, in².



The center axis bolt is locked to one half of the model with a locking nut and the model assembled by applying preselected torques to the other half of the test specimen. The threads on the center axis bolt are lubricated to insure that the primary frictional torques in the joint assembly are associated with the contacting surfaces on the interface ring. The full scale ring joints described in Section 5.2 have estimated compliances ranging from $0.75(10)^{-8}$ to $2.7(10)^{-8}$ rad/in # and fall in the moderate to good joint compliance classification scale. A corresponding range for the model joint compliance was provided by making three center axis couplers with diameters from 1/8 to 3/8 inches. A direct comparison between model and full scale joint compliance is obtained by multiplying the full scale values by the cube of the full scale to model diameter ratio as follows:

CONFIGURATION	$C_{\theta}(10)^6$ Rad/In #
Full Scale $\times (D_F/D_M)^3$.88 - 3.2
Model	.57 - 5.1

Where: D_F = Full scale Missile Diameter, 13.5 inches

D_M = Model Diameter, 2.75 inches

5.3.1 Model Joint Preload. The relationship between joint preload - measured by strain gages on the center axis tension bolt - and applied torque was investigated for three joint interface coatings in addition to the basic clean dry joint. The results of these measurements are shown in Figure 5-7. The teflon coating, approximately 3 mils thick,

was flame deposited by an application process identical to that used on the full scale rings discussed in Section 5.2. The Molybdenum Disulfide (MDS) Dry Film was applied using an aerosol spray; and the Silicon Grease, DC-4, was directly wiped on the joint interface surfaces. A thorough cleaning of the joint interfaces with solvent was performed between each test of a different coating material.

Both of the lubricants, MDS and DC-4, resulted, as might be expected, in a fairly significant increase in joint preload, ranging from 60 to 100 percent. The teflon coating, however, produced the largest increase in joint preload with a consistent and repeatable gain of greater than 5 over the basic unlubricated joint.

Teflon has a well recognized tendency to cold flow under load. To assess the implications of this behavior on the preload of a joint with teflon on the interface surfaces, a preload of 600 pounds was applied to the model joint and found to have been maintained with virtually no change after 64 hours. The estimated loading on the teflon for this condition was 318 psi, assuming uniform distribution over the joint interface.

5.3.2 Model Vibration Test Setup and Results. A sketch of the test setup used to evaluate the dynamic response characteristics of the ring joint model is shown in Figure 5-8. A free-free suspension was employed with the model oriented vertically to avoid any gravity moment bias on the joint. Force excitation was provided by an MB Electrodynamic Shaker, rated at 50 pounds peak force capability, monitored by a force gage at the input station on the test specimen. Triaxial response (acceleration) was monitored at the top end of the specimen to establish a total response reference, and both force and in-plane acceleration at the input station were monitored to provide a basis for estimating system damping. Although vibration induced by joint interface impact is propagated in all response coordinates, the longitudinal response (\ddot{x}) was concluded to provide the primary and most sensitive measure of joint impact induced response. The impact forcing function is assumed to be impulsive in nature with primary excitation at twice the transverse mode frequency with the response distributed over a broad frequency spectrum. Total impact induced noise was interpreted as the rms vibration over a 20-5000 K Hz bandwidth measured in the longitudinal coordinate (\ddot{x}) at the response station on the test specimen. This broadband vibration level was then normalized by the vector sum of the inplane and crossplane transverse response at the excitation frequency to establish a noise ratio for the particular test condition.

Table 5-2 presents response data for the basic configuration with uncoated metallic surfaces at the joint interface. Test parameters include variations in both joint preload and excitation level. Estimates of system damping shown are based on calculated generalized mass and

generalized force in the model response. The general trend is for frequency to increase with response level. Corresponding data for the test specimen with teflon at the joint interface is presented in Table 5-3. Considerable scatter in the response parameters is shown for both configurations at the lower preload and excitation levels, reflecting the nonlinearities and cross coupling in the test specimen response. The two higher values for joint preload used with the teflon configuration (200 and 400 pounds) are intended to represent a conservative estimate of the preload increase which would be realized over the basic configuration (50 to 100 pounds) for the same assembly torque. Particularly noteworthy is the fact that the teflon configuration at the higher preload levels exhibits pronounced decreases in impact noise ratio accompanied by significant increases in resonant frequency. The predicted relationship between test specimen 1st mode frequency and effective joint compliance is shown in Figure 5-9. Upper bound frequency test points are shown for the basic configuration assembled with 50 to 100 pounds for comparison with the teflon configuration assembled first with equal preload (50 to 100 pounds) and then with "equal" torque (200 to 400 pounds preload). Table 5-4 presents a comparison of the basic and teflon configuration response based on an arithmetic average of all test data with the following conclusions:

1. For comparable preloads, the teflon coating on the model joint interface reduced joint impact vibration by an average factor of greater than 2 while increasing mode damping by an average factor of greater than 2.
2. For comparable assembly torques, the teflon configuration reduced joint impact vibration by an average factor of nearly ten while maintaining and slightly increasing the improved damping attributed to the teflon. Additionally, the effective joint stiffness was found to be nearly a factor of 3 greater than the basic joint for the same torque, presumably because of the significantly higher joint preload realized with teflon.

5.4 FULL SCALE IMPLICATIONS OF MODEL TEST RESULTS

1. Joint interface impact can be a significant source of self-induced vibration.
2. The vibration generation mechanism requires physical separation at the joint interface for impact to occur.
3. Corrective measures would appear to include increasing preload to avoid interface separation and/or coating the impacting surfaces with a compliant material to attenuate the response.
4. Teflon as a candidate material for joint interface treatment has been shown in idealized model tests to produce a

substantial improvement in joint preload, reduction in self-induced vibration, and increase in joint contribution to structural damping.

5. Conflicting and mixed results obtained with partial teflon treatment of full scale noise susceptible joints are suspected to have been caused by neglecting to coat all of the primary joint interface surfaces.
6. The results to date in exploring joint interface coatings have shown some encouraging trends. Many questions remain unanswered, however, and more work is clearly needed before practical applications can be considered in actual missile structure.

Table 5-1
Measured Noise Ratios for Discontinuous Land
Joint with Different Surface Treatments
Constant Assembly Torque 4500 in #

Config.	Application	Response Level (1)	Noise Ratio (2)
Basic	Dry Film Lube (MDS) on All Surfaces	1	3.37
		2	8.30
Epoxy	All Surfaces (with parting agent) to Fill Voids	1	1.36
		2	5.45
RTV	All Surfaces	1	1.19
		2	2.62
Lead	Foil Tape on Non-Sliding Surfaces Only	1	1.35
		2	2.52
Aluminum	Foil Tape on Non-Sliding Surfaces Only	1	1.70
		2	1.98
Silicone	Thin Sheet Non-Sliding Surfaces Only	1	2.10
		2	2.01
Teflon	Flame Deposited on Coupling Ring Only	1	1.12
		2	1.14

(1) Response Dynamic Bending Moment
 Level Induced at Joint

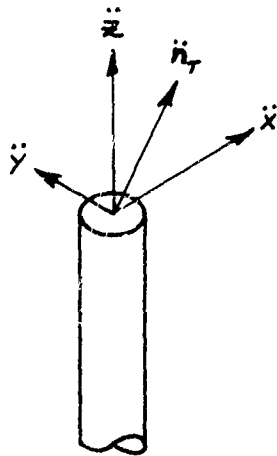
 1 3000 in #

 2 5000 in #

(2) Noise ratio defined as ratio of broadband
 response to fundamental response (g_{BB}/g_F)

Table 5-2
Basic Joint Model Dynamic Response

Preload #	Freq f_1 hz	\ddot{n}_T g's	% Cross Plane	Noise Ratio	Damping ξ
50	101	9.9	110	.19	.0078
50	106	16.7	117	.66	.0077
50	103	22.2	119	.72	.0049
75	107	7.4	93	.11	.022
75	108	18.6	124	.78	.0095
75	108	24.7	116	.63	.0079
100	110	9.9	108	1.42	.046
100	113	11.5	86	.45	.017
100	109	20.3	109	.84	.0098



Where:

\ddot{x} = inplane response at f_i

\ddot{y} = crossplane response at f_i

\ddot{n}_T = vector sum $\ddot{x} + \ddot{y}$

\ddot{z} = broadband (20-5000 hz) response

$$\text{Noise Ratio} = \ddot{z} / \ddot{n}_T$$

Table 5-3
Teflon Coated Joint Model Dynamic Response

Preload Comparable to Basic Joint

Preload #	Freq. Hz	g's	% Cross Plane	Noise Ratio	Damping
50	111	8.5	138	.088	.094
	110	18.7	124	.69	.0072
	111	21.0	107	.86	.0055
75	137	7.7	116	.072	.014
	134	8.1	127	.11	.013
	97	11.8	30	.13	.073
	101	18.8	20	.38	.060
100	94	6.1	35	.033	.042
	122	16.3	129	.41	.007
	101	13.5	27	.096	.059
	104	20.4	19	.27	.058

"Torque" Comparable to Basic Joint

Preload #	Freq. Hz	g's	% Cross Plane	Noise Ratio	Damping
200	114	7.9	51	.026	.031
	150	15.2	114	.19	.013
	119	12.4	45	.039	.037
	120	18.5	43	.092	.048
400	153	8.1	19	.031	.034
	151	15.9	22	.063	.053
	143	33.2	27	.048	.049

Table 5-4
Basic/Teflon Joint Model
Dynamic Response Comparison

Configuration	Comparison Basis	Preload Range #	Average Noise Factor	Average Damping ξ
Basic	Reference	50-100	.644	.015
Teflon	Equal Preload	50-100	.285	.032
Teflon	Equal Torque	200-400	.070	.038

Noise Factor Reduction:

Equal Preload $.285 / .644 = .44$

Equal Torque $.070 / .644 = .11$

Damping Increase:

Equal Preload $.032 / .015 = 2.1$

Equal Torque $.038 / .015 = 2.5$

FIGURE 5-1
DISCONTINUOUS LAND RING JOINT

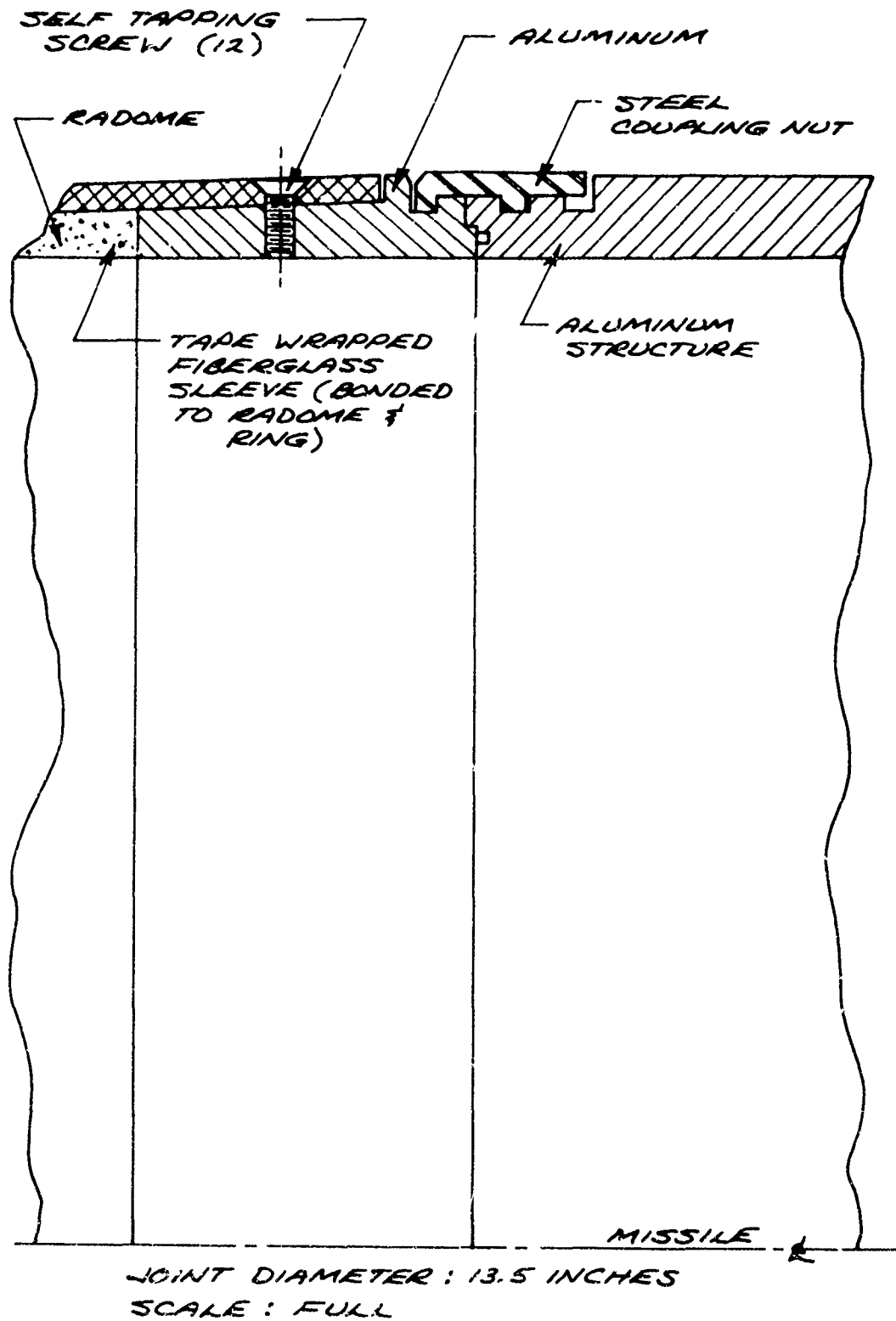


FIGURE 5-2
CONTINUOUS LAND RING JOINT

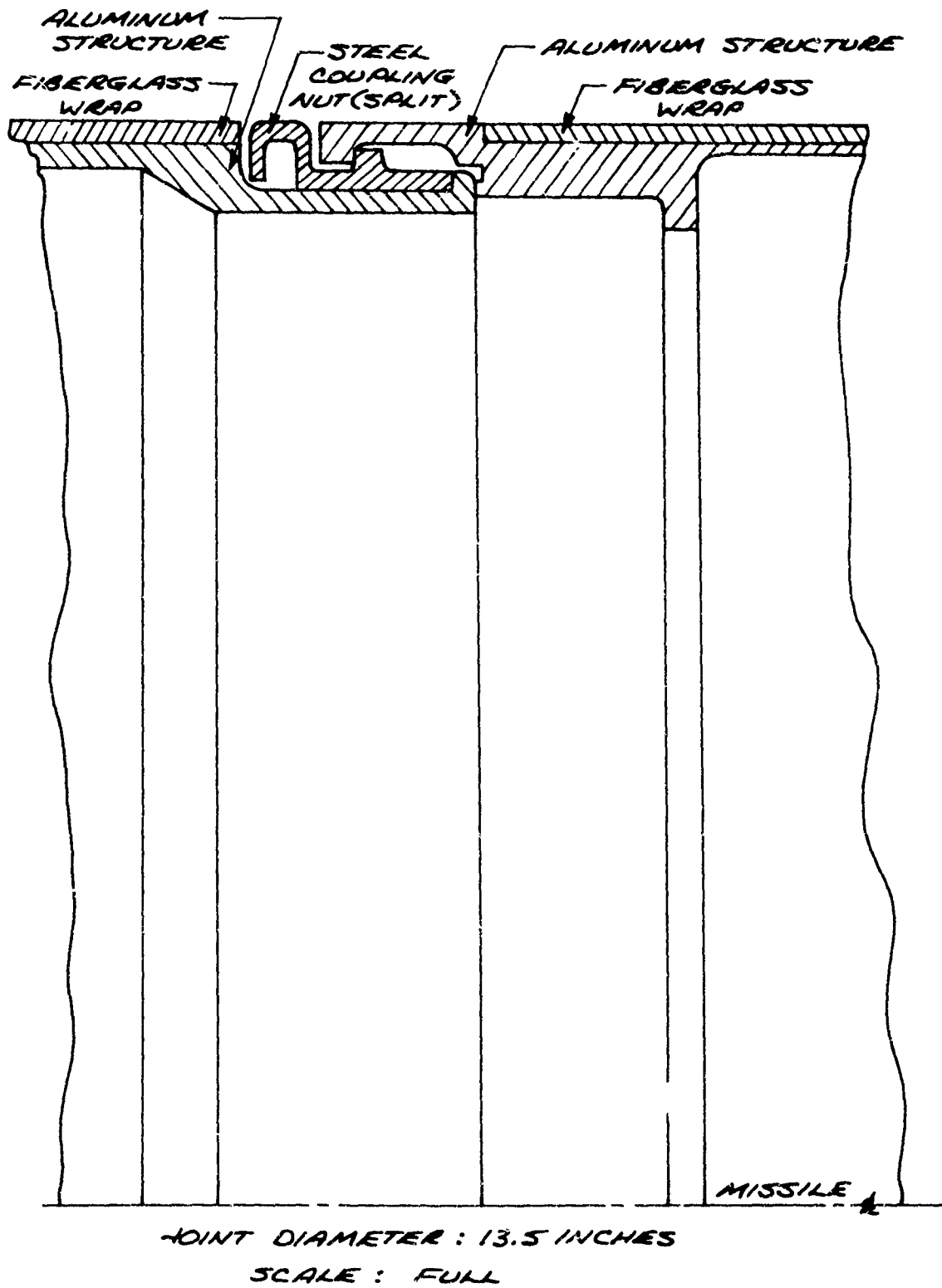


FIGURE 5-3
MISSILE JOINT INDUCED VIBRATION
TEST SET-UP

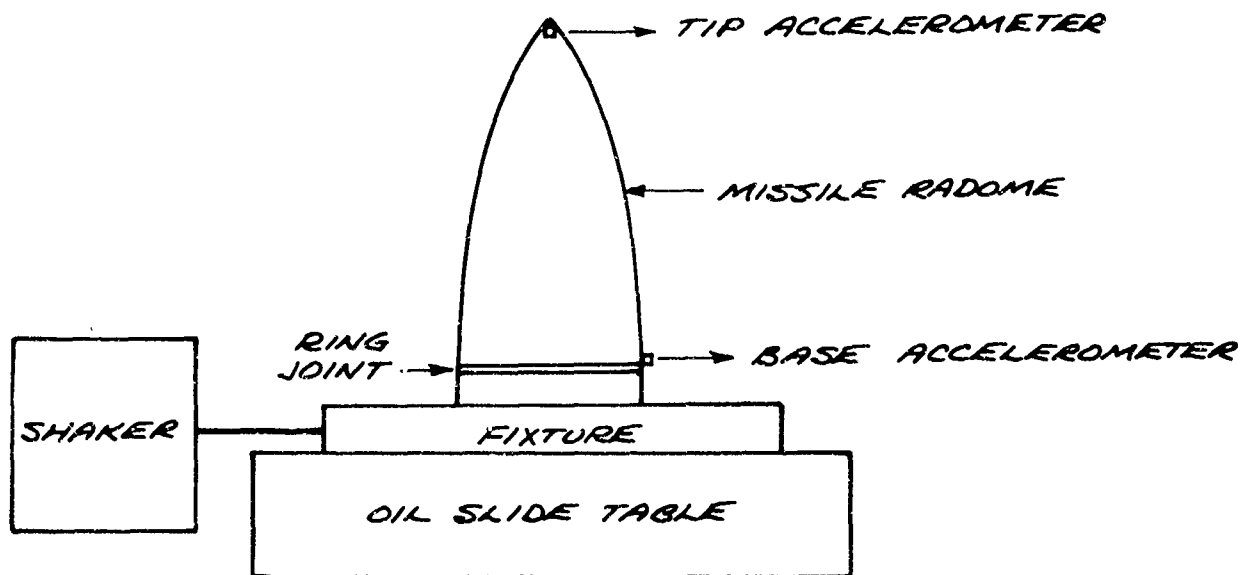


FIGURE 5-4
FLIGHT TEST MISSILE JOINT LOCATIONS

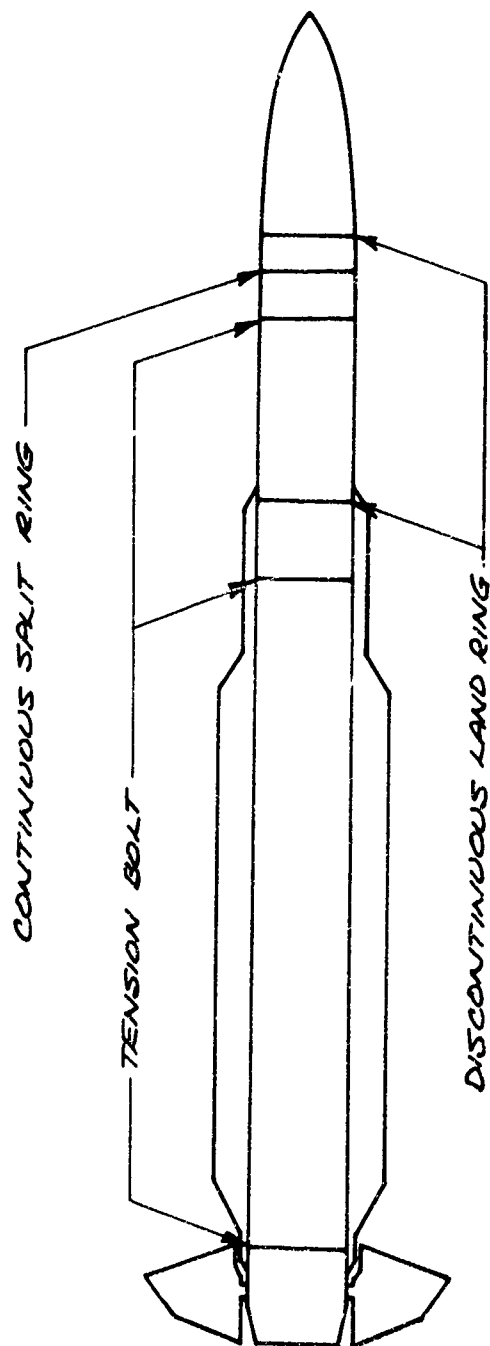


FIGURE 5-5
 TEFLON COUPLING RING
 JOINT IMPACT NOISE SUPPRESSION
 VERSUS BASIC JOINT NOISE FACTOR

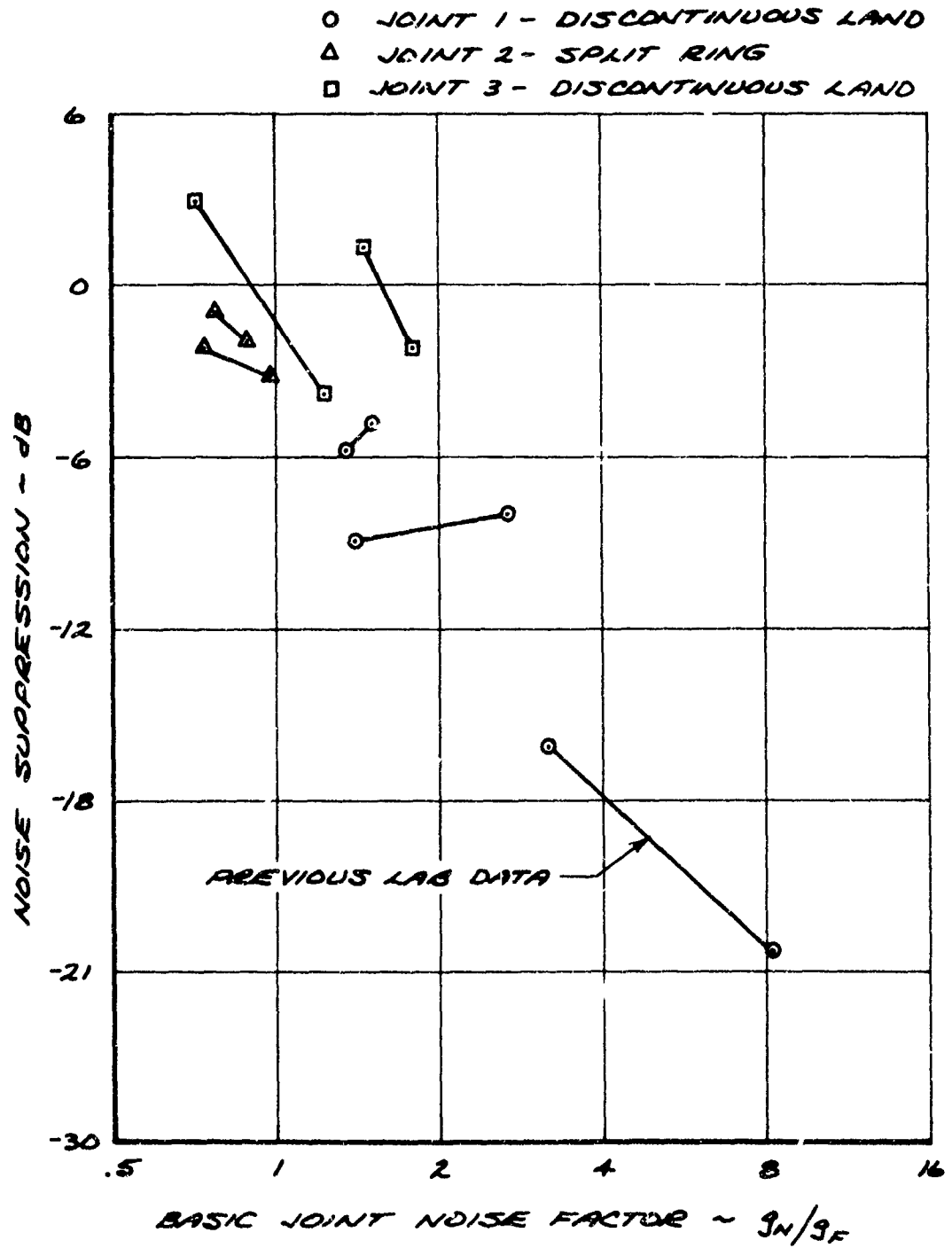
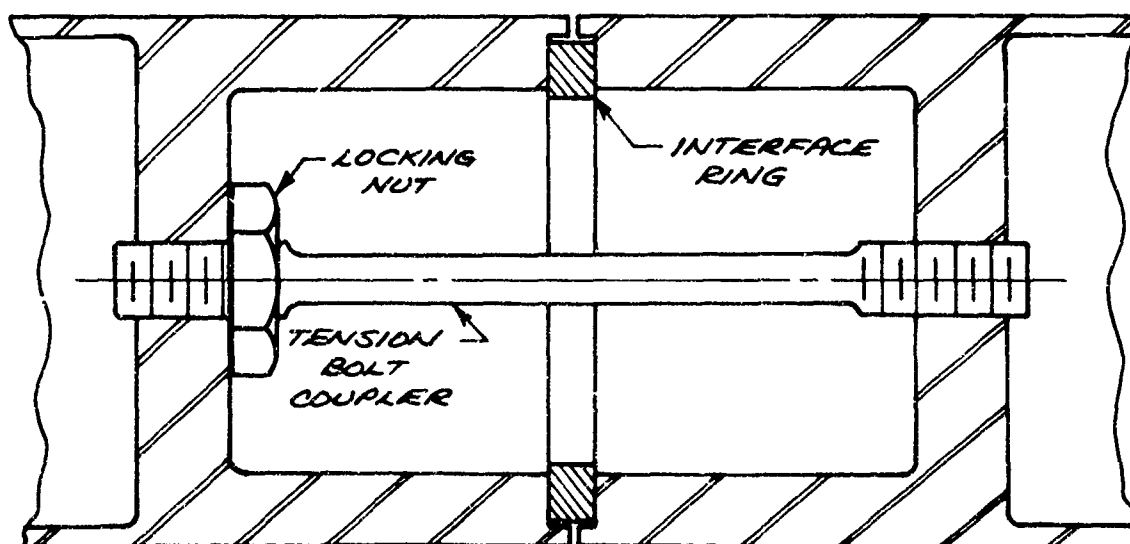
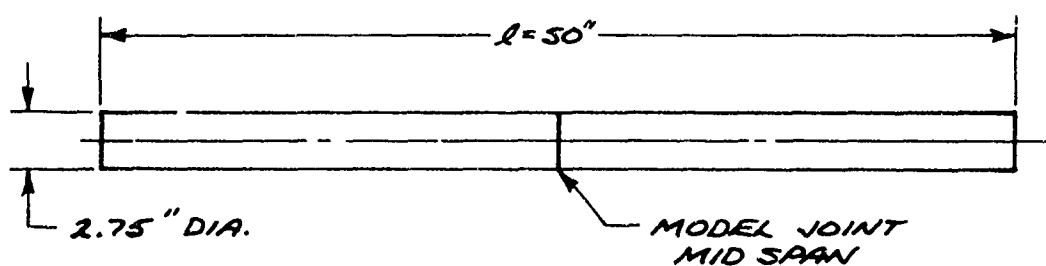


FIGURE 5-6
IDEALIZED RING JOINT MODEL



JOINT CROSS SECTION DETAIL

FIGURE 5-7
SCALE MODEL RING JOINT
PRELOAD VERSUS TORQUE

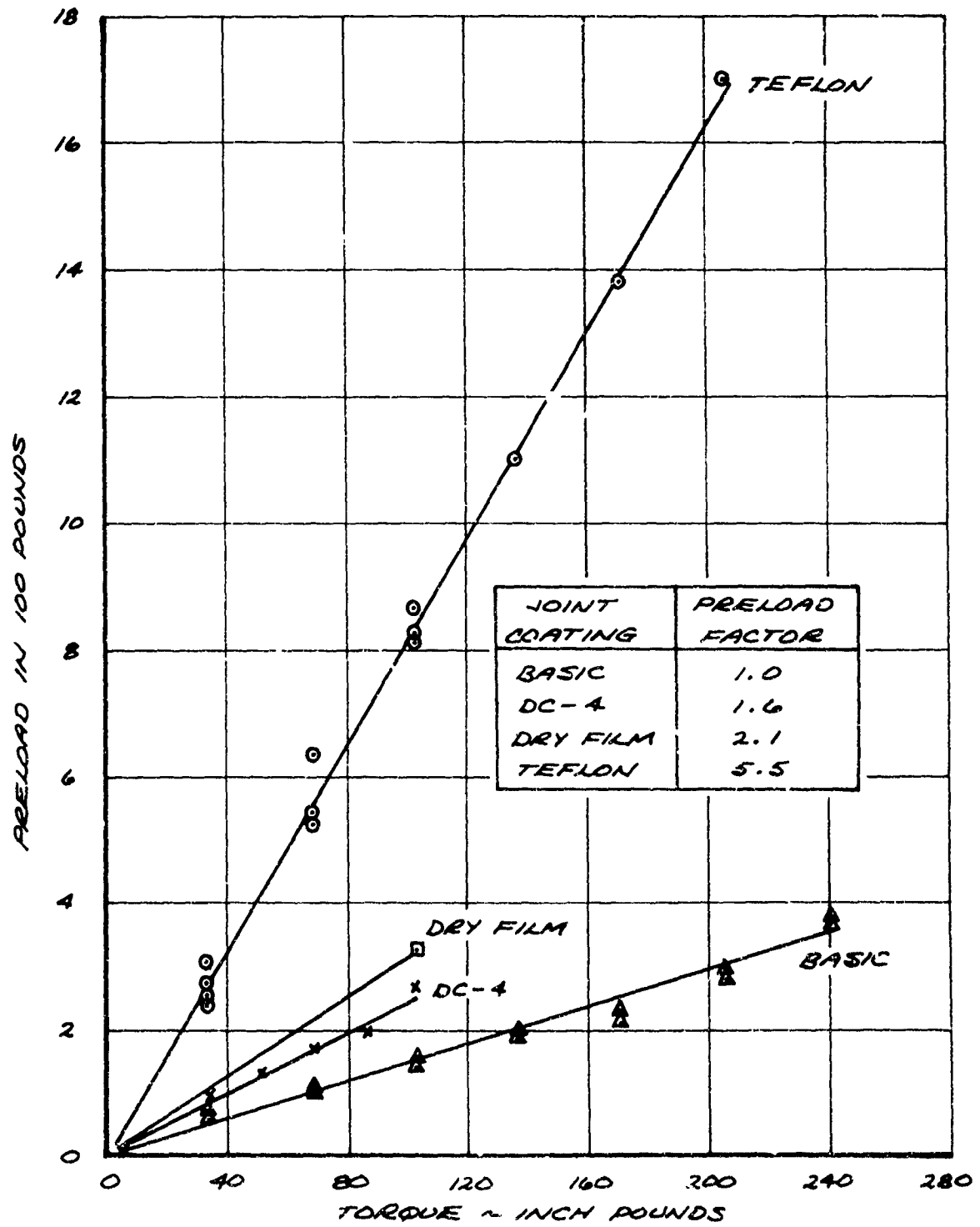


FIGURE 5-8
RING JOINT MODEL TEST SET-UP
(FREE-FREE SUSPENSION)

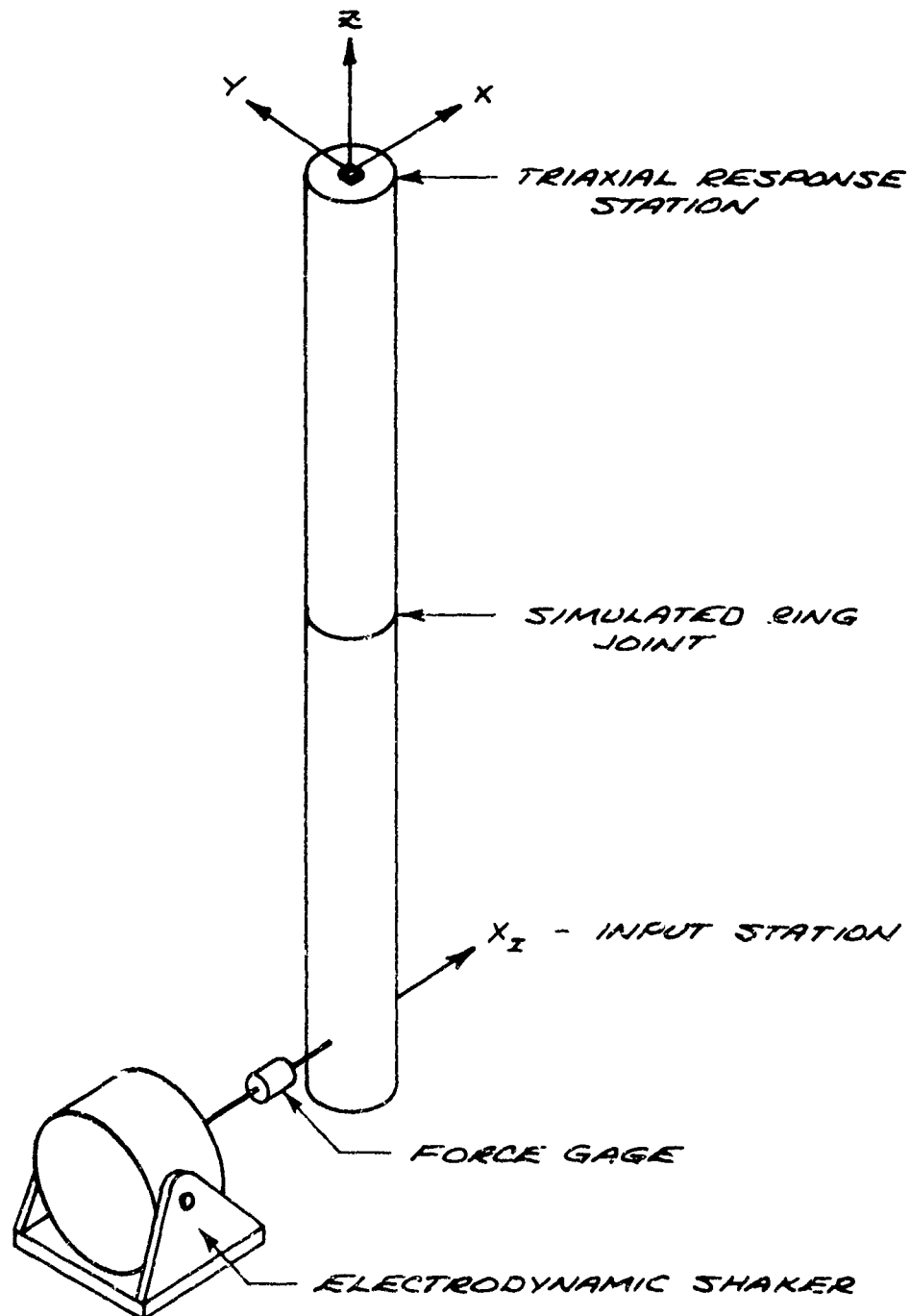
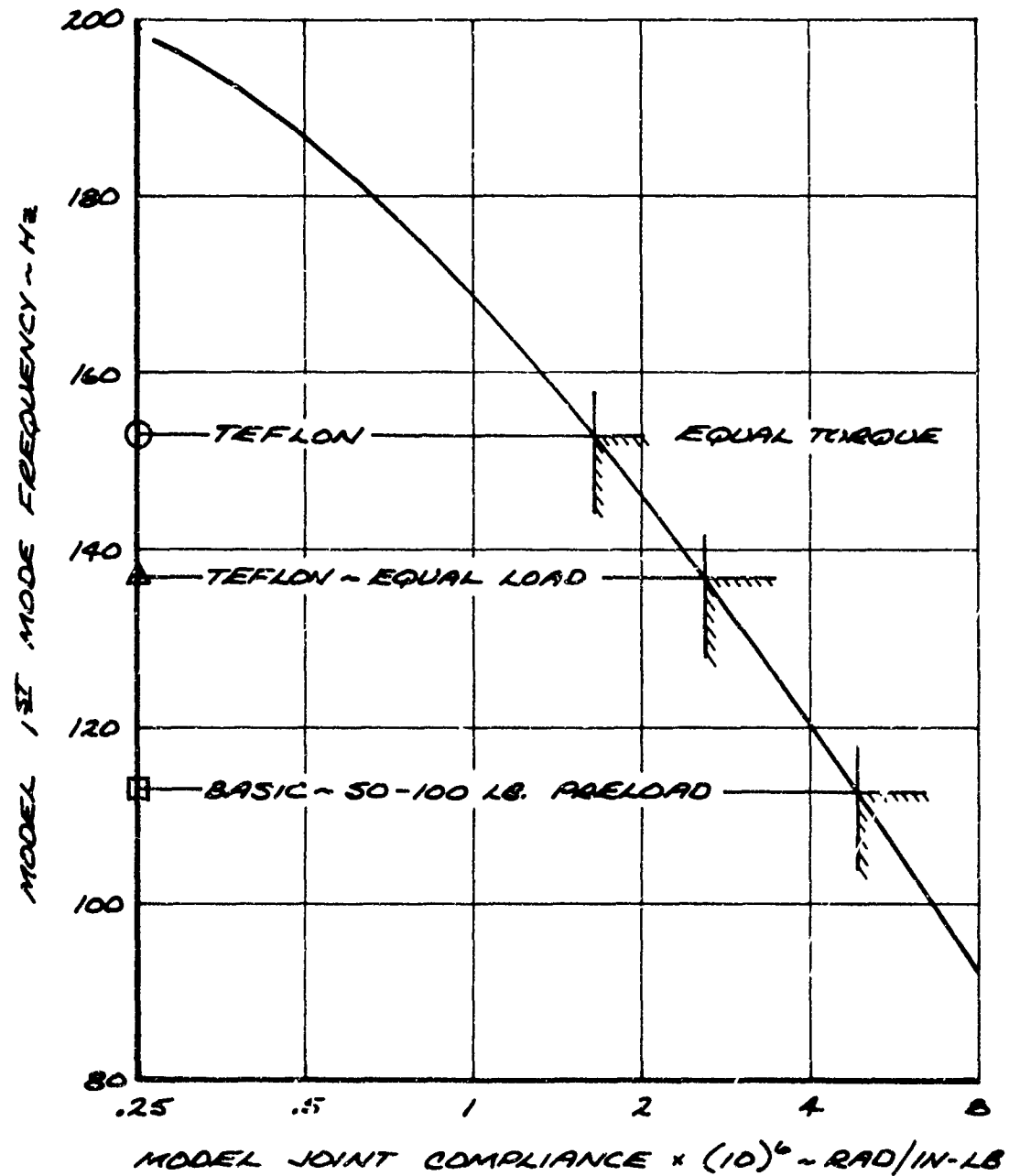


FIGURE 5-9

MODEL 1ST MODE FREQUENCY
VERSUS EFFECTIVE JOINT COMPLIANCE



Section 6.0

INTEGRATION INTO OVERALL SYSTEM REQUIREMENTS

The study thus far has been concerned with structural dynamic characteristics of joints such as stiffness, tightness and damping. There are a number of other characteristics that influence the design of tactical missile airframe joints. These include strength, weight, volumetric efficiency, degree of enclosure, producibility and maintainability. A brief discussion of each of these topics is now presented to provide an overview of airframe joint characteristics.

A rating scheme is then developed which is intended to facilitate the integration of these various characteristics into the overall system requirements. The rating scheme will then be applied to three different joints as an illustration. The three joints, which are used in the Medium Range Standard Missile (RIM-66), are shown in Figures 6-1 thru 6-3.

6.1 SYSTEM CONSIDERATIONS

The airframe joints of a tactical missile possess attributes which must satisfy a number of requirements. The dominant requirements which will be considered here are strength, weight, volumetric efficiency, degree of enclosure, producibility and missile maintainability.

6.1.1 Strength

The static load carrying capability of the airframe of a typical tactical missile is often determined by the airframe joints rather than the shell structure between joints. The fatigue capability of the airframe is also frequently determined by the joints. The reason that airframe joints are relatively inefficient load carrying members when compared to the adjacent shell structure is associated with the distortion of the load path created by the presence of the joint.

The critical static strength requirements for airframe joints are frequently the bending moments that arise from lateral loading conditions such as handling of the assembled missile or free flight steering maneuvers. There are of course shear, torque and longitudinal load requirements imposed on airframe joints. However, the strength requirement that drives the design of tactical missile airframe joints is usually the bending moment.

The strength of a joint can be quite sensitive to design details that are sometimes quite subtle. Since stress concentrations play an important role in the strength of joints, considerations such as ductility of the material and avoidance of sharp or rapid transitions are

important. The static strength of the three airframe joints that are studied in this section of the report provide an indication of the variation in strength. The strengths are listed below.

<u>Joint Type</u>	<u>Illustration (Figure No.)</u>	<u>Strength (Inch-Pounds)</u>
Continuous Land	6-1	104,000 to 209,000
Four Bolt Tension	6-2	231,000 to 347,000
Eight Bolt Tension	6-3	345,000 to 425,000

The variation in the strength for the first and third joints represent the effect of minor design changes that were implemented to improve the strength of the joint. The variation in the strength of the second joint is due to a combination of material property and dimensional differences.

A measure of the strength efficiency of a joint can be developed by ratioing the strength of the joint to the flexural strength of the adjacent shell structure.

<u>Joint Type</u>	<u>Strength Efficiency - (%)</u>
Continuous Land	28 to 57
Four Bolt Tension	41 to 62
Eight Bolt Tension	62 to 76

6.1.2 Weight

The weight of a joint is defined as the weight of the airframe in the vicinity of the joint less the weight of the thin shell sections if they were extended to the joint interface. Thus it is seen that the build-up in the shell adjacent to a joint is included as part of the weight of the joint. The weight of the fasteners, covers and fairings associated with the joint are also included in the weight figure. The weight of each of the three joints was calculated using the approach outlined above. The weight of the three joints is listed below.

<u>Joint Type</u>	<u>Weight (Pounds)</u>
Continuous Land	3.83
Four Bolt Tension	8.81
Eight Bolt Tension	8.80

A measure of the weight efficiency of a joint can be developed by ratioing the weight of the thin shell sections over half a body diameter if no joint were present to the weight of the same region of the structure with the joint present. This efficiency is of course referenced to the thin shell section which may not have been designed for minimum weight.

<u>Joint Type</u>	<u>Weight Efficiency - (%)</u>
Continuous Land	37
Four Bolt Tension	26
Eight Bolt Tension	48

6.1.3 Volumetric Efficiency

The presence of joints in an airframe influence the volume available to package the electronics, propulsion and ordnance. A measure of volumetric efficiency that reflects the influence that joints have on packaging volume is the open cross sectional area of the joint. The volumetric efficiency of the three joints are tabulated below.

<u>Joint Type</u>	<u>Volumetric Efficiency</u>
Continuous Land	86%
Four Bolt Tension	91%
Eight Bolt Tension	54%

The first and second joints are quite efficient with respect to volume required while the third joint is inefficient in that it occupies almost one half of the cross sectional area.

The significance of volumetric efficiency is dependent upon the design application. If the design is such that the packaged volume must pass thru the inside diameter of the joint, the volume penalty is experienced over the entire length of the packaged item. Thus a substantial volume penalty would be incurred for such an application. However, if the packaged volume need not pass thru the inside diameter of the joint, the volume penalty is experienced only over the relatively short length of the joint. Applications in which the packaged volume need not pass thru the inside diameter of the joint are usually those in which the entire packaged volume is loaded from the opposite end of the airframe section. The volume constraint of the joint on the opposite end is then of course the governing factor.

6.1.4 Degree of Enclosure

The sealing or degree of enclosure characteristics of joints are a consideration in most tactical missile applications. It

is generally preferable to provide sealing at the airframe joints for the entire interior of the missile rather than for selected sensitive components. The purpose of the seal is to preclude the entrance of moisture, sand and dust.

Sealing of airframe joints is generally accomplished by using elastomeric O-rings in the joint interface. Typically an annular groove is machined in one of the mating surfaces and the O-ring is sized such that it is stretched when installed in the groove. The tension in the installed O-ring provides for the retention of it during assembly of the joint.

The O-ring provides sealing of the primary potential leakage path to the interior of the airframe. There are however, a number of secondary leakage paths that must be sealed with certain joint designs. The eight bolt tension joint shown in Figure 6-3 is an example of a design that has potential secondary leakage paths. The eight fasteners pass from the exterior to the sealed interior of the airframe. This provides eight potential leakage paths. Sealing of the fastener assembly is accomplished by providing a spotfaced surface on the casting under the washer. The machined surfaces and the contact stresses generated on assembly of the joint provide sealing of the fastener areas. Other joint designs such as the discontinuous land shown in Figure 6-1 and the four bolt tension shown in Figure 6-2 preclude the existence of secondary leakage paths by keeping the fastener totally external to sealed interior.

6.1.5 Producibility

The producibility attribute of a joint design is concerned with the cost of manufacturing the joint hardware. Since costs are highly dependent upon production quantities, no attempt will be made here to generate quantitative cost figures. Rather the producibility of the joint will be based upon the complexity of the machining involved in fabrication of the hardware.

The continuous land joint shown in Figure 6-1 has three machined elements. Two of the machined elements are complex in that a large acme thread surface and tight tolerances are involved. The two elements are the split coupling nut and the mating female surface. Thus the producibility of this joint design is rated low.

The four bolt tension joint shown in Figure 6-2 has six machined elements, four of which are simply bolts. The two major elements require only straight forward machining to moderate tolerances. Thus the producibility of this joint design is rated high.

The eight bolt tension joint shown in Figure 6-3 has two major machined elements plus eight fastener assemblies. The tolerances involved are moderate, but the geometry of the assembly is such that an elaborate

casting is required for one member and considerable machining is required on the other member to minimize weight. Thus the producibility of this joint design is rated low.

6.1.6 Maintainability

The ease of assembly and disassembly of a joint design effects both the producibility and maintainability of tactical missiles. Extensive functional testing of the missile electronics is performed during both manufacturing and deployment. All repair work and certain types of functional testing require disassembly of the airframe joints. Logistic policies also commonly require periodic disassembly of the joints. The time and equipment required to assemble and disassemble as well as the opportunity for human error or damage to the hardware become important considerations when large quantities of hardware or frequent testing are involved.

The maintainability of the joint hardware itself is limited to inspection of the hardware such as the machined surfaces at disassembly and replacement of the O-rings and possibly certain of the fasteners at reassembly.

The ease of assembly and reassembly of the continuous land joint is somewhat greater than that of the four and eight bolt tension joints. Although the continuous land joint has a single fastener that requires roughly only one full turn to engage or disengage, it is difficult to position to start the thread engagement. The tension bolt joints are easier to position but the need to individually torque each fastener on assembly is time consuming.

6.2 INTEGRATION METHOD

The various attributes of airframe joints that were discussed in section 6.1 plus the structural dynamic attributes must be considered in an integrated fashion to produce an overall rating of different joint designs. This is accomplished by assigning a figure of merit to the individual joint attributes, a relative weighting among the attributes, and finally summing the ratings over the attributes.

The three joints shown in Figures 6-1 thru 6-3 will be rated as an illustration. Equal weightings among the attributes are used, although unequal weightings can of course be used to emphasize or deemphasize certain attributes relative to the others. The four ratings of excellent, good, fair and poor are used for the attributes based on the quantitative and qualitative factors proposed in Table 6-1. In addition to the joint attributes discussed in Section 6.1, the structural dynamic attributes of stiffness and tightness are included in Table 6-1. The stiffness rating is the NASA rating discussed in Reference 3. The tightness attribute

refers to self induced noise characteristics that are discussed in Section 5 of the present report.

The illustrative rating comparison for the three joints (Figures 6-1 thru 6-3) is presented in Table 6-2. Using equal weightings for each of the eight joint attributes results in the best overall rating for the four bolt tension joint. The overall rating using equal weighting factors, does not reveal large differences between the three joints. However, the use of unequal weighting factors in which certain attributes are assigned very high or very low emphasis would produce more dramatic differences in the overall ratings.

Table 6-1
Proposed Joint Attribute Rating Basis

Attribute	Measure or Units	Rating			
		Excellent	Good	Fair	Poor
Stiffness ⁽¹⁾	Inch-Pounds/Radian	$(10)^{10}/C$	$(10)^9/C$	$(10)^8/C$	$(10)^7/C$
Tightness	Noise generation	Low			High
Strength Efficiency	Per cent	>75	75 to 50	50 to 25	<25
Weight Efficiency	Per cent	>60	60 to 40	40 to 20	<20
Volumetric Efficiency	Per cent	>90	90 to 70	70 to 50	<50
Degree of Enclosure	No. of locations requiring sealing	1	2 to 5	>5	Unsealable
Producibility	Manufacturing cost	Low			High
Maintainability	Ease of assembly and disassembly	Simple			Difficult

(1) NASA stiffness rating as defined on page 16 of Reference 1, $C = (20/D)^3$, D = body diameter in inches.

Table 6-2
Illustrative Rating Comparison for Three Joints

Attribute	Ratings (1)		
	Continuous Land	Four Bolt Tension	Eight Bolt Tension
Stiffness	F	G	F
Tightness	P	G	G
Strength	G	G	E
Weight	G	F	G
Volume	G	E	F
Degree of Enclosure	E	E	F
Producibility	F	E	F
Maintainability	E	G	F
Overall	G(-)	G	F(+)

(1) E = Excellent, G = Good, F = Fair, P = Poor

FIGURE 6-1
CONTINUOUS LAND RING JOINT

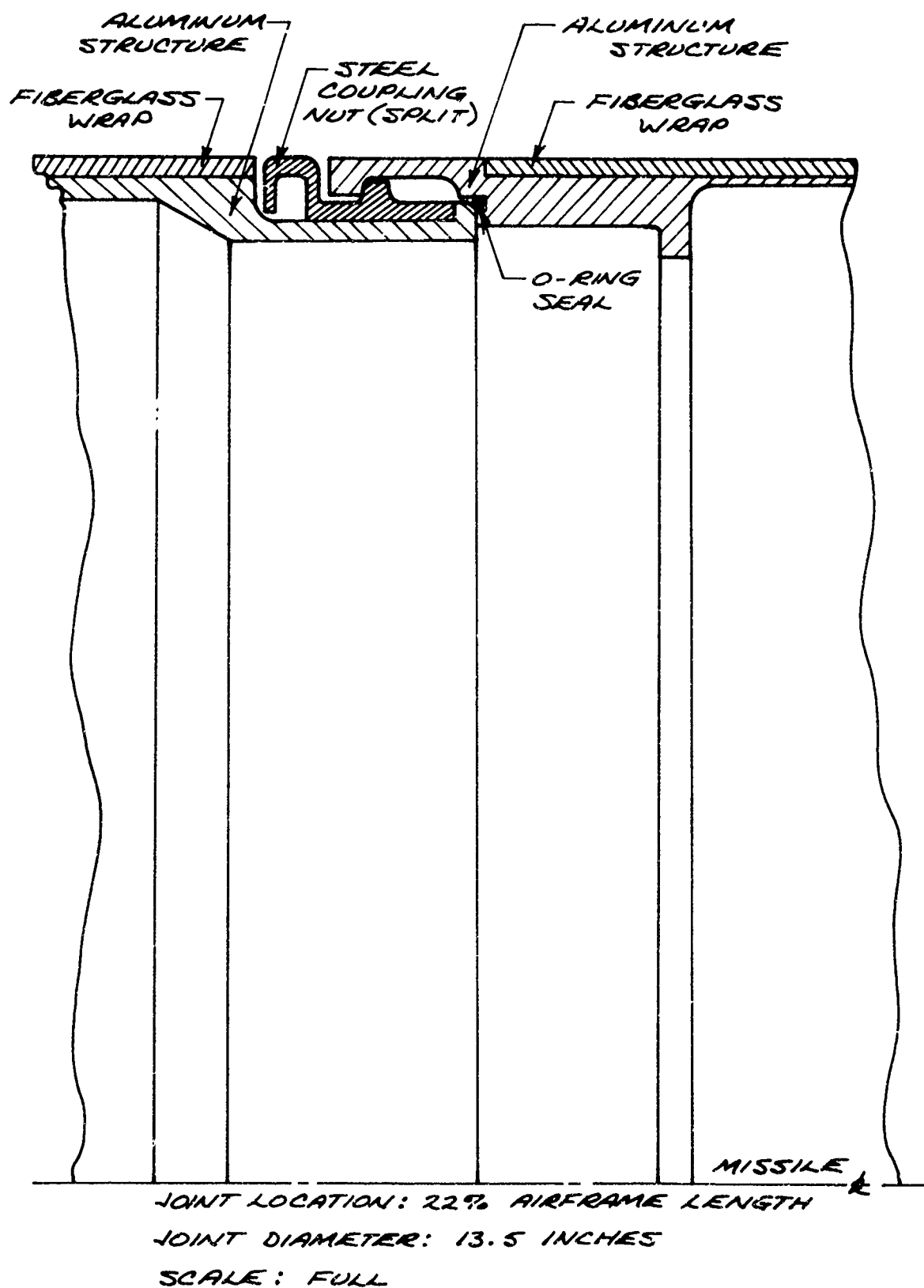
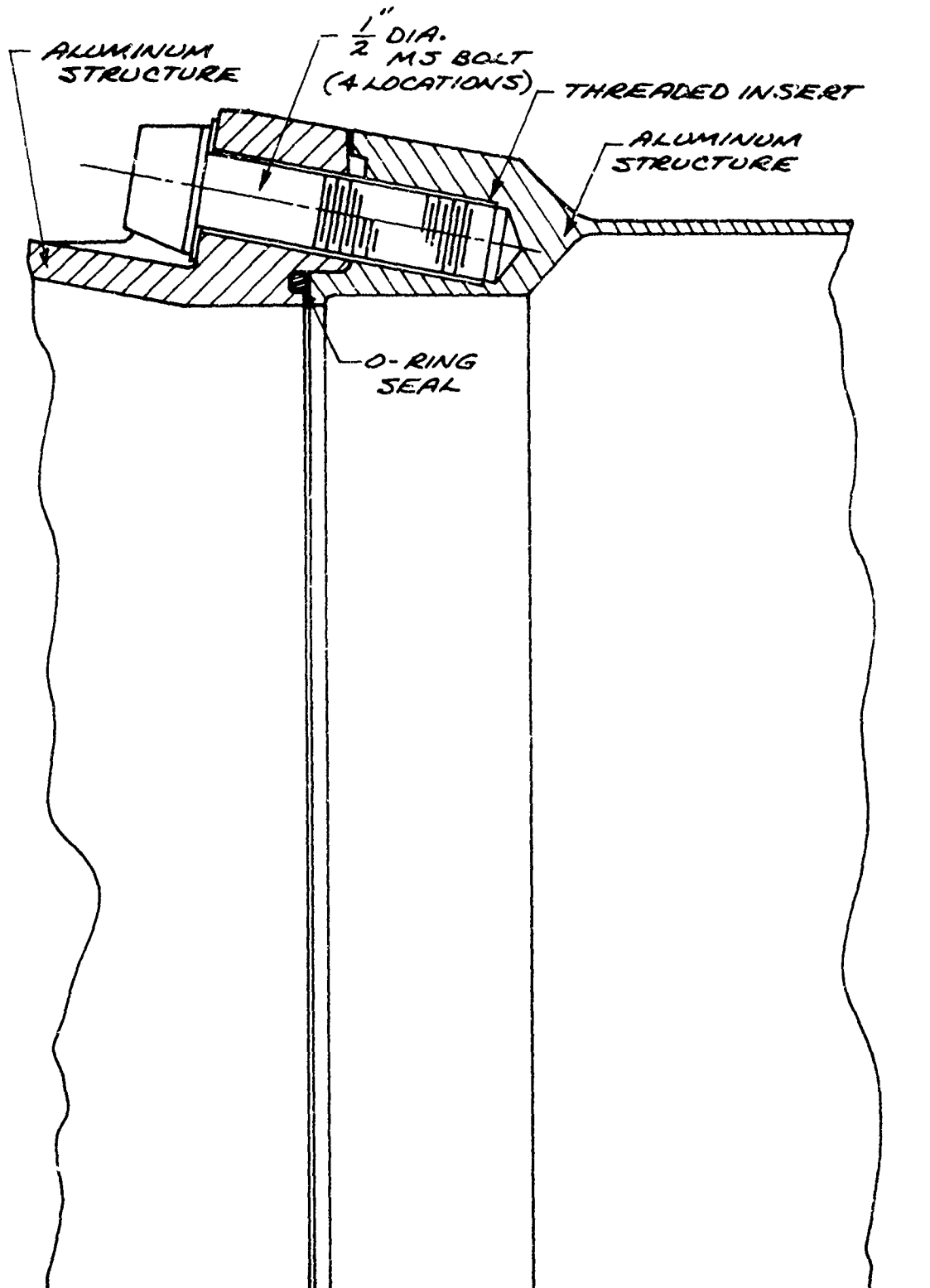
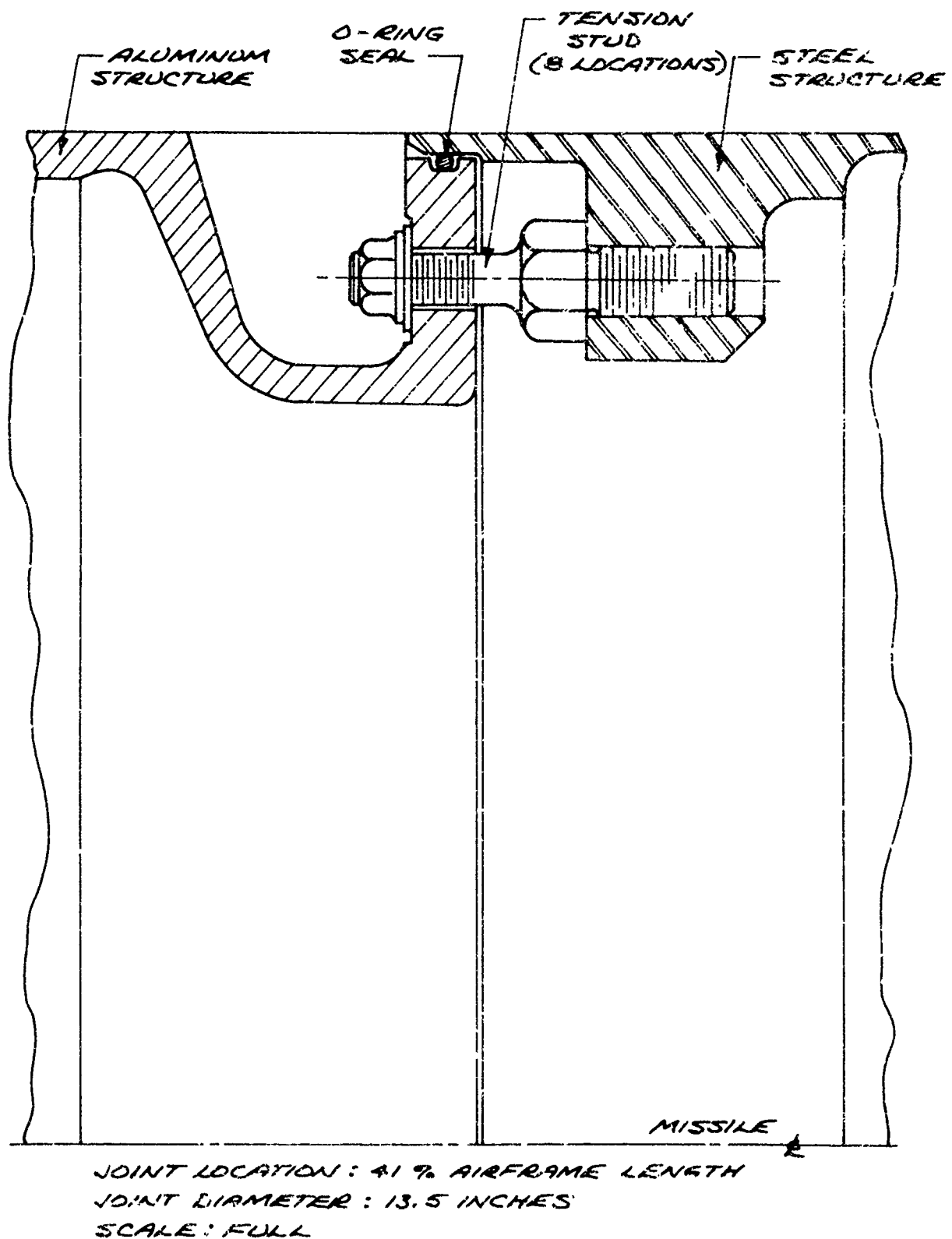


FIGURE 6-2
FOUR BOLT TENSION JOINT



JOINT LOCATION : 35% AIRFRAME LENGTH
JOINT DIAMETER : 13.5 INCHES
SCALE : FULL

FIGURE 6-3
EIGHT BOLT TENSION JOINT



REFERENCES

1. Maloney, J. G., Shelton, M. T., and Underhill, D. A., "Structural Dynamic Properties of Tactical Missile Joints - Phase I", General Dynamics, Pomona Division Report No. CR-6-348-945-001, June 1970.
2. Maloney, J. G. and Shelton, M. T., "Structural Dynamic Properties of Tactical Missile Joints - Phase 2", General Dynamics, Pomona Division Report No. CR-6-348-945-002, September 1971.
3. Alley, Jr., V. L. and Leadbetter, S. A., "The Prediction and Measurement of Natural Vibrations on Multistage Launch Vehicles", American Rocket Society Launch Vehicles: Structures and Materials Conference Report, April 1962.
4. Hall, B. M., Calkin, E. D. and Sholar, M. S., "Linear Estimation of Structural Parameters from Dynamic Test Data", AIAA/ASME 11th Structures, Structural Dynamics, and Materials Conference, Denver, Colorado, April 22-24, 1970.
5. McIntyre, K. L., "Modified Holzer-Myklestad Modal Analysis Final Report - CWA 245", General Dynamics/Pomona TM-348-15.1-3, July 24, 1961.
6. Householder, A. S., Principles of Numerical Analysis, McGraw Hill; New York, 1953.
7. Fox, R. L. and Kapoor, M. P., "Rates of Change of Eigenvalues and Eigenvectors", AIAA Journal, Vol. 6, Number 12, December 1968, p. 2426.

APPENDIX

JOINT COMPLIANCE EXTRACTION CODE
USER'S MANUAL

LIST OF TABLES AND FIGURES

<u>Table No.</u>	<u>Title</u>	<u>Page</u>
A-1	Input Data Sheets for Computer Program FILLIN	107
A-2	Flow Diagram of Computer Program JOINTS	110
A-3	Input Data Sheets for Computer Program JOINTS	111
A-4	FORTTRAN Listing of Program FILLIN	119
A-5	FORTTRAN Listing of Subroutine SQUARE	126
A-6	FORTTRAN Listing of Subroutine PARAB	127
A-7	FORTTRAN Listing of Subroutine LINFIT	128
A-8	FORTTRAN Listing of Program JOINTS	129
A-9	FORTTRAN Listing of Subroutine STEEP	141
A-10	FORTTRAN Listing of Subroutine ALTER	145
A-11	FORTTRAN Listing of Subroutine RENORM	146
A-12	FORTTRAN Listing of Subroutine MYKL	148
A-13	FORTTRAN Listing of Subroutine MEMSET	163
A-14	FORTTRAN Listing of Subroutine MATNF5	164
A-15	Sample Data Deck Listing of Program FILLIN	166
A-16	Sample Data Deck Listing of Program JOINTS	169
A-17	Key Output Data from Sample Data Deck	174

<u>Figure No.</u>	<u>Title</u>	<u>Page</u>
A-1	Sample Application Value of Unknown Joint Compliances and Cost Function Versus Cycle Number	175

INTRODUCTION

The computational system used for implementing the method of analysis described in Section 4 is composed of the following two digital computer programs:

- 1) Program FILLIN
- 2) Program JOINTS

Computer program FILLIN is a small prelude program that accepts measured modal data obtained at a set of test missile stations and interpolates these data to provide "measured" modal data at a set of missile stations consistent with theoretical modal data calculated within computer program JOINTS. This preliminary step is needed so that a comparison of experimental and theoretical modal data at identical missile stations can be made within computer program JOINTS.

Within the Appendix input data instructions, data output and program limitations are discussed for both computer programs FILLIN and JOINTS. Computer program FORTRAN listings and a sample application data deck listing are also presented.

PROGRAM FILLIN

Because comparisons between experimental and theoretical modal data are made at all modal analysis stations, within computer program JOINTS, computer program FILLIN was written to provide interpolated measured modal data for the modal analysis stations. The resulting interpolated measured mode shape deflections and slopes are punched on cards for the complete set of modal analysis missile stations in a format acceptable for subsequent input to computer program JOINTS.

Usually, only mode shape deflections are measured in the laboratory while both mode shape deflections and slopes are computed. Therefore, an added feature of computer program FILLIN is the computation of mode shape slopes from the measured mode shape deflection data.

Computer program FILLIN has the following restrictions:

- 1) There must be at least two experimental points on each appendage (to establish slope).
- 2) There must be at least two experimental points on either side of a joint (to establish shear discontinuity).

Computer program FILLIN and JOINTS were written to be run on the CDC 6400 digital computer with 32K words of memory storage, under control of the CDC 6000 Series Scope Monitor System (Version 3.3), at General

Dynamics, Pomona Division. All programs and subroutines are written in the CDC 6400 FORTRAN Extended Language (Version 3.0) and should be easily implemented on any machine having a FORTRAN IV compiler. Input/output devices required are the card reader (logical unit 60), the line printer (logical unit 6) and the card punch.

Computer program FILLIN is composed of the following routines:

- 1) Program FILLIN
- 2) Subroutine SQUARE
- 3) Subroutine PARAB
- 4) Subroutine LINFIT

In addition, FORTRAN library routines EOF (end of file) and EXIT are called. FORTRAN listings of these four routines comprising computer program FILLIN are presented in Tables A-4 through A-7.

The input data instructions showing card formats for computer program FILLIN are presented in Table A-1. A listing of a sample data deck is presented in Table A-15. Data output consists of a listing of the input data and the interpolated experimental data (mode shape deflections and slopes) computed at all modal analysis stations. It is suggested that the results obtained from computer program FILLIN be checked before using the punched output as input to program JOINTS.

PROGRAM JOINTS

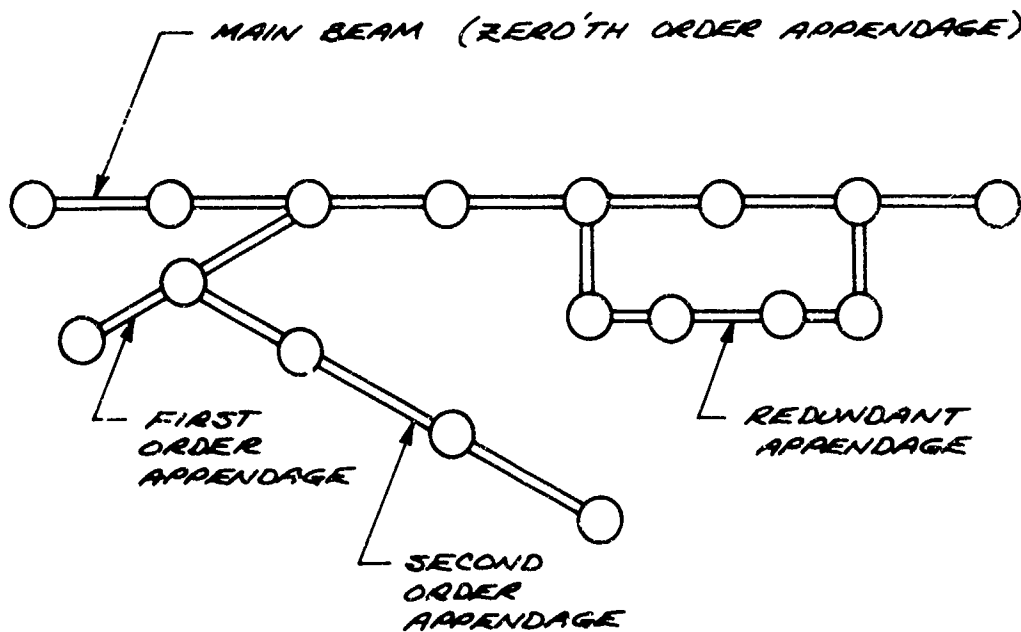
A simplified flow diagram of computer program JOINTS is presented in Table A-2. The procedure for joint compliance extraction is described as follows:

- 1) A starting value of joint compliance is assumed for each joint at which the compliance is unknown (initially from the input data).
- 2) Modes and the resulting cost function and first order gradients are computed for this initial configuration.
- 3) Each unknown joint compliance is varied independently from the trial configuration.
- 4) Modes and the resulting cost function and first order gradients are computed for each of these configurations obtained in Step 3.
- 5) Second order gradients are computed from the finite differences of the results obtained in Step 4.

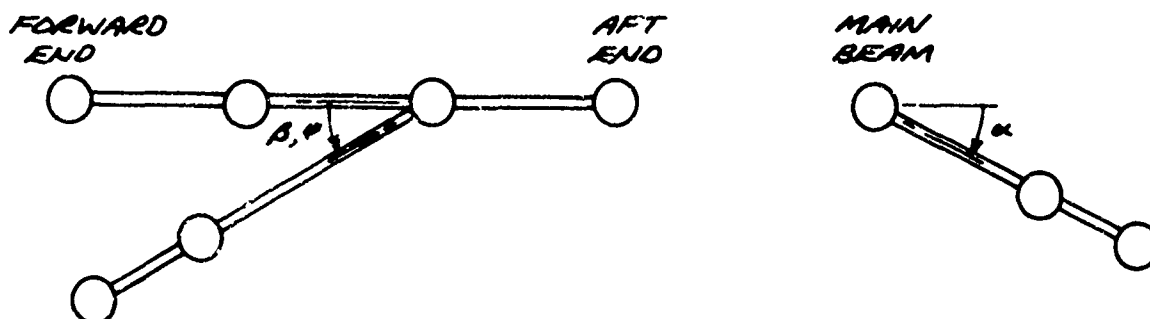
- 6) A new trial set of joint compliances is calculated using the first and second order gradients terms.
- 7) If the trial set of compliances has converged within a specified tolerance, the analysis stops. Otherwise Step 2 is reentered and the analysis continues.

These seven steps comprise a cycle of iterations (a configuration for each of the unknown springs plus the nominal configuration). A detailed description of the computational procedure for first and second order gradients and the new trial spring rates is presented in Section 4.

A brief description of the mathematical model of a missile is presented here to aid in understanding the input data to program JOINTS. A missile is modeled using a lumped parameter representation. A typical model is shown below.



Appendage attachment angles are defined by the following diagram.



If this is the top view, the marked angle is ψ . If this is the side view, the marked angle is α . End view of main beam looking aft.

The following five types of stations are available for modeling missile system:

- 1) mass
- 2) spring
- 3) appendage attachment
- 4) forward redundant appendage attachment
- 5) aft redundant appendage attachment

When modeling a system for input to the computer, each station input can perform only one function, that is, a mass station cannot have a spring associated with it or be an appendage attachment station.

The main beam or zero order appendage must be input first. The first station on the main beam must be labeled one. After that, any other positive integer may be used as a station identification number. As a general practice, station identification numbers should be unique since appendage attachment designations are made using these identification numbers. Simple appendages are entered next starting from their free end. Redundant appendages are entered last starting from their forward attachment end. Within the main beam or any appendages, station location values must be entered in increasing order (consecutive stations may have equal station locations). Redundant appendages must lie along the main beam and have the same type of motion (bending, torsion or longitudinal) as the main beam. Redundant appendages may not overlap but simple appendages may be attached to redundant appendages.

Complications arise due to the manner in which the Myklestad subroutine in Computer Program JOINTS functions. The number of stations in the actual mathematical model of a missile (input stations) is added to by the Myklestad subroutine for the following reasons:

- 1) A joint is represented by a single input station. However, for computations, a second station (at the same location) is needed to define the displacement and slope discontinuities at the joint.
- 2) At appendage attachment stations, an additional station is added (at the same location) to show the shear and moment discontinuities at the attachment station.
- 3) For each appendage and for the main beam, an additional station is added at the end of each beam system (at the same location as the last station) to allow for imposition of the boundary conditions.

Computer Program JOINTS is composed of the following routines.

- 1) Program JOINTS
- 2) Subroutine STEEL
- 3) Subroutine ALTER
- 4) Subroutine RENORM
- 5) Subroutine MYKL
- 6) Subroutine MEMSET
- 7) Subroutine MATNF5

In addition, FORTRAN library routines EOF (end of file), EXIT, SQRT, ABS, LABS, LOCF (storage address of variable in machine), SIN and COS are called. FORTRAN listings of these seven routines comprising computer program JOINTS are presented in Tables A-8 through A-14.

Computer program JOINTS and FILLIN have the following size limitations:

- 1) A maximum of 100 theoretical missile stations
- 2) A maximum of 10 experimental and theoretical modes
- 3) A maximum of 10 redundant appendages

The input data instructions showing card formats for computer program JOINTS are presented in Table A-3. A FORTRAN listing of the program and its subroutines is presented in Table A-8 thru A-14. A listing of a sample data deck is presented in Table A-16.

Data output from the program consists of a listing of the input data, the input configuration for each iteration, a comparison of experimental and theoretical modes (deflections and slopes) and frequencies and cost function data for each iteration.

SAMPLE APPLICATION

A sample application is included to assist the user in checkout of the codes. Assume three experimental modes for a missile have been measured in the laboratory. A 59 station mathematical model has been developed, which includes two simple appendages and one redundant appendage. Three theoretical modes are to be computed and four joint compliances are to be extracted from the measured data using computer program JOINTS.

First, computer program FILLIN is run to determine the experimental mode shape deflections and slopes at the modal analysis stations. The data deck listing for computer program FILLIN is presented in Table A-15.

With the experimental mode shape deflections and slopes defined at the desired stations, computer program JOINTS is then run. The data deck listing for computer program JOINTS is presented in Table A-16. The entire output listing from the computer program is not presented because of the large quantity of output. Key output data are given in Table A-17. Certain of the results are plotted in Figure A-1. Other application examples are presented in Section 4 of this report.

TABLE A-1
INPUT DATA INSTRUCTIONS FOR COMPUTER PROGRAM FILLIN
FORTRAN CODING AND DATA FORM

PROBLEM		PROGRAM FILLIN		NAME		DATE	
PROGRAMMER		D.O. RIFE		PHONE EXT.		DATE	
1	2	3	4	5	6	7	8
9	10	11	12	13	14	15	16
17	18	19	20	21	22	23	24
25	26	27	28	29	30	31	32
33	34	35	36	37	38	39	40
41	42	43	44	45	46	47	48
49	50	51	52	53	54	55	56
57	58	59	60	61	62	63	64
65	66	67	68	69	70	71	72
73	74	75	76	77	78	79	80
ONE GENERAL TITLE CARD							
MYKLESTAD FORMAT BEAM DESCRIPTIONS OF STATIONS AT WHICH MODE SHAPE DEFLECTIONS AND SLOPES ARE DESIRED (CARD FORMAT - 2IA, 3I2, 2X, 7E8.0)							
ID(1)	IA(1)	IT(1)	XSTA(1)		COMP1(1)		COMP2(1)
ID(2)	IA(2)	IT(2)	XSTA(2)		COMP1(2)		COMP2(2)
:	:	:	:		:		:
ID(K)	IA(K)	IT(K)	XSTA(K)		COMP1(K)		COMP2(K)
:	:	:	:		:		:
<p>ID(I) - STATION IDENTIFICATION COUNTER FOR STATION I.</p> <p>NOTE: THE FIRST STATION OF THE MAIN BEAM MUST BE LABELED 1, I.E. ID(1)=1</p> <p>AS A GENERAL PRACTICE, STATION IDENTIFICATION COUNTERS SHOULD BE UNIQUE SINCE APPENDAGE ATTACHMENT STATION NUMBERS REFER TO THESE IDENTIFICATION COUNTERS.</p> <p>IA(I) - APPENDAGE ATTACHMENT STATION IDENTIFICATION NUMBER FOR STATION I. IA(I) ≥ 0</p> <p>NOTE: EXCEPT FOR MAIN BEAM IN WHICH IA(I)=0, THE APPENDAGE ATTACHMENT STATION IDENTIFICATION NUMBER MUST REFER TO A STATION IN COUNTER, I.E., IA(I)=ID(J) FOR A STATION J IN WHICH IT(J)=2 (WITHIN AN APPENDAGE, ALL APPENDAGE ATTACHMENT NUMBERS ARE EQUAL)</p> <p>IT(I) - DESIGNATION OF STATION TYPE FOR STATION I</p> <p>0 - MASS STATION</p> <p>1 - SPRING STATION</p> <p>2 - APPENDAGE ATTACHMENT STATION</p> <p>3 - FORWARD REDUNDANT APPENDAGE ATTACHMENT STATION</p> <p>4 - AFT REDUNDANT APPENDAGE ATTACHMENT STATION</p> <p>NOTE: ENTER ALL REDUNDANT APPENDAGES LAST STARTING FROM THE FORWARD END.</p>							

TABLE A-1 (CONT'D)
FORTRAN CODING AND DATA FORM

PROBLEM										PROGRAMMER										DATE									
PROBLEM										PROGRAMMER										DATE									
1	2	3	4	5	6	7	8	9	10	11	12	13	14	15	16	17	18	19	20	21	22	23	24	25	26	27	28	29	30
XSTA(I) - STATION LOCATION OF STATION I - INCHES										NOTE: WITHIN THE MAIN BEAM OR ANY APPENDAGE, XSTA(I+1) ≥ XSTA(I)										(A STATION LOCATION IS NEEDED FOR EACH CARD INPUT, CAN BE ZERO)									
COMPL(I) - SHEAR COMPLIANCE FOR STATION I - IN/LB										NOTE: ENTER A VALUE HERE ONLY IF IT(I)=1										COMPL(I) > 0.0									
COMPL2(I) - FLEXURAL COMPLIANCE FOR STATION I - RAD/IN*LB										NOTE: ENTER A VALUE HERE ONLY IF IT(I)=1										COMPL2(I) > 0.0									
NOTE: ENTER ALL MAIN BEAM CARDS FIRST, THEN APPENDAGE CARDS - MAIN BEAM AND APPENDAGE CARDS MUST BE IN ORDER AS PROGRAM DOES NO SORTING.										ENTER SIMPLE APPENDAGES STARTING AT FREE END, ENDING AT ATTACHED END.										ID(I)=0 ENDS THE READING OF THE BEAM DESCRIPTION CARDS - READ A MAXIMUM OF 100 OF THESE CARDS (COUNTING THE ID(I)=0 CARD)									
OPTION CARD (CARD FORMAT - 315)																													
NSTA=NSTA NEXP																													
NSTA - NUMBER OF INTERNAL THEORETICAL STATIONS AT WHICH INTERPOLATED EXPERIMENTAL MODE SHAPE DEFLECTIONS AND SLOPES WILL BE PUNCHED.										(100 IS MAXIMUM BECAUSE OF PROGRAM JOINTS)										3=NSTA=100									
NEXP - NUMBER OF STATIONS AT WHICH EXPERIMENTAL MODES WERE MEASURED.										NOTE: NSTA > NEXP										2=NSTA=99									
NEXP - NUMBER OF EXPERIMENTAL MODES																				1=NEXP=10									

TABLE A-1 (CONT'D)

FORTRAN CODING AND DATA FORM

PROBLEM		NAME		DATE	
PROGRAMMER		NAME		DATE	
1	2	3	4	5	6
7	8	9	10	11	12
13	14	15	16	17	18
19	20	21	22	23	24
25	26	27	28	29	30
31	32	33	34	35	36
37	38	39	40	41	42
43	44	45	46	47	48
49	50	51	52	53	54
55	56	57	58	59	60
61	62	63	64	65	66
67	68	69	70	71	72
73	74	75	76	77	78
79	80				
81	82	83	84	85	86
87	88	89	90	91	92
93	94	95	96	97	98
99	100				
101	102	103	104	105	106
107	108	109	110	111	112
113	114	115	116	117	118
119	120	121	122	123	124
125	126	127	128	129	130
131	132	133	134	135	136
137	138	139	140	141	142
143	144	145	146	147	148
149	150	151	152	153	154
155	156	157	158	159	160
161	162	163	164	165	166
167	168	169	170	171	172
173	174	175	176	177	178
179	180				
181	182	183	184	185	186
187	188	189	190	191	192
193	194	195	196	197	198
199	200				
201	202	203	204	205	206
207	208	209	210	211	212
213	214	215	216	217	218
219	220	221	222	223	224
225	226	227	228	229	230
231	232	233	234	235	236
237	238	239	240	241	242
243	244	245	246	247	248
249	250	251	252	253	254
255	256	257	258	259	260
261	262	263	264	265	266
267	268	269	270	271	272
273	274	275	276	277	278
279	280				
281	282	283	284	285	286
287	288	289	290	291	292
293	294	295	296	297	298
299	300				
301	302	303	304	305	306
307	308	309	310	311	312
313	314	315	316	317	318
319	320	321	322	323	324
325	326	327	328	329	330
331	332	333	334	335	336
337	338	339	340	341	342
343	344	345	346	347	348
349	350	351	352	353	354
355	356	357	358	359	360
361	362	363	364	365	366
367	368	369	370	371	372
373	374	375	376	377	378
379	380				
381	382	383	384	385	386
387	388	389	390	391	392
393	394	395	396	397	398
399	400				
401	402	403	404	405	406
407	408	409	410	411	412
413	414	415	416	417	418
419	420	421	422	423	424
425	426	427	428	429	430
431	432	433	434	435	436
437	438	439	440	441	442
443	444	445	446	447	448
449	450	451	452	453	454
455	456	457	458	459	460
461	462	463	464	465	466
467	468	469	470	471	472
473	474	475	476	477	478
479	480				
481	482	483	484	485	486
487	488	489	490	491	492
493	494	495	496	497	498
499	500				
501	502	503	504	505	506
507	508	509	510	511	512
513	514	515	516	517	518
519	520	521	522	523	524
525	526	527	528	529	530
531	532	533	534	535	536
537	538	539	540	541	542
543	544	545	546	547	548
549	550	551	552	553	554
555	556	557	558	559	560
561	562	563	564	565	566
567	568	569	570	571	572
573	574	575	576	577	578
579	580				
581	582	583	584	585	586
587	588	589	590	591	592
593	594	595	596	597	598
599	600				
601	602	603	604	605	606
607	608	609	610	611	612
613	614	615	616	617	618
619	620	621	622	623	624
625	626	627	628	629	630
631	632	633	634	635	636
637	638	639	640	641	642
643	644	645	646	647	648
649	650	651	652	653	654
655	656	657	658	659	660
661	662	663	664	665	666
667	668	669	670	671	672
673	674	675	676	677	678
679	680				
681	682	683	684	685	686
687	688	689	690	691	692
693	694	695	696	697	698
699	700				
701	702	703	704	705	706
707	708	709	710	711	712
713	714	715	716	717	718
719	720	721	722	723	724
725	726	727	728	729	730
731	732	733	734	735	736
737	738	739	740	741	742
743	744	745	746	747	748
749	750	751	752	753	754
755	756	757	758	759	760
761	762	763	764	765	766
767	768	769	770	771	772
773	774	775	776	777	778
779	780				
781	782	783	784	785	786
787	788	789	790	791	792
793	794	795	796	797	798
799	800				
801	802	803	804	805	806
807	808	809	810	811	812
813	814	815	816	817	818
819	820	821	822	823	824
825	826	827	828	829	830
831	832	833	834	835	836
837	838	839	840	841	842
843	844	845	846	847	848
849	850	851	852	853	854
855	856	857	858	859	860
861	862	863	864	865	866
867	868	869	870	871	872
873	874	875	876	877	878
879	880				
881	882	883	884	885	886
887	888	889	890	891	892
893	894	895	896	897	898
899	900				
901	902	903	904	905	906
907	908	909	910	911	912
913	914	915	916	917	918
919	920	921	922	923	924
925	926	927	928	929	930
931	932	933	934	935	936
937	938	939	940	941	942
943	944	945	946	947	948
949	950	951	952	953	954
955	956	957	958	959	960
961	962	963	964	965	966
967	968	969	970	971	972
973	974	975	976	977	978
979	980				
981	982	983	984	985	986
987	988	989	990	991	992
993	994	995	996	997	998
999	1000				

TABLE A-2.

FLOW DIAGRAM OF COMPUTER PROGRAM JOINTS

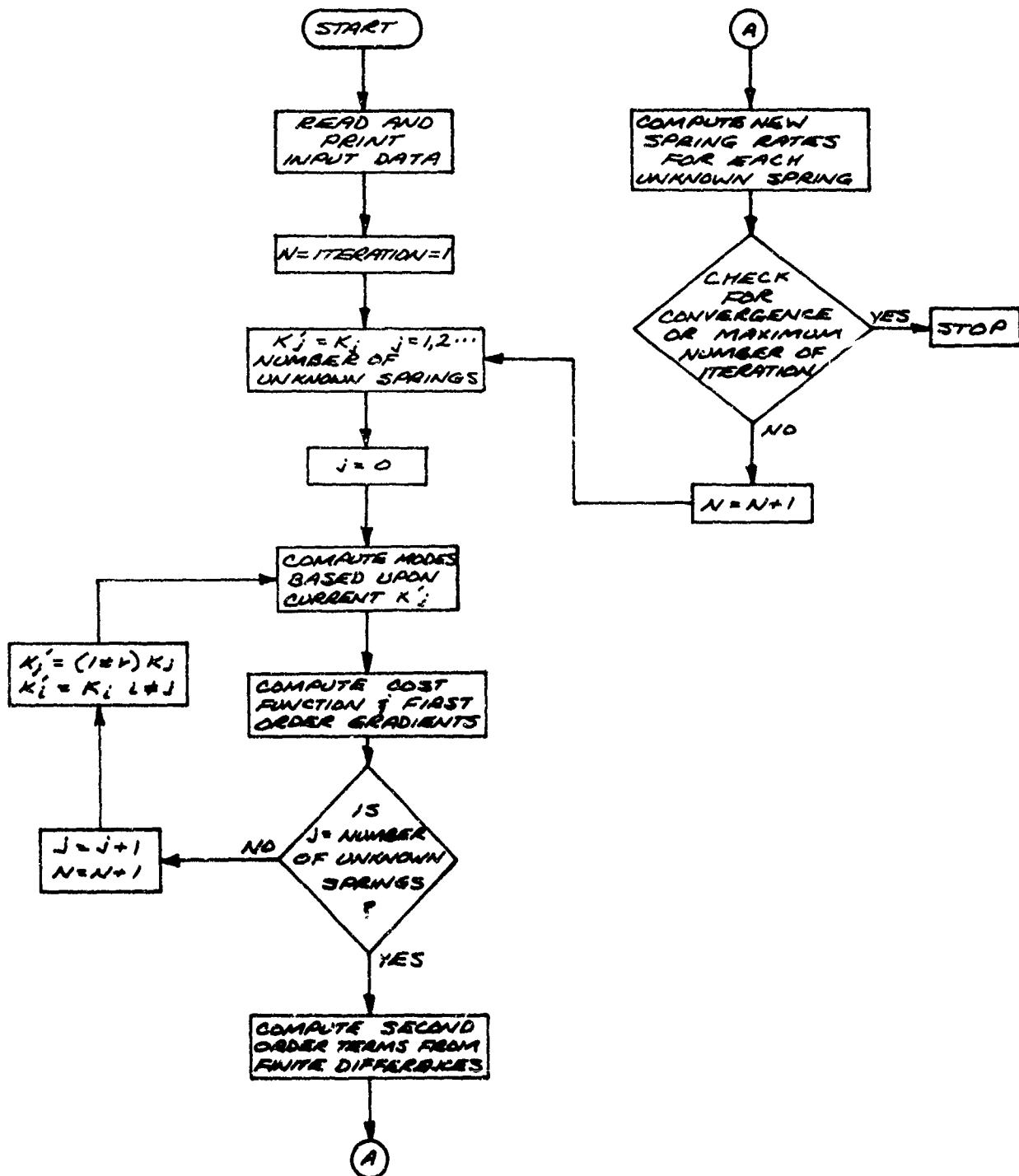


TABLE A-3

INPUT DATA INSTRUCTIONS FOR: COMPUTER PROGRAM JOINTS

PROBLEM		PROGRAMMER		NAME		DATE		TIME																					
PROGRAM		NAME		DATE		TIME		TIME																					
1	2	3	4	5	6	7	8	9	10	11	12	13	14	15	16	17	18	19	20	21	22	23	24	25	26	27	28	29	30
M.T. SHELTON, D.O. RIFE																													
OPTION CARDS (CARD FORMAT - BIS, TE10.0)																													
KNORM WT NEXP NUTITMAXVSPR NSTAMESTA STEP TOL CLOSE XCRATIO																													
KNORM - CARD NUMBER (NOT A STATION IDENTIFICATION COUNTER) AT WHICH																													
THEORETICAL MODES WILL BE NORMALIZED.																													
NOTE: THIS IS AN INTERNAL STATION CARD NUMBER, NOT AN INPUT CARD NUMBER																													
IF KNORM IS BLANK OR ZERO, PROGRAM SETS KNORM=1																													
NT - NUMBER OF THEORETICAL MODES TO BE COMPUTED																													
NEXP - NUMBER OF EXPERIMENTAL MODES BEING INPUT																													
NOTE: SAME VALUE AS IN PROGRAM FILE IN																													
NWT - MODE SHAPE AND MODE FREQUENCY WEIGHTING FACTOR OPTION																													
IF BLANK OR ZERO, PROGRAM COMPUTES WEIGHTING FACTORS.																													
OTHERWISE, WEIGHTING FACTORS ARE INPUT.																													
ITMAX - MAXIMUM NUMBER OF ITERATIONS FOR ANALYSIS																													
NOTE: THE PROGRAM COMPUTES ITERATIONS IN THE FOLLOWING MANNER:																													
THE NOMINAL CONFIGURATION OF A CYCLE OF ITERATIONS IS DESIGNATED																													
AS ITERATION NUMBER 1. EACH SPACING WHICH CAN VARY IS COUNTED AS																													
ANOTHER ITERATION. THEREFORE, TO COMPLETE ONE FULL CYCLE OF																													
ITERATIONS REQUIRES NUSP+1 ITERATIONS. AFTER EACH CYCLE OF																													
ITERATIONS, THE PROGRAM COMPUTES A NEW NOMINAL CONFIGURATION																													
AND THE PROCESS OF ITERATION COUNTING CONTINUES AS BEFORE. THE																													
PROGRAM ALWAYS COMPLETES A CYCLE OF ITERATIONS BEFORE STOPPING.																													

TABLE A-3 (CONT'D.)
FOR TRAN CODING AND DATA FORM

PROBLEM		NAME		PHONE-NUM		DATE																							
PROGRAMMER		NAME		PHONE-NUM		DATE																							
1	2	3	4	5	6	7	8	9	10	11	12	13	14	15	16	17	18	19	20	21	22	23	24	25	26	27	28	29	30
NUMBER OF SPRINGS WHOSE COMPLIANCES CAN BE VARIED.																													
NUMBER OF INTERNAL THEORETICAL STATIONS.																													
NOTE: SAME VALUE AS IN PROGRAM FILLIN.																													
NUMBER OF STATIONS AT WHICH EXPERIMENTAL MODES WERE MEASURED																													
NOTE: THIS PARAMETER HAS BEEN INCLUDED FOR USE WHEN PROGRAMS FILLIN AND JOINTS ARE COMBINED. SINCE THIS HAS NOT OCCURRED, SET NESTA=NSD																													
PARAMETER USED IN DETERMINING CHANGE IN SPRING RATES FOR VARYING SPRINGS. A VALUE OF STEP = 0.15 IS RECOMMENDED.																													
NOTE: $K_{MIN} = (1 \pm STEP) * K_{OLD}$																													
PARAMETER USED IN DETERMINING SOLUTION TOLERANCE FOR SPRING RATES. A VALUE OF TOL = 0.01 IS RECOMMENDED.																													
NOTE: IF $ABS(K_{CURRENT} / K_{PREVIOUS} - 1.0) < TOL$ FOR ALL VARYING SPRINGS, ANALYSIS IS STOPPED.																													
PARAMETER USED IN DETERMINING STARTING FREQUENCY FOR MYKLESTAD MODE SEARCH. A VALUE OF CLOSE = 0.90 IS RECOMMENDED.																													
NOTE: IF BLANK OR ZERO, PROGRAM MAKES A CONTINUOUS SEARCH STARTING FROM PREVIOUS MODE FREQUENCY. FOR STARTING FREQUENCY FOR MODE 1, SEE LAST CARD INPUT IN DATA DECK.																													
IF CLOSE # 0.0, $F_{START}(I) = CLOSE * FREQ(I)$ WHERE I IS THE MODE COUNTER. OTHERWISE, $F_{START}(I) = F_{MODE}(I-1)$.																													
PARAMETER USED IN DETERMINING NEXT CYCLE INITIAL SPRING RATE VALUES WHEN COST FUNCTION HAS INCREASED.																													
NOTE: IF XRATIO IS BLANK OR ZERO PROGRAM SETS XRATIO = 0.5																													

TABLE A-3 (CONT'D.)
FORTRAN CODING AND DATA FORM

PAGE 3 OF 8

PROBLEM		NAME		DATE																									
PROGRAMMER		PHONE-EXT		DATE																									
1	2	3	4	5	6	7	8	9	10	11	12	13	14	15	16	17	18	19	20	21	22	23	24	25	26	27	28	29	30
<p>OPTION FOR ASKING PROGRAM TO SEE IF A MODE MAY HAVE BEEN MISSED DURING THE MYKLESTAD MODE SEARCH PHASE OF THE ANALYSIS.</p> <p>NOTE: IF KCHECK=2, PROGRAM WILL CHECK TO SEE IF MODE HAS BEEN MISSED. OTHERWISE, NO CHECK WILL BE MADE.</p> <p>THIS OPTION SHOULD NOT BE EXERCISED IF MYKLESTAD MODEL CONTAINS REDUNDANT APPENDAGES.</p> <p>TOTAL SYSTEM MASS (REQUIRED)</p> <p>WEIGHTING FACTORS - DO NOT READ IF NWT=0 (CARD FORMAT - BE(10.0))</p> <p>PMAT(1) PMAT(2) PMAT(K) PMAT(NEXP)</p> <p>FMAT(1) FMAT(2) FMAT(K) FMAT(NEXP)</p> <p>PMAT(I) - RELATIVE MODE SHAPE DEFLECTION AND SLOPE WEIGHTING FACTOR FOR MODE I.</p> <p>FMAT(I) - RELATIVE MODE FREQUENCY WEIGHTING FACTOR FOR MODE I.</p> <p>EXPERIMENTAL FREQUENCIES (CARD FORMAT - BE(10.0))</p> <p>EFREQ(1) EFREQ(2) EFREQ(K) EFREQ(MT)</p> <p>EFREQ(I) - EXPERIMENTAL MODE FREQUENCY FOR MODE I - Hz. 0.0 < EFREQ(I) < EFREQ(I+1)</p> <p>NOTE: WHERE MODES HAVE BEEN MEASURED, ENTER MEASURED MODE FREQUENCIES. OTHERWISE, ESTIMATE WHERE MODES MAY BE FOUND.</p>																													

TABLE A-3 (CONT'D.)
FORTRAN CODING AND DATA FORM

PAGE 4 OF 8

PROBLEM		END		DATE																											
PROGRAMMER		PHONE-EXT.		DATE																											
1	2	3	4	5	6	7	8	9	10	11	12	13	14	15	16	17	18	19	20	21	22	23	24	25	26	27	28	29	30		
<p>1 VARIABLE SPRINGS (CARD FORMAT - 214, 258.0, 14)</p> <p>2</p> <p>3 KSTA(1) KVAR(1) SPRING(1) SPRINGU(1) KTYPE(1)</p> <p>4 KSTA(2) KVAR(2) SPRING(2) SPRINGU(2) KTYPE(2)</p> <p>5 :</p> <p>6 KSTA(K) KVAR(K) SPRING(K) SPRINGU(K) KTYPE(K)</p> <p>7 :</p> <p>8 KSTA KVAR SPRING SPRINGU KTYPE</p> <p>9 KUSTAR KVAR SPRING SPRINGU KTYPE</p> <p>10 KSTA(I) - CARD NUMBER (NOT A STATION IDENTIFICATION COUNTER) FROM INPUT</p> <p>11 MYKLESTAD BEAM DESCRIPTION OF VARYING SPRING NUMBER I</p> <p>12 / KSTA(I) = NESTA</p> <p>13</p> <p>14 KVAR(I) - CARD NUMBER (NOT A STATION IDENTIFICATION COUNTER) FROM INTERVAL</p> <p>15 MYKLESTAD BEAM DESCRIPTION OF VARYING SPRING NUMBER I</p> <p>16 / KVAR(I) = NESTA</p> <p>17</p> <p>18 SPRING(I) - LOWER LIMIT TO WHICH SPRING RATE MAY BE CHANGED FOR VARYING</p> <p>19 SPRING NUMBER I - LB/IN OR IN-LB/RAD</p> <p>20</p> <p>21 SPRINGU(I) - UPPER LIMIT TO WHICH SPRING RATE MAY BE CHANGED FOR VARYING</p> <p>22 SPRING NUMBER I - LB/IN OR IN-LB/RAD</p> <p>23 NOTE: SPRINGU(I) > SPRING(I)</p> <p>24</p> <p>25 KTYPE(I) - TYPE OF SPRING OPTION COUNTER FOR VARYING SPRING NUMBER I</p> <p>26 / KTYPE(I) = 2</p> <p>27 IF KTYPE(I) = 1, A SHEAR SPRING HAS BEEN INDICATED AND SPRINGU(I)</p> <p>28 AND SPRINGU(I) ARE INPUT IN UNITS OF LB/IN.</p> <p>29 IF KTYPE(I) = 2, A FLEXURAL SPRING HAS BEEN INDICATED AND SPRINGU(I)</p> <p>30 AND SPRINGU(I) ARE INPUT IN UNITS OF IN-LB/RAD.</p>																															

TABLE A-3 (CONT'D.)
FORTRAN CODING AND DATA FORM

PAGE 5 OF 8

PROBLEM																													
PROGRAMMER																													
1	2	3	4	5	6	7	8	9	10	11	12	13	14	15	16	17	18	19	20	21	22	23	24	25	26	27	28	29	30
EXPERIMENTAL MODE SHAPE DEFLECTIONS AND SLOPES (CARD FORMAT - 6X, 2I3, 5E12.5)																													
1	1	1	1	1	1	1	1	1	1	1	1	1	1	1	1	1	1	1	1	1	1	1	1	1	1	1	1	1	1
2	2	2	2	2	2	2	2	2	2	2	2	2	2	2	2	2	2	2	2	2	2	2	2	2	2	2	2	2	2
3	3	3	3	3	3	3	3	3	3	3	3	3	3	3	3	3	3	3	3	3	3	3	3	3	3	3	3	3	3
4	4	4	4	4	4	4	4	4	4	4	4	4	4	4	4	4	4	4	4	4	4	4	4	4	4	4	4	4	4
5	5	5	5	5	5	5	5	5	5	5	5	5	5	5	5	5	5	5	5	5	5	5	5	5	5	5	5	5	5
6	6	6	6	6	6	6	6	6	6	6	6	6	6	6	6	6	6	6	6	6	6	6	6	6	6	6	6	6	6
7	7	7	7	7	7	7	7	7	7	7	7	7	7	7	7	7	7	7	7	7	7	7	7	7	7	7	7	7	7
8	8	8	8	8	8	8	8	8	8	8	8	8	8	8	8	8	8	8	8	8	8	8	8	8	8	8	8	8	8
9	9	9	9	9	9	9	9	9	9	9	9	9	9	9	9	9	9	9	9	9	9	9	9	9	9	9	9	9	9
10	10	10	10	10	10	10	10	10	10	10	10	10	10	10	10	10	10	10	10	10	10	10	10	10	10	10	10	10	10
11	11	11	11	11	11	11	11	11	11	11	11	11	11	11	11	11	11	11	11	11	11	11	11	11	11	11	11	11	11
12	12	12	12	12	12	12	12	12	12	12	12	12	12	12	12	12	12	12	12	12	12	12	12	12	12	12	12	12	12
13	13	13	13	13	13	13	13	13	13	13	13	13	13	13	13	13	13	13	13	13	13	13	13	13	13	13	13	13	13
14	14	14	14	14	14	14	14	14	14	14	14	14	14	14	14	14	14	14	14	14	14	14	14	14	14	14	14	14	14
15	15	15	15	15	15	15	15	15	15	15	15	15	15	15	15	15	15	15	15	15	15	15	15	15	15	15	15	15	15
16	16	16	16	16	16	16	16	16	16	16	16	16	16	16	16	16	16	16	16	16	16	16	16	16	16	16	16	16	16
17	17	17	17	17	17	17	17	17	17	17	17	17	17	17	17	17	17	17	17	17	17	17	17	17	17	17	17	17	17
18	18	18	18	18	18	18	18	18	18	18	18	18	18	18	18	18	18	18	18	18	18	18	18	18	18	18	18	18	18
19	19	19	19	19	19	19	19	19	19	19	19	19	19	19	19	19	19	19	19	19	19	19	19	19	19	19	19	19	19
20	20	20	20	20	20	20	20	20	20	20	20	20	20	20	20	20	20	20	20	20	20	20	20	20	20	20	20	20	20
21	21	21	21	21	21	21	21	21	21	21	21	21	21	21	21	21	21	21	21	21	21	21	21	21	21	21	21	21	21
22	22	22	22	22	22	22	22	22	22	22	22	22	22	22	22	22	22	22	22	22	22	22	22	22	22	22	22	22	22
23	23	23	23	23	23	23	23	23	23	23	23	23	23	23	23	23	23	23	23	23	23	23	23	23	23	23	23	23	23
24	24	24	24	24	24	24	24	24	24	24	24	24	24	24	24	24	24	24	24	24	24	24	24	24	24	24	24	24	24
25	25	25	25	25	25	25	25	25	25	25	25	25	25	25	25	25	25	25	25	25	25	25	25	25	25	25	25	25	25
26	26	26	26	26	26	26	26	26	26	26	26	26	26	26	26	26	26	26	26	26	26	26	26	26	26	26	26	26	26
27	27	27	27	27	27	27	27	27	27	27	27	27	27	27	27	27	27	27	27	27	27	27	27	27	27	27	27	27	27
28	28	28	28	28	28	28	28	28	28	28	28	28	28	28	28	28	28	28	28	28	28	28	28	28	28	28	28	28	28
29	29	29	29	29	29	29	29	29	29	29	29	29	29	29	29	29	29	29	29	29	29	29	29	29	29	29	29	29	29
30	30	30	30	30	30	30	30	30	30	30	30	30	30	30	30	30	30	30	30	30	30	30	30	30	30	30	30	30	30

NOTE: THESE CARDS ARE PUNCHED BY PROGRAM FILLIN.

TABLE 19-3 (CONT'D.)

FORTRAN CODING AND DATA FORM

PROBLEM		PAGE 6 OF 8	
PROGRAMMER		NAME	DATE
		PHONE-EXT.	
1	MYKLESTAD	28 29 30 31 32 33 34 35 36 37 38 39 40 41 42 43 44 45 46 47 48 49 50 51 52 53 54 55 56 57 58 59 60 61 62 63 64 65 66 67 68 69 70 71 72 73 74 75 76 77 78 79 80	
2	BEAM DESCRIPTIONS OF STATIONS (CARD FORMAT - 2I4, 3I2, 2X, 7E8.0)		
3	ITEM1(I) = DATA1(1) DATA2(1) DATA3(1) DATA4(1) DATA5(1) DATA6(1) DATA7(1)		
4	ITEM2(I) = DATA1(2) DATA2(2) DATA3(2) DATA4(2) DATA5(2) DATA6(2) DATA7(2)		
5	ITEM3(I) = DATA1(3) DATA2(3) DATA3(3) DATA4(3) DATA5(3) DATA6(3) DATA7(3)		
6	ITEM4(I) = DATA1(4) DATA2(4) DATA3(4) DATA4(4) DATA5(4) DATA6(4) DATA7(4)		
7	ITEM5(I) = DATA1(5) DATA2(5) DATA3(5) DATA4(5) DATA5(5) DATA6(5) DATA7(5)		
8	ITEM6(I) = DATA1(6) DATA2(6) DATA3(6) DATA4(6) DATA5(6) DATA6(6) DATA7(6)		
9	ITEM7(I) = DATA1(7) DATA2(7) DATA3(7) DATA4(7) DATA5(7) DATA6(7) DATA7(7)		
10	ITEM8(I) = DATA1(8) DATA2(8) DATA3(8) DATA4(8) DATA5(8) DATA6(8) DATA7(8)		
11	ITEM9(I) = DATA1(9) DATA2(9) DATA3(9) DATA4(9) DATA5(9) DATA6(9) DATA7(9)		
12	ITEM10(I) = DATA1(10) DATA2(10) DATA3(10) DATA4(10) DATA5(10) DATA6(10) DATA7(10)		
13	ITEM11(I) = DATA1(11) DATA2(11) DATA3(11) DATA4(11) DATA5(11) DATA6(11) DATA7(11)		
14	ITEM12(I) = DATA1(12) DATA2(12) DATA3(12) DATA4(12) DATA5(12) DATA6(12) DATA7(12)		
15	ITEM13(I) = DATA1(13) DATA2(13) DATA3(13) DATA4(13) DATA5(13) DATA6(13) DATA7(13)		
16	ITEM14(I) = DATA1(14) DATA2(14) DATA3(14) DATA4(14) DATA5(14) DATA6(14) DATA7(14)		
17	ITEM15(I) = DATA1(15) DATA2(15) DATA3(15) DATA4(15) DATA5(15) DATA6(15) DATA7(15)		
18	ITEM16(I) = DATA1(16) DATA2(16) DATA3(16) DATA4(16) DATA5(16) DATA6(16) DATA7(16)		
19	ITEM17(I) = DATA1(17) DATA2(17) DATA3(17) DATA4(17) DATA5(17) DATA6(17) DATA7(17)		
20	ITEM18(I) = DATA1(18) DATA2(18) DATA3(18) DATA4(18) DATA5(18) DATA6(18) DATA7(18)		
21	ITEM19(I) = DATA1(19) DATA2(19) DATA3(19) DATA4(19) DATA5(19) DATA6(19) DATA7(19)		
22	ITEM20(I) = DATA1(20) DATA2(20) DATA3(20) DATA4(20) DATA5(20) DATA6(20) DATA7(20)		
23	ITEM21(I) = DATA1(21) DATA2(21) DATA3(21) DATA4(21) DATA5(21) DATA6(21) DATA7(21)		
24	ITEM22(I) = DATA1(22) DATA2(22) DATA3(22) DATA4(22) DATA5(22) DATA6(22) DATA7(22)		
25	ITEM23(I) = DATA1(23) DATA2(23) DATA3(23) DATA4(23) DATA5(23) DATA6(23) DATA7(23)		
26	ITEM24(I) = DATA1(24) DATA2(24) DATA3(24) DATA4(24) DATA5(24) DATA6(24) DATA7(24)		
27	ITEM25(I) = DATA1(25) DATA2(25) DATA3(25) DATA4(25) DATA5(25) DATA6(25) DATA7(25)		
28	ITEM26(I) = DATA1(26) DATA2(26) DATA3(26) DATA4(26) DATA5(26) DATA6(26) DATA7(26)		
29	ITEM27(I) = DATA1(27) DATA2(27) DATA3(27) DATA4(27) DATA5(27) DATA6(27) DATA7(27)		
30	ITEM28(I) = DATA1(28) DATA2(28) DATA3(28) DATA4(28) DATA5(28) DATA6(28) DATA7(28)		

NOTE: THE FIRST STATION OF THE MAIN BEAM MUST BE LABELED 1, I.E., ITEM1(I) = 1. AS A GENERAL PRACTICE, STATION IDENTIFICATION COUNTERS SHOULD BE UNIQUE SINCE APPENDAGE ATTACHMENT STATION NUMBERS REFER TO THESE IDENTIFICATION COUNTERS.

NOTE: EXCEPT FOR THE MAIN BEAM IN WHICH ITEM2(I) = 0, THE APPENDAGE ATTACHMENT STATION IDENTIFICATION NUMBER MUST REFER TO A STATION ID. COUNTER, I.E. ITEM2(I) = ITEM1(J) FOR A STATION J IN WHICH ITEM4(J) = 2

(WITHIN AN APPENDAGE, ALL ATTACHMENT NUMBERS ARE EQUAL)

NOTE: DESIGNATION OF APPENDAGE ORDER FOR STATION I

NOTE: IF MAIN BEAM, ITEM3(I) = 0

IF APPENDAGE ATTACHES TO MAIN BEAM, ITEM3(I) = 1

IF APPENDAGE ATTACHES TO A FIRST ORDER APPENDAGE, ITEM3(I) = 2

ETC.

FOR A REDUNDANT APPENDAGE, ITEM3(I) = -1

TABLE A-3 (CONT'D.)

FORTRAN CODING AND DATA FORM

PROBLEM										PROGRAMMER									
1	2	3	4	5	6	7	8	9	10	11	12	13	14	15	16	17	18	19	20
ITEM4(I)	-	DESIGNATION OF STATION	TYPE FOR STATION	I	1	2	3	4	5	6	7	8	9	10	11	12	13	14	15
0	-	MASS STATION																	
1	-	SARING STATION																	
2	-	APPENDAGE ATTACHMENT STATION																	
3	-	FORWARD REDUNDANT APPENDAGE ATTACHMENT STATION																	
4	-	AFT REDUNDANT APPENDAGE ATTACHMENT STATION																	
NOTE: ENTER ALL REDUNDANT APPENDAGES LAST STARTING FROM FORWARD END																			
ITEM5(I)	-	DESIGNATION OF TYPE OF MOTION FOR STATION																	
0	-	BENDING																	
1	-	TORSION																	
2	-	COMPRESSIVE																	
BENDING(ITEM5(I)=0)										TORSION(ITEM5(I)=1)									
DATA1(I)		ET	-	LG*IN ²															
DATA2(I)		WEIGHT	-	LG															
DATA3(I)		X	-	IN															
DATA4(I)		IR	-	LG*IN ²															
DATA5(I)		KR	-	IN/LG OR K - DEG															
DATA6(I)		KAR	-	KG/IN*LG OR K - DEG															
DATA7(I)		W	-	DEG															
NOTE: ENTER ALL MAIN BEAM CARDS FIRST, THEN APPENDAGE CARDS - MAIN BEAM AND APPENDAGE CARDS MUST BE IN ORDER AS PROGRAM DOES NO SORTING.																			
ENTER APPENDAGES STARTING AT FREE END, ENDING AT ATTACHED END.																			
EVERY STATION EXCEPT LAST SHOULD HAVE A VALUE IN DATA1(I). THIS IS THE STIFFNESS FROM X(I) TO X(I+1).																			
WEIGHT AND INERTIA VALUES ARE ASSUMED TO BE LUMPED AT X(I).																			
WEIGHTS AND INERTIA SHOULD ONLY BE ENTERED IF ITEM4(I)=0																			

TABLE A-3 (CONT'D.)
FORTRAN CODING AND DATA FORM

PROBLEM										NAME										DATA									
PROGRAMMER										NAME										DATA									
1	2	3	4	5	6	7	8	9	10	11	12	13	14	15	16	17	18	19	20	21	22	23	24	25	26	27	28	29	30
WITHIN THE MAIN BEAM OR ANY APPENDAGE, X(I+1) = X(I)																													
(A STATION LOCATION IS NEEDED FOR EACH CARD INPUT, CAN BE ZERO)																													
PARAMETERS SHOULD ONLY BE ENTERED IN DATA5(I), DATA6(I) AND DATA7(I)																													
IF ITEM4(I) = 1 OR 2																													
ITEM1(I) = 0 ENDS THE READING OF THE BEAM DESCRIPTION CARDS - READ A																													
MAXIMUM OF 100 OF THESE CARDS (COUNTING THE ITEM1(I) = 0 CARD)																													
ALSO CONTAINED ON THE ITEM1(I) = 0 CARD ARE THE FOLLOWING PARAMETERS:																													
ITEM2(I) - DESIGNATION OF BOUNDARY CONDITIONS FOR MAIN BEAM																													
1 - FREE FORWARD END, FREE AFT END																													
2 - FREE FORWARD END, CLAMPED AFT END																													
3 - CLAMPED FORWARD END, CLAMPED AFT END																													
4 - FREE FORWARD END, PINNED AFT END																													
5 - PINNED FORWARD END, CLAMPED AFT END																													
6 - PINNED FORWARD END, PINNED AFT END																													
DATA1(I) - STARTING FREQUENCY FOR MYKESTAD MODE SEARCH FOR MODE 1 - ME																													
NOTE: IF DATA1(I) IS BLANK OR ZERO, PROGRAM SETS DATA1(I) = 2.5 ME																													
DATA2(I) - TOLERANCE ON FREQUENCY FOR MODE DETERMINATION																													
NOTE: IF DATA2(I) IS BLANK OR ZERO, PROGRAM SETS DATA2(I) = 1.0 x 10 ⁻⁵																													
DATA3(I) - FREQUENCY CHANGE BYTE SIZE PARAMETER																													
(FREQUENCY = FREQUENCY * DATA3(I))																													
NOTE: IF DATA3(I) IS BLANK OR ZERO, PROGRAM SETS DATA3(I) = 1.0																													
DATA4(I) - UPPER MODE SEARCH FREQUENCY - ME																													
NOTE: IF DATA4(I) IS BLANK OR ZERO, PROGRAM SETS DATA4(I) = 250.0																													

NOTE: ADDITIONAL DATA CHECKS MAY BE SUBMITTED, STARTING WITH A NEW TITLE CARD, ETC.

Table A-4
FORTRAN Listing of Program FILLIN

PROGRAM FILLIN(INPUT=65,OUTPUT=65,TAPE 61=INPUT,PUNCH=65)	FIL 10
DIMENSION XSTA(200),XESTA(200),EPhi(200,10),EPHIP(200,10),PHI(200,	FIL 20
110),NAEND(11),NAAS(200),ITME(5,201),DAAT(7,201),TITLE(8),NAONE(11)	FIL 30
2,LABEL(200),ITYFE(200),PSAVE(10),NAS(200),	FIL 40
3SH=L(5),LAONE(11),LAEND(11)	FIL 50
COMMON Y(4),PH(4) A(3),X,P,PP,0,YSQ(4)	FIL 60
10 READ20,TITLE	FIL 70
20 FORMAT(8A10)	FIL 80
IF(E0F(60))30,40	FIL 90
30 CALL EXIT	FIL 100
40 PRINT 50,TITLE	FIL 110
50 FORMAT(1H1,15X,8A10)	FIL 120
C	FIL 130
C READ BEAM DESCRIPTION	FIL 140
C	FIL 150
NX=0	FIL 160
60 NX=NX+1	FIL 170
READ70,(ITME(LL,NX),LL=1,5),(DAAT(KK,NX),KK=1,7)	FIL 180
70 FORMAT(2I4,3I2,2X,7E8.0)	FIL 190
IF(ITME(1,NX).NE.0)GO TO 60	FIL 200
C READ CONTROL CARD	FIL 210
C	FIL 220
READ80,NSTA,NESTA,NEXP	FIL 230
80 FORMAT(3I5)	FIL 240
PRINT 90,NSTA,NESTA	FIL 250
90 FORMAT(///2)X,*NUMBER OF MYKLESTAD STATIONS=*,I5,10X,*NUMBER OF EX	FIL 260
PERIMENTAL POINTS=*,I5)	FIL 270
NCARD=NX	FIL 280
C	FIL 290
C PRINT BEAM DESCRIPTION	FIL 300
C	FIL 310
PRINT 100	FIL 320
100 FORMAT(///,20X,*MYKLESTAD INPUT*,///)	FIL 330
DO 110 I=1,NCARD	FIL 340
110 PRINT 120,I,(ITME(J,I),J=1,5),(DAAT(JJ,I),JJ=1,7)	FIL 350
120 FORMAT(6I4,4X,7E13.5)	FIL 360
C	FIL 370
C READ IN AND PRINT MEASUREMENT STATIONS AND APPENDAGE INDICATORS	FIL 380
C	FIL 390
READ130,(NAAS(I),XESTA(I),I=1,NESTA)	FIL 400
130 FORMAT((4(10,E10.0)))	FIL 410
PRINT 140,(I,NAAS(I),XESTA(I),I=1,NESTA)	FIL 420
140 FORMAT(1H1,10X,*MODAL MEASUREMENT STATIONS AND APPENDAGE ATTACHMEN	FIL 430
T STATION NUMBERS*,/(20X,2I10,10X,E13.5))	FIL 440
L=1	FIL 450
LAONE(1)=1	FIL 460
DO 150 I=2,NESTA	FIL 470
IF(NAAS(I).EQ.NAAS(I-1))GO TO 150	FIL 480
LAENU(L)=I-1	FIL 490
L=L+1	FIL 500

Table A-4
(Cont'd.)

LAONE(L)=I	FIL 510
150 CONTINUE	FIL 520
LAEND(L)=NESTA	FIL 530
C	FIL 540
C READ AND PRINT EXPERIMENTAL MODE SHAPES OR SLOPES	FIL 550
C	FIL 560
PRINT 160	FIL 570
160 FORMAT(1H1,20X,*EXPERIMENTAL MODE SHAPES*,//)	FIL 580
MSTA=NESTA	FIL 590
IF(NEXP.GT.5)MSTA=2*NESTA	FIL 600
DO 180 IT=1,MSTA	FIL 610
READ190,J,K,(SHEL(L),L=1,5)	FIL 620
PRINT 200,J,NAAS(IT),K,(SHEL(L),L=1,5)	FIL 630
DO 170 L=1,5	FIL 640
170 PHI(J,(K+L-1))=SHEL(L)	FIL 650
180 CONTINUE	FIL 660
190 FORMAT(6X,2I3,5E12.5)	FIL 670
200 FORMAT(6X,3I6,5X,5E12.5)	FIL 680
C	FIL 690
C DEFINE MYKLESTAD OUTPUT STATIONS	FIL 700
C DEFINE APPENDAGE END POINTS	FIL 710
C INITIALIZE NAT=NUMBER OF APPENDAGES, NA=APPENDAGE NUMBER,	FIL 720
C NAONE(NA),NAEND(NA)=NUMBERS OF FIRST AND LAST STATIONS,	FIL 730
C DEFINE STATION TYPE,ITYPE(J)=0(NO JOINT),1(LEFT SIDE ROTATIONAL	FIL 740
C SPRING), 2 (LEFT SIDE SHEAR SPRING), 3 (LEFT SIDE ROTATIONAL AND	FIL 750
C SHEAR SPRINGS), 4 (RIGHT SIDE ROTATIONAL SPRING), 5 (RIGHT SIDE	FIL 760
C SHEAR SPRINGS), 6 (RIGHT SIDE ROTATIONAL AND SHEAR SPRINGS)	FIL 770
C	FIL 780
NAT=NA=NAONE(1)=1	FIL 790
NN=1	FIL 800
K=0	FIL 810
DO 270 J=1,NSTA	FIL 820
XSTA(J)=DAAT(3,NN)	FIL 830
LABEL(J)=ITME(1,NN)	FIL 840
NAS(J)=ITME(2,NN)	FIL 850
ITYPE(J)=0	FIL 860
IF(K.NE.0)GO TO 210	FIL 870
IF(ITME(4,NN).EQ.0)GO TO 230	FIL 880
IF(ITME(4,NN).NE.1)GO TO 260	FIL 890
IF(DAAT(6,NN).NE.0)ITYPE(J)=1	FIL 900
IF(DAAT(5,NN).NE.0)ITYPE(J)=2	FIL 910
IF(DAAT(5,NN).NE.0.AND.DAAT(6,NN).NE.0)ITYPE(J)=3	FIL 920
GO TO 260	FIL 930
210 K=0	FIL 940
IF(ITME(4,NN).NE.1)GO TO 220	FIL 950
IF(DAAT(6,NN).NE.0)ITYPE(J)=4	FIL 960
IF(DAAT(5,NN).NE.0)ITYPE(J)=5	FIL 970
IF(DAAT(5,NN).NE.0.AND.DAAT(6,NN).NE.0)ITYPE(J)=6	FIL 980
GO TO 230	FIL 990
220 NN=1+NN	FIL1000

Table A-4
(Cont'd.)

GO TO 270	FIL1010
230 IF(ITME(1,NN+1).EQ.0)GO TO 240	FIL1020
IF(ITME(2,NN).NE.ITME(2,NN+1))GO TO 240	FIL1030
N'=1+NN	FIL1040
K=C	FIL1050
GO TO 270	FIL1060
240 NAEND(NA)=1+J	FIL1070
IF(ITME(1,NN+1).EQ.0)GO TO 250	FIL1080
NA=1+NA	FIL1090
NAONE(NA)=2+J	FIL1100
GO TO 260	FIL1110
250 NAT=NA	FIL1120
260 K=1	FIL1130
270 CONTINUE	FIL1140
VAEND(NAT)=NSTA	FIL1150
C	FIL1160
PRINT 280,NAT	FIL1170
280 FORMAT(/10X,*NUMBER OF APPENDAGES INCLUDING MAIN BEAM=*,I3)	FIL1180
PRINT 290	FIL1190
290 FORMAT(/10X*APPENDAGE NUMBER*,5X*FIRST STATION*,5X*END STATION*)	FIL1200
PRINT 300,(J,NAONE(J),NAEND(J),J=1,NAT)	FIL1210
300 FORMAT(20X,I3,12X,I3,12X,I3)	FIL1220
PRINT 310	FIL1230
310 FORMAT(1H1,T10*STATION NUMBER*T30*STATION*T50*LABEL*T70*TYPE*T90*A	FIL1240
1PPENDAGE LABEL*/)	FIL1250
PRINT 320,(J,XSTA(J),LABEL(J),ITYPE(J),NAS(J),J=1,NST;	FIL1260
320 FORMAT(I20,15X,13.5,I7,I18,I20)	FIL1270
C	FIL1280
DO 840 L=1,NAT	FIL1290
II=NAONE(L)	FIL1300
IFN=NAEND(L)	FIL1310
JI=LAONE(L)	FIL1320
JFN=LAEND(L)	FIL1330
JN=JFN-JI+1	FIL1340
DO 830 I=II,IFN	FIL1350
X=XSTA(I)	FIL1360
IT=ITYPE(I)+1	FIL1370
GO TO (330,450,540,630,690,760,790)IT	FIL1380
C	FIL1390
PLAIN STATION	FIL1400
330 IF(X.LE.XESTA(JI+1))GO TO 390	FIL1410
IF(X.GE.XESTA(JFN-1))GO TO 400	FIL1420
IF(JN.GT.4)GO TO 360	FIL1430
IF(JN.EQ.4)GO TO 410	FIL1440
JO=JI	FIL1450
JE=JI+1	FIL1460
Y(1)=XESTA(JO)	FIL1470
Y(2)=XESTA(JE)	FIL1480
340 D=1.0/(Y(2)-Y(1))	FIL1490
DO 350 M=1,NEXP	FIL1500
PH(1)=PHI(JO,M)	

Table A-4
(Cont'd.)

PH(2)=PHI(JE,M)	FIL1510
CALL LINFIT	FIL1520
EPHI(I,M)=P	FIL1530
350 EPHIP(I,M)=PP	FIL1540
GO TO (830,460,550,680,700,770,820)IT	FIL1550
360 JJ=JI+1	FIL1560
JM=JFN-2	FIL1570
DO 370 J=JJ, JM	FIL1580
IF(X.GT.XESTA(J).AND.X.LE.XESTA(J+1))GO TO 380	FIL1590
370 CONTINUE	FIL1600
380 JONE=J-1	FIL1610
GO TO 420	FIL1620
390 Y(1)=XESTA(JI)	FIL1630
Y(2)=XESTA(JI+1)	FIL1640
JO=JI	FIL1650
JE=JI+1	FIL1660
GO TO 340	FIL1670
400 Y(1)=XESTA(JFN-1)	FIL1680
Y(2)=XESTA(JFN)	FIL1690
JU=JFN-1	FIL1700
JE=JFN	FIL1710
GO TO 340	FIL1720
410 JONE=JI	FIL1730
420 CONTINUE	FIL1740
DO 440 M=1,NEXP	FIL1750
DO 430 K=1,4	FIL1760
Y(K)=XESTA(K+JONE-1)	FIL1770
430 PH(K)=PHI(K+JONE-1,M)	FIL1780
CALL SQUARE	FIL1790
CALL PARAB	FIL1800
EPHI(1,M)=P	FIL1810
440 EPHIP(I,M)=PP	FIL1820
GO TO (830,460,550,680,700,770,820)IT	FIL1830
450 KSAVE=1	FIL1840
GO TO 330	FIL1850
460 KSAVE=KSAVE+1	FIL1860
IF(KSAVE.EQ.3)GO TO 520	FIL1870
DO 470 M=1,NEXP	FIL1880
470 PSAVE(M)=EPHI(I,M)	FIL1890
DO 480 J=JI, JFN	FIL1900
JJ=J	FIL1910
IF(X.EQ.XESTA(J))GO TO 500	FIL1920
IF(X.LT.XESTA(J))GO TO 490	FIL1930
480 CONTINUE	FIL1940
GO TO 510	FIL1950
490 JFN=JJ-1	FIL1960
GO TO 510	FIL1970
500 JFN=JJ	FIL1980
510 JL=JJ-JI	FIL1990
IF(JL.GT.3)JI=JJ-3	FIL2000

Table A-4
(Cont'd.)

JN=JFN-JI+1	FIL2010
GO TO 330	FIL2020
520 DO 530 M=1,NEXP	FIL2030
530 EPHI(I,M)=PSAVE(M)	FIL2040
JI=LAONE(L)	FIL2050
JFN=LAEND(L)	FIL2060
JN=JFN-JI+1	FIL2070
GO TO 830	FIL2080
540 KSAVE=1	FIL2090
GO TO 630	FIL2100
550 KSAVE=1+KSAVE	FIL2110
IF(KSAVE.EQ.3) GO TO 610	FIL2120
DO 560 M=1,NEXP	FIL2130
560 PSAVE(M)=EPHIP(I,M)	FIL2140
DO 570 J=JI,JFN	FIL2150
JJ=J	FIL2160
IF(X.EQ.XESTA(J)) GO TO 590	FIL2170
IF(X.LT.XESTA(J)) GO TO 580	FIL2180
570 CONTINUE	FIL2190
GO TO 600	FIL2200
580 JFN=JJ-1	FIL2210
GO TO 600	FIL2220
590 JFN=JJ	FIL2230
600 JL=JJ-JI	FIL2240
IF(JL.GT.3) JJ=JJ-3	FIL2250
JN=JFN-JI+1	FIL2260
GO TO 330	FIL2270
610 DO 620 M=1,NEXP	FIL2280
620 EPHIP(I,M)=PSAVE(M)	FIL2290
JI=LAONE(L)	FIL2300
JFN=LAEND(L)	FIL2310
JN=JFN+1-JI	FIL2320
GO TO 830	FIL2330
C	FIL2340
C STATION TO LEFT OF A ROTATIONAL AND A SHEAR SPRING	FIL2350
C	FIL2360
630 DO 640 J=JI,JFN	FIL2370
JJ=J	FIL2380
IF(X.EQ.XESTA(J)) GO TO 660	FIL2390
IF(X.LT.XESTA(J)) GO TO 650	FIL2400
640 CONTINUE	FIL2410
GO TO 670	FIL2420
650 JFN=JJ-1	FIL2430
GO TO 670	FIL2440
660 JFN=JJ	FIL2450
670 JL=JJ-JI	FIL2460
IF(JL.GT.3) JJ=JJ-3	FIL2470
JN=JFN-JI+1	FIL2480
GO TO 330	FIL2490
680 JFN=LAEND(L)	FIL2500

Table A-4
(Cont'd.)

	JI=LAONE(L)	FIL2510
	JN=JFN+1-JI	FIL2520
	GO TO 830	FIL2530
C		FIL2540
C	STATION TO RIGHT OF A ROTATIONAL SPRING	FIL2550
C		FIL2560
	600 KSAVE=1	FIL2570
	GO TO 330	FIL2580
	700 KSAVE=1+KSAVE	FIL2590
	IF(KSAVE.EQ.3) GO TO 740	FIL2600
	DO 710 M=1,NEXP	FIL2610
	710 PSAVE(M)=EPHI(I,M)	FIL2620
	DO 720 J=JI,JFN	FIL2630
	JJ=J	FIL2640
	IF(X.LE.XESTA(J)) GO TO 730	FIL2650
	720 CONTINUE	FIL2660
	GO TO 830	FIL2670
	730 JI=JJ	FIL2680
	IF(JI+3.LE.JFN) JFN=JI+3	FIL2690
	JN=JFN-JI+1	FIL2700
	GO TO 330	FIL2710
	740 DO 750 M=1,NEXP	FIL2720
	750 EPHI(I,M)=PSAVE(M)	FIL2730
	JI=LAONE(L)	FIL2740
	JFN=LAEND(L)	FIL2750
	JN=JFN-JI+1	FIL2760
	GO TO 830	FIL2770
C		FIL2780
C	STATION TO RIGHT OF A SHEAR SPRING	FIL2790
C		FIL2800
	760 KSAVE=1	FIL2810
	GO TO 790	FIL2820
	770 DO 780 M=1,NEXP	FIL2830
	EPHIP(I,M)=0.5*(EPHIP(I-1,M)+EPHIP(I,M))	FIL2840
	780 EPHIP(I-1,M)=EPHIP(I,M)	FIL2850
	GO TO 830	FIL2860
C		FIL2870
C	STATION TO THE RIGHT OF A ROTATIONAL SPRING AND A SHEAR SPRING	FIL2880
C		FIL2890
	790 DO 800 J=JI,JFN	FIL2900
	JJ=J	FIL2910
	IF(X.LE.XESTA(J)) GO TO 810	FIL2920
	800 CONTINUE	FIL2930
	GO TO 830	FIL2940
	810 JI=JJ	FIL2950
	IF(JI+3.LE.JFN) JFN=JI+3	FIL2960
	JN=JFN-JI+1	FIL2970
	GO TO 330	FIL2980
	820 JFN=LAEND(L)	FIL2990
	JI=LAONE(L)	FIL3000

Table A-4
(Cont'd.)

JN=JFN+1-JI	FIL3010
IF(IT.EQ.6)GO TO 770	FIL3020
830 CONTINUE	FIL3030
840 CONTINUE	FIL3040
DO 860 I=1,NEXP	FIL3050
PRINT 850,I	FIL3060
850 FORMAT(1H1,20X*COMPLETE EXPERIMENTAL MODE*,I4,/,T15,*STATION NUMB	FIL3070
1ER*,T30,*STATION LABEL*,T45,*APPENDAGE LABEL*,T70,*STATION TYPE*,T	FIL3080
295,*STATION*,T96,*DISPLACEMENT*,T118,*SLOPE*,//)	FIL3090
DO 860 J=1,NSTA	FIL3100
860 PRINT 870,J,LABEL(J),NAS(J),ITYPE(J),XSTA(J),EPMI(J,I),EPHIP(J,I)	FIL3110
870 FORMAT(20X,I5,I10,2I20,5X,3E15.5)	FIL3120
880 CONTINUE	FIL3130
NP=1	FIL3140
890 IT=1	FIL3150
NE=NEXP	FIL3160
IF(NEXP.GT.5)NE=5	FIL3170
900 DO 920 J=1,NSTA	FIL3180
PUNCH 910,J,IT,(EPMI(J,L),L=IT,NE)	FIL3190
910 FORMAT(6X,2I3,5E12.5)	FIL3200
920 CONTINUE	FIL3210
IF(NEXP.GT.NE)GO TO 930	FIL3220
GO TO 940	FIL3230
930 IT=6	FIL3240
NE=NEXP	FIL3250
GO TO 900	FIL3260
940 NP=NP+1	FIL3270
IF(NP.EQ.3)GO TO 960	FIL3280
DO 950 L=1,NEXP	FIL3290
DO 950 J=1,NSTA	FIL3300
950 EPMI(J,L)=EPHIP(J,L)	FIL3310
GO TO 890	FIL3320
960 CONTINUE	FIL3330
GO TO 10	FIL3340
END	FIL3350

Table A-5
FORTRAN Listing of Subroutine SQUARE

SUBROUTINE SQUARE	SQU 10
COMMON Y(4),PH(4),A(3),X,P,PP,C,YSQ(4)	SQU 20
DIMENSION Z(4),F(4)	SQU 30
DO 10 I=1,4	SQU 40
Z(I)=Y(I)	SQU 50
F(I)=PH(I)	SQU 60
Y(I)=0.0	SQU 70
YSQ(I)=0.0	SQU 80
10 PH(I)=0.0	SQU 90
DO 20 I=1,4	SQU 100
PH(1)=PH(1)+F(I)	SQU 110
Y(1)=Y(1)+Z(I)	SQU 120
YSQ(1)=YSQ(1)+Z(I)*Z(I)	SQU 130
PH(2)=PH(2)+F(I)*Z(I)	SQU 140
YSQ(2)=YSQ(2)+Z(I)*Z(I)*Z(I)	SQU 150
PH(3)=PH(3)+F(I)*Z(I)*Z(I)	SQU 160
20 YSQ(3)=YSQ(3)+Z(I)**4	SQU 170
PH(1)=0.25*PH(1)	SQU 180
Y(1)=0.25*Y(1)	SQU 190
YSQ(1)=0.25*YSQ(1)	SQU 200
Y(2)=YSQ(1)/Y(1)	SQU 210
PH(2)=0.25*PH(2)/Y(1)	SQU 220
YSQ(2)=0.25*YSQ(2)/Y(1)	SQU 230
PH(3)=0.25*PH(3)/YSQ(1)	SQU 240
Y(3)=0.25*Y(3)/YSQ(1)	SQU 250
YSQ(3)=0.25*YSQ(3)/YSQ(1)	SQU 260
D=1.0/(Y(2)*YSQ(3)+Y(1)*YSQ(2)+Y(3)*YSQ(1)-Y(2)*YSQ(1)-Y(1)*YSQ(3)	SQU 270
1-Y(3)*YSQ(2))	SQU 280
END	SQU 290

Table A-6
FORTRAN Listing of Subroutine PARAB

SUBROUTINE PARAB	PAR 10
COMMON Y(4), PH(4), A(3), X, P, PP, D, YSQ(4)	PAR 20
A(1)=D*(PH(1)*(Y(2)*YSQ(3)-Y(3)*YSQ(2))+PH(2)*	PAR 30
1(Y(3)*YSQ(1)-Y(1)*YSQ(3))-PH(3)*(Y(2)*YSQ(1)-Y(1)*YSQ(2)))	PAR 40
A(2)=D*(PH(1)*(YSQ(2)-YSQ(3))+PH(2)*(YSQ(3)-YSQ(1))+PH(3)*(YSQ(1)-	PAR 50
1YSQ(2)))	PAR 60
A(3)=D*(PH(1)*(Y(3)-Y(2))+PH(2)*(Y(1)-Y(3))+PH(3)*(Y(2)-Y(1)))	PAR 70
P=A(1)+A(2)*X+A(3)*X*X	PAR 80
PP=A(2)+2*A(3)*X	PAR 90
END	PAR 100

Table A-7
FORTRAN Listing of Subroutine LINFIT

SUBROUTINE LINFIT	LIN	10
COMMON Y(4),PH(4),A(3),X,P,PP,D,YSQ(4)	LIN	20
A(1)=D*(Y(2)*PH(1)-Y(1)*PH(2))	LIN	30
A(2)=D*(PH(2)-PH(1))	LIN	40
P=A(1)+A(2)*X	LIN	50
PP=A(2)	LIN	60
END	LIN	70

Table A-8
FORTRAN Listing of Program JOINTS

	PROGRAM JOINTS (INPUT,OUTPUT,TAPE60=INPUT,TAPE6=OUTPUT)	JTS 10
C		JTS 20
C	PROGRAM JOINTS - PROBLEM 2049 02/26/71 VARIABLE DELTAK	JTS 30
C	WITH SHEAR SPRINGS	JTS 40
C		JTS 50
	DIMENSION MAXSIGN(10),NSMAXPH(10),NAONE(10),NAEND(10)	JTS 60
	DIMENSION TITLE(8), GM(10),SHFL(5),BB(10,10),CC(10,10)	JTS 70
	DIMENSION STFREQ(10),XESTA(100)	JTS 80
C		JTS 90
C	STORAGE COMMON TO SUBROUTINE MYKL	JTS 100
C		JTS 110
	COMMON FINK(300)	JTS 120
	COMMON A(4,4,101),SAP(4,4),AP(4,4),VINV(4,4),ALV(4,4),T(4,4),AL	JTS 130
	1VT(4,4),TAP(4,4,100),VEC(4,101),ITEM(6,101),CATA(8,101),I1(300),IR	JTS 140
	2(300),OM(300),FUNC(300),R(3),KKK(100),MODE(100),JOINT(101),AL(4,4)	JTS 150
	3,I6(101),PRNT(4),HOL(12)	JTS 160
	COMMON ICON(10),ICB(10),FPM(10,4,4),FOM(10,4,4),VSAVE(4),ARSTAR	JTS 170
	1(10,6,4), ARP(4,4),ARPA(4,4),APR(4,4),CANV(2,2),DENV(2,2)	JTS 180
	2),THMAN(6,6),BMAN(6,6),BINV(6,6),RMUL(6,4)	JTS 190
	COMMON I4(101)	JTS 200
	COMMON ITMF(5,101),DAAT(7,101),IETM(5),DTAA(7)	JTS 210
C		JTS 220
C	STORAGE COMMON TO SUBROUTINE STEEP	JTS 230
C		JTS 240
	COMMON/1/ MWH, ISTOP, NSTA, NT, NEXP, STEP, ITMAX, TOL, ITER	JTS 250
	COMMON/2/ KKKK, ALPHA, F, PFK(20), INTEG(20)	JTS 260
	COMMON/3/ PHMAT(10), FWMAT(10), EOMEGS(10), KVAR(20), SPRINGL(20), SPRIN	JTS 270
	1GU(20), EPHI(100,10), EPHIP(100,10), EFREQ(10), TFREQ(10)	JTS 280
	COMMON/4/ TOMECS(10), TPHI(100,10), TPHP(100,10)	JTS 290
	COMMON/5/ JA, JB, JD, FF, SPFK(10), AA(10,10), ASPRING(20)	JTS 300
	COMMON/6/ NVSPR, SPRING(10), SSPRING(10), KSTA(10), KTYPE(10), COMP(10)	JTS 310
	COMMON/7/ XRATIO, OLDSPR(10)	JTS 320
	COMMON/8/ KNORM, XSTA(100)	JTS 330
	CALL MEMSET (PINK(1),DTAA(7))	JTS 340
C		JTS 350
C	READ AND PRINT TITLE	JTS 360
C		JTS 370
	10 READ(20),TITLE	JTS 380
	20 FORMAT(8A10)	JTS 390
	IF(EOF(60))30,40	JTS 400
	30 CALL EXIT	JTS 410
	40 PRINT 50,TITLE	JTS 420
	50 FORMAT(1H1,20X*EXTRACTION OF JOINT COMPLIANCES FROM ELASTIC MODE T	JTS 430
	1EST DATA*//20X,8A10///)	JTS 440
C		JTS 450
C	INITIALIZATION PASS	JTS 460
C		JTS 470
	ISTOP=0	JTS 480
	ITER=1	JTS 490
C		JTS 500

Table A-8
(Cont'd.)

C	READING OPTIONS, WEIGHTING MATRICES, AND LIMITS	JTS 510
C		JTS 520
	READ60,KNORM,NT,NEXP,NWT,ITMAX,NVSPR,NSTA,NESTA,STEP,TOL,CLOSE, X	JTS 530
	1RATIO	JTS 540
60	FORMAT(4I5,4I5,4E10.0)	JTS 550
	IF(KNORM.EQ.0) KNORM=1	JTS 560
	NOTM=NT	JTS 570
	PRINT 70, NT,NEXP,ITMAX,NVSPR,NSTA,STEP,CLOSE,NWT,NESTA	JTS 580
70	FORMAT(//40X,* NT = *,I13,/40X,* NEXP = *,I13,/40X,* ITMAX	JTS 590
	1= *,I13,/40X,* NVSPR = *,I13,/40X,* NSTA = *,I13,/40X,* STEP	JTS 600
	2=*,E13.5,/40X,* CLOSE =*,E13.5,/40X,* NWT =*,I13,20X,*NESTA =*,I	JTS 610
	313)	JTS 620
	KCLOSE=0	JTS 630
	IF(CLOSE.EQ.0.0) KCLOSE=1	JTS 640
	PRINT 80,TOL	JTS 650
80	FORMAT(40X,* TOL = *,E13.5)	JTS 660
	READ90,KCHECK,XMASS	JTS 670
90	FORMAT(I5,E10.0)	JTS 680
	IF(KCHECK.NE.2)GO TO 110	JTS 690
	PRINT 100,XMASS	JTS 700
100	FORMAT(//20X*MODES WILL NOT BE CHECKED*,//20X,*XMASS = *,E13.5)	JTS 710
	GO TO 130	JTS 720
110	PRINT 120,XMASS	JTS 730
120	FORMAT(//20X*MODES WILL BE CHECKED*,//20X,*XMASS = *,E13.5)	JTS 740
130	IF(NWT.EQ.0)GO TO 145	JTS 750
	READ140,(PWMAT(I),I=1,NEXP)	JTS 760
140	FORMAT (8E10.0)	JTS 770
	READ140,(FWMAT(I),I=1,NEXP)	JTS 772
	GO TO 149	JTS 773
145	DO 146 I=1,NEXP	JTS 775
146	PWMAT(I)=FWMAT(I)=1.0	JTS 778
149	PRINT 150	JTS 780
150	FORMAT(//10X,* RELATIVE MODE SHAPE WEIGHTING FACTORS *)	JTS 790
	PRINT 160,(PWMAT(I),I=1,NEXP)	JTS 800
160	FORMAT(/ 1X,10E13.5)	JTS 810
	PRINT 170	JTS 830
170	FORMAT(//10X,* RELATIVE MODE FREQUENCY WEIGHTING FACTORS *)	JTS 840
	PRINT 160,(FWMAT(I),I=1,NEXP)	JTS 850
180	READ140,(EFREQ(I),I=1,NT)	JTS 860
	PRINT 190	JTS 870
190	FORMAT(//10X,* EXPERIMENTAL FREQUENCIES *)	JTS 880
	PRINT 160,(EFREQ(I),I=1,NT)	JTS 890
	DO 200 I=1,NT	JTS 900
200	EOMEGS(I)=(6.283185*EFREQ(I))**2	JTS 910
	RNST=XMASS/(2.0*NESTA)	JTS 950
	WF=ECMEGS(NEXP)**2	JTS 970
	DO 220 I=1,NEXP	JTS 980
	PWMAT(I)=RNST*WF*PWMAT(I)	JTS1000
220	FWMAT(I)=FWMAT(I)*WF/(EOMEGS(I)**2)	JTS1010
	PRINT 223	JTS1020

Table A-8
(Cont'd.)

223	FORMAT(//10X,* MODE SHAPE WEIGHTING FACTORS *)	JTS1025
	PRINT 160,(PWHAT(I),I=1,NEXP)	JTS1030
	PRINT 226	JTS1040
226	FORMAT(//10X,* MODE FREQUENCY WEIGHTING FACTORS *)	JTS1045
	PRINT 160,(FWHAT(I),I=1,NEXP)	JTS1050
230	READ 240,(KSTA(I),KVAR(I),SPRINGL(I),SPRINGU(I),KTYPE(I),I=1,NVSPR)	JTS1060
240	FORMAT(2I4,2E8.0,I4)	JTS1070
	PRINT 250	JTS1080
250	FORMAT(//22X,* K*,* KVAR(I)*,2X,* SPRINGL(I)*,2X,* SPRINGU(I)*,2X,* KTYPE*)	JTS1090
	PRINT 260,(KSTA(I),KVAR(I),SPRINGL(I),SPRINGU(I),KTYPE(I),I=1,NVSP	JTS1100
	1R)	JTS1110
260	FORMAT(/ (20X,I4,I8,2E13.5,I6))	JTS1120
	DO 270 I=1,10	JTS1130
	DO 270 J=1,NSTA	JTS1140
	EPHI(J,I)=0.0	JTS1150
270	EPHIP(J,I)=0.8	JTS1160
C		JTS1170
C	READING EXPERIMENTAL MODAL DATA	JTS1180
C		JTS1190
	IF(NSTA.EQ.NSTA)GO TO 290	JTS1200
	READ 140,(XESTA(I),I=1,NSTA)	JTS1210
	PRINT 280	JTS1220
280	FORMAT(//30X,*MODE MEASUREMENT STATIONS, XESTA(I)*)	JTS1230
	PRINT 160,(XESTA(I),I=1,NSTA)	JTS1240
290	PRINT 300	JTS1250
300	FORMAT(1H1,20X,25H EXPERIMENTAL MODE SHAPES,//)	JTS1260
	MSTA=NESTA	JTS1270
	IF(NEXP.GT.5)MSTA=2*NESTA	JTS1280
	DO 320 IT=1,MSTA	JTS1290
	READ 330,J,K,(SHEL(L),L=1,5)	JTS1300
	PRINT 330,J,K,(SHEL(L),L=1,5)	JTS1310
	DO 310 L=1,5	JTS1320
310	EPHI(J,(K+L-1))=SHEL(L)	JTS1330
320	CONTINUE	JTS1340
330	FORMAT(6X,2I3,5E12.5)	JTS1350
	PRINT 340	JTS1360
340	FORMAT(1H1,20X,25H EXPERIMENTAL MODE SLOPES,//)	JTS1370
	DO 360 IT=1,MSTA	JTS1380
	READ 330,J,K,(SHEL(L),L=1,5)	JTS1390
	PRINT 330,J,K,(SHEL(L),L=1,5)	JTS1400
	DO 350 L=1,5	JTS1410
350	EPHIP(J,(K+L-1))=SHEL(L)	JTS1420
360	CONTINUE	JTS1430
C		JTS1440
C	READ BEAM DESCRIPTION	JTS1450
C		JTS1460
	NX=0	JTS1470
370	NX=NX+1	JTS1480
	READ 380,(ITME(LL,NX),LL=1,5),(DAAT(KK,NX),KK=1,7)	JTS1490
		JTS1500

Table A-8
(Cont'd.)

380	FORMAT (2I4,3I2,2X,7E8.0)	JTS1510
	IF(ITME(1,NX).NE.0)GO TO 370	JTS1520
C		JTS1530
C	LAST DATA CARD HAS BEEN READ	JTS1540
C		JTS1550
	NCARD=NX	JTS1560
C		JTS1570
C	PRINT BEAM DESCRIPTION	JTS1580
C		JTS1590
	PRINT 390	JTS1600
390	FORMAT(1H1,* BEAM DESCRIPTION READ BY PROGRAM JOINTS*///)	JTS1610
	DO 410 I=1,NCARD	JTS1620
	PRINT 400,(ITME(J,I),J=1,5),(DAAT(JJ,I),JJ=1,7)	JTS1630
400	FORMAT ((5I4,4X,7E13.5))	JTS1640
410	CONTINUE	JTS1650
C		JTS1660
C	SETTING STATIONS TO INTERNAL COUNTERS	JTS1670
C	DEFINE APPENDAGE NUMBERS = NA, TOTAL NUMBER = NAT, FIRST AND LAST	JTS1680
C	STATION NUMBERS = NAONE(NA) AND NAEND(NA),	JTS1690
C		JTS1700
	NAT=NA=NAONE(1)+1	JTS1710
	NN=1	JTS1720
	K=0	JTS1730
	DO 460 J=1,NSTA	JTS1740
	XSTA(J)=DAAT(3,NN)	JTS1750
	IF(K.NE.0)GO TO 420	JTS1760
	IF(ITME(4,NN).NE.0)GO TO 450	JTS1770
	IF(ITME(1,NN+1).EQ.0)GO TO 430	JTS1780
	IF(ITME(2,NN).NE.ITME(2,NN+1))GO TO 430	JTS1790
420	NN=NN+1	JTS1800
	K=0	JTS1810
	GO TO 460	JTS1820
430	NAEND(NA)=J+1	JTS1830
	IF(ITME(1,NN+1).EQ.0)GO TO 440	JTS1840
	NA=NA+1	JTS1850
	NAONE(NA)=J+2	JTS1860
	GO TO 450	JTS1870
440	NAT=NA	JTS1880
450	K=1	JTS1890
460	CONTINUE	JTS1900
	PRINT 470,NAT	JTS1910
470	FORMAT(/10X,*NAT = *,I3)	JTS1920
	PRINT 480	JTS1930
480	FORMAT(/10X,* J*,5X,*NAONE(J)*,5X,*NAEND(J)*)	JTS1940
	PRINT 490,(J,NAONE(J),NAEND(J),J=1,NAT)	JTS1950
490	FORMAT(10X,I3,5X,I8,5X,I8)	JTS1960
C		JTS1970
C	COMPUTING GENERALIZED MASS FOR THE INPUT MODES	JTS1980
C		JTS1990
	DO 520 I=1,NEXP	JTS2000

Table A-8
(Cont'd.)

NN=0	JTS2010
JJ=0	JTS2020
GM(I)=0.0	JTS2030
500 NN=NN+1	JTS2040
JJ=JJ+1	JTS2050
IF(ITME(4,NN).NE.0) GO TO 510	JTS2060
GM(I)=GM(I)+DAAT(2,NN)*EPI(JJ,I)+EPI(JJ,I)+DAAT(4,NN)*EPI(JJ,I)	JTS2070
1)*EPI(JJ,I)	JTS2080
IF(ITME(2,NN).NE.ITME(2,NN+1)) JJ=JJ+1	JTS2090
IF(JJ.LT.NSTA) GO TO 500	JTS2100
GO TO 520	JTS2110
510 JJ=JJ+1	JTS2120
GO TO 500	JTS2130
520 GM(I)=GM(I)/386.4	JTS2140
PRINT 530	JTS2150
530 FORMAT(/5X,* THE GENERALIZED MASS ASSOCIATED WITH THE INPUT MODES*	JTS2160
1/)	JTS2170
PRINT 540,(GM(I),I=1,NEXP)	JTS2180
540 FORMAT(1X,5E20.8)	JTS2190
C DEFINE STATION NUMBER OF LARGEST DISPLACEMENT FOR EACH	JTS2200
C EXPERIMENTAL MODE NSMAXPH(I)	JTS2210
DO 550 I=1,NEXP	JTS2220
NSMAXPH(I)=1	JTS2230
MAXSIGN(I)=1	JTS2240
IF(EPI(1,I).LT.0.0) MAXSIGN(I)=-1	JTS2250
PHMAX=ABS(EPI(1,I))	JTS2260
NAE=NAEND(1)	JTS2270
DO 550 J=2,NAE	JTS2280
IF(ABS(EPI(J,I)).LE.PHMAX) GO TO 550	JTS2290
PHMAX=ABS(EPI(J,I))	JTS2300
MAXSIGN(I)=1	JTS2310
IF(EPI(J,I).LT.0.0) MAXSIGN(I)=-1	JTS2320
NSMAXPH(I)=J	JTS2330
550 CONTINUE	JTS2340
C	JTS2350
C NORMALIZING THE INPUT MODES TO A GENERALIZED MASS OF 1.0	JTS2360
C	JTS2370
DO 560 J=1,NEXP	JTS2380
FACT=SQRT(1.0/GM(I))	JTS2390
DO 560 J=1,NSTA	JTS2400
EPI(J,I)=FACT*EPI(J,I)	JTS2410
560 EPHIP(J,I)=FACT*EPHIP(J,I)	JTS2420
KKKK=0	JTS2430
DO 600 J=1,NVSPR	JTS2440
NN=KSTA(J)	JTS2450
IF(KTYPE(J).EQ.2) GO TO 570	JTS2460
IF(DAAT(5,NN).EQ.0.) GO TO 580	JTS2470
SPRING(J)=1.0/DAAT(5,NN)	JTS2480
GO TO 600	JTS2490
570 IF(DAAT(6,NN).EQ.0.) GO TO 580	JTS2500

Table A-8
(Cont'd.)

SPRING(J)=1.0/DAAT(6,NN)	JTS2510
GO TO 600	JTS2520
580 PRINT 590,J	JTS2530
590 FORMAT(/6H ****,18H COMPLIANCE NUMBER,I3,15H IS ZERO. ****)	JTS2540
ISTOP=1	JTS2550
600 CONTINUE	JTS2560
ITME(3,NCARD)=1	JTS2570
IF(DAAT(4,NCARD).EQ.0.0) DAAT(4,NCARD)=250.	JTS2580
IF(DAAT(3,NCARD).EQ.0.0) DAAT(3,NCARD)=1.10	JTS2590
IF(DAAT(1,NCARD).EQ.0.0) DAAT(1,NCARD)=2.5	JTS2600
SFREQ=DAAT(1,NCARD)	JTS2610
STOPFR=DAAT(4,NCARD)	JTS2620
DO 610 J=1,NVSPR	JTS2630
610 SSPRING(J)=SPRING(J)	JTS2640
JA=0	JTS2650
JB=0	JTS2660
JD=0	JTS2670
MIKE=0	JTS2680
DELF=DAAT(3,NCARD)	JTS2690
DO 620 I=1,NT	JTS2700
620 STFREQ(I)=EFREQ(I)	JTS2710
IF(ISTOP.EQ.1) GO TO 10	JTS2720
MWH=0	JTS2730
IF(XMASS.CT.0.0) GO TO 630	JTS2732
PRINT 625	JTS2734
625 FORMAT(/10X,62H* MISSILE MASS HAS BEEN READ AS ZERO. THIS CASE T	JTS2736
1ERMINATED. *)	JTS2737
GO TO 10	JTS2738
C	JTS2740
C	JTS2750
C	JTS2760
C	JTS2770
630 CONTINUE	JTS2780
DO 650 J=1,NVSPR	JTS2790
NN=KSTA(J)	JTS2800
IF(KTYPE(J).EQ.2) GO TO 640	JTS2810
DAAT(5,NN)=1.0/SPRING(J)	JTS2820
GO TO 650	JTS2830
640 DAAT(6,NN)=1.0/SPRING(J)	JTS2840
650 CONTINUE	JTS2850
IF(ITER.EQ.1) GO TO 670	JTS2860
DO 660 I=1,NT	JTS2870
660 STFREQ(I)=TFREQ(I)	JTS2880
670 CONTINUE	JTS2890
NT=NCTH	JTS2900
MTS=0	JTS2910
DO 680 I=1,NT	JTS2920
TFREQ(I)=0.0	JTS2930
DO 680 K=1,NSTA	JTS2940
TPHI(K,I)=0.0	JTS2950

Table A-8
(Cont'd.)

680	TPHIP(K,I)=0.0	JTS2960
	DAAT(1,NCARD)=SFREQ	JTS2970
		JTS2980
	SOLVE FOR NEW FREQUENCIES AND MODE SHAPES	JTS2990
		JTS3000
	PRINT 600,ITER	JTS3010
690	FORMAT(1H1,40X,21H INPUT FOR ITERATION ,I3/)	JTS3020
	LIME=0	JTS3030
	DO 930 I=1,NCTM	JTS3040
	DAAT(3,NCARD)=DELF	JTS3050
	DAAT(4,NCARD)=STOPFR	JTS3060
	IF(MTS.EQ.1)GO TO 930	JTS3070
	IF(I.EQ.1)GO TO 760	JTS3080
	IF(KCLOSE.EQ.1)GO TO 730	JTS3090
	IF(STFREQ(I).NE.0.0)GO TO 710	JTS3100
	PRINT 700,I	JTS3110
700	FORMAT(13H *** STFREQ(I,12,35H) EQUALS 0.0, THIS CASE TERMINATED.)	JTS3120
	MIKE=1	JTS3130
	GO TO 910	JTS3140
710	XFREQ=CLOSE*EFREQ(I)	JTS3150
	YFREQ=DELF*EFREQ(I-1)	JTS3160
	IF(XFREQ.GT.YFREQ)GO TO 720	JTS3170
	YFREQ=EFREQ(I-1)+(EFREQ(I)-EFREQ(I-1))/2.0	JTS3180
	DAAT(3,NCARD)=1.0+((EFREQ(I)-EFREQ(I-1))/(6.0*EFREQ(I)))	JTS3190
720	DAAT(1,NCARD)=XFREQ	JTS3200
	GO TO 740	JTS3210
730	DAAT(1,NCARD)=DAAT(3,NCARD)*TFREQ(I-1)	JTS3220
740	IF(DAAT(1,NCARD).GT.DAAT(4,NCARD))GO TO 810	JTS3230
	PRINT 750,(ITIME(J,NCARD),J=1,5),(DAAT(JJ,NCARD),JJ=1,7)	JTS3240
750	FORMAT(/(5I4,4X,7E13.5))	JTS3250
760	CALL MYKL(FREQ,GAM,LIME)	JTS3260
	LIME=1	JTS3270
	IF(FREQ.NE.0.)GO TO 780	JTS3280
	PRINT 770	JTS3290
770	FORMAT(/* ERROR IN COMPUTED MODE FREQUENCIES. FREQ=0.0, THIS CASE	JTS3300
	1 ABORTED *)	JTS3310
	MIKE=1	JTS3320
780	CONTINUE	JTS3330
	IF(I.EQ.1)GO TO 790	JTS3340
	IF(FREQ.EQ.TFREQ(I-1))GO TO 820	JTS3350
790	CONTINUE	JTS3360
	DO 800 K=1,NSTA	JTS3370
	TPHI(K,I)=VEC(4,K)	JTS3380
800	TPHIP(K,I)=VEC(3,K)	JTS3390
	TFREQ(I)=FREQ	JTS3400
	GM(I)=GAM	JTS3410
	GO TO 830	JTS3420
810	IF(MTS.EQ.1)GO TO 930	JTS3430
	NT=I	JTS3440
	MTS=1	JTS3450

Table A-8
(Cont'd.)

	GO TO 830	JTS3460
820	NT=I-1	JTS3470
	MTS=1	JTS3480
830	CONTINUE	JTS3490
	IF(MIKE.EQ.1)GO TO 10	JTS3500
C		JTS3510
C	MATCHING CORRESPONDING MODES	JTS3520
C		JTS3530
C	FIND MISSING MODES	JTS3540
C		JTS3550
	NT=NCTM	JTS3560
	DO 1070 I=1,NT	JTS3570
	IF(KCHECK.EQ.2)GO TO 1040	JTS3580
	LBITE=0	JTS3590
840	NSGNCH=0	JTS3600
	DO 860 NA=1,NAT	JTS3610
	NSGN=1	JTS3620
	IF(TPHIP(NAONE(NA),I).LT.0.0)NSGN=-1	JTS3630
	N1=NAONE(NA)+1	JTS3640
	N2=NAEND(NA)	JTS3650
	DO 850 J=N1,N2	JTS3660
	NSG=1	JTS3670
	IF(TPHIP(J,I).LT.0.0)NSG=-1	JTS3680
	IF(NSG.EC.NSGN)GO TO 850	JTS3690
	NSGN=NSG	JTS3700
	NSGNCH=NSGNCH+1	JTS3710
850	CONTINUE	JTS3720
860	CONTINUE	JTS3730
	IF(NSGNCH.EQ.I)GO TO 1040	JTS3740
	LBITE=LBITE+1	JTS3750
	GO TO (940,960,870)LBITE	JTS3760
870	PRINT 880	JTS3770
880	FORMAT(1H1,20X*MODES HAVE BEEN MISSED THREE TIMES.....CURRENT MODE	JTS3780
	15 AND SLOPES*//)	JTS3790
	NL=1	JTS3800
890	NN=NL+3	JTS3810
	IF(NN.GT.NT)NN=NT	JTS3820
	DO 900 KS=1,NSTA	JTS3830
900	PRINT 910,KS,(TPHI(KS,KM),TPHIP(KS,KM),KM=NL,NN)	JTS3840
910	FORMAT((2X,I4,4(3X,2F13.5)))	JTS3850
	NL=NL+4	JTS3860
	IF(NL.LE.NT)GO TO 890	JTS3870
	PRINT 920	JTS3880
920	FORMAT(//20X*FREQUENCIES AND GENERALIZED MASSES* ,//)	JTS3890
	PRINT 930,(KM,TFREQ(KM),GM(KM),KM=1,NT)	JTS3900
930	FORMAT((10X,I5,2(10XF17.7)))	JTS3910
	GO TO 10	JTS3920
940	PRINT 950,I	JTS3930
950	FORMAT(//20X*MODE*,I5,3X*HAS BEEN MISSED ONCE*)	JTS3940
	GO TO 980	JTS3950

Table A-8
(Cont'd.)

960 PRINT 970,I	JTS3960
970 FORMAT(/2JX*MODE*,I5,3X*HAS BEEN MISSED TWICE*)	JTS3970
980 CONTINUE	JTS3980
IF(NSGNCH.GI.NT)GO TO 1000	JTS3990
MN=NSGNCH	JTS4000
MM=MM+NI	JTS4010
MI=I+NT	JTS4020
DO 990 N=MM,NT	JTS4030
TFREQ(-M+MM)=TFREQ(-M+MI)	JTS4040
GM(-M+MM)=GM(-M+MI)	JTS4050
DO 990 L=1,NSTA	JTS4060
TPHI(L,-M+MM)=TPHI(L,-M+MI)	JTS4070
990 TPHIP(L,-M+MM)=TPHIP(L,-M+MI)	JTS4080
INF=MM-1	JTS4090
DAAT(4,NCARD)=0.99*TFREQ(INF+1)	JTS4100
GO TO 1010	JTS4110
1000 INF=NT	JTS4120
DAAT(4,NCARD)=0.99*TFREQ(NT)	JTS4130
1010 DAAT(3,NCARD)=1.0+0.2*(DAAT(3,NCARD)-1.0)	JTS4140
DO 1020 IN=I,INF	JTS4150
DAAT(1,NCARD)=SFREQ*(0.9*LBITE)	JTS4160
IF(IN.NE.1)DAAT(1,NCARD)=1.01*TFREQ(I-1)	JTS4170
PRINT 750,(ITHE(J,NCARD),J=1,5),(DAAT(JJ,NCARD),JJ=1,7)	JTS4180
CALL MYKL(FREQ,GAM,LINE)	JTS4190
DO 1020 K=1,NSTA	JTS4200
TPHI(K,IN)=VEC(4,K)	JTS4210
1020 TPHIP(K,IN)=VEC(3,K)	JTS4220
TFREQ(IN)=FREQ	JTS4230
1030 GM(IN)=GAM	JTS4240
GO TO 840	JTS4250
C COMPARE POLARITY TO THAT OF EXPERIMENTAL MODE	JTS4260
C	JTS4270
1040 CONTINUE	JTS4280
IF(1.GT.NEXP)GO TO 1070	JTS4290
NSIGN=1	JTS4300
IF(TPHI(NSMAXPH(I),I).LT.0.0)NSIGN=-1	JTS4310
IF(NSIGN.NE.MAXSIGN(I))GO TO 1050	JTS4320
GO TO 1070	JTS4330
1050 DO 1060 J=1,NSTA	JTS4340
TPHI(J,I)=-TPHI(J,I)	JTS4350
1060 TPHIP(J,I)=-TPHIP(J,I)	JTS4360
1070 CONTINUE	JTS4370
PRINT 1080	JTS4380
1080 FORMAT(/* COMPUTED GENERALIZED MASS FOR THE MYKL MODES ARE */)	JTS4390
PRINT 1090,(GM(I),I=1,NT)	JTS4400
1090 FORMAT(2X,10E13.5)	JTS4410
C	JTS4420
C NORMALIZING MYKL MODES TO A GENERALIZED MASS OF 1.0	JTS4430
C	JTS4440
DO 1100 I=1,NT	JTS4450

Table A-8
(Cont'd.)

TOMEGS(I)=(6.283185*TFREQ(I))**2	JTS4460
FACT=SQRT(1.0/GM(I))	JTS4470
DO 1100 J=1,NSTA	JTS4480
TPHI(J,I)=FACT*TPHI(J,I)	JTS4490
1100 TPHIP(J,I)=FACT*TPHIP(J,I)	JTS4500
PRINT 1110	JTS4510
1110 FORMAT(/* THE THEORETICAL MODES HAVE BEEN NORMALIZED *)	JTS4520
C	JTS4530
C CHECK MODE SHAPE AND FREQUENCY	JTS4540
C LOGIC FOR CONTROLLING PROGRAM MYKL WILL BE LOCATED HERE	JTS4550
C	JTS4560
C OBTAIN NEW ESTIMATES OF THE JOINT COMPLIANCES	JTS4570
C	JTS4580
CALL STEEP	JTS4590
IF(ITMAX.GT.1) GO TO 1115	JTS4593
ITER=1	JTS4594
CALL RENORM	JTS4595
GO TO 10	JTS4597
1115 IF((MWH.LT.1).OR.(MWH.GT.2))GO TO 1120	JTS4600
CALL ALTER	JTS4610
GO TO 630	JTS4620
1120 IF(ISTOP.EQ.0)GO TO 1130	JTS4630
CALL RENORM	JTS4640
GO TO 10	JTS4650
1130 IF(JA.EQ.2)GO TO 1140	JTS4660
GO TO 630	JTS4670
C	JTS4680
C CONVERGENCE CHECK ON SOLUTION	JTS4690
C	JTS4700
1140 KZERO=0	JTS4710
DO 1150 K=1,NVSPR	JTS4720
DELTAK=ASPRING(K)-SSPRING(K)	JTS4730
IF(DELTAK.EQ.0.0) KZERO=1	JTS4740
IF(KZERO.EQ.1)GO TO 1160	JTS4750
DO 1150 J=1,NVSPR	JTS4760
1150 BB(K,J)=(AA(J,K)-SPFK(J))/DELTAK	JTS4770
1160 CONTINUE	JTS4780
IF(KZERO.EQ.0)GO TO 1180	JTS4790
PRINT 1170	JTS4800
1170 FORMAT(10X,37H DELTAK = 0.0, THIS CASE TERMINATED.)	JTS4810
GO TO 10	JTS4820
1180 CONTINUE	JTS4830
C	JTS4840
C BB(J,K)=THE MATRIX OF SECOND ORDER DERIVATIVES	JTS4850
C	JTS4860
PRINT 1190	JTS4870
1190 FORMAT(/10X,* THE SECOND ORDER DERIVATIVES ARE */)	JTS4880
DO 1200 J=1,NVSPR	JTS4890
1200 PRINT 1210,(BB(J,K),K=1,NVSPR)	JTS4900
1210 FORMAT(1X,10E13.5)	JTS4910

Table A-8
(Cont'd.)

C		JTS4920
C	AVERAGING THE SECOND ORDER DERIVATIVES	JTS4930
C		JTS4940
	DO 1220 K=1,NVSPR	JTS4950
	DO 1220 J=1,NVSPR	JTS4960
1220	AA(K,J)=(BB(K,J)+BB(J,K))/2.0	JTS4970
	DO 1230 J=1,NVSPR	JTS4980
	DO 1230 K=1,NVSPR	JTS4990
1230	BB(J,K)=AA(J,K)	JTS5000
	PRINT 1240	JTS5010
1240	FORMAT(//10X,* THE AVERAGED SECOND ORDER DERIVATIVES ARE */)	JTS5020
	DO 1250 J=1,NVSPR	JTS5030
1250	PRINT 1210,(BB(J,K),K=1,NVSPR)	JTS5040
C		JTS5050
C	CALL INVERSION ROUTINE	JTS5060
C		JTS5070
	CALL MATNF 5 (BB,NVSPR,10, 1.0,DET,IERROR)	JTS5080
	PRINT 1260,DET	JTS5090
1260	FORMAT(/* DET = *,E16.7)	JTS5100
	PRINT 1270	JTS5110
1270	FORMAT(//10X,* THE INVERSE OF THE SECOND ORDER DERIVATIVES ARE */)	JTS5120
	DO 1280 J=1,NVSPR	JTS5130
1280	PRINT 1210,(BB(J,K),K=1,NVSPR)	JTS5140
C		JTS5150
C	CHECKING THE INVERSE OF THE SECOND ORDER TERMS	JTS5160
C		JTS5170
	DO 1290 I=1,NVSPR	JTS5180
	DO 1290 J=1,NVSPR	JTS5190
	CC(I,J)=0.0	JTS5200
	DO 1290 K=1,NVSPR	JTS5210
1290	CC(I,J)=CC(I,J)+AA(I,K)*BB(K,J)	JTS5220
	PRINT 1300	JTS5230
1300	FORMAT(//* THE INVERSE OF THE SECOND ORDER DERIVATIVES TIMES THE	JTS5240
	1 SECOND ORDER DERIVATIVES EQUAL */)	JTS5250
	DO 1310 J=1,NVSPR	JTS5260
1310	PRINT 1210,(CC(J,K),K=1,NVSPR)	JTS5270
C		JTS5280
C	COMPUTING NEW SPRINGS RATES UTILIZING SECOND ORDER TERMS	JTS5290
C		JTS5300
	DO 1340 J=1,NVSPR	JTS5310
	TEMP=0.0	JTS5320
	DO 1320 K=1,NVSPR	JTS5330
1320	TEMP=TEMP+BB(J,K)*SPFK(K)	JTS5340
	SPRING(J)=SSPRING(J)-TEMP	JTS5350
	RATIO=ABS(SPRING(J)/SSPRING(J)-1.0)	JTS5360
	IF(RATIO.LT.0.025)GO TO 1330	JTS5370
	XNUM=ASPRING(J)-SSPRING(J)	JTS5380
	XDEN=SPRING(J)-SSPRING(J)	JTS5390
	IF(XDEN.EQ.0.0)GO TO 1330	JTS5400
	RATIO=XNUM/XDEN	JTS5410

Table A-8
(Cont'd.)

	IF(RATIO.LT.0.0) SPRING(J)=ASPRING(J)	JTS5420
1330	CONTINUE	JTS5430
	IF((SPRING(J).LT.SPRINGL(J)) SPRING(J)=SPRINGL(J)	JTS5440
	IF((SPRING(J).GT.SPRINGU(J)) SPRING(J)=SPRINGU(J)	JTS5450
	COMP(J)=1.0/SPRING(J)	JTS5460
1340	CONTINUE	JTS5470
	PRINT 1350	JTS5480
1350	FORMAT(//20X,2H J,8X,5H K(J),9X,8H COMP(J),12X,8H SPFK(J),/)	JTS5490
	PRINT 1360,(J,SPRING(J),COMP(J),SPFK(J),J=1,NVSPR)	JTS5500
1360	FORMAT(18X,I4,2E16.6,E20.6)	JTS5510
	IF(ITER.LT.ITMAX)GO TO 1380	JTS5520
	PRINT 1370	JTS5530
1370	FORMAT(//* THE MAXIMUM NUMBER OF ITERATIONS HAS BEEN EXCEEDED *)	JTS5540
	ISTOP=1	JTS5550
1380	CONTINUE	JTS5560
	MM=0	JTS5570
	DO 1400 J=1,NVSPR	JTS5580
	RATIO=ABS((SPRING(J)/SSPRING(J)-1.0)	JTS5590
	IF(RATIO-TOL)1390,1400,1400	JTS5600
1390	MM=MM+1	JTS5610
1400	CONTINUE	JTS5620
	IF(MM.LT.NVSPR)GO TO 1420	JTS5630
	PRINT 1410	JTS5640
1410	FORMAT(//* THE MINIMUM COST FUNCTION HAS BEEN FOUND *)	JTS5650
	ISTOP=1	JTS5660
1420	CONTINUE	JTS5670
	DO 1430 J=1,NVSPR	JTS5680
	OLDSR(J)=SSPRING(J)	JTS5690
	SSPRING(J)=SPRING(J)	JTS5700
1430	CONTINUE	JTS5710
	IF(ISTOP.EQ.1)GO TO 630	JTS5720
	JD=0	JTS5730
	JA=1	JTS5740
	JB=0	JTS5750
	MWM=0	JTS5760
	GO TO 630	JTS5770
	END	JTS5780

Table A-9
FORTRAN Listing of Subroutine STEEP

	SUBROUTINE STEEP	STP 10
C		STP 20
C	ESTIMATE SPRING VALUES TO IMPROVE MATCH OF BEAM MODEL	STP 30
C		STP 40
	COMMON/1/ MHH, ISTOP, NSTA, NT, NEXP, STEP, ITMAX, TOL, ITER	STP 50
	COMMON/2/ KKKK, ALPHA, F, PFK(20), INTEG(20)	STP 60
	COMMON/3/ PHMAT(10), FWMAT(10), EOMEGS(10), KVAR(20), SPRINGL(20), SPRIN	STP 70
	15 U(20), EPHI(100,10), EPHIP(100,10), EFREQ(10), TFREQ(10)	STP 80
	COMMON/4/ TOMECS(10), TPHI(100,10), TPHIP(100,10)	STP 90
	COMMON/5/ JA, JB, JC, FF, SPFK(10), AA(10,10), ASPRING(20)	STP 100
	COMMON/6/ NVSPR, SPRING(10), SSpring(10), KSTA(10), KTYPE(10), COMP(10)	STP 110
	DIMENSION FACT(10), PXX(200), FWI(10), FXI(10)	STP 120
C		STP 130
C	PRINTING OUT A COMPARISON OF EXPERIMENTAL AND THEORETICAL MODES	STP 140
C		STP 150
	PRINT 10, ITER	STP 160
	10 FORMAT(1H1,* COMPARISON OF EXPERIMENTAL MODES TO THEORETICAL MODES	STP 170
	1 FOR ITERATION NUMBER*,I3/)	STP 180
	NL=1	STP 190
	20 NN=NL+3	STP 200
	IF(NN.GT.NT) NN=NT	STP 210
	DO 30 J=1,NSTA	STP 220
	30 PRINT 40, J,(EPHI(J,I),TPHI(J,I),I=NL,NN)	STP 230
	40 FORMAT(2X,I4, 3X,2E13.5,3X,2E13.5,3X,2E13.5,3X,2E13.5)	STP 240
	NL=NL+4	STP 250
	IF(NL.LE.NT) GO TO 20	STP 260
	PRINT 50	STP 270
	50 FORMAT(1H1,* COMPARISON OF SLOPES -- EXPERIMENTAL TO THEORETICAL*/	STP 280
	1)	STP 290
	NL=1	STP 300
	60 NN=NL+3	STP 310
	IF(NN.GT.NT) NN=NT	STP 320
	DO 70 J=1,NSTA	STP 330
	70 PRINT 40, J,(EPHIP(J,I),TPHIP(J,I),I=NL,NN)	STP 340
	NL=NL+4	STP 350
	IF(NL.LE.NEXP) GO TO 60	STP 360
	PRINT 80, ITER	STP 370
	80 FORMAT(1H1,47X,* ITERATION*,I4//)	STP 380
	PRINT 90	STP 390
	90 FORMAT(10X,* MODE*,10X,* EXPERIMENTAL FREQ*,10X,* THEORETICAL FREQ	STP 400
	(*//)	STP 410
	PRINT 100,(I,EFREQ(I),TFREQ(I),I=1,NT)	STP 420
	100 FORMAT(10X,I5,10X,E18.7,10X,E17.7)	STP 430
C		STP 440
C		STP 450
C	COMPUTATION OF THE QUADRATIC COST FUNCTION	STP 460
C		STP 470
	FW=0.0	STP 480
	FX=0.0	STP 490
	NSP1=NSTA+1	STP 500

Table A-9

(Cont'd.)

NSX2=NSTA*2	STP 510
DO 130 I=1,NEXP	STP 520
FWI(I)=0.5*FWMAT(I)*(EOMEGS(I)-TOMEGS(I))*(EOMEGS(I)-TOMEGS(I))	STP 530
FW=FW+FWI(I)	STP 540
FAC=0.0	STP 550
DO 110 J=1,NSTA	STP 560
110 FAC=FAC+(EPHI(J,I)-TPHI(J,I))*(EPHI(J,I)-TPHI(J,I))	STP 570
DO 120 J=NSP1,NSX2	STP 580
JJ=J-NSTA	STP 590
120 FAC=FAC+(EPHIP(JJ,I)-TPHIP(JJ,I))*(EPHIP(JJ,I)-TPHIP(JJ,I))	STP 600
FXI(I)=0.5*FAC*FWMAT(I)	STP 610
130 FX=FX+FXI(I)	STP 620
F=FW+FX	STP 630
PRINT 140,F,FW,FX	STP 640
140 FORMAT(/ / 22H THE COST FUNCTION = ,E13.5,10X,6H FW = ,E13.5,10X,6H	STP 650
1 FX = ,E13.5/)	STP 660
PRINT 150,(I,FWI(I),FXI(I),I=1,NEXP)	STP 670
150 FORMAT(38X,I3,10X,E13.5,16X,E13.5)	STP 680
IF(ITER.EQ.1) FF=F	STP 690
IF(JB.EQ.1) MWH=0	STP 700
IF(JB.NE.0) GO TO 160	STP 710
IF(ITER.EQ.1) GO TO 160	STP 720
IF(FF.GT.F) FF=F	STP 730
MWH=MWH+1	STP 740
IF(FF.GE.F) MWH=0	STP 750
IF((MWH.EQ.0).OR.(MWH.GT.2)) GO TO 160	STP 760
GO TO 390	STP 770
160 IF(ISTOP.EQ.1) GO TO 390	STP 780
C	STP 790
C COMPUTATION OF THE GRADIENTS FOR EACH UNKNOWN SPRING	STP 800
C POMEKG(PARTIAL DERIVATIVE OF OMEGA SQUARED WITH RESPECT TO SPRING	STP 810
C RATES K)	STP 820
C	STP 830
DO 280 J=1,NVSPR	STP 840
NN=KVAR(J)+1	STP 850
PFK(J)=0.0	STP 860
IF(JB.NE.0) AA(J,JB)=0.0	STP 870
DO 280 I=1,NEXP	STP 880
IF(KTYPE(J).EQ.1) GO TO 170	STP 890
POMEKG=(TPHIP(NN-1,I)-TPHIP(NN,I))**2	STP 900
GO TO 180	STP 910
170 POMEKG=(TPHI(NN-1,I)-TPHI(NN,I))**2	STP 920
180 CONTINUE	STP 930
C	STP 940
C P XK(PARTIAL DERIVATIVE OF PHI WITH RESPECT TO SPRING RATES K)	STP 950
C	STP 960
DO 190 NX=1,NSX2	STP 970
190 P XK(NX)=0.0	STP 980
DO 240 L=1,NT	STP 990
IF(L.EQ.1) GO TO 240	STP 1000

Table A-9
(Cont'd.)

	IF(KTYPE(J).EQ.1)GO TO 200	STP1010
	FACT(L)=(TPHIP(NN-1,L)*TPHIP(NN-1,I)-TPHIP(NN-1,L)*TPHIP(NN,I)-TPH	STP1020
	1IP(NN,L)*TPHIP(NN-1,I)+TPHIP(NN,L)*TPHIP(NN,I))/(TOMEGS(I)-TOMEGS(STP1030
	2L))	STP1040
	GO TO 210	STP1050
	200 FACT(L)=(TPHI(NN-1,L)*TPHI(NN-1,I)-TPHI(NN-1,L)*TPHI(NN,I)-TPHI(NN	STP1060
	1,L)*TPHI(NN-1,I)+TPHI(NN,L)*TPHI(NN,I))/(TOMEGS(I)-TOMEGS(L))	STP1070
	210 CONTINUE	STP1080
	DO 220 NX=1,NSTA	STP1090
	220 P XK(NX)=P XK(NX)+FACT(L)*TPHI(NX,L)	STP1100
	DO 230 NX=NSP1,NSX2	STP1110
	NY=NX-NSTA	STP1120
	230 P XK(NX)=P XK(NX)+FACT(L)*TPHIP(NY,L)	STP1130
	240 CONTINUE	STP1140
C		STP1150
C	COMPUTATION OF PFK(J)--PARTIAL DERIVATIVE OF F WRT K	STP1160
C		STP1170
	P FKX=0.0	STP1180
	P FKW=0.0	STP1190
	DO 250 N=1,NSTA	STP1200
	250 P FKX=P FKX+P HMAT(I)*(TPHI(N,I)-E PHI(N,I))*P XK(N)	STP1210
	DO 260 N=NSP1,NSX2	STP1220
	NY=N-NSTA	STP1230
	260 P FKX=P FKX+P HMAT(I)*(TPHIP(NY,I)-E PHIP(NY,I))*P XK(N)	STP1240
	P FKW=P HMAT(I)*(TOMEGS(I)-E OMEGS(I))*P OMEGK	STP1250
	P FK(J)=P FK(J)+P FKX+P FKW	STP1260
	IF(JB.EQ.0)GO TO 270	STP1270
	AA(J,JB)=AA(J,JB)+P FKX+P FKW	STP1280
	270 CONTINUE	STP1290
	280 CONTINUE	STP1300
	IF(JB.EQ.NVSPR)GO TO 380	STP1310
	IF(JD.EQ.1)GO TO 300	STP1320
	JA=1	STP1330
	JB=0	STP1340
	JD=1	STP1350
	DO 290 J=1,NVSPR	STP1360
	290 S PFK(J)=P FK(J)	STP1370
	300 CONTINUE	STP1380
C		STP1390
C	COMPUTING WHERE THE COST FUNCTION GOES TO ZERO	STP1400
C		STP1410
	JC=JB+1	STP1420
	IF(S PFK(JC).GT.0.0)GO TO 310	STP1430
	ALPHA=-STEP*SSPRING(JC)	STP1440
	GO TO 320	STP1450
	310 ALPHA=STEP*SSPRING(JC)	STP1460
	320 CONTINUE	STP1470
C		STP1480
C	COMPUTING NEW GUESSES FOR THE VARIABLE SPRINGS	STP1490
C		STP1500

Table A-9
(Cont'd.)

IF(JB.EQ.0)GO TO 330	STP1510
SPRING(JB)=SSPRING(JB)	STP1520
330 CONTINUE	STP1530
JB=JB+1	STP1540
SPRING(JB)=SSPRING(JB)-ALPHA	STP1550
IF(SPRING(JB).LT.SPRINGL(JB))SPRING(JB)=SPRINGL(JB)	STP1560
IF(SPRING(JB).GT.SPRINGU(JB))SPRING(JB)=SPRINGU(JB)	STP1570
ASPRING(JB)=SPRING(JB)	STP1580
DO 340 J=1,NVSPR	STP1590
340 COMP(J)=1.0/SPRING(J)	STP1600
PRINT 350	STP1610
350 FORMAT(/20X,2H J,8X,5H K(J),	11X,7H PFK(J),12X,6H COMP
1(J)/)	STP1620
PRINT 360,(J,SPRING(J),	PFK(J),COMP(J),J=1,NVSPR)
360 FORMAT(18X,I4,E16.5,	2E18.5)
PRINT 370,ALPHA	STP1650
370 FORMAT(/10X,* ALPHA = *,E16.5)	STP1660
ITER=ITER+1	STP1670
C	STP1680
GO TO 390	STP1690
C	STP1700
C	STP1710
380 JA=2	STP1720
ITER=ITER+1	STP1730
C	STP1740
C	STP1750
C	STP1760
RETURN TO PROGRAM JOINTS	STP1770
390 CONTINUE	STP1780
END	STP1790

Table A-10
FORTRAN Listing of Subroutine ALTER

	SUBROUTINE ALTER	ALT 10
C		ALT 20
C	ESTIMATE NEW SPRING RATES WHEN THE COST FUNCTION HAS INCREASED	ALT 30
C		ALT 40
	COMMON/6/NVSPR,SPRING(10),SSPRING(10),KSTA(10),KTYPE(10),COMP(10)	ALT 50
	COMMON/7/XRATIO,OLDSPR(10)	ALT 60
	DIMENSION RATIO(10)	ALT 70
	DO 10 J=1,NVSPR	ALT 80
	RATIO(J)=0.0	ALT 90
	IF(OLDSPR(J).EQ.0.)GO TO 10	ALT 100
	RATIO(J)=SSPRING(J)/OLDSPR(J)	ALT 110
10	CONTINUE	ALT 120
	IF(XRATIO.EQ.0.) XRATIO=0.5	ALT 130
	XRATIO=1.0+XRATIO	ALT 140
	YRATIO=1.0/XRATIO	ALT 150
	KOUNT=0	ALT 160
	DO 30 J=1,NVSPR	ALT 170
	IF(RATIO(J).LE.XRATIO)GO TO 20	ALT 180
	SSPRING(J)=XRATIO*OLDSPR(J)	ALT 190
	KOUNT=KOUNT+1	ALT 200
	GO TO 30	ALT 210
20	IF(RATIO(J).GE.YRATIO)GO TO 30	ALT 220
	SSPRING(J)=YRATIO*OLDSPR(J)	ALT 230
	KOUNT=KOUNT+1	ALT 240
30	CONTINUE	ALT 250
	IF(KOUNT.NE.0)GO TO 50	ALT 260
	DO 40 J=1,NVSPR	ALT 270
40	SSPRING(J)=(SSPRING(J)-OLDSPR(J))/2.0+OLDSPR(J)	ALT 280
50	DO 60 J=1,NVSPR	ALT 290
	SPRING(J)=SSPRING(J)	ALT 300
	COMP(J)=1.0/SSPRING(J)	ALT 310
60	CONTINUE	ALT 320
	PRINT 70	ALT 330
70	FORMAT(1H1,/,20X,76H SINCE THE COST FUNCTION HAS INCREASED, NEW SP	ALT 340
	RING RATES HAVE BEEN COMPUTED.//)	ALT 350
	PRINT 80	ALT 360
80	FORMAT(/20X,2H J,8X,5H K(J),9X,8H COMP(J),/)	ALT 370
	PRINT 90,(J,SPRING(J),COMP(J),J=1,NVSPR)	ALT 380
90	FORMAT(18X,I4,2E16.6)	ALT 390
	END	ALT 400

Table A-11
FORTRAN Listing of Subroutine RENORM

C	SUBROUTINE RENORM	REN 10
C	RENORMALIZATION OF THE EXPERIMENTAL AND THEORETICAL MODES	REN 20
C		REN 30
	COMMON/1/ MWH, ISTOP, NSTA, NT, NEXP, STEP, ITMAX, TOL, ITER	REN 40
	COMMON/3/ PWHAT(10), FWHAT(10), EOMEGS(10), KVAR(20), SPRINGL(20), SPRIN	REN 50
	16U(20), EPHI(100,10), EPHIP(100,10), EFREQ(10), TFREQ(10)	REN 60
	COMMON/4/ TOMEGS(10), TPHI(100,10), TPHIP(100,10)	REN 70
	COMMON/8/ KNORM, XSTA(100)	REN 80
	DATA (MODE=10H MODE), (NAME1=10H EPHI), (NAME2=10H TPHI	REN 90
	1), (NAME3=10H EPHIP), (NAME4=10H TPHIP)	REN 100
	DO 20 I=1, NEXP	REN 110
	IF (EPHI(KNORM, I).EQ.0.) GO TO 20	REN 120
	FACT=1.0/EPHI(KNORM, I)	REN 130
	DO 10 J=1, NSTA	REN 140
	EPHI(J, I)=FACT*EPHI(J, I)	REN 150
	EPHIP(J, I)=FACT*EPHIP(J, I)	REN 160
	10 CONTINUE	REN 170
	20 CONTINUE	REN 180
	DO 40 I=1, NT	REN 190
	IF (TPHI(KNORM, I).EQ.0.) GO TO 40	REN 200
	FACT=1.0/TPHI(KNORM, I)	REN 210
	DO 30 J=1, NSTA	REN 220
	TPHI(J, I)=FACT*TPHI(J, I)	REN 230
	TPHIP(J, I)=FACT*TPHIP(J, I)	REN 240
	30 CONTINUE	REN 250
	40 CONTINUE	REN 260
	50 PRINT 60, ITER	REN 270
	60 FORMAT(1H1, * COMPARISON OF EXPERIMENTAL MODES TO THEORETICAL MODES	REN 280
	1 FOR ITERATION NUMBER*, /3/)	REN 290
	NL=1	REN 300
	NN=NL+3	REN 310
	IF (NN.GT.NEXP) NN=NEXP	REN 320
	PRINT 70, (MODE, I, I=NL, NN)	REN 330
	70 FORMAT(10X, 4(18X, A6, I2))	REN 340
	PRINT 80, (NAME1, NAME2, I=NL, NN)	REN 350
	80 FORMAT(3X, 24 K, 6X, 6H XSTA, 4(8X, A6, 6X, A6))	REN 360
	DO 90 J=1, NSTA	REN 370
	90 PRINT 100, J, XSTA(J), (EPHI(J, I), TPHI(J, I), I=NL, NN)	REN 380
	100 FORMAT(1X, I4, 2X, E12.5, 4(2X, 2E12.5))	REN 390
	NL=NL+4	REN 400
	IF (NL.LE.NEXP) GO TO 50	REN 410
	110 PRINT 120	REN 420
	120 FORMAT(1H1, * COMPARISON OF SLOpes -- EXPERIMENTAL TO THEORETICAL*/	REN 430
	1)	REN 440
	NL=1	REN 450
	NN=NL+3	REN 460
	IF (NN.GT.NEXP) NN=NEXP	REN 470
	PRINT 70, (MODE, I, I=NL, NN)	REN 480
	PRINT 80, (NAME3, NAME4, I=NL, NN)	REN 490
		REN 500

Table A-11
(Cont'd.)

```
DO 130 J=1,NSTA
130 PRINT 100,J,XSTA(J),(EPHIP(J,I),TPHIP(J,I),I=NL,NN)
NL=NL+4
IF(NL.LE.NEXP)GO TO 110
END
```

```
REN 510
REN 520
REN 530
REN 540
REN 550
```

Table A-12
FORTRAN Listing of Subroutine MYKL

	SUBROUTINE MYKL (FREQ,GAM,LIME)	MYK	10
C	MYKL MODIFIED TO LIMIT NUMBER OF INTERNAL STATIONS TO 100	MYK	20
	COMMON FINK(300)	MYK	30
	COMMON A(4,4,101),SAP(4,4),AP(4,4),VINV(4,4),ALV(4,4),T(4,4),AL	MYK	40
C	COMMON A(4,4,300),SAP(4,4),AP(4,4),VINV(4,4),ALV(4,4),T(4,4),AL	MYK	50
	1 VT(4,4),TAP(4,4,100),VEC(4,101),ITEM(6,101),DATA(8,101),I1(300),IR	MYK	60
C	1 VT(4,4),TAP(4,4,100),VEC(4,300),ITEM(6,300),DATA(8,300),I1(300),IR	MYK	70
	2(300),OM(300),FUNC(300),R(3),KKK(100),MODE(100),JOINT(101),AL(4,4)	MYK	80
C	2(300),OM(300),FUNC(300),R(3),KKK(100),MODE(100),JOINT(300),AL(4,4)	MYK	90
	3,I6(101),PRNT(4),HOL(12)	MYK	100
C	3,I6(300),PRNT(4),HOL(12)	MYK	110
	COMMON ICON(10),ICB(10),FPM(10,4,4),FQM(10,4,4),VSAVE(4),ARSTAR	MYK	120
	1(10,6,4), ARP8(4,4),ARPA(4,4),APR(4,4),DANV(2,2),DENV(2,2	MYK	130
	2),THMAN(6,6),8MAN(6,6),8INV(6,6),RMUL(6,4)	MYK	140
	COMMON I4(101)	MYK	150
C	COMMON I4(300)	MYK	160
	COMMON ITME(5,101),DAAT(7,101),IETH(5),DTAA(7)	MYK	170
C	COMMON ITME(5,250),DAAT(7,250),IETH(5),DTAA(7)	MYK	180
	10 ITMIN=1	MYK	190
	ILAF=1	MYK	200
	N=0	MYK	210
	NX=0	MYK	220
20	N=N+1	MYK	230
	NX=N+1	MYK	240
	DO 30 I=1,5	MYK	250
30	ITEM(I,N)=ITME(I,NX)	MYK	260
	DO 40 I=1,7	MYK	270
40	DATA(I,N)=DAAT(I,NX)	MYK	280
	IF(LIME.EQ.1)GO TO 60	MYK	290
	WRITE(6,50) (ITEM(I,N),I=1,5), (DATA(J,N),J=1,7)	MYK	300
50	FORMAT(5I4,4X,7(E13.5))	MYK	310
60	CONTINUE	MYK	320
	IF(ITEM(1,N))70,100,70	MYK	330
70	ITEM(6,N)=ITEM(1,N)	MYK	340
	ITEM(1,N)=N	MYK	350
	IF(N.EQ.1)GO TO 20	MYK	360
	IF(ITEM(2,N).EQ.ITEM(2,N-1))GO TO 20	MYK	370
	DO 80 I=1,6	MYK	380
	ITEM(I,N+1)=ITEM(I,N)	MYK	390
80	ITEM(I,N)=ITEM(I,N-1)	MYK	400
	ITEM(1,N)=N	MYK	410
	ITEM(1,N+1)=N+1	MYK	420
	ITEM(4,N)=0	MYK	430
	DO 90 J=1,7	MYK	440
	DATA(J,N+1)=DATA(J,N)	MYK	450
90	DATA(J,N)=0.0	MYK	460
	DATA(3,N)=DATA(3,N-1)	MYK	470
	N=N+1	MYK	480
	GO TO 20	MYK	490
100	DO 110 I=1,6	MYK	500

Table A-12
(Cont'd.)

ITEM(I,N+1)=ITEM(I,N)	MYK 510
110 ITEM(I,N)=ITEM(I,N-1)	MYK 520
ITEM(1,N)=N	MYK 530
ITEM(4,N)=0	MYK 540
DO 120 J=1,7	MYK 550
DATA(J,N+1)=DATA(J,N)	MYK 560
120 DATA(J,N)=0.0	MYK 570
DATA(3,N)=DATA(3,N-1)	MYK 580
N=N+1	MYK 590
NN=N-1	MYK 600
M=N	MYK 610
DO 150 I=2,NN	MYK 620
N=I-1	MYK 630
DATA(8,N)=DATA(3,I)-DATA(3,N)	MYK 640
IF(ITEM(2,N)-ITEM(2,I))130,140,130	MYK 650
130 DATA(8,N)=0.0	MYK 660
140 DATA(8,I)=0.0	MYK 670
150 CONTINUE	MYK 680
DO 160 K=1,100	MYK 690
DO 160 I=1,4	MYK 700
DO 160 J=1,4	MYK 710
160 A(I,J,K)=0.0	MYK 720
KZ=0	MYK 730
KOWT=1	MYK 740
ITER=1	MYK 750
W2=DATA(1,M)	MYK 760
IF(W2)180,170,180	MYK 770
170 W2=2.5	MYK 780
180 W2=(W2*3.141593*2.0)**2	MYK 790
EPS=DATA(2,M)	MYK 800
IF(EPS)200,190,200	MYK 810
190 EPS=.1E-4	MYK 820
200 GAMA=DATA(3,M)	MYK 830
IF(GAMA)220,210,220	MYK 840
210 GAMA=1.10	MYK 850
220 SUMMA=1.+(GAMA-1.)*.05	MYK 860
JPBND=DATA(4,M)	MYK 870
IF(UPBND)240,230,240	MYK 880
230 JPBND=250.0	MYK 890
240 UPBND=UPBND*6.283185	MYK 900
K=1	MYK 910
SAMA=GAMA	MYK 920
DO 330 I=1,NN	MYK 930
IF(ITEM(4,I)-1)250,280,300	MYK 940
250 A(1,1,K)=1.0	MYK 950
A(2,2,K)=1.0	MYK 960
A(3,1,K)=-DATA(8,I)/DATA(1,I)	MYK 970
IF(DATA(1,I).EQ.0.0)A(3,1,K)=0.0	MYK 980
DATA(5,I)=DATA(5,I)/57.29578	MYK 990
DATA(6,I)=DATA(6,I)/57.29578	MYK1000

Table A-12

(Cont'd.)

	IF (ITEM(5,I)) 260,260,270	MYK1010
260	A(1,2,K)=-DATA(8,I)	MYK1020
	A(3,2,K)=.5*DATA(8,I)**2/DATA(1,I)	MYK1030
	IF (DATA(1,I).EQ.0.0) A(3,2,K)=0.0	MYK1040
	A(4,1,K)=-A(3,2,K)	MYK1050
	A(4,2,K)=DATA(8,I)**3/(6.0*DATA(1,I))	MYK1060
	IF (DATA(1,I).EQ.0.0) A(4,2,K)=0.0	MYK1070
270	K=K+1	MYK1080
	GO TO 330	MYK1090
280	A(3,1,K)=-DATA(6,I)	MYK1100
	IF (ITEM(5,I)) 290,290,300	MYK1110
290	A(4,2,K)=-DATA(5,I)	MYK1120
300	KK=K+1	MYK1130
	DATA(5,I)=DATA(5,I)/57.29578	MYK1140
	DATA(6,I)=DATA(6,I)/57.29578	MYK1150
	A(1,1,K)=1.0	MYK1160
	A(1,1,KK)=1.0	MYK1170
	A(2,2,K)=1.0	MYK1180
	A(2,2,KK)=1.0	MYK1190
	A(3,1,KK)=-DATA(8,I)/DATA(1,I)	MYK1200
	IF (DATA(1,I).EQ.0.0) A(3,1,KK)=0.0	MYK1210
	A(3,3,K)=1.0	MYK1220
	A(3,3,KK)=1.0	MYK1230
	A(4,4,K)=1.0	MYK1240
	A(4,4,KK)=1.0	MYK1250
	IF (ITEM(5,I)) 310,310,320	MYK1260
310	A(1,2,KK)=-DATA(8,I)	MYK1270
	A(3,2,KK)=DATA(8,I)**2*.5/DATA(1,I)	MYK1280
	IF (DATA(1,I).EQ.0.0) A(3,2,KK)=0.0	MYK1290
	A(4,1,KK)=-A(3,2,KK)	MYK1300
	A(4,2,KK)=DATA(8,I)**3/(6.0*DATA(1,I))	MYK1310
	IF (DATA(1,I).EQ.0.0) A(4,2,KK)=0.0	MYK1320
	A(4,3,KK)=DATA(8,I)	MYK1330
320	K=K+2	MYK1340
330	CONTINUE	MYK1350
	NSTA=K-1	MYK1360
	DO 340 I=1,NN	MYK1370
	DATA(7,I)=DATA(7,I)/57.29578	MYK1380
	DATA(2,I)=DATA(2,I)/386.4	MYK1390
340	DATA(4,I)=DATA(4,I)/386.4	MYK1400
	KORP=0	MYK1410
	DO 360 I=1,NN	MYK1420
	IF (ITEM(3,I)-KORP) 360,360,350	MYK1430
350	KORP = ITEM(3,I)	MYK1440
360	CONTINUE	MYK1450
	K=1	MYK1460
	DO 390 I=1,NN	MYK1470
	IF (ITEM(4,I)-1) 370,380,380	MYK1480
370	I1(K)=ITEM(1,I)	MYK1490
	I6(K)=ITEM(6,I)	MYK1500

Table A-12
(Cont'd.)

I4(K)=ITEM(4,I)	MYK1510
IR(K)=KORP-ITEM(3,I)	MYK1520
IF(ITEM(3,I).LT.0) IR(K)=-1	MYK1530
K=K+1	MYK1540
GO TO 390	MYK1550
380 KK=K+1	MYK1560
I1(K)=ITEM(1,I)	MYK1570
I6(K)=ITEM(6,I)	MYK1580
I1(KK)=I1(K)	MYK1590
I6(KK)=I6(K)	MYK1600
I4(K)=ITEM(4,I)	MYK1610
I4(KK)=I4(K)	MYK1620
IR(K)=KORP-ITEM(3,I)	MYK1630
IF(ITEM(3,I).LT.0) IR(K)=-1	MYK1640
IR(KK)=IR(K)	MYK1650
K=K+2	MYK1660
390 CONTINUE	MYK1670
NSUP=NSTA	MYK1680
DO 400 K=1,NSTA	MYK1690
I=I1(K)	MYK1700
IF(ITEM(3,I)) 410,400,400	MYK1710
400 CONTINUE	MYK1720
GO TO 420	MYK1730
410 NSTA=K-1	MYK1740
420 DIV=1.0	MYK1750
430 DO 450 I=1,4	MYK1760
DO 440 J=1,4	MYK1770
440 SAP(I,J)=0.0	MYK1780
450 SAP(I,I)=1.0	MYK1790
460 JNT=1	MYK1800
NDR=0	MYK1810
KIAP=KORP	MYK1820
470 K=1	MYK1830
480 CONTINUE	MYK1840
KS=K	MYK1850
IF(IR(K).LT.0) GO TO 490	MYK1860
IF(IR(K)+KIAP-KORP) 1110,490,1110	MYK1870
490 I=I1(K)	MYK1880
MF=I	MYK1890
J1=I+1	MYK1900
IF(IR(K).GE.0) GO TO 510	MYK1910
IF(J1-M) 500,980,500	MYK1920
500 IF(ITEM(2,I)-ITEM(2,J1)) 980,510,980	MYK1930
510 IF(ITEM(4,I)-1) 520,540,540	MYK1940
520 A(1,3,K)=W2*DATA(4,I)	MYK1950
A(1,4,K)=-W2*DATA(2,I)*DATA(8,I)	MYK1960
A(2,4,K)=W2*DATA(2,I)	MYK1970
A(3,3,K)=1.0+W2*DATA(4,I)*A(3,1,K)	MYK1980
A(3,4,K)=W2*DATA(2,I)*A(3,2,K)	MYK1990
A(4,3,K)=DATA(8,I)+W2*DATA(4,I)*A(4,1,K)	MYK2000

Table A-12
(Cont'd.)

A(4,4,K)=1.0+DATA(2,I)*M2*A(4,2,K)	MYK2010
IF(ITEM(5,I))540,540,530	MYK2020
530 A(4,3,K)=0.0	MYK2030
540 IF(I4(K)-3)670,590,600	MYK2040
550 NDR=NDR+1	MYK2050
DO 560 J=1,4	MYK2060
DO 560 L=1,4	MYK2070
560 APR(L,J)=AP(L,J)	MYK2080
KQR=I6(K)	MYK2090
ICB(NDR)=K	MYK2100
DO 580 J=1,4	MYK2110
DO 570 L=1,4	MYK2120
570 SAP(L,J)=0.0	MYK2130
580 SAP(J,J)=1.0	MYK2140
GO TO 670	MYK2150
590 IF(I4(K-1)-3)550,670,550	MYK2160
600 IF(I4(K-1)-4)610,670,610	MYK2170
610 KKEEP=K	MYK2180
DO 620 J=1,4	MYK2190
DO 620 L=1,4	MYK2200
620 ARPB(L,J)=AP(L,J)	MYK2210
KS1=NSTA+1	MYK2220
DO 640 J=1,4	MYK2230
DO 630 L=1,4	MYK2240
630 SAP(L,J)=0.0	MYK2250
640 SAP(J,J)=1.0	MYK2260
DO 650 LX=KS1,NSUP	MYK2270
IT=I1(LX)	MYK2280
IF(ITEM(2,IT)-KQR)650,660,650	MYK2290
650 CONTINUE	MYK2300
WRITE(6,790)KQR	MYK2310
GO TO 2190	MYK2320
660 K=LX	MYK2330
ICON(NDR)=K	MYK2340
GO TO 480	MYK2350
670 DO 690 L=1,4	MYK2360
DO 690 J=1,4	MYK2370
AP(L,J)=0.	MYK2380
DO 690 IC=1,4	MYK2390
AP(L,J)=AP(L,J)+A(L,IC,K)*SAP(IC,J)/DIV	MYK2400
IF(AP(L,J)-1.0E+19)690,680,680	MYK2410
680 DIV=DIV*1.0E+5	MYK2420
GO TO 430	MYK2430
690 CONTINUE	MYK2440
DO 700 L=1,4	MYK2450
DO 700 J=1,4	MYK2460
700 SAP(L,J)=AP(L,J)	MYK2470
IF(J1-M)710,720,710	MYK2480
710 IF(ITEM(2,I)-ITEM(2,J1))720,1110,720	MYK2490
720 AL(1,1)=SAP(1,3)	MYK2500

Table A-12
(Cont'd)

AL(1,2)=SAP(1,4)	MYK2510
AL(2,1)=SAP(2,3)	MYK2520
AL(2,2)=SAP(2,4)	MYK2530
IF(KIAP)730,1130,730	MYK2540
730 DETV=SAP(3,3)*SAP(4,4)-SAP(3,4)*SAP(4,3)	MYK2550
IF(DETV)740,2220,740	MYK2560
740 VINV(1,1)=SAP(4,4)/DETV	MYK2570
VINV(2,1)=SAP(4,3)/DETV*(-1.0)	MYK2580
VINV(1,2)=SAP(3,4)/DETV*(-1.0)	MYK2590
VINV(2,2)=SAP(3,3)/DETV	MYK2600
ALV(1,1)=AL(1,1)*VINV(1,1)+AL(1,2)*VINV(2,1)	MYK2610
ALV(1,2)=AL(1,1)*VINV(1,2)+AL(1,2)*VINV(2,2)	MYK2620
ALV(2,1)=AL(2,1)*VINV(1,1)+AL(2,2)*VINV(2,1)	MYK2630
ALV(2,2)=AL(2,1)*VINV(1,2)+AL(2,2)*VINV(2,2)	MYK2640
DO 750 K2=2, NSUP	MYK2650
KQ=K2	MYK2660
IF(ITEM(2,I)-I6(K2))750,770,750	MYK2670
750 CONTINUE	MYK2680
WRITE(6,760) I6(KQ)	MYK2690
760 FORMAT(25H NO APPENDAGE STATION FOR I3)	MYK2700
GO TO 2190	MYK2710
770 IQ=I1(KQ)	MYK2720
IF(ITEM(4,IQ)-2)780,800,780	MYK2730
780 WRITE(6,790) I6(KQ)	MYK2740
790 FORMAT(8H STATION I3,28H IS NOT AN APPENDAGE STATION)	MYK2750
GO TO 2190	MYK2760
800 IT=1+3*ITEM(5,IQ)+ITEM(5,I)	MYK2770
T(1,1)=0.0	MYK2780
T(1,2)=0.0	MYK2790
T(2,1)=0.0	MYK2800
T(2,2)=0.0	MYK2810
RAD=SQRT((COS(DATA(7,IQ)))**2+(SIN(DATA(7,IQ))*COS(DATA(6,IQ)))**2	MYK2820
1)	MYK2830
IF(RAD)820,820,810	MYK2840
810 CL=(COS(DATA(7,IQ))*COS(DATA(6,IQ)))/RAD	MYK2850
CU=SIN(DATA(7,IQ))*COS(DATA(6,IQ))/RAD	MYK2860
CV=COS(DATA(7,IQ))*SIN(DATA(6,IQ))/RAD	MYK2870
GO TO 830	MYK2880
820 CL=0.0	MYK2890
CU=SIN(DATA(5,IQ))	MYK2900
CV=COS(DATA(5,IQ))	MYK2910
830 GO TO (840,850,860,870,880,890,900,910,920),IT	MYK2920
840 T(1,1)=CL/SQRT(CL**2+CU**2)	MYK2930
T(2,2)=CL/SQRT(CL**2+CV**2)	MYK2940
T(2,2)=ABS(T(2,2))	MYK2950
GO TO 930	MYK2960
850 T(1,1)=CU	MYK2970
GO TO 930	MYK2980
860 T(2,1)=-CV	MYK2990
GO TO 930	MYK3000

Table A-12
(Cont'd.)

870	T(1,1)=-SQRT(1.0-CL**2)	MYK3010
	GO TO 930	MYK3020
880	T(1,1)=CL	MYK3030
	GO TO 930	MYK3040
890	GO TO 2200	MYK3050
900	T(1,2)=SQRT(1.0-CL**2)	MYK3060
	GO TO 930	MYK3070
910	GO TO 2200	MYK3080
920	T(1,1)=CL	MYK3090
930	ALVT(1,1)=ALV(1,1)*T(1,1)+ALV(1,2)*T(1,2)	MYK3100
	ALVT(1,2)=ALV(1,1)*T(2,1)+ALV(1,2)*T(2,2)	MYK3110
	ALVT(2,1)=ALV(2,1)*T(1,1)+ALV(2,2)*T(1,2)	MYK3120
	ALVT(2,2)=ALV(2,1)*T(2,1)+ALV(2,2)*T(2,2)	MYK3130
	A(1,3,KQ)=T(1,1)*ALVT(1,1)+T(1,2)*ALVT(2,1)	MYK3140
	A(1,4,KQ)=T(1,1)*ALVT(1,2)+T(1,2)*ALVT(2,2)	MYK3150
	A(2,3,KQ)=T(2,1)*ALVT(1,1)+T(2,2)*ALVT(2,1)	MYK3160
	A(2,4,KQ)=T(2,1)*ALVT(1,2)+T(2,2)*ALVT(2,2)	MYK3170
940	TAP(1,1,JNT)=VINV(1,1)*T(1,1)+VINV(1,2)*T(1,2)	MYK3180
	TAP(1,2,JNT)=VINV(1,1)*T(2,1)+VINV(1,2)*T(2,2)	MYK3190
	TAP(2,1,JNT)=VINV(2,1)*T(1,1)+VINV(2,2)*T(1,2)	MYK3200
	TAP(2,2,JNT)=VINV(2,1)*T(2,1)+VINV(2,2)*T(2,2)	MYK3210
	JOINT(K)=JNT	MYK3220
	KKK(JNT)=KQ	MYK3230
	JNT=JNT+1	MYK3240
950	DO 970 ISP=1,4	MYK3250
	DO 960 JSP=1,4	MYK3260
960	SAP(ISP,JSP)=0.0	MYK3270
970	SAP(ISP,ISP)=1.0	MYK3280
	GO TO 1110	MYK3290
980	DO 990 J=1,4	MYK3300
	DO 990 L=1,4	MYK3310
990	ARPA(L,J)=AP(L,J)	MYK3320
	DO 1000 I=1,2	MYK3330
	II=I+2	MYK3340
	DO 1000 J=1,2	MYK3350
1000	DANV(I,J)=ARPB(II,J)+ARPA(II,J)	MYK3360
	IF(ITEM(5,MF).NE.0) DANV(2,2)=1.0/DIV	MYK3370
	DEDET=1.0/(DANV(1,1)*DANV(2,2)-DANV(1,2)*DANV(2,1))	MYK3380
	DENV(1,1)=DANV(2,2)*DEDET	MYK3390
	DENV(2,2)=DANV(1,1)*DEDET	MYK3400
	DENV(1,2)=-DANV(1,2)*DEDET	MYK3410
	DENV(2,1)=-DANV(2,1)*DEDET	MYK3420
	DO 1010 J=1,6	MYK3430
	DO 1010 I=1,6	MYK3440
1010	THMAN(I,J)=0.0	MYK3450
	DO 1020 LL=1,5,2	MYK3460
	DO 1020 J=1,2	MYK3470
	JJ=J+LL-1	MYK3480
	DO 1020 I=1,2	MYK3490
	II=I+LL-1	MYK3500

Table A-12
(Cont'd.)

1020	THMAN(II,JJ)=DENV(I,J)	MYK3510
	BMAN(1,1)=-ARPA(3,1)-ARPB(3,1)	MYK3520
	BMAN(1,2)=-ARPA(3,2)-ARPB(3,2)	MYK3530
	BMAN(2,1)=-ARPA(4,1)-ARPB(4,1)	MYK3540
	BMAN(2,2)=-ARPA(4,2)-ARPB(4,2)	MYK3550
	BMAN(1,3)=ARPB(1,1)-ARPA(1,1)	MYK3560
	BMAN(1,4)=ARPB(1,2)-ARPA(1,2)	MYK3570
	BMAN(2,3)=ARPB(2,1)-ARPA(2,1)	MYK3580
	BMAN(2,4)=ARPB(2,2)-ARPA(2,2)	MYK3590
	BMAN(1,5)=-BMAN(1,3)	MYK3600
	BMAN(1,6)=-BMAN(1,4)	MYK3610
	BMAN(2,5)=-BMAN(2,3)	MYK3620
	BMAN(2,6)=-BMAN(2,4)	MYK3630
	BMAN(3,3)=-ARPA(3,1)	MYK3640
	BMAN(3,4)=-ARPA(3,2)	MYK3650
	BMAN(4,3)=-ARPA(4,1)	MYK3660
	BMAN(4,4)=-ARPA(4,2)	MYK3670
	BMAN(3,5)=-ARPB(3,1)	MYK3680
	BMAN(3,6)=-ARPB(3,2)	MYK3690
	BMAN(4,5)=-ARPB(4,1)	MYK3700
	BMAN(4,6)=-ARPB(4,2)	MYK3710
	BMAN(5,3)=-1.0	MYK3720
	BMAN(5,5)=1.0	MYK3730
	BMAN(6,4)=-1.0	MYK3740
	BMAN(6,6)=1.0	MYK3750
	DO 1030 I=1,6	MYK3760
	DO 1030 J=1,6	MYK3770
	BINV(I,J)=0.0	MYK3780
	DO 1030 MM=1,6	MYK3790
1030	BINV(I,J)=BINV(I,J)+BMAN(I,MM)*THMAN(MM,J)	MYK3800
	DO 1040 J=1,4	MYK3810
	DO 1040 I=1,6	MYK3820
1040	RMUL(I,J)=0.0	MYK3830
	DO 1050 J=1,2	MYK3840
	DO 1050 I=1,4	MYK3850
1050	RMUL(I,J)=-ARPB(I,J)	MYK3860
	DO 1060 J=3,4	MYK3870
	DO 1060 I=1,2	MYK3880
1060	RMUL(I,J)=-ARPB(I,J)-ARPA(I,J)	MYK3890
	DO 1070 J=3,4	MYK3900
	DO 1070 I=3,4	MYK3910
1070	RMUL(I,J)=-ARPB(I,J)	MYK3920
	DO 1080 I=3,4	MYK3930
	II=I+2	MYK3940
	DO 1080 J=3,4	MYK3950
1080	RMUL(II,J)=-ARPA(I,J)	MYK3960
	DO 1090 J=1,4	MYK3970
	DO 1090 I=1,6	MYK3980
	ARSTAR(NDR,I,J)=0.0	MYK3990
	DO 1090 MM=1,6	MYK4000

Table A-12

(Cont'd.)

1090	ARSTAR(NDR,I,J)=ARSTAR(NDR,I,J)+BINV(I,MM)*RMUL(MM,J)	MYK4010
	DO 1100 J=1,4	MYK4020
	DO 1100 I=1,4	MYK4030
	SAP(I,J)=0.0	MYK4040
	DO 1100 MM=1,4	MYK4050
1100	SAP(I,J)=SAP(I,J)+ARSTAR(NDR,I,MM)*APR(MM,J)	MYK4060
	K=KKEEP	MYK4070
	K=K+1	MYK4080
	GO TO 480	MYK4090
1110	K=K+1	MYK4100
	IF(K.LE.NSTA)GO TO 480	MYK4110
	IF(KIAP)480,480,1120	MYK4120
1120	KIAP=KIAP-1	MYK4130
	GO TO 470	MYK4140
1130	I2N=ITEM(2,M)	MYK4150
	KK(JNT)=1	MYK4160
	JOINT(K)=JNT	MYK4170
	MODE(JNT)=ITEM(5,1)+1	MYK4180
	IF(I2N-7)1140,2240,2240	MYK4190
1140	IF(I2N)2190,2190,1150	MYK4200
1150	GO TO (1160,1190,1200,1230,1240,1250),I2N	MYK4210
1160	IF(ITEM(5,1))1180,1180,1170	MYK4220
1170	AP(2,4)=1.0/DIV	MYK4230
1180	FUNC(ITER)=AP(1,3)*AP(2,4)-AP(1,4)*AP(2,3)	MYK4240
	GO TO 1260	MYK4250
1190	FUNC(ITER)=AP(3,3)*AP(4,4)-AP(3,4)*AP(4,3)	MYK4260
	GO TO 1260	MYK4270
1200	IF(ITEM(5,1))1220,1220,1210	MYK4280
1210	AP(4,2)=1.0/DIV	MYK4290
1220	FUNC(ITER)=AP(3,1)*AP(4,2)-AP(3,2)*AP(4,1)	MYK4300
	GO TO 1260	MYK4310
1230	FUNC(ITER)=AP(1,3)*AP(4,4)-AP(1,4)*AP(4,3)	MYK4320
	GO TO 1260	MYK4330
1240	FUNC(ITER)=AP(3,2)*AP(4,3)-AP(4,2)*AP(3,3)	MYK4340
	GO TO 1260	MYK4350
1250	FUNC(ITER)=AP(1,2)*AP(4,3)-AP(1,3)*AP(4,2)	MYK4360
1260	OM(ITER)=SQRT(W2)	MYK4370
	PRNT(1)=ITER	MYK4380
	PRNT(2)=OM(ITER)/6.283185	MYK4390
	PRNT(3)=FUNC(ITER)	MYK4400
	GO TO (1270,1380),ILAF	MYK4410
1270	IF(KOMT.GT.1)GO TO 1330	MYK4420
1280	IF(ITHIN.LT.3)GO TO 1300	MYK4430
	OM(ITER+1)=OM(ITER)*GAMA	MYK4440
	IF(OM(ITER+1).GE.THIS)GO TO 1290	MYK4450
	GO TO 1310	MYK4460
1290	KOMT=1	MYK4470
	ITHIN=1	MYK4480
1300	OM(ITER+1)=OM(ITER)*GAMA	MYK4490
1310	ITER=ITER+1	MYK4500

Table A-12
(Cont'd.)

IF(ITER-298) 1320, 2190, 2190	MYK4510
1320 IF(OM(ITER).GT.OP8ND) GO TO 2190	MYK4520
KOWT=KOWT+1	MYK4530
W2=OM(ITER)**2	MYK4540
IF(W2.EQ.0.0) GO TO 2190	MYK4550
GO TO 420	MYK4560
1330 IF((FUNC(ITER)/FUNC(ITER-1)).GT.0.0) GO TO 1350	MYK4570
ITHIN=1	MYK4580
1340 ILAF=2	MYK4590
SINLO=FUNC(ITER-1)	MYK4600
SMX=ABS(SINLO)	MYK4610
SINH1=FUNC(ITER)	MYK4620
BIX=ABS(SINH1)	MYK4630
GOL0=OM(ITER-1)	MYK4640
GOMI=OM(ITER)	MYK4650
GO TO 1410	MYK4660
1350 IF(ITHIN.EQ.3) GO TO 1280	MYK4670
FINK(ITER)=FUNC(ITER)-FUNC(ITER-1)	MYK4680
IF(KOWT.LT.3) GO TO 1280	MYK4690
IF((FINK(ITER)/FINK(ITER-1)).LE.0.0) ITHIN=ITHIN+1	MYK4700
GO TO (1280, 1360, 1370), ITHIN	MYK4710
1360 THAT=OM(ITER-1)	MYK4720
THEM=FUNC(ITER-1)	MYK4730
GO TO 1280	MYK4740
1370 THIS=OM(ITER)	MYK4750
OM(ITER)=THAT	MYK4760
FUNC(ITER)=THEM	MYK4770
GO TO 1280	MYK4780
1380 IF(FUNC(ITER)/SINLO) 1390, 1390, 1400	MYK4790
1390 SINHI=FUNC(ITER)	MYK4800
GOMI=OM(ITER)	MYK4810
GO TO 1410	MYK4820
1400 SINLO=FUNC(ITER)	MYK4830
GOL0=OM(ITER)	MYK4840
1410 IF(KZ.LE.3) GO TO 1420	MYK4850
OM(ITER+1)=(SINH1*GOL0-SINLO*GOMI)/(SINH1-SINLO)	MYK4860
OM(ITER+1)=ABS(OM(ITER+1))	MYK4870
GO TO 1430	MYK4880
1420 OM(ITER+1)=(GOMI+GOL0)*.5	MYK4890
IF(KZ.EQ.0) GO TO 1440	MYK4900
1430 CONTINUE	MYK4910
IF(ABS(1.0-(OM(ITER+1)/OM(ITER))).LE.EPS) GO TO 1460	MYK4920
1440 KZ=KZ+1	MYK4930
IF(KZ-16) 1310, 1310, 1450	MYK4940
1450 KOWT=1	MYK4950
KZ=0	MYK4960
ITHIN=1	MYK4970
ILAF=1	MYK4980
OM(ITER)=GOMI	MYK4990
FUNC(ITER)=SINH1	MYK5000

Table A-12
(Cont'd.)

GO TO 1280	MYK5010
1460 SAMBO=ABS(FJNC(ITER))	MYK5020
IF(SAMBO-BIX)1470,1470,1450	MYK5030
1470 IF(SAMBO-SMX)1480,1480,1450	MYK5040
1480 OMEG=OM(ITER)	MYK5050
IF(NDR.EQ.0)GO TO 1530	MYK5060
DO 1520 LAP=1,NDR	MYK5070
DO 1500 J=1,4	MYK5080
DO 1490 I=1,4	MYK5090
FPM(LAP,I,J)=0.0	MYK5100
1490 FQM(LAP,I,J)=0.0	MYK5110
FPM(LAP,J,J)=1.0	MYK5120
1500 FQM(LAP,J,J)=1.0	MYK5130
DO 1510 I=1,2	MYK5140
II=I+4	MYK5150
DO 1510 J=1,4	MYK5160
FQM(LAP,I,J)=ARSTAR(LAP,II,J)	MYK5170
1510 FPM(LAP,I,J)=FPM(LAP,I,J)-ARSTAR(LAP,II,J)	MYK5180
1520 CONTINUE	MYK5190
1530 CONTINUE	MYK5200
KZ=0	MYK5210
GO TO (1540,1580,1620,1660,1680,1700),I2N	MYK5220
1540 IF(ITEM(5,1))1550,1550,1560	MYK5230
1550 VEC(3,1)=-AP(1,4)/AP(1,3)	MYK5240
VEC(4,1)=1.0	MYK5250
GO TO 1570	MYK5260
1560 VEC(3,1)=1.0	MYK5270
VEC(4,1)=0.0	MYK5280
1570 VEC(1,1)=0.0	MYK5290
VEC(2,1)=0.0	MYK5300
GO TO 1720	MYK5310
1580 IF(ITEM(5,1))1590,1590,1600	MYK5320
1590 VEC(3,1)=-AP(3,4)/AP(3,3)	MYK5330
VEC(4,1)=1.0	MYK5340
GO TO 1610	MYK5350
1600 VEC(3,1)=1.0	MYK5360
VEC(4,1)=0	MYK5370
1610 VEC(1,1)=0	MYK5380
VEC(2,1)=0.0	MYK5390
GO TO 1720	MYK5400
1620 IF(ITEM(5,1))1630,1630,1640	MYK5410
1630 VEC(1,1)=-AP(3,2)/AP(3,1)	MYK5420
VEC(2,1)=1.0	MYK5430
GO TO 1650	MYK5440
1640 VEC(1,1)=1.0	MYK5450
VEC(2,1)=0.0	MYK5460
1650 VEC(3,1)=0.0	MYK5470
VEC(4,1)=0.0	MYK5480
GO TO 1720	MYK5490
1660 IF(ITEM(5,1))1670,1670,2240	MYK5500

Table A-12
(Cont'd.)

1670	VEC(1,1)=0.0	MYK5510
	VEC(2,1)=0.0	MYK5520
	VEC(3,1)=-AP(1,4)/AP(1,3)	MYK5530
	VEC(4,1)=1.0	MYK5540
	GO TO 1720	MYK5550
1680	IF(ITEM(5,1))1690,1690,2240	MYK5560
1690	VEC(1,1)=0.0	MYK5570
	VEC(2,1)=-AP(3,3)/AP(3,2)	MYK5580
	VEC(3,1)=1.0	MYK5590
	VEC(4,1)=0.0	MYK5600
	GO TO 1720	MYK5610
1700	IF(ITEM(5,1))1710,1710,2240	MYK5620
1710	VEC(1,1)=0.0	MYK5630
	VEC(2,1)=-AP(4,3)/AP(4,2)	MYK5640
	VEC(3,1)=1.0	MYK5650
	VEC(4,1)=0.0	MYK5660
1720	NSH=0	MYK5670
	DO 1870 K=2,KS	MYK5680
	I=I1(K)	MYK5690
	IF(I4(K)-3)1850,1730,1820	MYK5700
1730	IF(I4(K-1)-3)1850,1740,1850	MYK5710
1740	NSH=NSH+1	MYK5720
	DO 1750 J=1,4	MYK5730
1750	VSAVE(J)=VEC(J,K-1)	MYK5740
	DO 1760 J=1,4	MYK5750
	VEC(J,K)=0.0	MYK5760
	DO 1760 MM=1,4	MYK5770
1760	VEC(J,K)=VEC(J,K)+FPM(NSH,J,MM)*VSAVE(MM)	MYK5780
	KL=ICON(NSH)	MYK5790
	DO 1770 J=1,4	MYK5800
	VEC(J,KL)=0.0	MYK5810
	DO 1770 MM=1,4	MYK5820
1770	VEC(J,KL)=VEC(J,KL)+FQM(NSH,J,MM)*VSAVE(MM)	MYK5830
1780	KL=KL+1	MYK5840
	IF(KL.GT.NSJP)GO TO 1810	MYK5850
	I=I1(KL)	MYK5860
	IF(I.EQ.I1(KL-1))GO TO 1790	MYK5870
	IF(ITEM(2,I)-ITEM(2,I-1))1810,1790,1810	MYK5880
1790	DO 1800 J=1,4	MYK5890
	VEC(J,KL)=0.0	MYK5900
	DO 1800 MM=1,4	MYK5910
1800	VEC(J,KL)=VEC(J,KL)+A(J,MM,KL-1)*VEC(MM,KL-1)	MYK5920
	GO TO 1780	MYK5930
1810	CONTINUE	MYK5940
	GO TO 1870	MYK5950
1820	IF(I4(K-1)-4)1850,1830,1850	MYK5960
1830	DO 1840 J=1,4	MYK5970
	VEC(J,K)=0.0	MYK5980
	DO 1840 MM=1,4	MYK5990
1840	VEC(J,K)=VEC(J,K)+ARSTAR(NSH,J,MM)*VSAVE(MM)	MYK6000

Table A-12
(Cont'd.)

GO TO 1870	MYK6010
1850 DO 1860 J=1,4	MYK6020
VEC(J,K)=0.0	MYK6030
DO 1860 MM=1,4	MYK6040
1860 VEC(J,K)=VEC(J,K)+A(J,MM,K-1)*VEC(MM,K-1)	MYK6050
1870 CONTINUE	MYK6060
IF(KORP)2010,2010,1880	MYK6070
1880 KIAP=1	MYK6080
1890 DO 1990 K=KS,NSTA	MYK6090
I=I1(K)	MYK6100
IF(ITEM(2,I)-ITEM(2,I-1))1910,1900,1910	MYK6110
1900 IF(IR(K)+KIAP-KORP)1990,1970,1990	MYK6120
1910 IF(IR(K)+KIAP-KORP)1990,1920,1990	MYK6130
1920 DO 1930 K2=1,NSUP	MYK6140
KQ=K2	MYK6150
IF(ITEM(2,I)-I6(KQ))1930,1940,1930	MYK6160
1930 CONTINUE	MYK6170
GO TO 2190	MYK6180
1940 VEC(1,K)=0.0	MYK6190
VEC(2,K)=0.0	MYK6200
DO 1950 J1=1,JNT	MYK6210
J=J1	MYK6220
IF(KKK(J1)-KQ)1950,1960,1950	MYK6230
1950 CONTINUE	MYK6240
1960 VEC(3,K)=TAP(1,1,J)*VEC(3,KQ)+TAP(1,2,J)*VEC(4,KQ)	MYK6250
MODE(J)=ITEM(5,I)+1	MYK6260
VEC(4,K)=TAP(2,1,J)*VEC(3,KQ)+TAP(2,2,J)*VEC(4,KQ)	MYK6270
GO TO 1990	MYK6280
1970 DO 1980 I=1,4	MYK6290
VEC(I,K)=0.0	MYK6300
DO 1980 J=1,4	MYK6310
1980 VEC(I,K)=VEC(I,K)+A(I,J,K-1)*VEC(J,K-1)	MYK6320
1990 CONTINUE	MYK6330
IF(KIAP-KORP)2000,2010,2000	MYK6340
2000 KIAP=KIAP+1	MYK6350
GO TO 1890	MYK6360
2010 GAM=0.0	MYK6370
DO 2020 K=1,NSUP	MYK6380
KN=K	MYK6390
IF(ITEM(4,M)-I6(K))2020,2030,2020	MYK6400
2020 CONTINUE	MYK6410
GO TO 2080	MYK6420
2030 IF(ITEM(5,KV)-1)2040,2050,2050	MYK6430
2040 B=VEC(4,KN)	MYK6440
GO TO 2060	MYK6450
2050 B=VEC(3,KN)	MYK6460
2060 DO 2070 K=1,NSUP	MYK6470
DO 2070 J=1,4	MYK6480
2070 VEC(J,K)=VEC(J,K)/B	MYK6490
2080 DO 2090 K=1,NSUP	MYK6500

Table A-12
(Cont'd.)

I=11(K)	MYK6510
2030 GAM=GAM+DATA(4,1)*VEC(3,K)**2+DATA(2,I)*VEC(4,K)**2	MYK6520
JK=GAM*OMEG**2	MYK6530
IF(NDR)2100,2120,2100	MYK6540
2100 JUG=JNT+NDR	MYK6550
KKK(JUG)=KKK(JNT)	MYK6560
MODE(JUG)=MODE(JNT)	MYK6570
JU1=JUG-1	MYK6580
J1=0	MYK6590
DO 2110 J=JNT, JU1	MYK6600
J1=J1+1	MYK6610
KKK(J)=ICB(J1)	MYK6620
2110 MODE(J)=MODE(JUG)	MYK6630
JNT=JUG	MYK6640
2120 CONTINUE	MYK6650
DO 2170 JJ=1, JNT	MYK6660
KQ=KKK(JJ)	MYK6670
IQ=I6(KQ)	MYK6680
II=MODE(JJ)	MYK6690
IF(II)2190,2190,2130	MYK6700
2130 GO TO (2140,2150,2160),II	MYK6710
2140 GO TO 2170	MYK6720
2150 GO TO 2170	MYK6730
2160 GO TO 2170	MYK6740
2170 CONTINUE	MYK6750
FREQ=OMEG/6.283185	MYK6760
FREQ=OM(ITER+1)/6.283185	MYK6770
ITEM(3,M)=ITEM(3,M)-1	MYK6780
IF(ITEM(3,M))2190,2190,2100	MYK6790
2190 KONT=2	MYK6800
OM(1)=GOHI	MYK6810
FUNC(1)=SINH I	MYK6820
IF(FUNC(1).EQ.0.0)FUNC(1)=-SINLO	MYK6830
GAMA = SAMA	MYK6840
ILAF=1	MYK6850
OM(2)=GOHI*SAMA	MYK6860
ITER=2	MYK6870
MFAP=1	MYK6880
W2=OM(2)**2	MYK6890
ITMIN=1	MYK6900
GO TO 420	MYK6910
2190 RETURN	MYK6920
2200 WRITE(6,2210)IT	MYK6930
2210 FORMAT(29H NO T GIVEN FOR JOINT TYPE = I3)	MYK6940
GO TO 2190	MYK6950
2220 WRITE(6,2230)I6(KQ),KIAP	MYK6960
2230 FORMAT(24H DETERMINANT V OF JOINT I3,17H APPENDAGE ORDER I3,5H = 0	MYK6970
1.)	MYK6980
GO TO 2190	MYK6990
2240 WRITE(6,2250)I2N	MYK7000

Table A-12
(Cont'd.)

2250 FORMAT(25H BOUNDARY NOT IN TABLE = I3)
GO TO 2190
END

MYK7010
MYK7020
MYK7030

Table A-13
FORTRAN Listing of Subroutine MEMSET

SUBROUTINE MEMSET (IA,IB)	MST	10
DIMENSION IA(1)	MST	20
K=IABS(LOC(IA)-LOC(IB))+1	MST	30
DO 10 J=1,K	MST	40
10 IA(J)=0	MST	50
END	MST	60

SUBROUTINE MATNF5(A,N,NDIM,DETSCL,DET,IROAR)	MTN 10
DIMENSION A(1)	MTN 20
DIMENSION PIVOT(170),INDEX(170,2),IPIVOT(170)	MTN 30
10 EQUIVALENCE(IROW,JROW),(ICOL,JCOL),(AMAX,T,SWAP)	MTN 40
C	MTN 50
C BLOCK 100 INITIALIZE	MTN 60
C	MTN 70
20 IROAR=0	MTN 80
DET=DETSCL	MTN 90
30 DO 40 J=1,N	MTN 100
40 IPIVOT(J)=0	MTN 110
DO 210 I=1,N	MTN 120
C	MTN 130
C BLOCK 200 SEARCH FOR PIVOT ELEMENT	MTN 140
C	MTN 150
50 AMAX=0.0	MTN 160
DO 100 J=1,N	MTN 170
IF(IPIVOT(J)-1)60,100,60	MTN 180
60 DO 90 K=1,N	MTN 190
IF(IPIVOT(K)-1)70,90,290	MTN 200
70 JK=J+NDIM*(K-1)	MTN 210
IF(ABS(AMAX)-ABS(A(JK)))80,90,90	MTN 220
80 IROW=J	MTN 230
ICOL=K	MTN 240
AMAX=A(JK)	MTN 250
90 CONTINUE	MTN 260
100 CONTINUE	MTN 270
110 IF(AMAX)120,300,120	MTN 280
C	MTN 290
C BLOCK 300 INTERCHANGE ROWS TO PUT PIVOTAL ELEMENT ON DIAGONAL	MTN 300
C	MTN 310
120 IPIVOT(ICOL)=IPIVOT(ICOL)+1	MTN 320
IF(IROW-ICOL)130,150,130	MTN 330
130 DET=-DET	MTN 340
DO 140 L=1,N	MTN 350
LD=NDIM*(L-1)	MTN 360
IROL=IROW+LD	MTN 370
ICLL=ICOL+LD	MTN 380
SWAP=A(IROL)	MTN 390
A(IROL)=A(ICLL)	MTN 400
140 A(ICLL)=SWAP	MTN 410
150 INDEX(I,1)=IROW	MTN 420
INDEX(I,2)=ICOL	MTN 430
ILOC=ICOL+NDIM*(ICOL-1)	MTN 440
PIVOT(I)=A(ILOC)	MTN 450
DET=DET*PIVOT(I)	MTN 460
C	MTN 470
C BLOCK 400 DIVIDE PIVOT ROW BY PIVOT ELEMENT	MTN 480
C	MTN 490
160 A(ILOC)=1.0	MTN 500

Table A-14
(Cont'd.)

	DO 170 L=1,N	MTN 510
	ICLL=ICOL+NDIM*(L-1)	MTN 520
	A(ICLL)=A(ICLL)/PIVOT(I)	MTN 530
170	CONTINUE	MTN 540
C		MTN 550
C	BLOCK 500 REDUCE NON-PIVOT ROWS	MTN 560
C		MTN 570
180	DO 210 L1=1,N	MTN 580
	IF(L1-ICOL)190,210,190	MTN 590
190	ICOL=NDIM*(ICOL-1)	MTN 600
	L10=L1+ICOL	MTN 610
	T=A(L10)	MTN 620
	A(L10)=0.0	MTN 630
	DO 200 L=1,N	MTN 640
	LD=NDIM*(L-1)	MTN 650
	L10=L1+LD	MTN 660
	ICL=ICOL+LD	MTN 670
200	A(L10)=A(L10)-A(ICL)*T	MTN 680
210	CONTINUE	MTN 690
C		MTN 700
C	BLOCK 600 INTERCHANGE COLUMNS	MTN 710
C		MTN 720
220	DO 250 I=1,N	MTN 730
	L=N+1-I	MTN 740
	IF(INDEX(L,1)-INDEX(L,2))230,250,230	MTN 750
230	JROW=INDEX(L,1)	MTN 760
	JCOL=INDEX(L,2)	MTN 770
	JROW=NDIM*(JROW-1)	MTN 780
	JCOL=NDIM*(JCOL-1)	MTN 790
	DO 240 K=1,N	MTN 800
	KR=K+JROW	MTN 810
	KC=K+JCOL	MTN 820
	SWAP=A(KR)	MTN 830
	A(KR)=A(KC)	MTN 840
	A(KC)=SWAP	MTN 850
240	CONTINUE	MTN 860
250	CONTINUE	MTN 870
	RETURN	MTN 880
C		MTN 890
C	BLOCK 9000 ERROR INDICATIONS	MTN 900
C		MTN 910
260	WRITE(6,270)IROAR	MTN 920
270	FORMAT(31H0 SUBROUTINE MATNF4 ERROR TYPE I5)	MTN 930
280	CALL EXIT	MTN 940
290	IROAR=1	MTN 950
	GO TO 260	MTN 960
300	IROAR=-5	MTN 970
	RETURN	MTN 980
	END	MTN 990

TABLE B-15
SAMPLE DATA DECK LISTING FOR PROGRAM FILLIN

----- CARD COLUMNS -----
0000000001111111112222222222333333333344444444445555555555666666666677777777778
1234567890123456789012345678901234567890123456789012345678901234567890

FILLIN TEST CASE		TYPICAL MISSILE AIRFRAME			
1		0.16 +7	.040	7.8	
15		1.16 +8	.412	15.	2.447
20		2.75 +8	.629	20.	7.002
25		4.72 +8	.728	25.	11.50
30		6.92 +8	1.003	30.15	20.13
35		3.90 +8	.783	35.5	10.93
37	2	3.83 +8		37.3	
39		2.51 +8	4.138	39.8	22.15
45		3.59 +8	1.016	45.4	24.36
46	1	5.81 +8		46.8	.93 -7
47		5.81 +8	.614	47.2	13.83
48	3	1.57 +8		48.	
49		1.57 +8	.323	49.4	7.92
55		1.57 +8	.560	55.	13.75
60		1.57 +8	1.161	59.5	28.46
61		4.53 +8		61.8	
62	1	4.53 +8		62.59	.62 -8
63	4	3.23 +8		63.	
66		2.59 +8	3.106	66.	41.24
67		3.56 +8	.809	67.97	11.32
70	1	7.07 +8		70.	.12 -6
71		1.29 +8	.687	71.38	19.42
76		4.88 +8	.925	7.4	26.13
77	1	4.98 +8		77.6	.62 -8
78	2	4.54 +8		78.25	
79		4.54 +8	.846	79.	19.89
80	1	8.02 +8		80.5	.93 -7
82		7.10 +8	7.075	82.	92.66
90		5.26 +8	2.791	90.	81.50
100		5.26 +8	3.000	100.	92.34
110		5.26 +8	2.883	110.	88.78
120		5.26 +8	2.883	120.	88.78
130		5.26 +8	2.883	130.	88.78
140		5.26 +8	2.883	140.	88.78
150		5.26 +8	2.883	150.	88.78
157		1.20 +9		157.5	
160		9.41 +8	4.468	160.	138.91
168		1.23 +9	7.011	170.4	94.76
170	1	2.47 +8		170.5	.43 -7
171		2.47 +8	1.387	171.7	26.71
174		3.88 +8		174.	
178		5.98 +7	8.351	177.38	109.66
182		5.98 +7	2.508	182.2	24.63
191	37 1:	2.43 +5	1.132	30.3	
192	37 1: 1	2.43 +5		30.31	.19 -3

[illegible]

```

-----CARD COLUMNS-----
0000000001111111122222222233333333344444444455555555566666666677777777778
1234567890123456789012345678901234567890123456789012345678901234567890

```

167

(Cont'd.)

```

-----CARD COLUMNS-----
0000000011111111222222223333333344444444555555556666666677777777
123456789012345678901234567890123456789012345678901234567890
-----

```

16	1	-.315	-.435	.069
17	1	-.311	-.436	.079
18	1	-.304	-.501	.126
19	1	-.306	-.616	.202
20	1	-.296	-.663	.250
21	1	-.280	-.701	.281
22	1	-.260	-.710	.308
23	1	-.242	-.709	.324
24	1	-.223	-.732	.342
25	1	-.198	-.755	.344
26	1	-.170	-.674	.336
27	1	-.143	-.641	.321
28	1	-.113	-.571	.298
29	1	-.079	-.504	.268
30	1	-.043	-.420	.229
31	1	.030	-.217	.141
32	1	.068	-.112	.09
33	1	.111	.072	.02
34	1	.148	.176	-.05
35	1	.161	.215	-.068
36	1	.237	.392	-.173
37	1	.268	.567	-.278
38	1	.797	-10.28	-.64
39	1	.78	-9.35	-.6
40	1	.65	-5.6	-.28
41	1	.53	-3.0	-.03
42	1	.42	-0.5	.17
43	1	.362	.691	.278
44	1	.36	.69	.275
45	1	.354	.687	.268
46	1	-.345	-.429	-.036
47	1	-.325	-.436	.013
48	1	-.321	-.439	.041
49	1	-.319	-.44	.046
50	1	-.311	-.441	.049
51	1	.2	.635	.09
52	1	.135	.59	.01
53	1	.103	.635	-.155
54	1	-.01	.68	-.265
55	1	-.10	.54	-.36
56	1	-.161	.487	-.422
57	1	-.15	.19	-.13
58	1	-.19	.1	-.115

TABLE A-1E
SAMPLE DATA DECK LISTING FOR PROGRAM JOINTS

----- CARD COLUMNS -----

00000000111111112222222233333333334444444455555555666666666677777777778
1234567890123456789012345678901234567890123456789012345678901234567890

PROGRAM JOINTS TEST CASE										
1	3	3	1	10	4	78	78	0.15	0.001	.9
2	0.264									
1.0	1.0		1.0							
1.0	1.0		1.0							
59.7	116.		153.							
10	11	.1	+8	1.	+8	2				
21	26	.5	+7	5.	+7	2				
27	35	.1	+8	1.	+8	2				
48	58	.1	+6	1.	+6	2				
1	1	.99305E+00 .99665E+00 .99142E+00								
2	1	.82618E+00 .91618E+00 .78559E+00								
3	1	.77703E+00 .99471E+00 .73663E+00								
4	1	.66545E+00 .84066E+00 .60805E+00								
5	1	.53995E+00 .77872E+00 .46133E+00								
6	1	.41282E+00 .71442E+00 .31713E+00								
7	1	.37409E+00 .70447E+00 .27764E+00								
8	1	.37409E+00 .70447E+00 .27764E+00								
9	1	.31913E+00 .67842E+00 .21627E+00								
10	1	.19196E+00 .61390E+00 .86290E-01								
11	1	.15979E+00 .59723E+00 .57824E-01								
12	1	.15979E+00 .59723E+00 .57824E-01								
13	1	.15042E+00 .59237E+00 .49532E-01								
14	1	.13144E+00 .58253E+00 .32737E-01								
15	1	.13144E+00 .58253E+00 .32737E-01								
16	1	.10106E+00 .55586E+00 .96847E-02								
17	1	-.14839E-01 .41939E+00 -.66610E-01								
18	1	-.93783E-01 .29449E+00 -.98593E-01								
19	1	-.13327E+00 .22284E+00 -.11155E+00								
20	1	-.14322E+00 .19475E+00 -.11030E+00								
21	1	-.14322E+00 .19475E+00 -.11030E+00								
22	1	-.14322E+00 .18249E+00 -.10969E+00								
23	1	-.14822E+00 .18249E+00 -.10969E+00								
24	1	-.18578E+00 .90383E-01 -.10511E+00								
25	1	-.20661E+00 .25042E-01 -.88056E-01								
26	1	-.22617E+00 -.42329E-01 -.67804E-01								
27	1	-.22617E+00 -.42329E-01 -.67804E-01								
28	1	-.23708E+00 -.92267E-01 -.50985E-01								
29	1	-.29274E+00 -.32567E+00 .31853E-01								
30	1	-.29464E+00 -.33381E+00 .34456E-01								
31	1	-.29464E+00 -.33381E+00 .34456E-01								
32	1	-.30085E+00 -.36042E+00 .42963E-01								
33	1	-.30085E+00 -.36042E+00 .42963E-01								
34	1	-.30908E+00 -.39140E+00 .52867E-01								
35	1	-.31141E+00 -.42991E+00 .71247E-01								
36	1	-.31141E+00 -.42991E+00 .71247E-01								

Table A-16

(cont'd.)

 CARD COLUMNS
 00000000111111112222222233333333444444445555555566666666777777778
 1234567890123456789012345678901234567890123456789012345678901234567890

37	1	-.31075E+00	-.45913E+00	.91805E-01
38	1	-.30233E+00	-.58973E+00	.19073E+00
39	1	-.27819E+00	-.68768E+00	.27681E+00
40	1	-.24224E+00	-.71739E+00	.32324E+00
41	1	-.19671E+00	-.71957E+00	.33832E+00
42	1	-.14245E+00	-.63215E+00	.31740E+00
43	1	-.78407E-01	-.49883E+00	.26426E+00
44	1	-.75292E-02	-.31738E+00	.18385E+00
45	1	.49843E-01	-.14328E+00	.10883E+00
46	1	.69465E-01	-.82199E-01	.82546E-01
47	1	.15548E+00	.20953E+00	-.65211E-01
48	1	.15636E+00	.21245E+00	-.66965E-01
49	1	.15636E+00	.21245E+00	-.66965E-01
50	1	.16575E+00	.23778E+00	-.83601E-01
51	1	.18630E+00	.30551E+00	-.12344E+00
52	1	.21903E+00	.42658E+00	-.19370E+00
53	1	.26103E+00	.54700E+00	-.26600E+00
54	1	.26103E+00	.54700E+00	-.26600E+00
55	1	.78000E+00	-.93500E+01	-.60000E+00
56	1	.77943E+00	-.93190E+01	-.59867E+00
57	1	.65071E+00	-.56155E+01	-.28149E+00
58	1	.54672E+00	-.33377E+01	-.73377E-01
59	1	.41079E+00	-.31895E+00	.18714E+00
60	1	.36169E+00	.69730E+00	.27857E+00
61	1	.36377E+00	.58673E+00	.26450E+00
62	1	.35960E+00	.60980E+00	.27453E+00
63	1	.35400E+00	.68700E+00	.26800E+00
64	1	.35400E+00	.68700E+00	.26800E+00
65	1	-.33433E+00	-.43273E+00	-.28667E-02
66	1	-.32051E+00	-.43896E+00	.38411E-01
67	1	-.32020E+00	-.43960E+00	.46600E-01
68	1	-.31933E+00	-.43996E+00	.45875E-01
69	1	-.31100E+00	-.44100E+00	.49000E-01
70	1	-.31100E+00	-.44100E+00	.49000E-01
71	1	.13478E+00	.58985E+00	.97324E-02
72	1	.13382E+00	.87727E+00	-.12500E+00
73	1	.82455E-01	.80682E+00	-.17500E+00
74	1	-.10000E-01	.68000E+00	-.26500E+00
75	1	-.10000E+00	.54000E+00	-.36000E+00
76	1	-.18540E+00	.46580E+00	-.44680E+00
77	1	-.14987E+00	.19030E+00	-.13005E+00
78	1	-.14987E+00	.19030E+00	-.13005E+00
1	1	-.23176E-01	-.11176E-01	-.28588E-01
2	1	-.23176E-01	-.11176E-01	-.28588E-01
3	1	-.19867E-01	-.96208E-02	-.22895E-01
4	1	-.24768E-01	-.12001E-01	-.28537E-01

----- CARD COLUMNS -----
0000000001111111112222222222333333333344444444445555555555666666666677777777778
1234567890123456789012345678901234567890123456789012345678901234567890

5	1	-.21830E-01	-.11839E-01	-.24761E-01
6	1	-.25695E-01	-.12996E-01	-.29145E-01
7	1	-.21270E-01	-.10882E-01	-.23752E-01
8	1	-.21270E-01	-.10882E-01	-.23752E-01
9	1	-.22695E-01	-.10757E-01	-.25343E-01
10	1	-.22627E-01	-.11727E-01	-.20844E-01
11	1	-.22222E-01	-.35556E-02	-.21111E-01
12	1	-.20857E-01	-.16571E-01	-.14000E-01
13	1	-.23524E-01	-.12192E-01	-.20818E-01
14	1	-.23923E-01	-.12399E-01	-.21171E-01
15	1	-.23923E-01	-.12399E-01	-.21171E-01
16	1	-.21405E-01	-.22829E-01	-.15240E-01
17	1	-.19312E-01	-.27955E-01	-.10185E-01
18	1	-.16843E-01	-.30562E-01	-.55264E-02
19	1	-.17494E-01	-.31743E-01	-.57399E-02
20	1	-.16200E-01	-.28200E-01	-.56000E-02
21	1	-.71429E-02	-.34800E-01	.97143E-02
22	1	-.12229E-01	-.29990E-01	.14927E-02
23	1	-.12229E-01	-.29990E-01	.14927E-02
24	1	-.12812E-01	-.31418E-01	.15639E-02
25	1	-.94716E-02	-.33228E-01	.89118E-02
26	1	-.71429E-02	-.34800E-01	.97143E-02
27	1	-.92000E-02	-.35200E-01	.12600E-01
28	1	-.91541E-02	-.37813E-01	.12965E-01
29	1	-.94904E-02	-.40664E-01	.13000E-01
30	1	-.92000E-02	-.35200E-01	.12600E-01
31	1	-.40000E-02	-.38000E-01	.20000E-01
32	1	-.95946E-02	-.41111E-01	.13142E-01
33	1	-.95946E-02	-.41111E-01	.13142E-01
34	1	-.90866E-02	-.41505E-01	.13268E-01
35	1	-.40000E-02	-.38000E-01	.20000E-01
36	1	.17500E-02	-.16250E-01	.11750E-01
37	1	.82451E-03	-.17875E-01	.12834E-01
38	1	.92996E-03	-.17279E-01	.12805E-01
39	1	.31500E-02	-.65641E-02	.71598E-02
40	1	.38679E-02	-.18828E-02	.40726E-02
41	1	.49226E-02	.16749E-02	.77617E-03
42	1	.57506E-02	.11929E-01	-.31200E-02
43	1	.88015E-02	.14865E-01	-.62313E-02
44	1	.73400E-02	.19740E-01	-.88800E-02
45	1	.77870E-02	.24240E-01	-.10429E-01
46	1	.79106E-02	.24624E-01	-.10595E-01
47	1	.87572E-02	.29155E-01	-.17539E-01
48	1	.74000E-02	.20800E-01	-.14000E-01
49	1	.92000E-02	.35400E-01	-.21000E-01
50	1	.88731E-02	.29253E-01	-.17205E-01

Table A-16
(Cont'd.)

----- CARD COLUMNS -----
0000100001111111112222222222333333333344444444445555555555666666666677777777778
12345678901234567890123456789012345678901234567890123456789012345678901234567890

51	1	.89920E-02	.29645E-01	-.17435E-01	
52	1	.87143E-02	.25600E-01	-.15000E-01	
53	1	.87143E-02	.25000E-01	-.15000E-01	
54	1	.87143E-02	.25000E-01	-.15000E-01	
55	1	-.56667E-01	.31000E+01	.13333E+00	
56	1	-.56667E-01	.31000E+01	.13333E+00	
57	1	-.56667E-01	.31000E+01	.13333E+00	
58	1	-.40809E-01	.89668E+00	.78299E-01	
59	1	-.30688E-01	.63016E+00	.57143E-01	
60	1	-.30688E-01	.63016E+00	.57143E-01	
61	1	-.20000E-01	-.10000E-01	-.23333E-01	
62	1	-.20000E-01	-.10000E-01	-.23333E-01	
63	1	-.20000E-01	-.10000E-01	-.23333E-01	
64	1	-.20000E-01	-.10000E-01	-.23333E-01	
65	1	.44444E-02	-.15556E-02	.10889E-01	
66	1	.35587E-02	-.15063E-02	.11415E-01	
67	1	.16080E-02	-.12000E-02	.11200E-01	
68	1	.33333E-01	-.41667E-02	.12500E-01	
69	1	.33333E-01	-.41667E-02	.12500E-01	
70	1	.33333E-01	-.41667E-02	.12500E-01	
71	1	-.0207	-.0283	-.0202	
72	1	-.0207	-.0283	-.0202	
73	1	-.20545E-01	-.28182E-01	-.20000E-01	
74	1	-.20545E-01	-.28182E-01	-.20000E-01	
75	1	-.24400E-01	-.21200E-01	-.24800E-01	
76	1	-.24400E-01	-.21200E-01	-.24800E-01	
77	1	-.13378E-01	-.30100E-01	.0015056	
78	1	-.13378E-01	-.30100E-01	.0015056	
1		0.16 +7	.040	7.8	
15		1.16 +8	.412	15.	2.447
20		2.75 +8	.629	20.	7.002
25		4.72 +8	.728	25.	11.50
30		6.92 +8	1.003	30.15	20.13
35		3.90 +8	.783	35.5	10.93
37	2	3.83 +8		37.3	
39		2.51 +8	4.138	39.8	22.15
45		3.59 +8	1.016	45.4	24.36
46	1	5.81 +8		46.8	
47		5.81 +8	.614	47.2	13.83
48	3	1.57 +8		48.	
49		1.57 +8	.323	49.4	7.92
55		1.57 +8	.560	55.	13.75
60		1.57 +8	1.161	59.5	28.46
61		4.53 +8		61.8	
62	1	4.53 +8		62.59	
63	4	3.23 +8		63.	

.93 -7

.62 -8

Table A-16
(Cont'd.)

		CARD COLUMNS																			
		0100000001111111111222222222233333333334444444444555555555566666666																			
		123456789012345678901234567890123456789012345678901234567890123456																			
66																					
67																					
70	1																			.12	-6
71																					
76																					
77	1																			.62	-8
78	2																				
79																					
80	1																			.93	-7
82																					
90																					
100																					
110																					
120																					
130																					
140																					
150																					
157																					
160																					
168																					
170	1																			.43	-7
171																					
174																					
178																					
182																					
191	37 1																				
192	37 1 1																			.19	-3
193	37 1																				
194	37 1																				
195	37 1 1																			.80	-5
196	37 1																				
198	37 1																				
315	78 1																				
325	78 1																				
328	78 1 1																			.26	-4 .32 -6
330	78 1																				
265	48-1 1																			.28	-4
267	48-1																				
268	48-1																				
269	48-1																				
271	48-1 1																			.62	-4 1.
	1 3																				

Table A-17

Key Output Data from Sample Data Deck

Parameter	Iteration		
	0	1	2
Cost Functions			
Overall	.68164 E + 12	.65905 E + 11	.36836 E + 11
Frequency	.17047 E + 12	.39695 E + 11	.96240 E + 10
Mode Shape	.51117 E + 12	.26210 E + 11	.27212 E + 11
Compliances			
C ₁	.93000 E - 7	.83152 E - 7	.53820 E - 7
C ₂	.12060 E - 6	.12038 E - 6	.80930 E - 7
C ₃	.93000 E - 7	.60380 E - 7	.40304 E - 7
C ₄	.30000 E - 5	.69565 E - 5	.59244 E - 5
Frequencies			
f ₁	.4888485 E + 2	.4894103 E + 2	.5546776 E + 2
f ₂	.1435402 E + 3	.1078903 E + 3	.1124721 E + 3
f ₃	.1435414 E + 3	.1441162 E + 3	.1485364 E + 3

FIGURE A-1
 SAMPLE APPLICATION
 VALUES OF UNKNOWN JOINT
 COMPLIANCES AND COST FUNCTION
 VERSUS CYCLE NUMBER

